THE MINERALOGY AND SIZE OF AIRBORNE CHRYSOTILE AND ROCK FRAGMENTS: RAMIFICATIONS OF USING THE NIOSH 7400 METHOD

Ann G. Wylie*
Kelly F. Bailey*

ᵃLaboratory for Mineral Deposits Research, Department of Geology, University of Maryland, College Park, MD 20742; ᵇVulcan Materials Company, One Metroplex Dr., Birmingham, AL 35209

The length and width of chrysotile and rock fragments that were collected on nine air-monitoring filters in the mine and plant of the Lowell asbestos mine in Vermont have been measured by transmission electron microscopy (TEM). Selective area electron diffraction (SAED) and energy dispersive x-ray analysis (EDS) were used to identify particles longer than 5 µm with a length-to-width aspect ratio of at least 3:1 (federal fiber). All federal fibers were found to be chrysotile or serpentinite rock fragment; no tremolite or other amphiboles were detected. Magnifications of 400× and 19 000× were used on five filters in an attempt to compare the size distributions of the federal fibers likely to be measured by using phase contrast optical microscopy (PCM) at 400× to those measured by TEM at higher magnification. The data from the mine show that (1) the size distribution of chrysotile determined at 19 000× differs substantially from that determined at 400× but the size distribution of rock fragment is nearly independent of the magnification; and (2) at 400×, 34% of the federal fibers were chrysotile, 39% were serpentinite rock fragment, and 27% were composite particles, not fibers. At 19 000×, the proportion of chrysotile increased to 77%, reflecting the increased visibility of chrysotile at high magnification. The proportions of chrysotile, serpentinite rock, and composite particles are such that if an air filter were analyzed at 400×, and 1.0 f/cc were determined to be the exposure, 0.3 f/cc would be chrysotile, 0.4 f/cc would be serpentinite rock, and 0.3 f/cc would be composite particles. If TEM were used at high magnification, the total federal fiber burden would rise to 1.6 f/cc with 1.2 f/cc chrysotile and 0.4 f/cc rock fragment. These results suggest that the proportion of federal fibers obtained by the standard PCM method that are actually asbestos may be lower in the chrysotile asbestos mining environment than that obtained in the commercial asbestos handling environments that were used in government quantitative risk assessments. The Occupational Safety and Health Administration excluded epidemiologic studies of asbestos miners and millers from its quantitative risk assessment because evidence showed the risk to be lower than in other industrial environments because of fiber size. Likewise, the use of the PCM National Institute for Occupational Safety and Health 7400 method, which was developed from data taken in commercial asbestos handling as an "index" of exposure, may not be valid in mining environments. TEM analysis of air filters may be necessary to assess chrysotile exposure adequately in mining environments.

Within any given industrial setting, there exists a positive correlation between the incidence of the asbestos-related diseases and the level of exposure to asbestos as established by phase contrast optical microscopy (PCM) and the membrane filter method.[1] However, it is generally not possible to predict closely the risk of disease within one industry by comparing exposures of its workers to exposures and disease incidence from a different industrial environment. For example, the incidence of asbestos-related diseases among Canadian chrysotile miners is less than would be predicted from the experience of textile workers or asbestos insulation workers.[2-5] Also, there is no elevated incidence of mesothelioma among anthophyllite asbestos miners of Paakila, Finland, although high incidence would be predicted based on the experience of crocidolite miners in Australia and South Africa.[6-8]

These observations lead to several possible hypotheses to explain the discrepancies. First, it may be that there are significant differences in the biological activity among the different asbestos minerals. For example, chrysotile fibers appear to dissolve or in some other way be removed from the body but crocidolite fibers do not, and because of this, the long-term effects of exposure to chrysotile may be quite different from the same level of exposure to crocidolite.[9] In fact, because of the behavior of chrysotile fibers in vivo, tremolite-asbestos, which in some cases has been identified as a contaminant in chrysotile, has received much attention as the possible etiologic agent for the diseases that are observed in those "solely" exposed to chrysotile.[10-13] Second, there may be significant differences in the size and shape of the respirable mineral particles making up the dust clouds in different industrial settings; differences that are simply not reflected in the PCM exposure measurements.[14]

For example, because the average width of amosite fiber is greater than the average width of crocidolite fiber, more of the amosite fiber will be visible by PCM. In this case, therefore, more of the total airborne amosite fiber will be counted to assess exposure than of the total airborne crocidolite fiber when the total airborne fiber concentrations of the two are actually the same. Third, there may be differences in the aerodynamic characteristics among the asbestos minerals, such as chrysotile's propensity to curl compared to the relatively straight amosite fiber, that affect the fate of an inhaled fiber in the body. Although the relative importance of these variables is not well known, the explanation for the observed differences in risk for the same PCM-measured exposure is likely that both fiber type and fiber size play a role, and it is important that both of these variables be examined more closely.

This study was undertaken in order to examine the mineralogy and size distribution of the airborne particles at the Lowell chrysotile mine in Vermont. The Lowell mine is located in the upper Missisquoi Valley just south of the international boundary with the Canadian province of Quebec. Chrysotile has been produced from this mine and nearby pits for more than 100 yr. More than 80% of the asbestos mined in the United States has come from this mining district, and the Lowell mine is the largest and most productive mine in the area. It is located in the same geologic terrane as the larger asbestos deposits in Quebec.[15] The geology of the Lowell mine and vicinity is described in detail by Cady et al.[16]

Specifically, the authors were interested in determining what minerals would be included in a PCM fiber count, how the specific minerals differ in particle size and shape, and how the use of transmission electron microscopy (TEM) affects determination of fiber exposure. The authors also wanted to determine if tremolite was an important constituent of airborne dust in the mine because it is widely assumed that tremolite is ubiquitous in chrysotile deposits.[10-13,17-19] Estimates of tremolite asbestos contamination in chrysotile mines range as high as 1.5%.[20]

EXPERIMENTAL MATERIALS AND METHODS

Samples

Nine air filters from the Lowell mine were provided by the United States Mine Safety and Health Administration (MSHA). No information was provided on the airflow or duration of collection. Six of the filters contained particles collected in the mine, two of the filters were from the mill, and one was from the bagging room. The filters were collected in 1987. The samples were prepared for TEM analysis by AMA Laboratories in Laurel, Md., according to the procedures specified by the Environmental Protection Agency[21] for air filter analysis in school buildings. Two 200-mesh copper grids were prepared from each filter.

High Magnification

Randomly chosen grid openings were scanned at a magnification of 19 000×. All particles longer than 5 μm with an

aspect ratio of 3:1 or greater (federal fibers) were identified and their length and width determined directly from the screen by comparison to a calibrated scale. The precision of this method of measurement is estimated at 10%.[22] Identification was based on selective area electron diffraction (SAED) pattern, qualitative chemical analysis by energy dispersive x-ray analysis (EDS), and morphology. For a federal fiber to be positively identified as chrysotile, it had to have the appropriate chemical composition and possess either an obvious tubular structure or a characteristic diffraction pattern. Fiber analysis continued until at least 50 federal fibers from each filter were measured and identified.

Low Magnification

Randomly chosen grid openings were first scanned at a magnification of 400×. All particles that met the federal fiber size criteria, as determined by comparison to a calibrated scale on the screen, were designated. A diagram of the grid opening with the position of these federal fibers was made. Each designated federal fiber was then examined at a magnification of 19 000×. The federal fibers were identified as chrysotile or "other" based on the diffraction pattern and tubular morphology and, if necessary, EDS. For federal fibers exhibiting diffraction patterns that could be amphibole, EDS would have been used to identify the amphibole tentatively. However, no amphibole particles were found. The length and width of all chrysotile and other federal fibers were measured in the same manner described above.

RESULTS

Mineralogy

In this study, a total of 517 federal fibers were measured and identified. A total of 63% were found to be chrysotile and 37% were identified as other. For the 256 federal fibers examined at high magnification, all those identified as "other" had a Si:Mg ratio and a diffraction pattern (when obtainable) consistent with the serpentinite minerals antigorite or lizardite. MSHA, by using an automated imaging system, had previously studied these filters and identified 477 federal fibers on the basis of qualitative chemical composition and, in part, diffraction patterns.[23] MSHA identified a large portion of the federal fibers as antigorite/lizardite and found small amounts of a number of other minerals, including magnetite, plagioclase feldspar, chlorite, quartz, enstatite, olivine, diopside, and calcite. MSHA did not identify tremolite or any other amphibole.

When the federal fibers designated at low magnification were examined at 19 000×, a large portion were not fibers at all but were composed of a linear array of smaller particles. These particles were sometimes both chrysotile and serpentinite rock fragments, and they sometimes were only serpentinite rock fragments. A total of 29% of the elongated particles from the mine were found to be such "composite particles." Of the elongated particles from the mill sample, 10% were also composite particles. Although there is a significant difference between the number of composite particles found in

TABLE I. Distribution of Particles at 400× Magnification

Filter	Chrysotile (No.)	(%)	Other Minerals (No.)	(%)	Composite Particles (No.)	(%)
Mine 3	20	30	27	40	20	30
Mine 4	14	29	21	44	13	27
Mine 6	18	31	17	29	23	40
Mine 7	12	20	36	61	11	19
Mine 9	36	49	15	20	23	31
Mine total	100	33	116	38	90	29
Mill 5	22	44	23	46	5	10
Total mine and mill	122	34	139	39	95	27

Size Distributions

The frequency distributions of log length, log width, and log aspect ratio of federal fibers collected from the mine at 400× and 19 000× magnification that are not chrysotile are given in Figure 1a–f. Log values are used to approximate normal distributions. The similarity of these distributions indicates that there is little evidence for systematic bias in the characterization of these federal fibers introduced by changing magnifications over this range. The ranges, modal classes, and means are similar. However, only the means of log length from the low and high magnifications are statistically indistinguishable (t-test). Mean log width and mean log aspect ratio are not identical even though they are close in magnitude.

the mill (one filter) and in the mine, it is impossible to tell whether this is caused by real differences in the nature of the airborne dust cloud in these two environments or to a difference in filter loading (see Table I). Because "composite particles" were not fibers, they are not used in comparing the size distributions at 400× and 19 000×.

Table II gives the distributions of chrysotile and federal fibers identified as "other" according to sample location and the magnification. At low magnification, more than half of the federal fibers were found to be a mineral other than chrysotile. When the filters were first examined at high magnification, most of the federal fibers were found to be chrysotile and the proportion of other federal fibers was significantly less than at low magnification. The difference between the proportion of airborne chrysotile in the mine and the proportion of airborne chrysotile in the mill or bagging room is statistically insignificant (5% level of significance).

TABLE II. Mineralogical Distribution of Single Particles at 400× and 19 000× Magnification

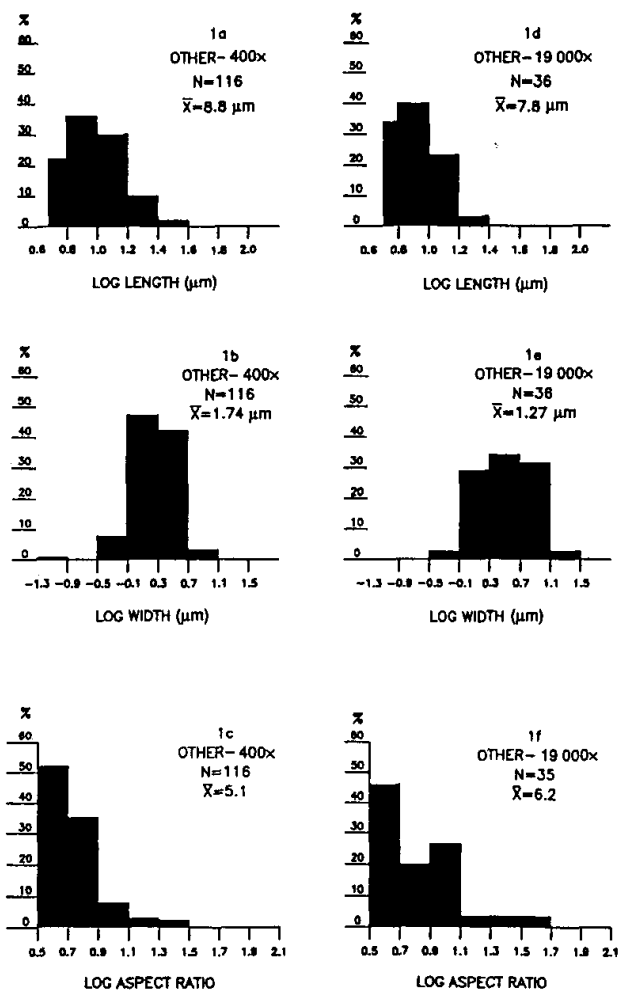| Filter	Chrysotile (No.)	(%)	Other Minerals (No.)	(%)
400×				
Mine 3	20	43	27	57
Mine 4	14	40	21	60
Mine 6	18	51	17	49
Mine 7	12	25	36	75
Mine 9	36	71	15	29
Mine total	100	46	116	54
Mill 5	22	49	23	51
19 000×				
Mine 8	38	70	16	30
Mine 6	46	92	4	8
Mine 4	35	69	16	31
Mine total	119	77	36	23
Mill 1	44	88	6	12
Bagging room 10	43	84	8	16
Plant total	87	86	14	14

FIGURE 1. Nonasbestos particle dimension distributions

The frequency distributions of log length, log width, and log aspect ratio of chrysotile collected from the mine at 400× and 19 000× are given in Figure 2a–f. Changing magnification has had a significant impact on the distributions of these variables. Thin, short, high-aspect-ratio fibers dominate the populations analyzed at high magnification.

A comparison of the size distributions of serpentinite rock fragment and chrysotile shows that these two populations are distinct, whether examined at low or high magnification. However, there is significant overlap at both low and high magnification in all three dimensional parameters, and it is not possible to discriminate effectively between these populations by introducing a simple dimensional parameter such as an aspect ratio of 20:1 or a width of 1 μm as may be appropriate in other environments and has been suggested elsewhere.[24–26]

DISCUSSION

Estimates of the minimum width of a fiber that can be seen by phase contrast microscopy at 400× range from 0.1 to 0.5 μm.[27]
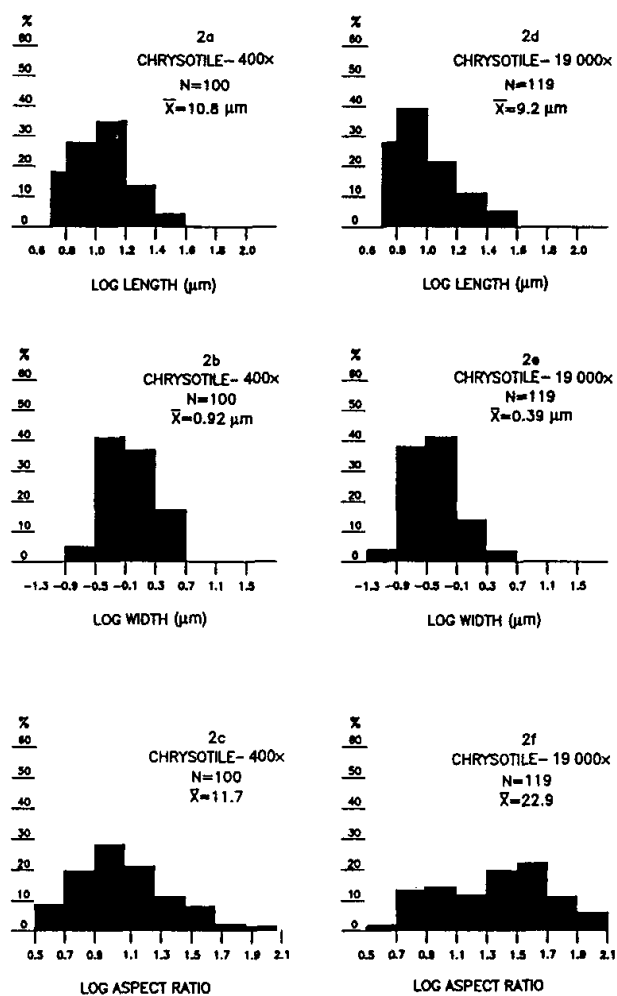

FIGURE 2. Chrysotile particle dimension distributions

Whether the observations made at 400× by TEM duplicate what would be seen optically by phase contrast microscopy is difficult to evaluate. Visibility is not only a function of the resolution of the system, it is also a function of the magnification, the difference in the index of refraction of the fiber and the substrate, and the visual acuity of the observer.

A comparison of width distributions of chrysotile at 400× (Figure 2b) and at 19 000× (Figure 2e) shows abundant chrysotile fibers with widths less than 0.4 μm present on the air filters. It is also evident that most of these fibers are not visible at 400×.

Figure 3 shows the aspect ratio frequency distribution of chrysotile fibers with widths greater than 0.4 μm and those that are visible at 400×, scaled so that the frequency of the modal class at 400× is equivalent to the frequency at 19 000×. The similarity in the distributions between the chrysotile greater than 0.4 μm and that visible at 400× reinforces the conclusion that the visibility of chrysotile at 400× on the TEM is comparable to the visibility of chrysotile by phase contrast microscopy.

Accurate assessment of the airborne fiber content in occupational settings where epidemiologic studies have shown a correlation between exposure to airborne fiber and incidence of asbestos-related diseases is essential for risk assessment and forms the basis for establishing acceptable exposure limits in occupational settings. If federal fibers other than asbestos are included in unequal proportions in different occupational settings, the reliability of the occupational exposure standard for all environments is suspect. Very few data are available on what proportion of a fiber count, as established by the membrane filter method, is composed of federal fibers that are *not* asbestos.[14] This study clearly indicates that for this mining environment, the proportion is large (54%); it would be inappropriate to use exposure data from this mine to assess risk in another environment where the proportion of asbestos is different.

Because the distributions of length, width, and aspect ratio of serpentinite rock fragments visible at 400× are so similar to the distributions visible at 19 000×, it is reasonable to assume that most serpentinite rock federal fibers that are visible at 19 000× would also be visible at 400×. Of the serpentinite rock federal fibers visible at 19 000×, 3% have widths less than 0.3 μm and none visible at 400× have widths this small, so the populations are clearly not identical. Nonetheless, the populations are similar enough that predictions based on the assumption that they are the same can be reasonably made. Accepting this assumption, the concentration in fibers per cubic centimeter of serpentinite rock federal fibers would be the same whether the filters were examined with low or high magnification. If an air filter from this mine were analyzed at 400× and the total fiber concentration were determined to be 1.0 f/cc, the proportion of serpentinite rock fragment, chrysotile, and composite particles would be 0.4, 0.3, and 0.3, respectively. If the same filter were examined at 19 000× and the concentration of serpentinite fragments would remain constant at 0.4 f/cc, the likely concentration of chrysotile would be 1.2 f/cc.

The proportions of chrysotile and rock fragment found on an air filter may vary greatly as a function of the environment. That the proportion of rock fragment will be considerably greater in a mining environment than in an industrial setting where a commercial asbestos product was applied is certainly reasonable; it may also vary from one mine to another. Not only will the amount of rock fragment meeting the dimensional criteria for a fiber as defined by the Occupational Safety and Health Administration (OSHA) vary from one mine to another, but the proportion of asbestos meeting these criteria may also vary. For example, the distribution of length and width of airborne chrysotile at the Lowell mine differs significantly from that at the chrysotile mines in Quebec as described by Gibbs and Hwang.[28] Therefore, these data cannot be applied directly to all other mining environments.

■ =CHRYSOTILE VISIBLE AT 400×

▥ =CHRYSOTILE FIBERS GREATER THAN 0.4-μm DIAMETER

FIGURE 3. Chrysotile asbestos aspect ratio distributions

These results do suggest that the proportion of federal fibers obtained by the standard PCM method that are actually asbestos may be lower in the chrysotile asbestos mining environment than that obtained in the commercial asbestos handling environments (i.e., textile, insulation). The quantitative risk assessments were calculated from these commercial asbestos environments; ultimately, the levels of permitted exposure in regulatory standards were established. OSHA, in its rulemaking deliberations on asbestos, stated that "There is some evidence that risks in asbestos mining and milling operations are lower than other industrial operations due to differences in fiber size." For this reason, the epidemiologic data from mining and milling operations were not considered.[29] These data show that the use of the PCM National Institute for Occupational Safety and Health 7400 method, which was developed from data taken in commercial asbestos handling environments for the purpose of providing an "index" of actual asbestos exposure, may not be valid in the mining environments. The use of the PCM method in mining environments can present a significant problem in determining true asbestos exposure levels. This problem must be addressed by using more sophisticated means of analysis such as TEM.

The fact that neither tremolite or actinolite were found among the airborne federal fibers from the Lowell chrysotile mine points up the need to determine the abundance of tremolite-asbestos throughout the chrysotile mining industry. These data indicate that tremolite may not contaminate all chrysotile deposits at measurable levels. Before tremolite-asbestos can be assumed to be the active agent in all chrysotile exposure, more data on its abundance are needed.
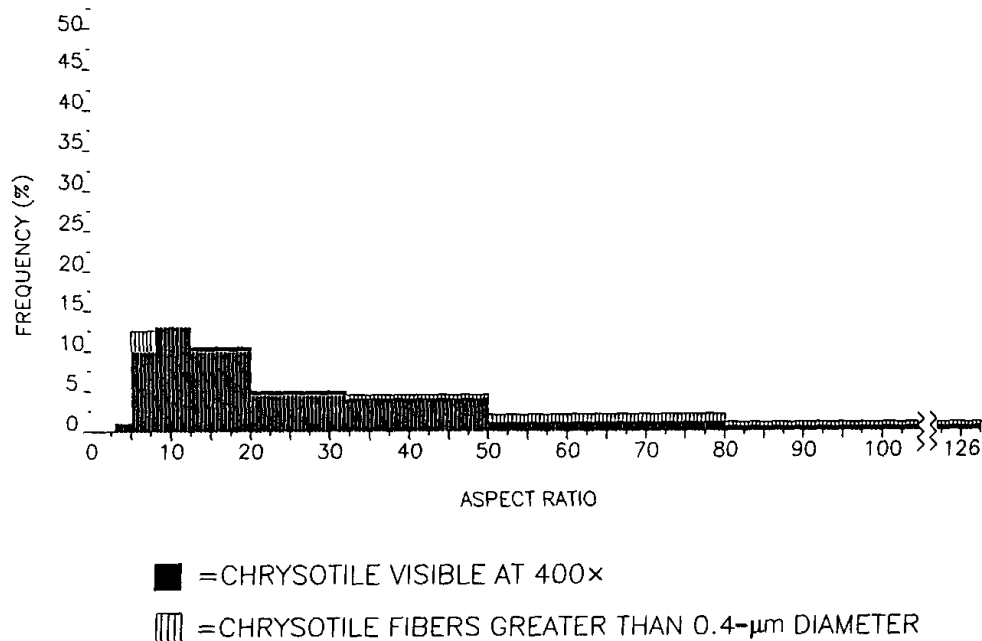
REFERENCES

1. United States Public Health Service/National Institute for Occupational Safety and Health: Membrane Filter Method for Evaluating Airborne Asbestos Fibers. DHEW (NIOSH) Technical Report Pub. No. 79-127. Cincinnati, Ohio: National Institute for Occupational Safety and Health, 1979.

2. McDonald, J.C.: Asbestos-Related Disease: An Epidemiological Review. In Biological Effects of Mineral Fibers. Vol. 2. IARC Scientific Publication Number 30. Geneva, Switzerland: International Agency for Research on Cancer, 1980. pp. 587–601.

3. Sebastien, P., J.C. McDonald, A.D. McDonald, B. Case, and R. Harley: Respiratory Cancer in Chrysotile Textile and Mining Industries: Exposure Inferences from Lung Analysis. Br. J. Ind. Med. 46:180–187 (1989).

4. Dement, J.M., R.L. Harris, Jr., M.J. Symons, and C. Shy: Exposures and Mortality among Chrysotile Asbestos Workers: Part II. Mortality. Am. J. Ind. Med. 4:421–434 (1983).

5. Selikoff, I.J., E.C. Hammond, and H. Seidman: Mortality Experience of Insulation Workers in the United States and Canada, 1943–1976. Ann. N.Y. Acad. Sci. 330:91–116 (1979).

6. Meurman, L.O., R. Kiviluoto, and M. Hakama: Mortality and Morbidity among the Working Population of Anthophyllite Asbestos Miners in Finland. Br. J. Ind. Med. 31:105–112 (1974).

7. Hobbs, M.S.T., S.D. Woodward, B. Murphy, A.W. Musk, and J.E. Elder: The Incidence of Pneumoconiosis, Mesothelioma and Other Respiratory Cancer in Men Engaged in Mining and Milling Crocidolite in Western Australia. In Biological Effects of Mineral Fibers. Vol. 2. IARC Scientific Publication November 30. Geneva, Switzerland: International Agency for Reasearch on Cancer, 1980. pp. 615–625.

8. Wagner, J.C., C.A. Sleggs, and P. Marchand: Diffuse Pleural Mesothelioma and Asbestos Exposure in the North Western Cape Province. Br. J. Ind. Med. 17:260–271 (1960).

9. **Health Effects Institute—Asbestos Research:** Asbestos in Public and Commercial Buildings: A Literature Review and Synthesis of Current Knowledge. Cambridge, Mass.: Health Effects Institute, 1991. pp. 6-4–6-7, 6-74–6-75.

10. **Churg, A. and B. Wiggs:** Fiber Size and Number in Workers Exposed to Processed Chrysotile Asbestos, Chrysotile Miners, and the General Population. *Am. J. Ind. Med. 9*:143–152 (1986).

11. **McConnochie, K., L. Simonato, P. Mavrides, P. Christofidis, F.D. Pooley, and J.C. Wagner:** Mesothelioma in Cyprus: The Role of Tremolite. *Thorax 42*:342–347 (1987).

12. **Addison, J. and L.S.T. Davies:** Analysis of Amphibole Asbestos in Chrysotile and Other Minerals. *Ann. Occup. Hyg. 34*:159–175 (1990).

13. **McDonald, J.C.:** Tremolite, Other Amphiboles, and Mesothelioma. *Am. J. Ind. Med. 14*:247–249 (1988).

14. **Cherrie, J., J. Addison, and J. Dodgson:** Comparative Studies of Airborne Asbestos in Occupational and Non-Occupational Environments Using Optical and Electron Microscope Techniques. In *Non-Occupational Exposure to Mineral Fibers*, edited by J. Bignon, J. Peto, and R. Saracci. IARC Scientific Publication Number 90. Geneva, Switzerland: International Agency for Research on Cancer, 1989. pp. 304–309.

15. **Lamarch, R.V. and P.H. Riordan:** Geology and Genesis of the Chrysotile Asbestos Deposits of Northern Appalachia. In *Geology of Asbestos Deposits*, edited by P.H. Riordon. New York: Society of Mining Engineers, 1981. pp. 11–25.

16. **United States Geological Survey:** *Bedrock Geology and Asbestos Deposits of the Upper Missisquoi Valley and Vicinity, Vermont.* USGS Bulletin 1122-B. Washington, D.C.: United States Geological Survey, 1963.

17. **Weill, H., J.L. Abraham, J.R. Balmes, B. Case, A.M. Churg, J. Hughes, M. Schenker, and P. Sebastien:** Health Effects of Tremolite. *Am. Rev. Respir. Dis. 142*:1453–1458 (1990).

18. **Churg, A.M., B. Wiggs, L. DePaoli, B. Kampe, and B. Stevens:** Lung Asbestos Content in Chrysotile Workers with Mesothelioma. *Am. Rev. Respir. Dis. 130*:1042–1045 (1984).

19. **Churg, A.M. and J.L. Wright:** Fibre Content of Lung in Amphibole and Chrysotile-Induced Mesothelioma Implications for Environmental Exposure. In *Non-Occupational Exposure to Mineral Fibers*, edited by J. Bignon, J. Peto, and R. Saracci. IARC Scientific Publication Number 90. Geneva, Switzerland: International Agency for Research on Cancer, 1989. pp. 314–318.

20. **McDonald, J.C. and A.D. McDonald:** "Asbestos and Carcinogenicity." Letter to Editor. *Science 249*:844 (1990).

21. "Asbestos Containing Materials in Schools, Final Rule and Notice." *Code of Federal Regulations* Title 40, Part 763. 1987. pp. 41826–41905.

22. **Dye, C.:** "Measurement Precision." June 1, 1989. [Private Conversation]. Chip Dye, AMA Analytical Services, 4475 Forbes Blvd., Lanham, MD 20706.

23. **Goodwin, A.:** "MSHA Fiber Identification Techniques." May 1988. [Private Conversation]. Aurel Goodwin, MSHA Safety and Health Technology Center, P.O. Box 25367, Denver Federal Center, Denver, CO 80225.

24. **Wylie, A., R. Virta, and E. Russek:** Characterizing and Discriminating Airborne Amphibole Cleavage Fragments and Amosite Fibers: Implications for the NIOSH Method. *Am. Ind. Hyg. Assoc. J. 46(4)*:197–201 (1985).

25. **Wylie, A.:** Testimony on the Regulation of the Non-Asbestiform Amphiboles Tremolite, Actinolite, and Anthophyllite. In *OSHA Public Hearings*, Docket H033d. Washington, D.C.: Government Printing Office, May 8, 1990.

26. **Lee, R.J.:** Testimony on the Regulation of the Non-Asbestiform Amphiboles Tremolite, Actinolite, and Anthophyllite. In *OSHA Public Hearings*, Docket H033d. Washington, D.C.: Government Printing Office, May 8, 1990.

27. **Lynch, J.R., H.E. Ayer, and D.L.O. Johnson:** The Interrelationship of Selected Asbestos Exposure Indices. *Am. Ind. Hyg. Assoc. J.: 31(5)*:598–604 (1970).

28. **Gibbs, G.W. and C.Y. Hwang:** Dimensions of Airborne Asbestos Fibers. In *Biological Effects of Mineral Fibers*, edited by J.C. Wagner and W. Davis. Vol. I. IARC Scientific Publication Number 30. Geneva, Switzerland: International Agency for Research on Cancer, 1980. pp. 69–78.

29. "Occupational Exposure to Asbestos, Tremolite, Anthophyllite, and Actinolite, Final Rule." *Code of Federal Regulations*, Title 29, Parts 1910 and 1926. 1986. p. 22637.

Relationship of Mineral Habit to Size Characteristics for Tremolite Cleavage Fragments and Fibers

By William J. Campbell, Eric B. Steel, Robert L. Virta, and Michael H. Eisner

UNITED STATES DEPARTMENT OF THE INTERIOR

CONTENTS

ILLUSTRATIONS

ii

TABLES

RELATIONSHIP OF MINERAL HABIT TO SIZE CHARACTERISTICS FOR TREMOLITE CLEAVAGE FRAGMENTS AND FIBERS

by

William J. Campbell, [1] Eric B. Steel, [2] Robert L. Virta, [2] and Michael H. Eisner [2]

ABSTRACT

This Bureau of Mines report describes a study conducted to determine the relationship of mineral habit to particle size and shape characteristics for prismatic, acicular, fibrous, and asbestiform varieties of tremolite. Particle measurements were made with the petrographic microscope at X 1,250 and the scanning electron microscope at magnifications up to X 10,000. All of the varieties of tremolite, upon Wiley milling, produced a significant percentage of particles that meet the Federal regulatory criteria for counting as asbestos fibers. However, only the asbestiform variety gave milled particles that fell into a size range of >10 um in length and <0.5 um in width; some medical scientists consider this range significant for production of adverse health effects.

INTRODUCTION

In September 1976 the Bureau of Mines established a Particulate Mineralogy Unit to assist local, State, and Federal agencies by establishing precise and workable mineral definitions and by developing improved methods of particulate identification and quantitative measurement (1).[3] Attention to adverse health effects associated with asbestos have been focused on occupational exposure in industries involved in the mining, milling, fabrication, and utilization of asbestos. Now there is increasing concern regarding the effects on industrial employees and the general public from long-term, low-level and short-term, high-level exposure to various elongate mineral particulates present as minor or major constituents in ores, crushed stone, and various industrial minerals. These particulates include both the more common and the asbestos varieties of serpentine and amphibole minerals.

---

[1] Supervisory research chemist.
[2] Geologist (mineralogy).
  All authors are with the Avondale Metallurgy Research Center, Bureau of Mines, Avondale, Md.
[3] Underlined numbers in parentheses refer to items in the list of references at the end of this report.

Asbestos regulatory procedures are based on counting elongated serpentine and amphibole mineral particles at 450 to 500 magnification using phase-contrast microscopy. To be counted as "regulatory," the silicate particles must meet the following size criteria: ≥ 5 um in length, ≤ 3 um in diameter, and an aspect ratio of ≥ 3 to 1. These elongate particles are generated by natural growth as fibers (for example, tremolite asbestos) or are produced as cleavage fragments by the crushing and grinding of the common nonasbestos varieties of the amphibole minerals. The present definition of a fiber used by the regulatory agencies does not distinguish between cleavage fragments and fibers produced by natural growth, and existing regulatory practices count all particles that meet the above criteria as equally hazardous. That is, a short-cleavage fragment of a nonasbestos variety amphibole 6 um long and 2 um wide is currently counted as being equivalent to an amphibole asbestos fiber 10 um in length and 0.1 um wide.

The principal objective of this study is to correlate the size characteristics of particles generated from grinding a typical amphibole mineral--tremolite--with the habit of the mineral. The second objective is to point out that amphibole minerals range in habit from common equant grains to the much rarer asbestiform variety. Regulatory personnel and health scientists should be aware of the strong dependence of particle size and shape characteristics on the mineral's original crystallization habit.

Studies on the biological effects of human and animal exposure to asbestos minerals do not fall within the mission of the Bureau of Mines. However, it is important that mineralogical identification-characterization procedures be applicable to health-related studies. The ultimate goal of all concerned groups--regulatory, medical, and industrial--is to distinguish between particles known to be hazardous and particles for which no adverse effects have been identified so that the workers and general public are protected properly and the domestic minerals industry is not subjected to unnecessary regulations. Measurement of the size characteristics of particles derived from different habits of the same mineral should assist medical scientists in evaluating the various types of elongate silicate particles (2).

PREVIOUS STUDIES

Stanton and Layard of the National Institutes of Health conducted extensive studies on tumor production in rats by introducing various types of particles in the pleural space and observing tumor production over a 2-year span (5). They concluded that implantation of long, thin, durable fibers resulted in tumors in a high percentage of the test animals, and that compositional variables such as trace metals and organics had a significantly lower, if any, effect on tumor probability. Stanton and Layard suggest there is a dimensional range of fibers that is related to tumor probability.

They tested seven durable fibrous materials, each of differing compositions and size characteristics. The order of probability of inducing pleural sarcomas with these test materials ranged from approximately 0 to 100 percent. Fibers of the size range of the International Union Against Cancer (UICC) asbestos standards fell in the 65- to 80-percent probability range. Linear

regression of the tumor probability versus size characteristics indicated that the size class with a diameter of ≤0.25 um and a length ≥8 um was the single variable that best correlated to sarcoma.[*] Histologic observations suggested that shorter and thicker particles are not as biologically active.

The relationship of fiber length and diameter characteristics to tumor formation has been the subject of extensive discussion in the occupational and environmental health sciences literature. For example, Wagner (6) states, "Fibers with a diameter below 0.5 um if injected into the pleural cavity will cause mesothelioma." Wright (7) comments that "Although the fibre diameter should be less than 1/2 um for tumors to develop also it appears that the fibre must be longer than 10 um." Davis (3) concluded that "the long fibre theory of asbestos pathogenesis and especially carcinogenicity does, at the present time, appear to be correct but the biochemical reasons why only long fibres should be dangerous are still obscure." Thus, there is agreement, at least among some medical scientists, that long, thin, durable fibers are essential for tumor production in test animals.

In this present study on size characteristics by the Bureau of Mines, emphasis was given to the number of particles in the following size range: length ≥10 um and diameter <0.5 um. Durable particles meeting these specifications would be classified as hazardous by most health researchers. There is also general interest in the relationship, if any, between the total number of regulatory particles and those meeting the above criteria for a long, thin fiber. Existing regulatory standards are based on the assumption that there is a constant distribution of asbestos particle sizes ranging from macroscopic to submicroscopic so that the counting methods can be limited to those readily visible by optical microscopy. Whether or not this relationship holds for nonasbestos particles is an important phase of this study.

CRYSTAL HABIT

The amphiboles, a common group of rock-forming minerals in the earth's crust, are found in many geologic settings. They crystallize in a wide variety of habits displayed in a progression from equant or equidimensional to fibrous (fig. 1); a detailed discussion on terminology is presented in Information Circular 8751 (1). All terms shown in figure 1 are general descriptive terms for the crystal habits of grains. There are gray areas between all of these terms; for example, an equant habit means approximately equidimensional, and the break between equant and elongate habits is not precise. However, these terms still have distinctly different meanings and apply to specific particle morphologies.

Traditionally, rock textures are described at a macroscopic or hand-sample level using the types of terms shown in figure 1. A change of

---

[*]Width rather than diameter is the correct terminology because amphibole particles are rectangular slabs rather than cylinders. The ratio of the width to the height in cross section ranges from approximately 2.5 to 1 to 10 to 1. In general, the amphibole particles are positioned on the slide or support with the widest dimension exposed to view.
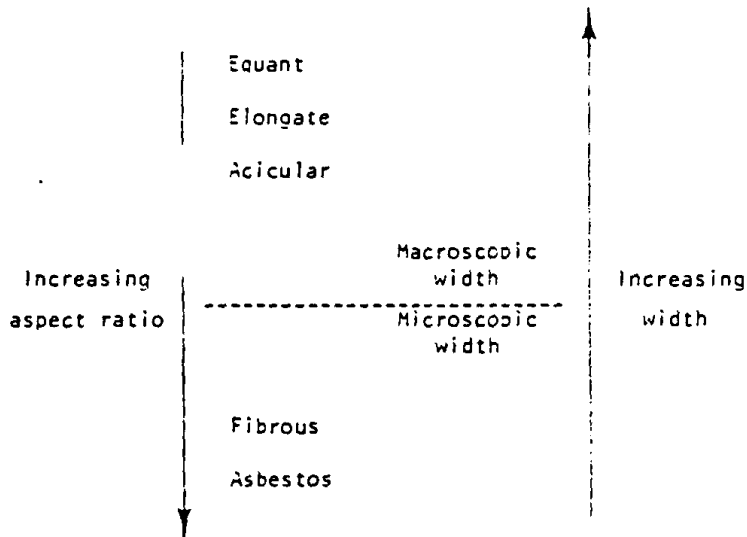
4

```
           Equant

           Elongate

           Acicular


                    Macroscopic
Increasing            width          Increasing
                -------------------
aspect ratio         Microscopic       width
                       width


           Fibrous

           Asbestos
```

FIGURE 1. - Examples of terminology used to describe grains
in hand samples. At some indefinite point be-
tween acicular and fibrous habits, the aggregate
of grains can still be seen with the unaided eye;
however, owing to their thinness the individual
grains become very difficult to observe without
magnification.

perspective occurs when going from observation with the unaided eye to the high magnifications of the light and electron microscopes. Grains that appear to be fibrous to the unaided eye obviously appear thicker using the microcope and, therefore, might be termed acicular or elongate. It is important to stress that the terms in figure 1 are primarily meant for hand-sample macroscopic examination, and their use becomes much less meaningful once the perspective is changed by using high magnification.

The term fibrous is used in a general mineralogical way to describe any aggregates of grains that crystallize in a needlelike habit and appear to be composed of fibers. The term "thin," as used in this report, means that the width of the grains is difficult to see with the unaided eye. In the terminology in figure 1, "fibrous" has a much more general meaning than "asbestos". While it is correct that all asbestos minerals are fibrous, not all minerals having a fibrous habit are asbestos. Asbestos has properties that make it unique and different from other fibrous minerals and even from other fibrous habits of the same amphibole. The asbestos minerals of commercial importance have the following characteristics:

1. Aspect ratios ranging upward to 1,000:1 or higher.

2. Very thin fibrils, generally less than 0.5 um in width.

3. Very high flexibility and tensile strength compared to nonasbestos minerals.

4. Parallel fiber growth in veins.

The classic crystal habit of asbestos includes all four of these properties. With the exception of mass fiber deposits, which have reticulated or random direction of fiber growth, all commercial asbestos has these crystal habit characteristics.
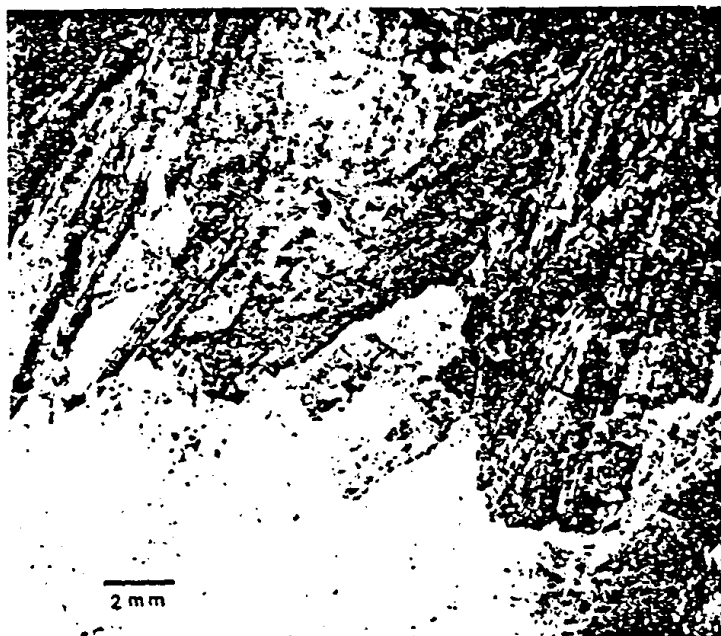
FIGURE 2. - Macrophotograph of prismatic tremolite showing the large euhedral grains in a medium-grained marble.

FIGURE 3. - Photomicrograph of thin section of prismatic tremolite under crossed nicols displaying cleavage traces within the very large grain of tremolite. Some calcite can be observed within the grain.

The large aspect ratio, very thin fibers and fibrils, flexibility, and tensile strength are the unique properties that make asbestos commercially valuable. However, there are variations in these properties from mineral to mineral, from deposit to deposit, and even within the same deposit. For instance, chrysotile does not have the tensile strength of crocidolite. The mass fiber chrysotile has shorter fibers than the other forms of "vein" chrysotile, and within a deposit the fiber lengths vary considerably. All of this variation takes place within the bounds of the characteristics of asbestos listed above. It is important to note that not all amphiboles have been found with asbestos habits; for instance, there is no verified occurrence of hornblende asbestos.

PETROGRAPHY OF SAMPLES

Samples were selected for this study to cover a wide range of crystallization habit from essentially equant grains to asbestiform. Where available, approximately monomineralic samples were used. The texture of the prismatic, acicular, fibrous, and asbestos tremolite-actinolite samples can be observed in the macrophotographs and the photomicrographs of thin sections included in this report. Light optical properties of the samples are listed in table 1.

TABLE 1. - Optical data for tremolite of various habits

Sample	Optical parameters				
	n_α	n_ε	n_γ	2V, degrees	Extinction angle, degrees
Prismatic.................	1.607	1.618	1.628	[1]87	19
Acicular..................	1.598	1.622	1.626	[2]84	18
Fibrous...................	1.616	1.630	1.638	[2]79	20
Tremolite asbestos 1......	1.612	1.628	1.638	[1]76	14
Tremolite asbestos 2......	1.612	1.628	1.638	[1]76	19
FD-72.....................	1.610	1.622	ND	ND	ND
FD-275....................	1.598	1.620	ND	ND	ND

ND Not determined.
[1]Calculated values.
[2]Measured values.

The sample in figure 2 from Adirondack, N.Y., is a coarse-grained prismatic tremolite in a medium-grained marble. The prismatic grains of tremolite are approximately 1 to 5 mm wide and 15 to 30 mm long. Prominent striations parallel to the long direction of the grains were observed. A thin section of the sample shows evidence of cleavage planes but no distinct grain boundaries (fig. 3). A few sections with crystals 2 to 3 mm wide and 10 to 15 mm long were picked out of the rock for grinding and subsequent size measurements.

The acicular amphibole sample (figs. 4-5) consists of subparallel crystals approximately 0.05 to 1 mm wide and 0.2 to 8 mm long, with the average grains being approximately 0.15 by 1 mm. Note that the width of most of the grains is visible with the unaided eye. The grains generally have tapering to pointed terminations. The specimen is listed by Ward's National Science Establishment, Rochester, N.Y.,[5] as tremolite even though the chemical composition varied considerably throughout the sample. The chemical composition, determined by the energy-dispersive X-ray spectrographic mode on the scanning electron microscope, varied over a wide range, including magnesium amphibole with a trace of calcium, magnesium-iron amphibole, and calcium-magnesium amphibole, and calcium-magnesium amphibole with a trace of iron. The optical data in table 1 for the acicular sample are only approximate because of the variations in composition. The elongate grains characteristic of the acicular habit are readily visible in the thin section (fig. 5). Although many of these grains have an aspect ratio of greater than 3 to 1 and exceed 5 um in length, these grains, if released intact during grinding, would not be regulatory particles because of their large width. Extensive preferential breakage parallel to the long dimension would be required to produce particles meeting the regulatory criterion for width.

---

[5]Reference to specific suppliers is made for identification only and does not imply endorsement by the Bureau of Mines.

FIGURE 4. - Macrophotograph of acicular amphibole.

FIGURE 5. - Photomicrograph of thin section of acicular amphibole under crossed nicols.

The fibrous tremolite (figs. 6-7) was collected from a rodingite vein in a Maryland serpentinite quarry. The grains range in orientation from random to subparallel and are approximately 0.7 um to 75 um wide and 50 um to 500 um long with an average grain being approximately 15 by 80 um. The width of these grains is not visible with the unaided eye; one can only see the masses or bundles of the individual fibers.

The tremolite asbestos samples (figs. 8-9) are composed of fiber bundles ranging from 30 mm to 100 mm in length and approximately 0.5 um to 10 um in width. Asbestos 1, from California, contains a minor amount of fine fibrous talc. Asbestos 2 is a museum sample collected in Rajasthan, India. Both samples are more brittle than the typical commercial asbestos, and neither consistently had the random orientation about the c-axis characteristic of amphibole asbestos.

Samples FD-72 and FD-275 were obtained as fine powders from William E. Smith, Fairleigh Dickinson University. Sample FD-275 was isolated from a sample of tremolite taken from a tremolitic talc ore body; asbestos variety tremolite was the source of FD-72 (4). The FD-72 tremolite was reported by Smith (4) to produce tumors in hamsters using intrapleural injection methods. In contrast, no tumors were observed in the hamsters injected with FD-275. Therefore, comparison of the particle size and shape characteristics of these

8

FIGURE 6. - Macrophotograph of fibrous (nonasbestos) tremolite.

FIGURE 7. - Photomicrograph of thin section of fibrous tremolite under crossed nicols showing the interlocking texture of the grains.

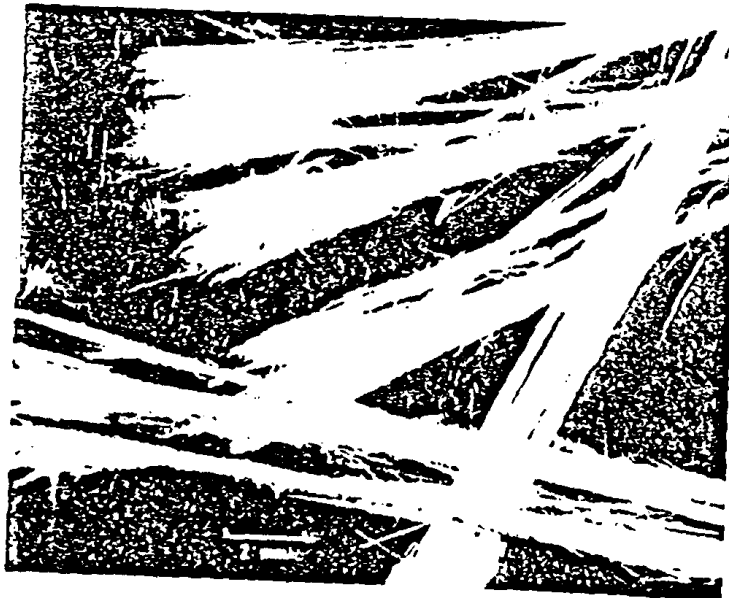FIGURE 8. - Macrophotograph of tremolite asbestos 1.

FIGURE 9. - Macrophotograph of tremolite asbestos 2.

10

FD samples with the particles derived from Wiley-milled tremolites of various habit may provide some insight into their relative biological activity. The UICC amosite standard was included in the scanning electron microscope studies in order to compare our size distribution measurements with published data; no significant differences were noted.[7]

CRUSHING AND GRINDING OF AMPHIBOLES

Important factors controlling the size and shape of amphibole particulates that may be released during mining and milling operations are the original crystal habit of the amphibole grains in the rock, the way in which these grains break or cleave, and the method of crushing. Breakage of asbestos fibrils and fiber bundles appears to be significantly different from that of the nonasbestos forms.

FIGURE 10. - Lengthwise splitting of amphibole grain to form two elongate particles.

In figure 10 a relatively blocky grain can be seen cleaving lengthwise along the {110} surface to form two elongate particles. This direction of cleavage competes with another direction of breakage or parting on the {001} or {10$\bar{1}$} surface (fig. 11) that is perpendicular to the long direction and produces particles that are shorter and more blocky. In the nonasbestos grains the probability of breaking in the long direction is somewhat higher than that of breaking in the short direction; therefore, elongate
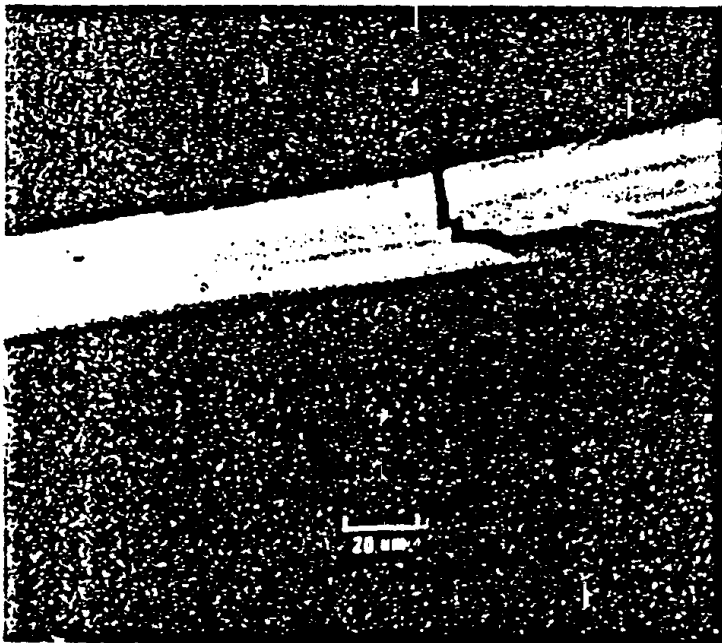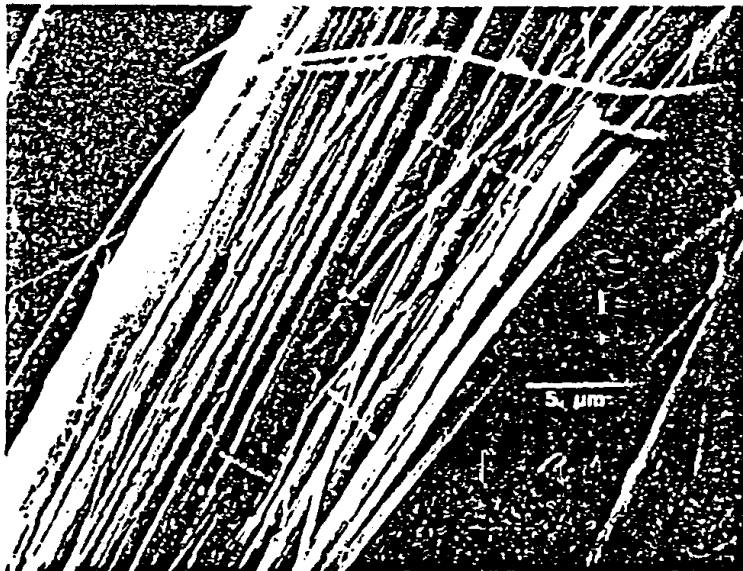

FIGURE 11. - Amphibole breaking perpendicular to the long axis to form two shorter, lower-aspect-ratio particles.

[7]UICC asbestos standards are available from Particle Information Services, P.O. Box 702, Grants Pass, Oreg. 97526.

particles with aspect ratios in the range of 3:1 to 10:1 are produced, together with a few particles of higher aspect ratio.

X 65

X 1,400

FIGURE 12. - Asbestos fiber bundle splitting into thinner, higher-aspect-ratio fibers.

With asbestos the probability of separating the fiber bundles to smaller bundles and to fibrils (see fig. 12) is one or more orders of magnitude greater than that of breakage in the short (perpendicular to the fiber axis) direction. Therefore, thin fiber bundles and fibrils are produced that have aspect ratios of several hundred to 1 and greater.

The next step in this study was to examine the size and characteristics of particles derived from crushing and grinding of tremolites of various habit. Ideally, occupational air samples representative of various mining and mineral processing operations would have been included, however; tremolites are present as trace, minor, or major constituents in talcs, quarry products, etc., rather than as a single mineral. Therefore, it was decided to limit these preliminary studies to essentially monominerallic samples.

To produce the desired particles, each of the tremolite-actinolite varieties (prismatic, acicular, fibrous, and asbestos) was ground by a single pass through a Wiley mill, and the ground samples that passed through a 20-mesh screen were collected. The other samples, FD-72, FD-275, and UICC amosite, were examined for particle size distribution as received.

MICROSCOPY

Sample Preparation

Grain mounts for the petrographic microscope were prepared by dispersing a small amount of each milled sample in an oil with a refractive index of 1.400 to obtain high contrast. Several mounts were prepared for each sample.

The sample preparation for scanning electron microscopy varied depending on the sample. The following procedure was used for asbestos 1, asbestos 2, prismatic tremolite, fibrous tremolite, and the UICC amosite. A small amount of sample was placed in a vial and then dispersed in distilled water to produce samples with little or no overlap of the particles. The vial was agitated by hand for 30 seconds, and then the larger grains were allowed to settle for 3 to 5 seconds. Approximately 1 ml of solution was withdrawn from the vial and several drops were placed onto carbon-coated scanning electron microscope stubs. These stubs were heated to ~95° C to evaporate the water, and then the sample was carbon-coated.

The acicular amphibole and the two FD samples were prepared for counting by the following method. A small amount of sample was placed in a vial and dispersed in water. The acicular amphibole was agitated by hand for 30 seconds, and the larger grains were allowed to settle for 3 to 5 seconds. About 1 ml of solution was withdrawn from the vial and mixed with about 20 ml of water in the funnel apparatus for the nuclepore filters. The solution then was filtered through the 0.1-um nuclepore filter. A section of the filter was cut out, mounted on scanning electron microscope stubs, and copper-coated.

The FD-72 and FD-275 samples were prepared similarly except that instead of using hand agitation, it was necessary to place the samples in a low-energy ultrasonic bath for 1 to 3 minutes to disperse the samples.

Particle Counting

Field of view counts were made at X 1,250 with the petrographic microscope. All particles with one dimension of 1 um or greater were counted. Emphasis was given to counting only those particles identified petrographically as tremolite-actinolite.

Counting was performed on the scanning electron microscope by first randomly selecting an area on the tab at low magnifications (~X 100) and then increasing the magnification to X 500, X 1,000, or X 2,000. This region was photographed, and all particles in the field of view or intersecting only the top and left side of the field of view were counted. The magnification used to define the field of view varied according to the size distribution of the samples; for the asbestos samples the field of view was defined at X 500, and for the FD-72 it was X 2,000. The particles were sized using a scale calibrated with 0.1-um latex spheres at magnifications ranging from X 500 to X 20,000. On each scanning electron microscope stub several fields of view were counted on the center and edges of the stubs.

Size Characteristics

The primary objective of this study was to correlate the size characteristics of the ground tremolites with the habit of the mineral. The number of long, thin particles (>10 um long, <0.5 um wide) in each of the milled samples was of particular interest.

The wide variation in size characteristics is qualitatively obvious in the photomicrographs and scanning electron micrographs for each of the samples (figs. 13-20). Size characteristics are presented in a more quantitative format in table 2. These data represent size measurements on 200 to 400 particles for each sample; for ease of comparison, all data were normalized to 200 particles. All particles with one dimension greater than 1 um were counted. The particles were placed in six classes--a nonregulatory group, and five groups of increasing aspect ratio that meet the regulatory size criteria. Differences in the data in table 2 for the petrographic microscope and the scanning electron microscope are primarily a reflection of the range of magnification available with the two techniques together with some variations in the sample preparation. Also the measurement error using optical microscopy becomes significant for particles less than 0.5 to 1 um wide. In general, a larger percentage of smaller particles is counted in the electron microscope. Because of the very limited number of particles measured for each sample, the results should be considered as semiquantitative; however, the conclusions derived from this study are not expected to change significantly with more data.

TABLE 2. - Aspect ratio of particles from milled tremolites of various habits

	Aspect ratio range					
	NR[1]	3:1 to 5:1	>5:1 to 10:1	>10:1 to 20:1	>20:1 to 50:1	>50:1
NUMBER OF PARTICLES USING PETROGRAPHIC MICROSCOPY[2]						
Prismatic............	174	13	10	2	1	0
Acicular[3]...........	173	8	12	6	1	0
Fibrous..............	114	37	37	11	1	0
Asbestos 1...........	97	13	26	27	27	10
Asbestos 2...........	107	7	29	24	26	7
FD-72................	142	10	25	14	3	1
FD-275...............	192	4	4	0	0	0
NUMBER OF PARTICLES USING SCANNING ELECTRON MICROSCOPY[4]						
Prismatic............	147	27	20	5	0	1
Acicular[3]...........	187	7	3	1	1	1
Fibrous..............	138	30	25	7	0	0
Asbestos 1...........	78	18	27	34	35	8
Asbestos 2...........	90	4	18	28	33	27
FD-72................	166	9	6	8	9	2
FD-275...............	195	1	3	1	0	0
UICC amosite[5]......	138	2	10	21	21	8

[1]NR designates nonregulatory particles that do not meet the length ≥ 5 um, width ≤ 3 um, and aspect ratio ≥ 3 criteria.

[2]Size measurements on 200 particles at X 1,250 with petrographic microscope.

[3]Low-calcium amphibole.

[4]Size measurements of 200 particles with scanning electron microscope. Magnification up to X 50,000 was used where necessary to measure small-diameter particles.

[5]UICC standards were prepared in South Africa by attrition grinding. This grinding was more extensive than used by the Bureau on asbestos 1 and asbestos 2.

14

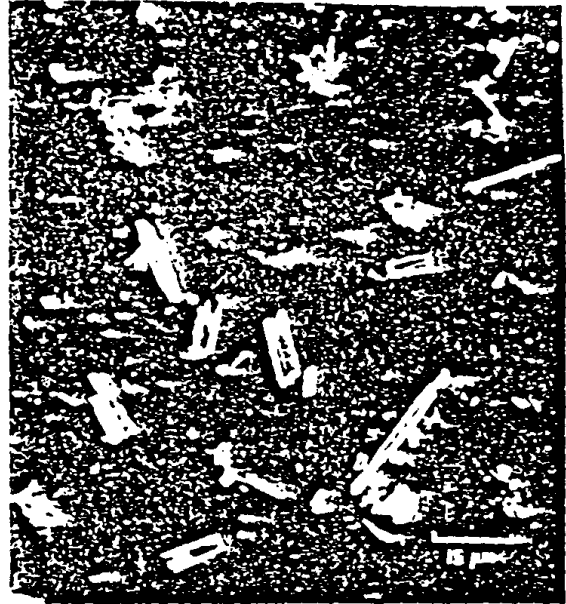FIGURE 13. - Photomicrograph of particles from Wiley-milled prismatic tremolite.

FIGURE 14. - Scanning electron micrograph of particles from Wiley-milled acicular amphibole.

FIGURE 15. - Photomicrograph of particles from Wiley-milled fibrous tremolite.
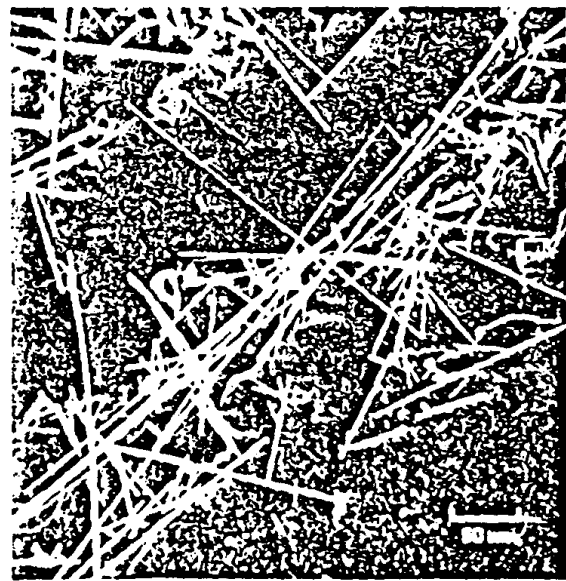

FIGURE 16. - Scanning electron micrograph of particles from Wiley-milled tremolite asbestos 1.
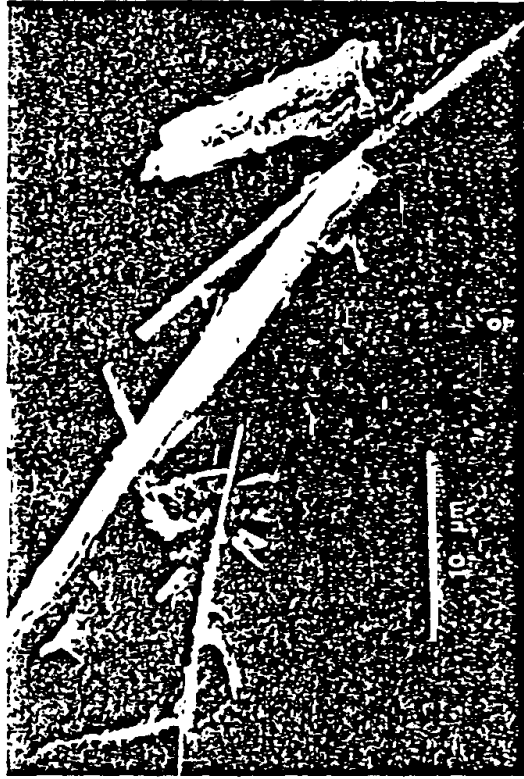
FIGURE 18. - Scanning electron micrograph of FD-72 particles.

FIGURE 20. - Scanning electron micrograph of UICC amosite particles.

FIGURE 17. - Photomicrograph of particles from Wiley-milled asbestos 2.

FIGURE 19. - Scanning electron micrograph of FD-275 particles.

The important feature of the data in table 2 is the very small number of particles with an aspect ratio ≥20 for the prismatic, acicular, fibrous, and FD-275 samples. In contrast, there is a significant percentage of particles with high aspect ratios for asbestos 1 and 2, FD-72, and UICC amosite. This type of size distribution is, as anticipated, directly related to the crystal habit of the samples prior to grinding.

The size characteristics of the samples are organized in a different format in table 3. For this table, particles longer than 10 um that also met the regulatory criteria were placed in three groupings, depending on the width of the particle. For the prismatic, acicular, and fibrous samples, zero to three particles (based on 200 particles) fell in the 0.5- to 0.99-um-width group, and no particles were found in the <0.5-um-width class. In contrast, asbestos 1 and 2, FD-72, and UICC amosite had a large number of long particles in the width ranges 0.5 um to 0.99 um and in the critical width range of <0.5 um. It should be emphasized that the UICC amosite had been subjected to significantly more severe grinding than the asbestos 1 and 2 samples; therefore, no comparison should be made of the size distributions between the two tremolite asbestos samples and UICC amosite.

TABLE 3. - Classification by width of tremolite particles
≥10 um in length

	Width, um		
	0.1-0.49	0.5-0.99	1-3
NUMBER OF PARTICLES USING PETROGRAPHIC MICROSCOPY[1]			
Prismatic......................	0	1	4
Acicular[2].....................	0	3	8
Fibrous........................	0	1	26
Asbestos 1.....................	8	11	23
Asbestos 2.....................	14	12	42
FD-72..........................	3	5	10
FD-275.........................	0	0	2
NUMBER OF PARTICLES USING SCANNING ELECTRON MICROSCOPY[3]			
Prismatic......................	0	1	20
Acicular[2].....................	0	1	3
Fibrous........................	0	0	21
Asbestos 1.....................	3	21	59
Asbestos 2.....................	10	16	51
FD-72..........................	4	5	6
FD-275.........................	0	0	0
UICC amosite...................	6	15	10

[1]Data normalized to 200 particles measured at X 1,250
with petrographic microscope.

[2]Low-calcium amphibole.

[3]Data normalized to 200 particles measured with scanning
electron microscope. Magnification up to X 50,000 was
used when necessary to measure particles of small
width.

SUMMARY

Based on this limited study, there is a relationship between the number of particles of "critical" dimensions, ≥10 um in length and ≤0.5 um in width, and the habit of the tremolite-actinolite prior to grinding. Although all the Wiley-milled tremolites (prismatic, acicular, fibrous, and asbestos) have a significant percentage of particles meeting the current regulatory asbestos criteria, only the asbestos variety gave long, thin particles of the dimensions established by some medical scientists as necessary to produce adverse biological effects in laboratory animals.

The asbestos regulatory counting criteria were established for air sampling in an occupational environment where commercial asbestos was being mined, milled, fabricated, or installed. Under these restricted conditions, the assumption probably is valid that, for each occupational setting and type of asbestos, there is a relatively constant distribution of particle sizes and shapes, ranging from macroscopic to particles below the limit of resolution of the optical microscope. On that basis, measurement of elongate particles at X 450 reflects the presence of a certain percentage of fibers longer than 10 um and less than 0.25 to 0.50 um wide. Particles from Wiley-milled tremolite asbestos exhibit a continuum of particle size ranging from very thin to medium width, resulting in some particles with aspect ratios of 100 or greater. In contrast, particles derived from the nonasbestos varieties are skewed toward thicker particles, and the distribution is characterized by the absence of long, thin particles of high aspect ratio.

The existing asbestos regulatory criteria have had an increasingly negative impact on the nonasbestos mining and mineral-processing industries. These criteria equate all particles meeting the regulatory dimensions as equally harmful, whereas there is a significant body of data indicating that only the particles having critical dimensions produce adverse effects in test animals. With minor exceptions, all of the epidemiology and most of the laboratory studies on test animals relate to exposure to commercial asbestos (chrysotile, crocidolite, "amosite," and anthophyllite asbestos). There are no comparable data on exposure to cleavage fragments of the common amphibole minerals found in many mineral-processing industries such as crushed stone quarries and gold and talc operations; currently these operations are being subjected to the same criteria as applied to the mining and milling of commercial asbestos. In consideration of the dual need to establish effective environmental and occupational controls to safeguard the population and the worker, and to avoid unnecessary economic impact on the domestic minerals industry, it is recommended that appropriate experiments be conducted to obtain conclusive data as to the relative effects of the various size particles. The key question to be resolved is the relative biological effect of elongate particles 1 to 3 um wide as compared to particles of the same length that are less than 0.5 um wide.

REFERENCES

1. Campbell, W. J., R. L. Blake, L. L. Brown, E. E. Cather, and J. J. Sjoberg. Selected Silicate Minerals and Their Asbestiform Varieties: Mineralogical Definitions and Identification-Characterization. BuMines IC 8751, 1977, 56 pp.

2. Campbell, W. J., E. B. Steel, R. L. Virta, and M. H. Eisner. Characterization of Cleavage Fragments and Asbestiform Amphibole Particulates. Proc. Soc. for Occupational and Environmental Health, Symp. on Occupational Exposures to Fibrous and Particulate Dust and Their Extension Into the Environment, Washington, D.C., Dec. 4-7, 1977 (pub. as Dust and Disease).

3. Davis, J. M. G. Current Concepts in Asbestos Fibre Pathogenicity. Proc. Soc. for Occupational and Environmental Health, Symp. on Occupational Exposure to Fibrous and Particulate Dust and Their Extension Into the Environment, Washington, D.C., Dec. 4-7, 1977 (pub. as Dust and Disease).

4. Smith, W. E., D. D. Hubert, H. J. Sobel, and E. Marquet. Biologic Tests of Tremolite in Hamsters. Proc. Soc. for Occupational and Environmental Health, Symp. on Occupational Exposure to Fibrous and Particulate Dust and Their Extension Into the Environment, Washington, D.C., Dec. 4-7, 1977 (pub. as Dust and Disease).

5. Stanton, M. F., and M. Layard. The Carcinogenicity of Fibrous Minerals. Workshop on Asbestos: Definitions and Measurement Methods. National Bureau of Standards Spec. Tech. Pub. 506, Nov., 1978, pp. 143-151.

6. Wagner, J. C. Comments in "Fibres for Biological Experiments," ed. by P. V. Pelnar. 1974, p. 10; available from Institute of Occupational and Environmental Health, Montreal, Quebec, Canada.

7. Wright, G. W. Comments in "Fibres for Biological Experiments," ed. by P. V. Pelnar. 1974, p. 11; available from Institute of Occupational and Environmental Health, Montreal, Quebec, Canada.

Relationship between the growth habit of asbestos and the dimensions of asbestos fibers

A.G. Wylie

Abstract — *The dimensions and shape of both airborne and bulk amphibole-asbestos fibers are different from those of both airborne and bulk of cleavage fragments of the amphiboles. These differences are related to the mineralogical properties unique to the habit of asbestos, including the fibrillar structure, small fibril widths and distinctive crystallographic faces of fibrils. Criteria for distinguishing amphibole cleavage fragments from amphibole-asbestos include mineralogical properties observable in bulk samples and the dimensions of particles collected on air filters. It would be very helpful to the mining and mineral industry if these properties were recognized in the regulation of asbestos.*

Introduction

Asbestos is a term applied to a group of highly fibrous silicate minerals that readily separate into long, thin, strong fibers of sufficient flexibility to be woven, are heat resistant and chemically inert, and possess a high electrical insulation and, therefore, are suitable for uses where incombustible, nonconducting or chemically resistant material is required (Gary et al., 1974).

Heat resistance, chemical inertia and high electrical insulation are properties of almost all silicates. Therefore, they are not unique to asbestos. However, long, thin, strong flexible fibers are limited almost exclusively to asbestos and are the properties that made the use of asbestos in building materials so widespread.

Nonetheless, in the regulation of asbestos, the federal government, and many state and local governments following the federal government's lead, define asbestos as anyone of six minerals: chrysotile, crocidolite (riebeckite), amosite (grunerite or cummingtonite), tremolite, actinolite, and anthophyllite. Further, asbestos is regulated on the exposure to or content of particles that are longer than 5 μm and have aspect ratios (length:width) of 3:1 or greater. This has the effect of making cleavage fragments of any of these minerals into asbestos fibers.

This paper will describe the mineralogical characteristics of asbestos and the shape of both airborne and bulk asbestos particles. The properties and dimensions relate to the habit of asbestos, distinguish asbestos from the more common varieties of the same silicate minerals, and could provide a basis for the regulation of asbestos without the inclusion of cleavage fragments for which no carcinogenic potential has been established.

A.G. Wylie is associate professor, Department of Geology, College Park Campus, University of Maryland, College Park, MD. SME preprint 88-85, SME-AIME Annual Meeting, Phoenix, AZ. Manuscript October 1987. Discussion of this paper must be submitted, in duplicate, prior to Feb. 28, 1989.

Mineralogical properties of asbestos

Chemical composition and atomic structure

In modern times, only four minerals have been mined as asbestos on a large scale: anthophyllite-asbestos $(Mg_7Si_8O_{22}(OH)_2)$; grunerite-asbestos (amosite) $((Fe,Mg)_7Si_8O_{22}(OH)_2))$; riebeckite-asbestos (crocidolite) $(Na_2Fe_5Si_8O_{22}(OH)_2$; and chrysotile $(Mg_3Si_2O_5(OH)_4)$. In earlier times, actinolite-asbestos $(Ca_2(Fe,Mg)_5Si_8O_{22}(OH)_2)$ and tremolite-asbestos $(Ca_2(Mg,Fe)_5Si_8O_{22}(OH)_2)$ have been used locally. Other minerals, including arfvedsonite (Deer et al., 1962), potassian winchite (Wylie and Huggins, 1980) and richterite (Malyshonok et al., 1986), talc, and erionite, may occasionally occur in an asbestiform habit.

All of the major types of asbestos, except chrysotile, have essentially the same atomic structure and, because of it, are known as amphiboles. Amphiboles have a double chain of SiO_4-4 tetrahedra as their basic building block. Amphibole asbestos fibers are elongated parallel to the double chain. Chrysotile is a sheet silicate, so-called because its basic structural unit is a sheet of connected SiO_4-4 tetrahedra. Rolling up of the sheet forms its fibers.

Fibrillar structure

Asbestos of all types is composed of bundles of individual fibrils. These fibrils vary in size among the different asbestos types and occurrences. South African and Australian crocidolite have fibrils that range in width from about 500 to 2000 A. Grunerite-asbestos (amosite) from South Africa ranges from about 2000-6000 A and chrysotile fibrils from most localities range from about 200 to 500 A in width.

These fibrils share a common axis of elongation but are randomly oriented with respect to the other crystallographic directions. There have been reports of other minerals forming between these fibrils (talc, brucite), but generally asbestos fibers are monomineralic. The fibrils are held together by weak bonds and are easily separated by gentle pressure of the hand. Separation of the fibrils in this manner is not cleavage; no structural bonds are broken.

The fibrillar structure of asbestos hinders the use of single crystal X-ray techniques to study it. Instead of producing a pattern of spots, which can be interpreted to determine symmetry and structure, an asbestos fiber with a diameter of about 0.1 mm (0.004 in.) will produce a pattern consisting of lines derived from spot patterns of thousands of individual fibrils that share only one crystallographic axis in common. For many years, the inability to study asbestos by classical X-ray techniques left the determination of symmetry to the optical properties (which also are affected by the fibrillar structure)

and the common amphibole-asbestoses crocidolite and amosite were thought to be orthorhombic rather than monoclinic, which they are now known to be.

Monoclinic amphiboles exhibit the property of oblique extinction when viewed under the petrographic microscope. This property arises because the principal optic directions (X, Y, and Z) are not parallel to the principal crystallographic axes (a, b, and c). It is found in minerals that belong to the monoclinic and triclinic crystal systems, but is lacking in minerals that are orthorhombic, hexagonal, or tetragonal.

Minerals of the latter group exhibit parallel extinction. However, all types of asbestos exhibit parallel extinction, regardless of the crystal system to which they belong. This is because the individual fibrils are generally smaller than the resolution of the light microscope and their properties cannot be examined individually. Instead, a group is always observed.

In some samples of asbestos, some individual fibrils approach 1 μm in width. These fibrils are individually resolvable by light microscopy and should show the properties characteristic of the crystal system to which they belong. In some specimens they do, but in others, they do not. Amosite, for example, has fibrils that approach 5000A. These are large enough to be seen optically. However, they always exhibit anomalous parallel extinction. {100} twinning is very common in amphibole asbestos, and if pervasive, could account for this anomalous behavior (Wylie, 1979).

The parallel extinction of chrysotile arises because of the tubular structure of the fibrils. While chrysotile also occurs in fiber bundles, even if the fibrils were singular and large enough to be viewed optically, this structure would preclude oblique extinction even though chrysotile is monoclinic.

Tensile strength

The high tensile strength of asbestos is clearly related to the fibrillar structure. Asbestos has a 10- to 30-fold increase in tensile strength over nonasbestos forms of the same mineral. In the case of the amphiboles, the tensile strength varies inversely with the size of the fibril cross section (Zoltai, 1984; Sinclair, 1959). This means that the tensile strength of South African crocidolite is greater than that of the South African amosite, which, in turn has a tensile strength greater than Finnish anthophyllite.

Zoltai (1984) suggested that the high tensile strength is related to the surface structure of the fibrils as well as to their size. Under the scanning electron microscope, the surface of asbestos fibers are very smooth (Dorling and Zussman, 1987). They lack cracks and other imperfection that contribute to a decrease in the ideal tensile strength.

By contrast, cleaved fragments of the same mineral always have rough, irregular surfaces. While direct comparisons of tensile strength between cleavage fragments and fibers of the same width have never been made, the surface structure theory of tensile strength predicts higher tensile strength for smooth-surfaced fibers. .

Crystal forms

Cleavage in amphiboles takes place along the {110} surfaces ({210} in the orthoamphiboles). Therefore, most amphibole particles that have been cleaved are bounded by these surfaces. However, some amphiboles may also exhibit parting along {100} and/or {010}. Parting in common amphiboles is not usually well developed. So, amphibole cleavage frag-

ments are bounded by parting surfaces only rarely.

By contrast, amphibole asbestos fibrils are frequently bounded by {100} and {010} in addition to {110} faces with {100} being the most well developed (Harlow et al., 1984). These are dominantly crystal faces formed during the growth of the fibers, not cleavage surfaces, although parting developed along {100} twinning surfaces may contribute to the dominance of the {100} surface in some samples.

In amphiboles, the {110} surfaces meet at 120° angles. Furthermore, all {110} surfaces are equally likely to develop. Therefore, particles bounded by {110} cleavage planes will have cross sections that approximate a diamond shape: a parallelogram with internal angles of 120° and 60°.

By contrast, {100} and {010} surfaces are not equivalent in the amphiboles. The {100} surfaces are generally larger, and the cross sectional shape of amphibole particles bounded by {100} and {010} will be rectangles with a width to thickness ratio of between two and three (Wylie et al., 1982).

Size and shape of asbestos fibers

Bulk samples

Length, width, and aspect ratio distributions of populations of bulk samples of many types of asbestos have been determined (Campbell et al., 1980; Siegrist and Wylie, 1980; Shedd, 1985; Stanton et al., 1981). To some extent, the dimensional characteristics of these populations depend on the sample preparation techniques, primarily the degree of grinding. However, except under the most extreme conditions, when grinding has been so prolonged that the particles are reduced to nearly equidimensional masses, certain characteristics of asbestos are retained.

Sample preparation disaggregates asbestos fibers and, to a greater or lesser degree, separates individual fibrils. Because the cross sectional dimension of a fibril is established during the formation of asbestos, it cannot be easily altered. However, width distributions of asbestos are affected by the instrumentation used to measure this dimension (width is defined as the size of the fiber perpendicular to the direction of elongation). Studies done on TEM emphasize the distribution of the smaller fibrils, while studies based on scanning electron microscopy (SEM) often overlook the smallest fibrils. Studies done on the same instrument, however, produce width distribution that are comparable.

Another dimensional characteristic that is normally unaffected by sample preparation is the relationship between width and length. The width of an asbestos fiber is essential independent of its length (Siegrist and Wylie, 1980). Small widths are characteristic of both long and short fibers. This behavior contrasts sharply with that of cleavage fragments. For populations of cleavage fragments, as the length of a particle increases, so does its width.

Aspect ratio (length/width) has been used frequently to characterize asbestos. However, to be used effectively, aspect ratio comparisons must be restricted to particular ranges in length. For example, Table 1 gives the mean aspect ratio for particles with a length of 5 μm and 10 μm. The samples used in this and other tables were prepared or collected in a variety of different ways. The details of collection and preparation are provided in the references.

Despite the differences in sample preparation and collection, the contrast between all samples of asbestos and cleavage fragments is striking. For both, the aspect ratio is greater for 10 μm particles than for 5 μm particles, but the effect is much

more pronounced in asbestos populations. This is because there is very little difference between the width of 10 μm fibers and 5 μm fibers because the width of asbestos is established during growth, and the width is independent of the length. Therefore, there is a marked increase in aspect ratio as length increases. For cleavage fragments, on the other hand, longer particles have wider widths so the increase in aspect ratio is minimal.

Table 1 — Mean Aspect Ratios of 5 μm and 10 μm Asbestos Fibers and Amphibole Cleavage Fragments

	Mean Aspect Ratio Length	
Asbestos	5 μm	10 μm
amosite - Transvaal South Africa[1]	13	24
crocidolite - Kurman Hills South Africa[1]	24	40
crocidolite - Cape Province South Africa[2]	42	66
crocidolite - Australia[3]	35	56
actinolite-asbestos - South Africa[3]	13	27
tremolite-asbestos - India[3]	8	13
Cleavage Fragments		
tremolite - New York[1]	3	5
actinolite - Virginia[4]	4	5
riebeckite - Colorado[3]	4	5
grunerite - Minnesota[4]	5	6
cummingtonite - South Dakota[4]	4	7

Collection, preparation and characterization are described in the following:

[1]Campbell et al., 1980 (bulk samples)
[2]Shedd, 1986 (bulk samples)
[3]Wylie and Schweitzer, 1982 (bulk samples)
[4]Wylie et al., 1985 (airborne particles)

Table 2 presents dimensional data from bulk samples of asbestos and cleavage fragments. Two of the four cleavage fragment populations are not amphibole and would not be regulated as asbestos, although wollastonite is occasionally marketed as asbestos substitute. The high proportion of asbestos fibers with widths less than 0.5 μm reflects the growth of fibrils with the lower percentages found in samples with larger average fibril width. Among these samples, chrysotile has the smallest fibril and amosite and tremolite-asbestos the largest. Due to their small widths, virtually all of the asbestos particles have aspect ratios in excess of 10:1 (fibers longer than 5 μm). While there are some high aspect ratio cleavage fragments, most have aspect ratios less than 10:1, and less than 6% of any population of cleavage fragments have both aspect ratios in excess of 10:1 and widths less than 0.5 μm.

Airborne samples

Dimensions have been used as the basis for identifying and counting asbestos collected on air filters in occupational settings for many years. However, the dimensions that have been used (longer than 5 μm with aspect ratios greater than or equal to three to one) have very little relevance to the actual dimensions and shape of asbestos fibers. In certain occupational settings (the asbestos textile industry), this presents no problem to the accurate assessment of the quantity of asbestos in the air. In the mining and mineral industries (other than asbestos mining), however, mineral particulates can be mistakenly classified as asbestos under this definition. The problem is particularly acute when minerals that can occur as asbestos in some localities are also found in forms other than asbestos, e.g., the amphiboles.

The dimensions of airborne fibers of asbestos differ very little from the dimensions of bulk samples. There is a slightly narrower range in the width of the fibers and the extremely long fibers (greater than 500 μm) rarely become airborne. However, comparison with airborne particles of ordinary amphiboles, airborne asbestos fibers are quite distinctive. The longest particles reported from airborne amphibole cleavage fragment populations are generally less than 20 μm, while fibers of greater than 100 μm may be routinely found in airborne asbestos populations. However, the distinction between asbestos and cleavage fragments is most obvious when aspect ratio distributions are compared.

Two comprehensive studies examine in detail the size distributions of airborne asbestos. They are studies of Gibbs and Hwang (1980) and Pooley and Clarke (1980). Table 3 presents their data in terms of aspect ratio distributions. All 5μm particles have aspect ratios in excess 10:1 and greater than 50% have aspect ratios greater than 20:1 Similar data from published studies of the size distributions of airborne cleavage fragments are presented in Table 4. Among this population, 20:1 particles are extremely rare.

Table 5 presents the aspect ratio distribution of airborne asbestos fibers and airborne cleavage fragments that are longer than 5 μm and have widths greater than or equal to 0.25 μm. These are particles that should be visible by the phase contrast method for analyzing air filters (Leidel et al., 1979). While a small proportion of the total asbestos fiber is visible using optical microscopy rather than electron microscopy (column (a) in Table 6 vs. column (a) in Table 3), the prevalence of high aspect ratio remains unchanged. For airborne cleavage fragments longer than 5 μm, the additional constraint of widths greater than or equal to 0.25 μm has no effect on the aspect ratio distribution or in the proportion of airborne fiber included in this category. Essentially all airborne cleavage fragments longer than 5 μm have widths greater than 0.25 μm and are visible by optical microscopy.

Table 2 — SEM Characterization of Bulk Samples of Asbestos and Cleavage Fragments

	(a) % longer than 5 μm	(b) % of (a) with widths < 1.0 μm	(c) % of (a) with widths < 0.5 μm	(d) % of (a) with aspect ratio greater than 3:1	(e) % of (a) with aspect ratio greater than 10:1	(f) % of (a) with aspect ratio greater than 15:1	(g) % of (a) with aspect ratio greater than 20:1
A. Asbestos							
crocidolite - South Africa[1]	48	98	85	100	99	95	89
amosite - South Africa[1]	73	91	50	100	98	84	75
chrysotile - Quebec[1]	38	99	94	100	100	98	96
chrysotile - California[1]	54	98	94	100	99	97	94
actinolite-asbestos - South Africa[2]	10	96	70	100	86	70	52
tremolite-asbestos - Libby, MT[3]	43	87	54	100	88	70	52
B. Cleavage Fragments							
tremolite - New York[1]	30	7	1	47	3	2	2
riebeckite - California[2]	50	27	5	78	35	21	12
antigorite and talc - New York[1]	15	0	0	32	4	0	0
Wollastonite - New York[3]	22	22	6	82	20	9	4

Collection, Preparation and Characterization of the Samples are Described in the Following:

[1]Campbell, et al., 1980
[2]Wylie and Schweitzer, 1982
[3]Atkinson et al., 1982

Table 3 — Aspect Ratio Distributions of Airborne Asbestos Fiber, All Widths

	(a) % of total airborne fiber longer than 5 μm	(b) % of (a) with aspect ratio >3:1	(c) % of (a) with aspect ratio >10:1	(d) $ of (a) with aspect ratio >15:1	(e) % of (a) with aspect ratio >20:1
crocidolite[1]					
mining	4.1	100	100	98	93
bagging	7.1	100	100	99	96
amosite[1]					
mining	12.7	100	100	92	70
bagging	24.6	100	100	93	73
chrysotile[1]					
mining	1.3	100	100	90	62
bagging	4.2	100	100	95	79
crocidolite[2][3]	10.60	100	100	96	89
amosite[2][3]	25.20	100	100	88	75
Asbestos in lung tissue					
crocidolite[2][3]		100	100	98	95
amosite[2][3]		100	100	93	75
chrysotile[2][3]		100	100	100	97

[1]Gibbs and Hwang, 1980
[2]Pooley and Clark, 1980
[3]Maximum width assumed to be ≤ 0.5 μm. This is based on the data of Gibbs and Hwang (1980)

Table 4 — Aspect Ratio Distributions of Airborne Cleavage Fragments, All Widths.

	(a) % of total airborne fiber longer than 5 μm	(b) % of (a) with aspect ratio ≥3:1	(c) % of (a) with aspect ratio ≥10:1	(d) $ of (a) with aspect ratio ≥15:1	(e) % of (a) with aspect ratio ≥20:1
cummingtonite South Dakota[1]	42	67	16	7	4
cummingtonite South Dakota[2]	44	28	9	2	1
Actinolite Virginia[1]	39	75	11	3	2
Grunerite and actinolite Minnesota[3]	17	12	1	0	0

[1]Wylie, et al., 1985. Collected on location by MSHA.
[2]Eckert, 1981. Collected on location by Homestake Mining Company.

Table 5 — Airborne Asbestos Fibers and Cleavage Fragments With Widths Greater Than or Equal to 0.25 μm

Total Airborne Particles	(a) % longer than 5 μm	(b) % of (a) with aspect ratio >3:1	(c) % of (a) with aspect ratio >10:1	(d) $ of (a) with aspect ratio >15:1	(e) % of (a) with aspect ratio >20:1
Cleavage Fragments					
cummingtonite South Dakota[1]	42	67	16	7	4
cummingtonite South Dakota[2]	44	28	9	2	1
actinolite Virginia[1]	39	75	11	3	2
grunerite and actinolite Minnesota[3]	17	12	1	0	0
Asbestos					
crocidolite[3]					
mining	0.69	100	100	90	57
bagging	1.20	100	100	93	72
amosite[3]					
mining	8.32	100	100	88	54
bagging	17.79	100	100	91	62
chrysotile[3]					
mining	0.82	100	100	84	25
bagging	1.72	100	100	88	49
crocidolite[4]	3.36	100	100	86	65
amosite[4]	14.58	100	100	91	69

[1]Wylie et al., 1985 Collected on location by MSHA.
[2]Eckert, 1981. Collected on location by Homestake Mining Company.
[3]Gibbs and Hwang, 1980.
[4]Pooley and Clark, 1980.

Conclusions

The dimensions of asbestos fibers are unique in the mineral world. The fibers are characterized by extremely small and uniform widths and very high aspect ratios. These properties are characteristic of both bulk and airborne samples, whether they are characterized by optical or electron microscopy. They are retained under all but the most extreme conditions because they arise from the mineralogical properties of asbestos.

Asbestos fibers attain their shape by growth, not cleavage. They are easily separated but their extremely high tensile strength makes any other manipulation extremely difficult. Their surfaces are bounded by unequal crystallographic planes making their cross sectional shape rectangular. It would be extremely helpful to the mining and mineral industries if these properties were recognized in the regulation of asbestos. Using a three to one aspect ratio for the definition of an asbestos fiber has no mineralogical justification and is not supported by any studies on the carcinogenicity of mineral fibers. ♦

References

Atkinson, G.R., et al., 1982. Collection, Analysis and Characterization of Vermiculite Samples for Fiber Content and Asbestos Contamination. Report to EPA Contract No. 68-01-5915.

Campbell, W.J., Huggins, C.W., and Wylie, A.G., 1980. "Chemical and Physical Characterization of Amosite, Chrysotile, Crocidolite and Nonfibrous Tremolite for Oral Ingestion Studies by the National Institute of Environmental Health Sciences," US Bureau of Mines Report of Investigation No. 8452, 66 pp.

Deer, W.A., Howie, R.A., and Zussman, J., 1962. Rock-forming Minerals Vol. 2, 356 pp.

Dorling, M., and Zussman, J., 1987. "Characteristics of Asbestiform and Nonasbestiform Calcic Amphiboles." Lithos, Vol. 20, pp. 469-489.

Eckert, J., 1981. "Dimensions of Airborne Cummingtonite Particles from the Homestake Mine. Lead, South Dakota," unpublished senior thesis, Department of Geology, University of Maryland, 10 pp.

Gary, M., McAfee, R., Wolf, C., eds., 1974. Glossary of Geology. American Geological Institute, 801 pp.

Gibbs, G.W., and Hwang, C.Y., 1980. "Dimensions of Airborne Asbestos Fibers." in Biological Effects of Mineral Fibers Vol. 1, J.C. Wagner, ed., IARC Scientific Publication No. 30 Lyon, France. pp. 79-86.

Harlow, G.E., et al., 1985, "Observations on Amosite/Grunerite Dusts," in Applied Mineralogy, W.C. Park, D.M. Hausen, and R.D. Hagni, eds., AIME, pp. 1147-1157.

Langer, A.M., and Nolan, R.P., 1985. "Physio-chemical Properties of Minerals Relevant to Biological Activities: State of Art," in In Vitro Effects of Mineral Dusts. E.G. Beck and J. Bignon, eds., NATO ASI Series, Vol. G3, pp. 9-24.

Leake, B.E., 1978. "Nomenclature of Amphiboles." American Mineralogist, Vol. 63, pp. 1023-1052.

Leidel, N.A., et al., 1979. "USPHS/NIOSH Membrane Filter Method for Evaluating Airborne Asbestos Fibers." US Department. of Health, Education, and Welfare, NIOSH, Technical Report No. 79-127, Cincinnati, OH.

Malyshonok, Y.V., Vorob'yev, Y.I., and Beyseyev, O.B., 1986. "Geology and Origin of Richterite Asbestos," International Geology Review, Vol. 28, pp. 318-326.

Pooley, F.D. and Clark, N., 1980. "A Comparison of Fiber Dimensions in Chrysotile, Crocidolite, and Amosite Particles from Sampling of Airborne Dust and from Post Mortem Lung Tissue Specimens," in Biological Effects of Mineral Fiber Vol. 1, J.C. Wagner, ed., IARC Scientific Publications No. 30 pp. 79-86.

Shedd, K.B., 1985. "Fiber Dimensions of Crocidolites from Western Australia, Australia, Bolivia, and the Cape and Transvaal Provinces of South Africa." US Bureau of Mines Report of Investigations No. 8998, 33 pp.

Siegrist, H.G., and Wylie, A.G., 1980. "Characterizing and Discriminating the Shape of Asbestos Particles," Environmental Research, Vol. 23, pp. 348-361.

Sinclair, W.E., 1959. "Asbestos: Its Origin, Production, and Utilization," Mineral Publications.Ltd., Salisbury House, London, 879 pp.

Stanton, M.F et al., 1981. "Relation of Particle Dimension to Carcinogenicity in Amphibole Asbestos and Other Fibrous Minerals." Journal of the National Cancer Institute, Vol 67, pp. 965-975.

Wylie, A.G., 1979. "Optical Properties of the Fibrous Amphiboles." Annals of the New York Academy of Sciences, Vol 330, pp 611-620.

Wylie, A.G., and Huggins, C., 1980, "Characteristics of a Potassian Winchite asbestos from the Allamoore Talc District, Texas," American Mineralogist, Vol 18, pp. 101-107.

Wylie, A.G., and Schweitzer, P., 1982. "The Effects of Sample Preparation and Measuring Techniques on the Shape and Shape Characterization of Mineral Particles: The Case of Wollastonite," Environmental Research, Vol. 27, pp. 52-73.

THE IMPORTANCE OF WIDTH IN ASBESTOS FIBER CARCINOGENICITY AND ITS IMPLICATIONS FOR PUBLIC POLICY

A. G. Wylie[a]*

K. F. Bailey[b]

J. W. Kelse[c]

R. J. Lee[d]

[a]Laboratory for Mineral Deposits Research, Department of Geology, University of Maryland. College Park, MD 20742; [b]Vulcan Materials Company, Birmingham, AL 35209; [c]R.T. Vanderbilt Company, Inc., Norwalk, CT 06855; [d]RJ Lee Group, Inc., Monroeville, PA 15146.

Evidence from human epidemiology, experimental animal implantation and inoculation studies, and lung burden studies shows that fibers with widths greater than 1 μm are not implicated in the occurrence of lung cancer or mesothelioma. Furthermore, it is generally believed that certain fibers thinner than a few tenths of a micrometer must be abundant in a fiber population in order for them to be a causative agent for mesothelioma. These conclusions are fully consistent with the mineralogical characteristics of asbestos fibers, which, as fibrils, have widths of less than 1 μm and, as bundles, easily disaggregate into fibrils. Furthermore, the biological behavior of various habits of tremolite shows a clear dose-response relationship and provides evidence for a threshold between fiber width and tumor experience in animals. Public policy in regulating mineral fibers should incorporate this knowledge by altering the existing federal asbestos fiber definitions to reflect it.

Width and length of fibers are both important parameters in determining the carcinogenic potential of asbestos and other specific fibrous materials. Most investigators who have examined this subject agree that there exists a minimum length and maximum width below which and above which fibers are not related to tumor induction. Although fiber dimension is linked to the pathogenic effects of asbestos and certain other fibrous materials, it is also recognized that fiber characteristics other than dimension (i.e., durability, harshness, surface chemistry, surface area or activity, etc.) likely play an important role in the pathogenetic process. Whatever fiber characteristics contribute to the pathogenicity of asbestos, however, it is important to ensure that size parameters used for regulatory purposes reflect those most closely associated with asbestos and known carcinogenic effects.

*Author to whom correspondence should be addressed

Although it is common to see the dimensions of asbestos fibers discussed in terms of a ratio of length to width, or aspect ratio, the use of such a dimensionless parameter results in the loss of information about the size of fibers and, therefore, is of little use in the discussion of fiber carcinogenicity or exposure. While asbestos fiber length is recognized in federal regulatory policy, width is ignored entirely. It is the purpose of this paper to examine the relationship between asbestos fiber width and fiber carcinogenicity, to suggest how this parameter might be used to identify other potentially harmful mineral fibers and to enhance the specificity of existing asbestos regulations.

The National Institute for Occupational Safety and Health (NIOSH) has established the definitions and analytical methods for asbestos used to one degree or another by all asbestos regulatory bodies in the United States. Under the NIOSH scheme, asbestos is simply defined as any fiber of chrysotile, crocidolite, amosite, anthophyllite, tremolite, or actinolite. A "fiber" is defined as a particle with a length to width ratio (aspect ratio) of at least 3:1 and a length of 5 μm or more as determined by the phase-contrast optical microscope (PCM) at a magnification of 450X–500X.[1-2] In this paper a "NIOSH fiber" refers to any particle with these dimensional parameters as determined by any accepted analytical technique.

PREVIOUS WORK

Mesothelioma and Fiber Width

Several investigators have examined the question of what particle sizes are most likely associated with the induction of mesothelioma. Merle Stanton first proposed that a distinct relationship exists between the shape or dimensions of durable fibers and mesothelial tumors in rats.[3] Stanton and co-workers concluded from these experiments that populations with abundant fibers longer than 8 μm and narrower

TABLE I. Bulk and Airborne Particles—Cleavage Fragments

Mineral and Reference	Instrumentation	Length Restriction	Percent less than stated widths or mean width (μm)
Wollastonite			
a. Bulk Samples			
(75) New York	TEM	None	90%<2.3; 50%<1.1
			10%<0.62
Tremolite			
a. Bulk Samples			
(78) New York	SEM	> 5 μm	9%<1.0; 0%<0.5
b. Airborne			
(58) New York	SEM	> 5 μm	0%<0.25
Cummingtonite			
a. Airborne			
(61) S. Dakota	SEM	> 5 μm	22%<1.0; 7%<0.5; 0%<0.25
(70) S. Dakota	SEM	> 5 μm	11%<1.0; 2%<0.5
Actinolite			
a. Airborne			
(75) Virginia	SEM	> 5 μm	15%<1.0; 0.5%<0.5
			0%<0.25
Grunerite and Actinolite			
a. Airborne			
(61) Minnesota	SEM	> 5 μm	1% <1; 0%<0.25
Antigorite			
a. Airborne			
(74) Vermont	TEM 400X	> 5 μm	22%<1.0; 2%<0.5
(74) Vermont	TEM 20KX	> 5 μm	37%<1.0; 10%<0.5
Riebeckite			
a. Bulk Samples			
(75) California	SEM	> 5 μm	27%<1.0; 5%<0.5

than 0.25 μm were most closely linked to pleural tumor response irrespective of fiber type.[4] Most other researchers who use the animal model support the position that only narrow fibers are capable of inducing tumors.[5-7]

Evidence for the importance of narrow fibers in regard to mesothelioma also comes from human experience. Timbrell and co-workers observed that the differences in the incidence of mesothelioma among two groups of asbestos miners in South Africa noted by Harington is most likely related to width.[8,9] In the northwestern Cape, where miners experienced elevated mesothelioma, the mean fiber diameter for crocidolite is 0.073 μm. In the Transvaal crocidolite and Transvaal amosite regions, mean diameters of 0.212 μm and 0.243 μm, respectively, were noted and mesotheliomas are rare. Among vermiculite miners and millers in Libby, Montana who were exposed to tremolite-asbestos, mesothelioma was elevated.[10,11] Studies by Atkinson and co-workers on bulk samples from the Libby vermiculite mine show that 87% of tremolite fibers longer than 5 μm have widths equal to or less than 1 μm and 54% have widths less than or equal

to 0.5 μm.[12] The high incidence of mesothelioma in Turkey has been attributed to fibers of asbestiform (wooly) erionite that are on the order of 0.1 μm in width.[13-15] In contrast, no evidence of mesothelioma has been found in mining environments where NIOSH fibers produced by cleavage of massive amphiboles are abundant.[16-20] In these mining environments 78% or more of the 5 μm long particles have widths greater than 1.0 μm while 93% or more have widths greater than 0.5 μm. Few, if any, show widths below 0.25 μm (Table I).

Some have suggested that the carcinogenic potential of mineral fibers extends to those with widths as large as 2 μm, and there is some evidence from animal experimentation to support this position. For example, Pott et al. have induced tumors in Wistar rats by intraperitoneal injection with basalt and ceramic fibers with median diameters close to or in a few cases greater than 1 μm.[21,22] Hesterberg et al. report tumors in Syrian hamsters after inhalation of refractory ceramic fibers with an average diameter of 0.95 μm.[23] However, the effect of the wide fibers in these studies is most evident when the fibers are very long (up to 50 μm) or when a significant number of narrow fibers are part of the population, a fact that may not be evident from reporting mean or median widths of the population. Many populations of shorter fibers (still longer than 5 μm) with widths predominantly greater than 0.5 μm, such as wollastonite, gypsum, and certain fibrous glasses, have been shown to produce no significant tumor responses after instillation in animals.[22,24,25] Furthermore, the tumor potential of wide fibers has not been demonstrated by inhalation experiments, in part, at least, because such fibers deposit in the conductive airways in the head and lung and do not reach the lung alveoli.[26]

An opportunity to examine in humans the carcinogenic potential of a naturally occurring population of relatively wide mineral fiber is provided by the experience of anthophyllite-asbestos miners and millers in Paakkila, Finland. Anthophyllite-asbestos from this locality has a mean width of approximately 0.6 μm, and in the fiber population, widths less than 0.1 μm are quite rare.[27] In his study of lung tissue

from four individuals exposed to Paakkila anthophyllite-asbestos, Timbrell reports one fiber of 4 μm in width, some fibers between 2 and 4 μm and more than 50% of the fibers with widths less than 0.7 μm. In fact, Timbrell has shown that the distribution of amphibole fiber widths in lung tissue closely resembles the distribution of fiber widths in air.[28] Among the occupational cohort of miners and millers exposed to Paakkila anthophyllite-asbestos, asbestosis is common and the incidence of lung cancer is elevated, primarily in smokers.[29] However, the incidence of mesothelioma is not elevated.[27] The fact that Paakkila anthophyllite-asbestos will induce malignant tumors in animals after intraperitoneal inoculation[22] and inhalation[30] demonstrates that it has a detectable carcinogenic potential in animals under certain experimental conditions. However, the human experience tells us that either because of aerodynamic characteristics and/or the body's defenses, a population of durable fibers with the dimensions of Paakkila anthophyllite-asbestos does not represent the same occupational or environmental mesothelioma risk as other types of asbestos. The best explanation for these observations, in conformity with the Stanton hypothesis, is that the most abundant fibers of Paakkila anthophyllite-asbestos are by and large too wide and the thin fibers are too scarce for the population to induce mesothelioma even with the high exposures associated with this occupational setting.

Lung Cancer and Fiber Width

There are fewer data on the relationship between fiber width and lung cancer than there are for fiber width and mesothelioma. However, studies of human populations exposed to asbestos and animal inhalation studies involving asbestos consistently show an association between asbestos exposure and lung cancer as well as between mesothelioma and asbestos exposure.[8-11,29] In contrast, exposures to the nonasbestiform analogs of asbestos minerals (cleavage fragments) have not shown an elevated lung cancer risk in man.[16,18-20] Lippmann has reviewed the literature in this area and concludes that lung cancer is associated with fibers with widths between 0.3 and 0.8 μm (and length > 10 μm).[31] His conclusions rest in part on the work of Timbrell who has shown that lung retention is greatest for fibers with these widths and lengths.[32] Such dimensions are consistent with those commonly associated with asbestos fibers but not for common cleavage fragments (see Tables I and III). Thinner fibers migrate to the pleura and peritoneum. Thicker fibers are usually rare in an airborne population of asbestos, and when present, disaggregate into thinner fibrils.

Lung Burden Studies in Asbestos-Related Diseases and Fiber Width

During the past 15 years, there have been a significant number of lung burden studies of persons occupationally exposed to asbestos who have developed asbestos-related diseases. Numerous investigators have published information on the sizes of asbestos fibers found in these persons and only rarely are fibers with widths greater than 1.0 μm detected (See Table II). In fact, most asbestos fibers found in lung tissue have widths less than a few tenths of a micrometer. The data are summarized in Table II. While there may be a gradual transition in the carcinogenic potential of fibers from greater to lesser as fiber width increases, as suggested by Pott, wide fibers are not implicated in mesothelioma in humans because they appear to be incapable of translocating to pleural regions, and they are not found in the lungs of people who have developed this disease.[33]

Fibers longer than 5 μm with widths greater than 1 μm are not often found in lung tissue of asbestos miners, millers, and fabricators for several reasons. First, wider fibers contain more mass than narrow fibers of the same length and are thus less likely to become airborne. Wider fibers are also likely to be intercepted in the upper respiratory tract before they reach the lung. Work by numerous investigators has shown that the penetrability of airborne fibers into the peripheral rat lung drops sharply with an aerodynamic diameter above two, which corresponds to a diameter of approximately 0.67 μm.[5] Pott and co-workers assert that fibers with a diameter range of 1–5 μm cannot be tested for carcinogenicity by inhalation because they deposit in the upper respiratory tract and do not reach the lung.[21]

There are also two very important mineralogical reasons why wide fibers of asbestos are rare in lung tissue. First, populations of asbestos fibers of all types are composed of fibers that are less than 1 μm in width, and, therefore, wide fibers are simply not readily available for inhalation (Table III). Second, asbestos fibers wider than 1 μm are composed of bundles of fibrils that readily split longitudinally into individual fibers of much smaller width. Even if wider fibers were inhaled, because of the fibrillar structure of asbestos, the fibers disaggregate. Cook and co-workers demonstrated the effectiveness of this process in their animal intratracheal instillation experiments with ferroactinolite-asbestos.[34] In these experiments they showed that the number of fibers found in lung tissue increased following cessation of exposure and that the increase was due to longitudinal splitting of fiber bundles. Other natural fibers that have been shown to exhibit a significant carcinogenic potency such as asbestiform (wooly) erionite are also characterized by very narrow widths and the ability to split longitudinally. The fibrillar structure is the hallmark of asbestiform fibers.[35] All asbestos minerals that have been implicated as carcinogens in humans exhibit this unique habit of crystal growth structure.

In summary, human epidemiology, experimental animal studies, and the information on size distributions of fibers found in human lung tissue strongly suggest that fibers wider than 1 μm are not likely to be a significant factor in the production of mesothelioma or lung cancer in man. To test the hypothesis that 1 μm is a reasonable upper limit for critical width, we have examined data from tremolite-asbestos and nonasbestiform tremolite. This analysis will show that a clear dose-response relationship and evidence for a threshold exist between the abundance of fibers less than 1 μm in width and carcinogenic response. While fibers wider than 1 μm that are actually fiber bundles might also be important in

producing a carcinogenic response they are usually uncommon in terms of fiber number in an airborne asbestos population. We have therefore neglected these bundles in analyzing fiber abundance data although it may be inappropriate to ignore them for regulatory purposes.

MATERIALS AND METHODS

Tremolite occurs naturally as a gangue and as a component of ore at a number of mines producing industrial talc, vermiculite, play sand, marble, crushed stone, and chrysotile-asbestos. Health risks associated with tremolite have been the source of considerable debate in both the scientific community and regulatory arena for many years.[36-38] Tremolite, in its massive and most common habit, when crushed, forms elongated cleavage fragments that are similar in size and shape to cleavage fragments of other common amphiboles. In this form, there are no epidemiological studies that clearly implicate tremolite as the cause of mesothelioma or lung cancer in man despite its prevalence in some mining environments.[36] In its rare asbestiform habit, on the other hand, it appears to be the cause of both mesothelioma and lung cancer in man.[10,11,39] In animals, mesothelioma has been observed after exposure to tremolite asbestos.[4,40,41] One animal inhalation study involving tremolite asbestos showed elevated lung tumors as well as mesothelioma.[42] There is a modern source of commercial tremolite-asbestos in Korea, and in the past tremolite-asbestos has been mined locally in Europe, Asia, and North America. Tremolite-asbestos possesses the characteristics that distinguish the more commercially important amphibole-asbestos types (crocidolite, amosite, anthophyllite-asbestos) including flexibility, thin fibrils, and a fibrillar structure.[35] Therefore, tremolite is an ideal mineral to study because it occurs naturally in the full range of amphibole habits, its asbestiform variety is known to cause mesothelioma and lung cancer in both man and animals, it is widely distributed, and it is known to occur in a number of important industrial mineral products.

TABLE II. Fibers in Lung Tissue of Humans Exposed to Asbestos

Mineral and Reference	Instrumentation	Length Restriction	Percent less than stated widths or mean width (μm)
Amphibole and Chrysotile			
[76] lung parenchyma	TEM	None	mean = 0.13; range: 0.05–0.32
[76] parietal pleura	TEM	None	mean = 0.06; range: 0.03–0.09
Amphibole			
[76]	TEM	>4 μm	100%<1.0; 63%<0.25
[73] pleura	TEM	None	mean width = 0.15 ± 0.07
[73] parenchyma	TEM	None	mean width = 0.19 ± 0.21
[73] node	TEM	None	mean width = 0.21 ± 0.12
Crocidolite			
[28] mining	TEM	None	100%<1.0
[68]	TEM	None	mean widths = 0.13, 0.09, 0.14, 0.15
[52] lung parenchyma	TEM	>4 μm	96%<0.375
[55] shipyard and construction	TEM	>1 μm	25%<0.07; 75%<0.16
[47]	TEM	None	100%<0.12 ± 0.10
Amosite			
[28] mining	TEM	None	>95%<1
[68]	TEM	None	mean widths = 0.27, 0.24, 0.35, 0.20
[52] lung parenchyma	TEM	>4 μm	66%<0.375
[55] shipyard and construction	TEM	>1 μm	25%<0.09; 75%<0.29
[55] shipyard and construction	TEM	>4 μm	74%<0.31
[47] shipyard and construction	TEM	None	100%<0.43 ± 0.29

A number of well-characterized samples of nonasbestiform tremolite and tremolite-asbestos have been used in animal experimentation and made available to us for study. The importance of these samples is that they represent a range in naturally occurring mineral habit that has not been evaluated for any other mineral. The tremolites include samples with numerous fibers of a fibrillar or asbestiform habit, samples in which only part of the tremolite is fibrillar, and samples lacking tremolite particles of a fibrillar habit altogether (nonasbestiform). We have examined the tumor response of these samples (established through animal experimentation by independent researchers) as a function of the dose of fibers longer than 5 μm with widths less than and greater than 1 μm. Only tremolite particles with a length to width ratio of 3:1 or greater (NIOSH fibers) were included.

Davis and co-workers have recently released the results of injection experiments that used six samples of tremolite: California tremolite-asbestos from Jamestown; Korean

TABLE II. Continued

Mineral and Reference	Instrumentation	Length Restriction	Percent less than stated widths or mean width (μm)
Chrysotile			
[54] referent	TEM	>5 μm	mean width = 0.15 ± 0.18
[54] environmental	TEM	>5 μm	mean width = 0.13 ± 0.25
[54] occupational	TEM	>5 μm	mean width = 0.13 ± 0.16
[53] textile plant	TEM	>5 μm	mean width = 0.10 ± 0.02
[53] mine	TEM	>5 μm	mean width = 0.07 ± 0.01
[68]	TEM	None	mean widths = 0.07, 0.07, 0.07, 0.07, 0.04, 0.11
[76]	TEM	>4 μm	100%<0.25
[55] shipyard and construction	TEM	>1 μm	25%<0.03; 75%<0.06
[47]	TEM	None	100%<0.07 ± 0.02
[73]	TEM	None	mean width 0.09 ± 0.15 mean width 0.07 ± 0.06 mean width 0.08 ± 0.06
Anthophyllite			
[28]	TEM	None	80%<1
[55]	TEM	>1 μm	25%<0.17; 75%<0.44
[65]	TEM	None	50%<0.67
Tremolite			
[57]	TEM	None	100%<1.0; 80%<0.5
[54] referent	TEM	>5 μm	mean width = 0.66 ± 0.48
[54] environmental	TEM	>5 μm	mean width = 0.62 ± 0.74
[54] occupational	TEM	>5 μm	mean width = 0.30 ± 0.25
[53] textile plant	TEM	>5 μm	mean width = 0.35 ± 0.04
[53] mine	TEM	>5 μm	mean width = 0.32 ± 0.02
[68]	TEM	None	mean widths = 0.24, 0.31
[55] shipyard and construction	TEM	>1 μm	25%<0.23; 75%<0.57
Actinolite			
[55]	TEM	>1 μm	25%<0.15; 75%<0.37

tremolite-asbestos; tremolite-asbestos from a laboratory in Swansea; fibrous Italian tremolite (Ala de Stura); tremolite from Carr Brae, Dornie, Scotland; and tremolite from Shinness, Scotland.[40] In this paper, these samples are identified as tremolite A, B, C, E, F, and G, respectively. Tremolite A, B, and C are composed primarily of tremolite-asbestos. Fiber bundles, curved flexible fibers, and small fibril widths are evident from optical microscopic examination of the samples. Tremolite E (Italian) consists of very long, highly unusual, single, needle-like crystals, with limited flexibility. Many of these fibers are twinned and in subsequent analysis, an asbestos subpopulation was reported.[43] Sample F (Dornie) is composed primarily of tremolite cleavage fragments. However, a small portion of the sample contains fiber bundles of tremolite-asbestos. Tremolite G (Shinness) was obtained by crushing large prismatic crystals, and it is composed entirely of cleavage fragments. Davis and co-workers packed the samples into cylinders of Timbrell dust dispensers and airborne dusts were generated. They collected the respirable fraction of these dusts and administered it to rats by using the intraperitoneal injection technique. Measurements of width and length for the fibers in the populations were collected by scanning electron microscopy after deposition on 0.2 μm pore-size polycarbonate filters. Davis and co-workers provide dimensional data for approximately 450 particles from each sample. The dose in terms of number of particles per milligram of dust was obtained directly from the data of Davis and co-workers.[40]

In earlier work Stanton reported the results of 72 rat pleural implantation experiments involving approximately 30 different inorganic materials.[4] Among these materials, one tremolite-asbestos sample was implanted on two different occasions. The sample comes from California, but its exact origin is unknown. Like tremolite A, B, and C, this tremolite possesses all the characteristics of commercial asbestos. In this paper it is referred to as tremolite D. Another Stanton sample identified as Talc 6 is a commercial tremolitic talc from the state of New York identified from Stanton's laboratory notes as Nytal 300. This sample contains 40–50% tremolite cleavage fragments. It is referred to as tremolite H in this paper.

Stanton and co-workers did not provide adequate dimensional data to evaluate width satisfactorily, and it was necessary to re-examine both tremolite D and H. Samples of tremolite-asbestos 1 and 2 (tremolite D) and of Talc 6 (tremolite H) were obtained from the National Cancer Institute and prepared for analysis by gentle sonication in distilled water and filtration on a polycarbonate filter. Portions of the filters were mounted on a polished SEM stub and carbon coated. For Talc 6, the filters were scanned at 5000X and the chemical composition of particles longer than 4 μm was established by energy dispersive spectroscopy (EDS). The particles were identified as tremolite or "other" from their chemical spectra, and their dimensions were measured and recorded. For tremolite D, the samples were photographed at 5000X. All particles in the photograph with lengths longer than 4 μm were measured. From each population 100–150 particles were measured.

Stanton provided estimates of the number of particles longer than 4 μm in a microgram.[41] From our measurements of tremolite-asbestos D, we determined that 74% of the particles longer than 4 μm met the definition of a NIOSH fiber. We also determined that 99% of the NIOSH fibers of tremolite had widths less than or equal to 1.5 μm, 88% had widths less than or equal to 1.0 μm, and 52% had widths less than or equal to 0.5 μm. From these data we calculated the number of NIOSH fibers per total dose and the number of fibers within each of the width categories.

From Talc 6 (tremolite H), we used the number of particles per microgram longer than 4 μm provided by Stanton. From our analysis, we determined that 30% of those particles longer than 4 μm were NIOSH fibers of tremolite. Of these, 9% had widths less than or equal to 1.5 μm, 9% had widths less than or equal to 1.0 μm and 0% had widths less than or equal to 0.5 μm. As was the case for tremolite D, we calculated the number of tremolite NIOSH fibers per total dose and the number within each of the width categories.

Smith and co-workers reported the results of intrapleural injection of four tremolite samples into Syrian hamsters.[44] Only limited information on the size distributions of these samples was published, but one sample, FD-14, was available for additional analysis. Sample FD-14 was an off-the-shelf sample of tremolitic talc from the state of New York that contained approximately 50% nonasbestiform tremolite. The samples were examined by SEM at 2000X and the particles were identified as tremolite based on their chemical composition. Five hundred tremolite particles were measured of which 64 met the definition of a NIOSH fiber. Data regarding the number of tremolite NIOSH fibers in a microgram were not available for this sample. Interestingly, very long fibers of the mineral talc

that have narrow widths and a fibrillar structure occur in this sample. This sample is referred to as tremolite I in this paper.

RESULTS

There are several ways to examine the width data. First, the correlation between tumor incidence and the dose of NIOSH

TABLE III. Bulk and Airborne Particles—Asbestos and Other Fibers

Mineral and Reference		Instrumentation	Length Restriction	Percent less than stated widths or mean width (μm)
Crocidolite Cape Province				
a.	Bulk Samples			
[50]		SEM	>5 μm	98%<1.0; 85%<0.5
[56]	UICC	TEM	None	>99%<1.0; >90%<0.5
[63]	UICC	TEM	None	mean width = 0.23 ± 0.06
[64]		TEM	>2 μm	99%<1.0; 99%<0.5
[22]	UICC	TEM	None	median width = 0.20
[60]		SEM	None	mean width = 0.35 (2S.D. = 0.78 – 0.16)
[60]		TEM	None	mean width = 0.12 (2S.D. = 0.31 – 0.05)
b.	Airborne			
[69]		TEM	None	98%<0.4
[69]		TEM	>5 μm	90%<0.3
[52]		TEM	>4 μm	88%<0.375
[45]		TEM	>5 μm	98%<1.0; 82%<0.5
[46]	UICC	TEM	>0.25 μm	99%<1.0; 88%<0.5
[9]		TEM	None	99%<0.5
Crocidolite Transvaal				
a.	Bulk Samples			
[64]		TEM	>2 μm	89%<1.0; 65%<0.5
Crocidolite Australia				
a.	Bulk Samples			
[64]		TEM	>2 μm	100%<1.0; 99%<0.5
Crocidolite Bolivia				
a.	Bulk Samples			
[64]		TEM	>2 μm	85%<1.0; 60%<0.5
Amosite Transvaal				
a.	Bulk Samples			
[50]		SEM	>5 μm	91%<1.0; 50%<0.5
[56]	UICC	TEM	None	98%<1.0; 80%<0.5
[72]	UICC		>5 μm	92%<1.0; 72%<0.5
[63]	UICC	TEM	None	mean width = 0.47 ± 0.17
[60]		SEM	None	mean width = 0.55 (2S.D. = 1.29 – 0.23)
[60]		TEM	None	mean width = 0.35 (2S.D. = 1.22 – 0.10)

TABLE III. Continued

Mineral and Reference	Instrumentation	Length Restriction	Percent less than stated widths or mean width (μm)
b. Airborne			
(69)	TEM	None	95%<0.4
(69)	TEM	>5 µm	45%<0.3
(52)	TEM	>4 µm	66%<0.375
(62)	PCM	>5 µm	99.4%<1; 94.2%<0.5
(61)	SEM	None	95%<1.0; 80%<0.5
(9) (inc. croc.)	TEM	None	95%<1.0; 70%<0.5
Chrysotile			
Quebec			
a. Bulk Samples			
(50)	SEM	>5 µm	99%<1.0; 94%<0.5
(63) UICC	TEM	None	mean width = 0.17 ± 0.03
(22) UICC	TEM	None	median width = 0.15
(67)	PCM	82% >5 µm	81%<1.0
b. Airborne			
(69)	TEM	None	98%<0.4
(69)	TEM	>5 µm	61%<0.3
Chrysotile			
California			
a. Bulk Samples			
(50)	SEM	>5 µm	99%<1.0; 94%<0.5
(50)	TEM	>5 µm	100%<1.0; 98%<0.5
Chrysotile			
Rhodesia			
a. Bulk Samples			
(63) UICC	TEM	None	mean width = 0.16 ± 0.04
Chrysotile			
Vermont			
b. Airborne			
(74)	TEM 400X	>5 µm	63%<1.0
(74)	TEM 20KX	>5 µm	90%<1.0; 71%<0.5
Anthophyllite			
Finland			
a. Bulk Samples			
(56) UICC	TEM	None	90%<1.0; 60%<0.5
(22) UICC	TEM	None	median width = 0.61
b. Airborne			
(51)	TEM	None	70%<1.0; 40%<0.5

fibers wider than 1 μm is illustrated in Figure 1. It is clear that the dose of wide fibers (>1 μm) shows no relationship to the likelihood of producing tumors. It is important to note that the number of wide (>1 μm) NIOSH fibers in the dose of tremolite in the cleavage fragment samples (G, F, and H) is comparable to that in the tremolite asbestos samples. Thus, the argument that more tumors might have been observed if there had been more wide NIOSH fibers in these samples is not supported. In contrast, the correlation

between tumor incidence and the number of NIOSH fibers per total dose administered with widths less than or equal to 1 μm is shown in Figure 2. This figure shows a dose-response relationship in the form of an s-shaped curve suggesting a threshold and a rapid increase in tumor incidence as the number of these thin (<1 μm) fibers increases. The curve in Figure 2 is derived from a least-squares linear regression of the form:

$$logit = m(\log \text{ of total dose} \leq 1 \ \mu m) + b$$

where

$$logit = \ln\left(\frac{\% \text{ tumor}}{1 - \% \text{ tumor}}\right)$$

The equation for the curve in Figure 2 is shown below and is highly significant ($R^2 = 0.84$, $p < 0.005$):

$$logit = 3.04(\log \text{ total dose} < 1 \ \mu m) - 6.25$$

A straight linear regression of the form below is also highly significant ($R^2 = 0.90$, $p < 0.005$). In the data in Figure 2, this equation is:

$$\% \text{ Tumor} = 49.3(\log \text{ total dose} \leq 1 \ \mu m) - 54.6$$

Another way to illustrate the importance of width relative to tumor response is to characterize the samples in terms of the percentage of NIOSH fibers that have widths of less than 1 μm. It has been shown in most cases that up to 30% of ordinary cleavage fragments of amphibole longer than 5 μm have widths less than 1 μm, and more than 90% of asbestos fibers have widths less than 1 μm (all asbestos fibrils will be less than 1 μm). (See Tables I and III.) Therefore, the proportion of a fiber population with small widths is a measure of the asbestos-like nature of the population or of the abundance of the asbestiform components in a sample. Figure 3 shows the correlation between tumor incidence and the percentage of the tremolite NIOSH fiber population that has widths less than 1.0 μm. By

TABLE III. Continued

Mineral and Reference		Instrumentation	Length Restriction	Percent less than stated widths or mean width (μm)
Actinolite-asbestos				
a.	Bulk Samples			
[34]	Minnesota	TEM	None	mean width = 0.41 50%<0.24
[75]	South Africa	SEM	>5 μm	96%<1.0; 70%<0.5
[49]		TEM	None	90%<0.33; 50%<0.06
[75]		SEM	>5 μm	98%<1.0; 90%<0.5
[22]	Fed. Rep. Ger.	TEM	None	median width = 0.17
Tremolite-asbestos				
a.	Bulk Samples			
[12]	Montana	TEM	>5 μm	87%<1.0; 54%<0.5
[77]	Montana	TEM	None	81%<0.6; 67%<0.4
[77]	Metsovo	TEM	None	96%<0.6; 85%<0.4; 64%<0.2
b.	Airborne			
[66]	Korea	TEM	>0.4 μm	99%<1.0; 90%<0.5
[11]	Montana	TEM	>5 μm	for w >0.45: 98%<1.24; 93%<0.88; 68%<0.62
Tremolite-asbestos and tremolite				
a.	Bulk Samples			
[12]	S. Carolina	TEM	>5 μm	81%<1.0; 48%<0.5
[75]	India	SEM	>5 μm	61%<1.0; 34%<0.5
Asbestos, mineral ID not specified				
b.	Airborne			
[59]		TEM	None	80%<0.43
Wooly Erionite				
a.	Bulk Samples			
[22]	Turkey	TEM	None	median width = 0.38
[22]	Oregon	TEM	None	median width = 0.21
[71]	Oregon	TEM	None	width range = 0.01–0.13 mean width = 0.03
Nemalite				
a.	Bulk Samples			
[22]		TEM	None	mean width = 0.06

this measure an increase in tumor incidence is again observed as the proportion of tremolite fibers <1.0 μm in width increases in the population. The curve in Figure 3 is derived from a least-squares linear regression of the form:

$$\text{logit} = m(\% \text{ fibers} \leq 1 \ \mu\text{m}) + b$$

The equation for the curve in Figure 3 is shown below and is highly significant ($R^2 = 0.85$, p <0.005):

$$\text{logit} = 0.008(\% \text{ fibers} \leq 1 \ \mu\text{m}) - 4.6$$

A straight linear regression of the data using the equation below is also highly significant ($R^2 = 0.93$, p <0.005):

$$\% \text{ Tumors} = 1.2(\% \text{ fibers} \leq 1 \ \mu\text{m}) - 14.4$$

DISCUSSION

Figures 1 and 2 contrast the pleural and peritoneal tumor response (mesothelioma) produced by wide and thin tremolite NIOSH fibers. For wide NIOSH fibers alone, there is no regular dose-response relationship, whereas for thin fibers, the s-shaped curve indicates a strong relationship between dose and carcinogenicity. Furthermore, as illustrated by Figure 3, as the proportion of tremolite NIOSH fibers with widths greater than 1 μm increases, the tumor incidence produced by the sample decreases. Complicating this somewhat simple picture is the fact that as the width of fibers increases, the number of fibers per microgram must decrease. Hence, the number of wide fibers will always be less than the number of narrow fibers in samples of equal weight. Notwithstanding this reality, however, is the observation that without thin fibers, tremolite NIOSH fiber populations are not associated with the induction of pleural or peritoneal tumors in animals. It is also made clear in these figures that characterization of populations of nonasbestiform tremolite by the NIOSH aspect ratio criterion for fibers produces an index that shows no relationship to mesothelioma risk.

The tremolite samples can be divided into three groups based on their carcinogenic potential: those without significant response, those with intermediate responses, and those that produce tumors in almost all the experimental animals. Criteria for a "significant" response varies according to the experimental animal, the level of total dose, the method and location of sample introduction of the fibers, latency, and experience of controls. Davis and co-workers indicate that by intraperitoneal injection, tumor responses in less than 10% of the animals are insignificant. For Stanton and
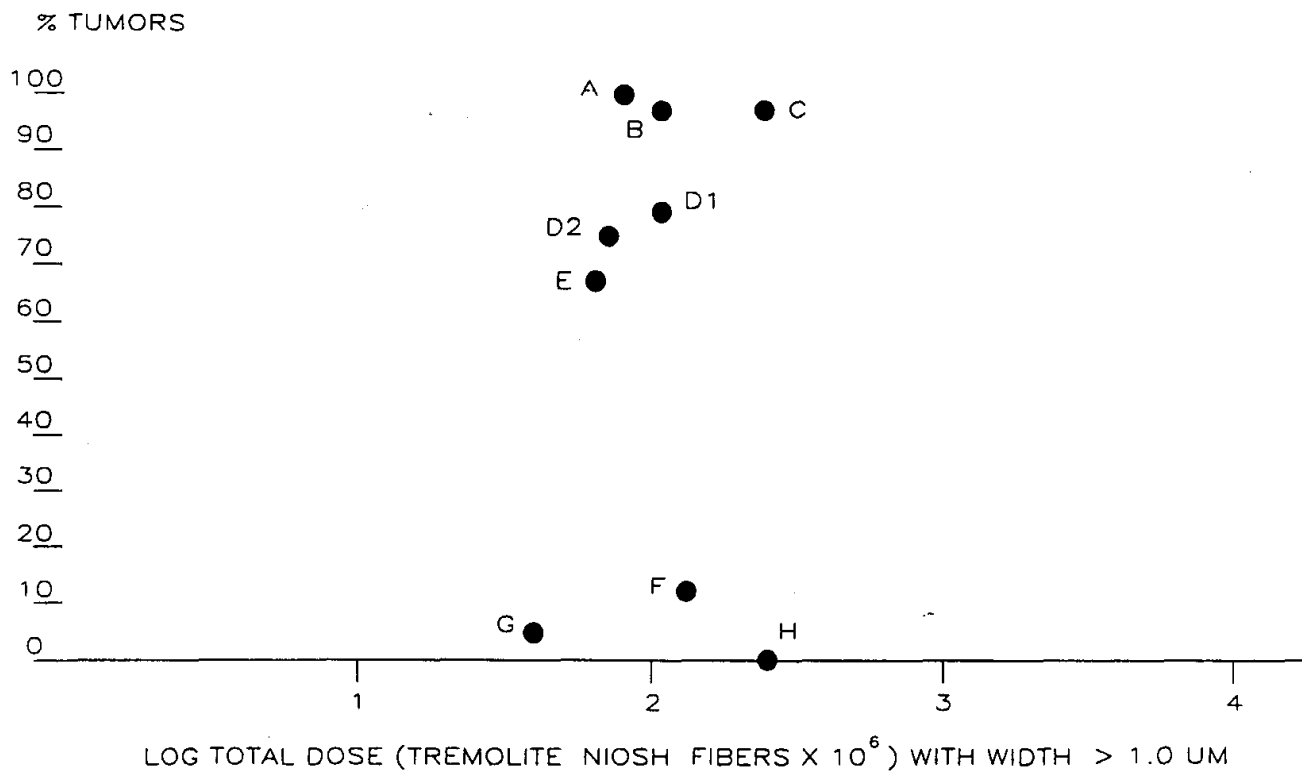
% TUMORS

LOG TOTAL DOSE (TREMOLITE NIOSH FIBERS X 10^6) WITH WIDTH > 1.0 UM

A: Addison—Davis California Tremolite Asbestos
B: Addison—Davis Korean Tremolite Asbestos
C: Addison—Davis Swansea Tremolite Asbestos
D1: Stanton Tremolite Asbestos 1
D2: Stanton Tremolite Asbestos 2
E: Addison—Davis Italian Tremolite Asbestos/Cleavage Fragments

F: Addison—Davis Dornie Tremolite Cleavage Fragments/ Asbestos
G: Addison—Davis Shinness Tremolite Cleavage Fragments
H: Stanton Talc 6 Tremolite (Non—asbestiform)

Figure 1. Percentage of tumors observed in experimental animals after exposure to tremolite as a function of the total dose of tremolite (number of fibers) equal to or longer than 5 μm, wider than 1 μm, and with an aspect ratio equal to or greater than 3

co-workers, 30% tumors were necessary for a significant response by pleural implantation.

Samples G, H, and I fall into the first category. Two of these samples are tremolitic talc from the state of New York (H and I). The high proportion of wide tremolite fibers in these samples is a clear indicator that the tremolite is nonasbestiform.

Samples E and F produced intermediate tumor responses in the animals. However, while sample E produced a high proportion of tumors, the mean survival time of the animals was almost twice that of the animals injected with tremolite A, B, and C, leading Davis and co-workers to conclude that tremolite E represented one-fortieth the hazard of tremolite C, a relationship not evident from the total tumor response. The intermediate responses might be expected from these two samples based on their mineralogical characteristics. Sample E contains a large proportion of highly unusual mineral fibers that lack a recognizable fibrillar structure. Other researchers, employing higher resolution electron microscopic techniques, report an asbestos subpopulation in

this sample.[43] The long latency observed in the animals injected with this material might reflect a slow disaggregation of twinned or possibly asbestiform fibers. This hypothesis is further supported by the fact that the number of fibers per microgram, whether defined as total NIOSH fibers or as NIOSH fibers with widths less than 1 μm, in sample E is less than in sample F. The inverse correlation between dose and response could be explained by sample alteration in vivo as well as by several other mechanisms resulting from differences in surface properties. A comparison between the width distribution of the sample and the width distribution of the fibers found in the lung is necessary to evaluate the hypothesis that disaggregation occurs in vivo.

Sample F contains a small proportion of asbestiform fibers. The limited response of the animals to this material is most likely due to a low dose of asbestos. Davis and co-workers characterize this sample as unlikely to be carcinogenic to man given the marginal biological response observed in what is generally regarded as the most sensitive animal tumor induction technique (intraperitoneal
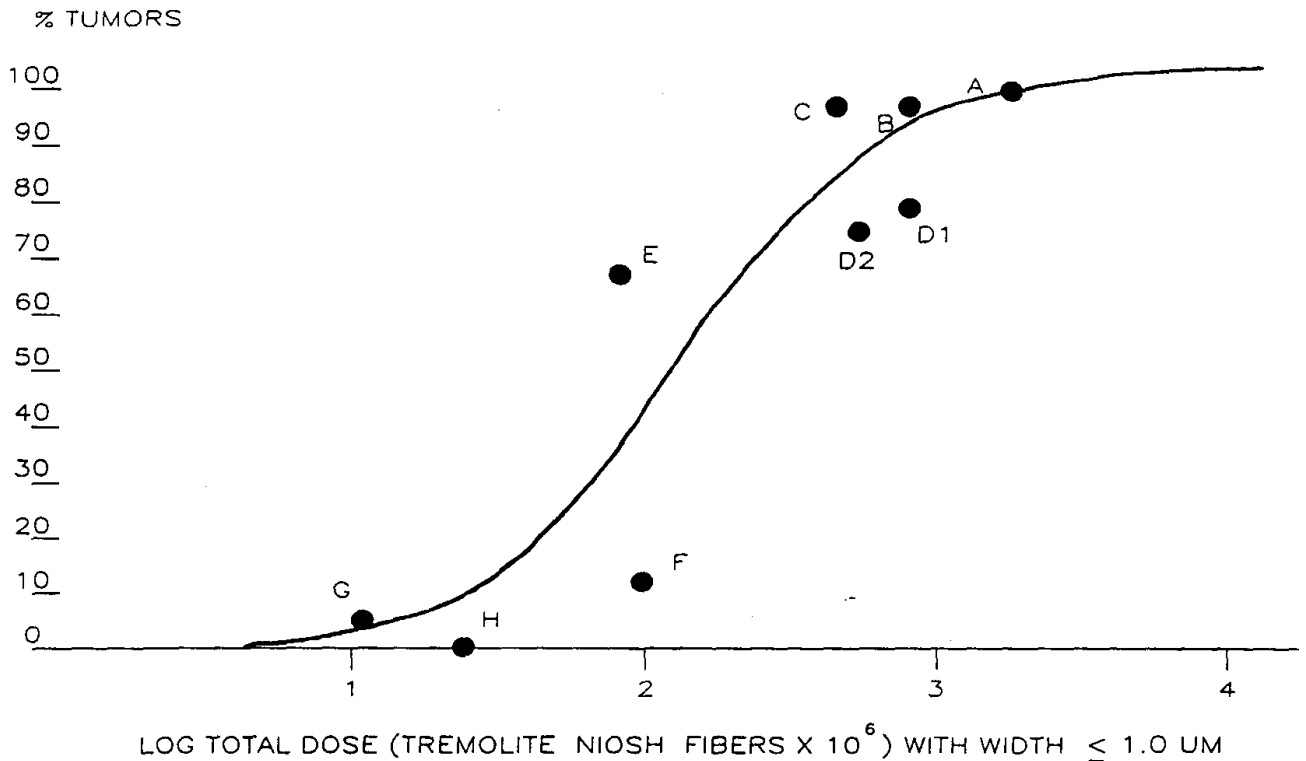
% TUMORS

LOG TOTAL DOSE (TREMOLITE NIOSH FIBERS X 10^6) WITH WIDTH $\leq$ 1.0 UM

A: Addison–Davis California Tremolite Asbestos
B: Addison–Davis Korean Tremolite Asbestos
C: Addison–Davis Swansea Tremolite Asbestos
D1: Stanton Tremolite Asbestos 1
D2: Stanton Tremolite Asbestos 2
E: Addison–Davis Italian Tremolite Asbestos/Cleavage
   Fragments

F: Addison–Davis Dornie Tremolite Cleavage Fragments/
   Asbestos
G: Addison–Davis Shinness Tremolite Cleavage Fragments
H: Stanton Talc 6 Tremolite (Non–asbestiform)

Figure 2. Percentage of tumors observed in experimental animals after exposure to tremolite as a function of the total dose of tremolite (number of fibers) equal to or longer than 5 μm, less than or equal to 1 μm wide, and with an aspect ratio equal to or greater than 3

injection).[40] Tumors have been induced with this test through the introduction of substances as benign as saline solution.[22]

Tremolite-asbestos samples A, B, and C produced pleural tumor incidences in excess of 95% with very short latency periods. While tremolite-asbestos samples D1 and D2 produced 75%- and 79% tumor incidences, respectively, Stanton considered this response equivalent to a 100% tumor probability.

Because the tremolite studies did not involve inhalation exposures in either man or animals, they do not directly test carcinogenic potential relative to lung cancer. However, human epidemiology, lung burden data, and animal experimentation previously discussed support the hypothesis that as the number of asbestos and certain other fibers with widths below 1 μm (and 5 μm or longer) increases, the risk of both lung cancer and mesothelioma increases as well. Therefore, to the extent mesothelioma tumor experience observed in these tremolite animal studies is consistent with both fiber-size observations and biological response reported

elsewhere, reasonable assumptions about lung cancer can be made with respect to the tremolite samples discussed here. It has already been established that excess lung cancer and mesothelioma are not evident in human populations exposed only to amphibole cleavage fragments but they are evident for human populations exposed to tremolite asbestos.

CONCLUSIONS

Combining tremolite samples that have been administered in different ways and to different animal groups such as we have done may appear to overlook important distinctions among these approaches. Despite this simplification, the data show a systematic relationship between dose based on width and mesothelioma tumor response in animals. It should also be noted that by using only the Addison and Davis data, the relationship of tumor response to fiber width remains strong. Furthermore, the fact that asbestos, with its unique dimensions, is known to cause lung cancer and pneumoconiosis suggests that width is related to respiratory

% TUMORS

% TREMOLITE NIOSH FIBERS ≤ 1.0 UM

A: Addison–Davis California Tremolite Asbestos
B: Addison–Davis Korean Tremolite Asbestos·
C: Addison–Davis Swansea Tremolite Asbestos
D: Stanton Tremolite Asbestos
E: Addison–Davis Italian Tremolite Asbestos/Cleavage Fragments

F: Addison–Davis Dornie Tremolite Cleavage Fragments/ Asbestos
G: Addison–Davis Shinness Tremolite Cleavage Fragments
H: Stanton Talc 6 Tremolite Cleavage Fragments
I: Smith FD–14 Tremolite Cleavage Fragments

Figure 3. Percentage of tumors observed in experimental animals after exposure to tremolite as a function of the percentage of tremolite equal or longer than 5 μm with an aspect ratio equal to or greater than 3 that have widths less than or equal to 1 μm.

diseases other than mesothelioma. It seems clear that width is an extremely important variable that to date has been overlooked in regulatory policy. While fibers from a tenth to 200 μm long have been found in human lung tissue, it is the narrow width of these fibers that has given them access. A fiber 15 μm long and 5 μm wide meets the NIOSH criteria for a fiber, but such a particle is highly unlikely to cause disease in humans because it cannot gain access to a human lung. Not only is width a useful indicator of mesothelioma tumor induction, but a dose-response with a threshold is indicated as well.

We propose that NIOSH fiber size parameters used in the quantification of asbestos be modified to include only particles longer than 5 μm with widths less than 1 μm and that the use of the aspect ratio criterion be abandoned. Furthermore, in monitoring airborne asbestos particles or in determining the weight percentage of asbestos in bulk mineral samples, all 5 μm or longer particles that exhibit a fibrillar structure should be included as possible asbestos regardless of width. The potential of fiber bundles to disaggregate, in the air or in vivo, appears to be one of the most hazardous aspects of asbestos. The observation of fiber bundles should be included as part of the asbestos identification procedure. Electron and/or polarized light microscopy of the bundles would be necessary to determine the mineral composition.

Regulatory policy should also recognize that there exists a natural background of mineral particles that are longer than 5 μm and have widths less than 1 μm, which are not asbestos and which, from all evidence, are not associated with any carcinogenic risk. Nonasbestiform amphiboles, pyroxenes, feldspar alumino-silicates, and even phyllosilicates may form elongated fragments when they are crushed, and some will be of this size. However, *populations* of these elongated mineral fragments are easily distinguished from *populations* of asbestiform mineral fibers and vice versa. By establishing thresholds and meaningful definitions, asbestos regulations will not be extended to harmless rock fragments unnecessarily. While we may advocate asbestos regulation based on specific widths, we fully recognize that the scientific basis for regulation comes from populations of mineral fibers and that if asbestos is present in a population of mineral particles, the full range of its dimensions will also be present. It must be stressed that our recommendations have been derived from data and literature references on minerals whose asbestiform variety is known to be carcinogenic. Given the broad range and complexity of physio-chemical properties typically associated with mineral dusts, it is not reasonable to assume similarly sized particles of different minerals will act the same way once in the human lung. Therefore, the authors do not advocate the untested application of dimensional

observations addressed in this paper to all elongated particles. Rather, their application should be restricted to asbestos until such time that their relevance to other materials can be empirically demonstrated.

It is clear, however, that dimensional parameters can be effectively applied to distinguish asbestos dust populations and other fibrous dust exposures from common cleavage fragment dust exposures. This distinction appears to be both dose and risk dependent as well. It is also reasonable to conclude that all fiber populations of similar width, length, and crystal morphology as asbestos should be viewed with caution and perhaps given deference with respect to biological testing.

REFERENCES

1. **National Institute for Occupational Safety and Health:** *USPHS/NIOSH Membrane Filter Method for Evaluating Airborne Asbestos Fibers,* by N.A. Leidel, S.G. Bayer, R.D. Zumwalde, and K.A. Busch (Technical Report No. 79-127). Cincinnati, Ohio: National Institute for Occupational Safety and Health, 1979.
2. **National Institute for Occupational Safety and Health:** *NIOSH Manual of Analytical Methods.* 3d ed. (DHH/NIOSH Publ. No. 84-100). Washington, D.C.: Government Printing Office, 1984. Method #7400. pp. 7400-1–7400-14.
3. **Stanton, M.F.:** Some Etiological Considerations of Fibre Carcinogenesis. In *Biological Effects of Asbestos,* IARC Scientific Publication Number 8, P. Bogovski, J.C. Gilson, V. Timbrell, and J.C. Wagner, eds. Lyon, France: IARC, 1973. pp. 289–294.
4. **Stanton, M. F., M. Layard, A. Tergeris, E. Miller, M. May, E. Morgan, and A. Smith:** Relation of Particle Dimension to Carcinogenicity in Amphibole Asbestos and Other Fibrous Minerals. *J. Natl. Cancer Inst. 67:*965–975 (1981).
5. **Lippmann, M.:** Effects of Fiber Characteristics on Lung Deposition, Retention, and Disease. *Environ. Health Perspect. 88:*311–317 (1990).
6. **Wagner, J.C., G. Berry, and V. Timbrell:** Mesotheliomata in Rats After Inoculation with Asbestos and Other Materials. *Br. J. Cancer. 28:*175–185 (1973).
7. **Wagner, J.C.:** Biological Effects of Short Fibers. In *Proceedings of the VIIth International Pneumoconioses Conference, Part II.* (Department of Health and Human Services Publication No. 90-108). Cincinnati, OH: National Institute for Occupational Safety and Health, 1990. pp. 835–839.
8. **Harington, J.C., J.C. Gilson, and J.C. Wagner:** Asbestos and Mesothelioma in Man. *Nature 232:*54–55 (1971).
9. **Timbrell, V., D.M. Griffiths, and F.D. Pooley:** Possible Biological Importance of Fibre Diameter of South African Amphiboles. *Nature 232:*55–56 (1971).
10. **McDonald, J.C., A.C. McDonald, B. Armstrong, and P. Sebastian:** Cohort Study of Mortality of Vermiculite Miners Exposed to Tremolite. *Br. J. Ind. Med. 43:*436–444 (1986).
11. **Amandus, H., R. Wheeler, J. Jankovic, and J. Tucker:** The Morbidity and Mortality of Vermiculite Miners and Millers Exposed to Tremolite-Actinolite: Part 1–2. Exposure Estimates. *Am. J. Ind. Med. 11:*1–14 (1987).
12. **U. S. Environmental Protection Agency:** *Collection, Analysis and Characterization of Vermiculite Samples for Fibre Content and Asbestos Contamination,* by G. R. Atkinson, D. Rose,

K. Thomas, D. Jones, E. Chatfield, and J. Going (USEPA Contract No. 68-01-5915). Washington, D.C.: U. S. Environmental Protection Agency, 1982.
13. **Baris, Y., A. Sahin, and M. Ozesmie:** An Outbreak of Pleural Mesothelioma and Chronic Fibrosing Pleurisy in the Village of Karain in Anatolia. *Thorax 33:*181–192 (1978).
14. **Baris, I., L. Simonato, M. Artvinli, F. Pooley, R. Saracci, J. Skidmore, and C. Wagnrk:** Epidemiological and Environmental Evidence of the Health Effects of Exposure to Erionite Fibers: A Four-Year Study in the Cappadocian Region of Turkey. *Int. J. Cancer 39:*10–17 (1987).
15. **Elmes, P.C.:** Fibrous Minerals and Health. *J. Geol. Soc. London 137:*525–235 (1980).
16. **McDonald, J.C., G.W. Gibbs, F.D.K. Liddell, and A.D. McDonald:** Mortality After Long Exposure to Cummingtonite-Grunerite. *Am. Rev. Respir. Dis. 118:*271–277 (1978).
17. **National Institute for Occupational Safety and Health:** *Occupational Exposure to Talc Containing Asbestos,* by D.P. Brown, J.M. Dement, R.D. Zumwalde, J.F. Gamble, W. Fellner, M.J. Demco, and J.K. Wagoner (DHEW/NIOSH Publication No. 80-115). Washington, D.C.: Government Printing Office, 1980.
18. **Higgins, I.T.T., J.H. Glassman, S.O. Mary, and R.G. Cornell:** Mortality of Reserve Mining Company Employees in Relation to Taconite Dust Exposure. *Am. J. Epidemiol. 118(5):*710–719 (1983).
19. **Brown, D. P., S.D. Kaplan, R.D. Zumwalde, M. Kaplowitz, and V.E. Archer:** Retrospective Cohort Mortality Study of Underground Gold Mine Workers. In *Silica, Silicosis, and Cancer—Controversy in Occupational Medicine. Cancer Research Monograph, Volume 2,* by D. F. Goldsmith, D. M. Winn, and C. M. Shy. eds. Westport, Connecticut: Praeger Publishers Div., 1986. pp. 335–350.
20. **Cooper, W.C., O. Wong, and R. Graeber:** Mortality of Workers in Two Minnesota Taconite Mining and Milling Operations. *J. Occup. Med. 30:*507–511 (1988).
21. **Pott, F., H. Blome, J. Bruch, K. Friedbers, K. Rodelsperger, and H. Woitowitz:** Classification Proposal for Inorganic and Organic Fibers, Testimony of the Task Group "Determination of Limiting Values for Dusts". In *Senate Commission of the German Research Council for the Examination of Hazardous Substances.* Bonn, Germany: October 1990.
22. **Pott, F., U. Zien, F. Reiffer, F. Huth, H. Ernst, and U. Mohn:** Carcinogenicity Studies on Fibres, Metal Compounds, and Some Other Dusts in Rats. *Exp. Pathol. 32:*129–152 (1987).
23. **Hesterberg, T.W., R. Mast, E.E. McConnell, J. Chevalier, D.M. Bernstein, W.B. Bunn, and R. Anderson:** Chronic Inhalation Toxicity of Refractory Ceramic Fibers in Syrian Hamsters. In *Mechanisms in Fibre Carcinogenesis,* R.C. Brown, J.A. Hoskins, and N.F. Johnson. New York and London: Plenum Press, 1991. pp. 531–538.
24. **Pott, F., M. Roller, R. Rippe, P. Germann, and B. Bellmann:** Tumours by the Intraperitoneal and Intrapleural Routes and their Significance for the Classification of Mineral Fibres." In *Mechanisms in Fibre Carcinogenesis,* ed. by R.C. Brown, J.A. Hoskins, and N.F. Johnson. New York and London: Plenum Press, 1991. pp. 547–565.
25. **Stanton, M.F. and C. Wrench:** Mechanisms of Mesotheliomas Induction with Asbestos and Fibrous Glass. *J. Natl. Cancer Inst. 48(3):*797–821 (1972).
26. **Timbrell, V.:** An Aerosol Spectrometer and its Applications. In *Assessment of Airborne Particles,* T. Mercer, P. Marrow, and W. Stober, eds. Springfield, IL: Charles C. Thomas, 1972. pp. 290–330.

27. **Timbrell, V.:** Review of the Significance of Fibre Size in Fibre-related Lung Disease: A Centrifuge Cell for Preparing Accurate Microscope-evaluation Specimens from Slurries Used in Inoculation Studies. *Ann. Occup. Hyg 33*:483-505 (1989).

28. **Timbrell, V., F.D. Pooley, and J.C. Wagner:** Characteristics of Respirable Asbestos Fibres. In *Pneumoconiosis: Proceedings of the International Conference in Johannesburg.* Cape Town: Oxford University Press, 1970 pp. 120–125.

29. **Meurman, L., R. Kiviluoto, and M. Hakama:** Combined Effect of Asbestos Exposure and Tobacco Smoking on Finnish Anthophyllite Miners and Millers In Health Hazards of Asbestos Exposure. *Ann. N. Y. Acad. Sci. 330*:491–495 (1979).

30. **Wagner, J. C., G. Berry, J. W. Skidmore and V. Timbrell:** The Effects of the Inhalation of Asbestos in Rats. *Br. J. Cancer 29*:252-269 (1974).

31. **Lippmann, M.:** Asbestos Exposure Indices. *Environ. Res. 46*:86–106 (1988).

32. **Timbrell, V.:** Deposition and Retention of Fibers in the Human Lung. *Ann. Occup. Hyg. 26*:347–369 (1982).

33. **Pott, F.:** Some Aspects on the Dosimetry of the Carcinogenic Potency of Asbestos and Other Fibrous Dusts. *Staub-Reinhalt. Luft. 38*:486–490 (1978).

34. **Cook, P.M., L.D. Palekar, and D.L. Coffin:** Interpretation of the Carcinogenicity of Amosite Asbestos and Ferroactinolite on the Basis of Retained Fiber Dose and Characteristics In Vivo. *Toxicol. Lett. 13*:151–158 (1982).

35. **Steel, E. and A. Wylie:** Mineralogical Characteristics of Asbestos Fibers. In *Geology of Asbestos Deposits*, P.H. Riordon, ed. Littleton, Colorado: Society of Mining Engineers, 1981. pp. 93–100.

36. **American Thoracic Society:** Health Effects of Tremolite. *Am. Rev. Resp. Dis. 142*:1453–1458 (1990).

37. **Reger, R., W.K.C. Morgan:** On Talc, Tremolite and Tergiversation, *Br. J. Ind. Med. 47*:505–507 (1990).

38. **Occupational Safety and Health Administration:** "Occupational Exposure of Asbestos, Tremolite, Anthophyllite and Actinolite," *Federal Register 55* (1990). pp. 4938–54.

39. **Langer, A.M., R.P. Nolan, S.H. Constantopoulos, H.M. Moutsopoulos:** Association of Metsoro Lung and Pleural Mesothelioma with Exposure to Tremolite Containing Whitewash. *Lancet i*:965–967 (1987).

40. **Davis, J.M.G., J. Addison, G. McIntosh, G. Miller, and K. Niven:** Variations in the Carcinogenicity of Tremolite Dust Samples of Differing Morphology. In *The Third Wave of Asbestos Disease: Exposure to Asbestos in Place*, ed. by P.J. Landrigan and H. Kazemi. New York: The New York Academy of Sciences, 1991. *643*: pp. 473–490.

41. **Wagner, J.C., M. Chamberlain, R.C. Brown, G. Berry, F.D. Pooley, R. Davis, and D.M. Griffiths:** Biological Effects of Tremolite. *Br. J. Cancer 45*:352–60 (1982).

42. **Davis, J.C.G., J. Addison, R.E. Bolton, K. Donaldson, A.D. Jones, B.G. Miller:** Inhalation Studies on the Effects of Tremolite and Brucite Dust. *Carcinogenesis 6*:667–674 (1985).

43. **Langer, A.M., R.P. Nolan, J.M.G. Davis, J. Addison, and B.G. Miller:** Critique of a NIOSH Review of Submission (Ex. 479-22). In *OSHA Docket H033d*, August 1991.

44. **Smith, W.E., D. Hubert, H. Sobel, and E. Marquet:** Biologic Tests of Tremolite in Hamsters. In *Dusts and Disease*, R. Lemen and J. Dement, eds. Park Forest South, Illinois: Pathotox Publishers, 1979. pp. 335–339.

45. **Griffis, L.C., J.A. Pickrell, R.L. Carpenter, R.K. Wolff, S.J. McAllen, and K.I. Yerkes:** Deposition of Crocidolite Asbestos and Glass Microfibers Inhaled by the Beagle Dog. *Am. Ind. Hyg. Assoc. J. 44*:216–222 (1983).

46. **Evans, J.C., R.J. Evans, A. Holmes, R.F. Hounam, D.M. Jones, A. Morgan, and M. Walsh:** Studies on the Deposition of Inhaled Fibrous Material in the Respiratory Tract of the Rat and its Subsequent Clearance Using Radioactive Tracer Techniques. *Environ. Res. 6*:180–201 (1973).

47. **Gibbs, A.R., D.M. Griffiths, F.D. Pooley, and J.S.P. Jones:** Comparison of Fibre Types and Size Distributions in Lung Tissue of Paraoccupational and Occupational Cases of Malignant Mesothelioma, *Br. J. Ind. Med. 47*:621–626 (1990).

48. **Coffin, D.L., L.D. Palekar, and P.M. Cook:** Tumorigenesis by a Ferroactinolite Mineral, *Toxicol. Lett. 13*:143–150 (1982).

49. **Pott, F., M. Roller, U. Ziem, F. Reiffer, B. Bellmann, M. Rosenbruck, and F. Huth:** "Carcinogenicity Studies on Natural and Man-Made Fibres with the Intraperitoneal Test in Rats". Paper presented at the Symposium on Mineral Fibres in the Non-occupational Environment, Lyon, France, 1987.

50. **U. S. Department of the Interior:** *Chemical and Physical Characterization of Amosite, Chrysotile, Crocidolite and Non-fibrous Tremolite for Oral Ingestion Studies by the National Institute of Environmental Health Sciences* by W. J. Campbell, C.W. Huggins, and A.G. Wylie (U. S. Bureau of Mines Report of Investigations #8452). Washington, D.C.: United States Department of the Interior, Bureau of Mines, 1980.

51. **Harington, J.S.:** Fiber Carcinogenesis: Epidemiologic Observations and the Stanton Hypothesis. *J. Natl. Cancer Inst. 67*:977–989 (1981).

52. **Pooley, F.D. and N.J. Clark:** A Comparison of Fibre Dimensions in Chrysotile, Crocidolite and Amosite Particles from Samples of Airborne Dust and from Post-mortem Lung Tissue Specimens. In *Biologic Effects of Mineral Fibers*, IARC Scientific Publication Number 30, J.C. Wagner and W. Davis, eds. Lyon, France: IARC, 1980. pp. 79–86.

53. **Sebastien, P., J.C. McDonald, A.D. McDonald, B. Case, and R. Harley:** Respiratory Cancer in Chrysotile Textile and Mining Industries: Exposure Inferences from Lung Analysis. *Br. J. Ind. Med. 46*:180–187 (1989).

54. **Case, B.W. and P. Sebastien:** Environmental and Occupational Exposure to Chrysotile Asbestos: A Comparative Microanalytic Study. *Arch. Environ. Health 42*:185–191 (1987).

55. **Warnock, M.L.:** Lung Asbestos Burden in Shipyard and Construction Workers with Mesothelioma: Comparison with Burdens in Subjects with Asbestosis or Lung Cancer. *Environ. Res. 50*:68–85 (1989).

56. **Brown, R.C., M. Chamberlain, D.M. Griffiths, and V. Timbrell:** The Effect of Fibre Size on the In Vitro Biological Activity of Three Types of Amphibole Asbestos. *Int. J. Cancer 22*:721–727 (1978).

57. **McConnochie, K., L. Simonato, P. Mavrides, P. Christofidis, F.D. Pooley, and J.C. Wagner:** Mesothelioma in Cyprus: The Role of Tremolite. *Thorax 42*:342–347 (1987).

58. **Kelse, J.W. and C.S. Thompson:** The Regulatory and Mineralogical Definitions of Asbestos and Their Impact on Amphibole Dust Analysis. *Am. Ind. Hyg. Assoc. J. 50*:613–622 (1989).

59. **Crankshaw, O.:** Factors Affecting Incompatibility of Airborne Fiber Concentration Determinations of the Same Atmosphere by PCM and TEM. *Exp. Pathol. 32*:129–152 (1989).

60. **Wylie, A.G., K.B. Shedd, and M.E. Taylor:** Measurement of the Thickness of Amphibole Asbestos Fibers with the Scanning Electron Microscope and the Transmission Electron Microscope. In *Microbeam Analysis*, K.F. Hernrich, ed. San Francisco: San Francisco Press, 1982. pp. 181–187.

61. **Wylie, A.G., R.L. Virta, and E. Russek:** Characterizing and Discriminating Airborne Amphibole Cleavage Fragments and Amosite Fibers: Implications for the NIOSH Method. *Am. Ind. Hyg. Assoc. J. 46*:197–201 (1985).

62. **Roach, S. A.:** Measurement of Airborne Asbestos Dust by Instruments Measuring Different Parameters. *Ann. N. Y. Acad. Sci. 330*:306–315 (1965).

63. **Spurny, K.R., W. Stober, H. Opiela, and G. Weiss:** On the Problem of Milling and Ultrasonic Treatment of Asbestos and Glass Fibers in Biological and Analytical Applications. *Am. Ind. Hyg. Assoc. J. 41*:198–203 (1980).

64. **U. S. Department of the Interior:** *Fiber Dimensions of Crocidolite from Western Australia, Bolivia, and the Cape and Transvaal Provinces of South Africa* by K. B. Shedd (U. S. Bureau of Mines Report of Investigations #8998) Washington, D.C.: United States Department of the Interior, Bureau of Mines, 1985.

65. **Timbrell, V.:** Measurement of Fibres in Human Lung Tissue. In *Biologic Effects of Mineral Fibers*, IARC Scientific Publication Number 30, J.C. Wagner and W. Davis, eds. Lyon, France: IARC, 1980. pp. 113–126.

66. **Davis, J.M.G., J. Addison, R.E. Bolton, K. Donaldson, A.O. Jones, and B.G. Miller:** Inhalation Studies on the Effects of Tremolite and Brucite Dust. *Carcinogenesis 6*:667–674 (1985).

67. **Assuncao, J. and M. Corn:** The Effects of Milling on Diameters and Lengths of Fibrous Glass and Chrysotile Asbestos Fibers. *Am. Ind. Hyg. Assoc. J. 36*:811–819 (1975).

68. **Gaudichet, A., P. Sebastien, N.J. Clark, and F.D. Pooley:** Identification and Quantification of Asbestos Fibres in Human Tissues. In *Biologic Effects of Mineral Fibers*, IARC Scientific Publication Number 30, J.C. Wagner and W. Davis, eds. Lyon, France: IARC, 1980. pp. 61–68.

69. **Gibbs, G.W. and C.Y. Hwang:** Dimensions of Airborne Asbestos Fibres. In *Biologic Effects of Mineral Fibers*, IARC Scientific Publication Number 30, J.C. Wagner and W. Davis, eds. Lyon, France: IARC, 1980. pp. 69–78.

70. **Eckert, J.:** "Dimensions of Airborne Cummingtonite Particles from the Homestake Mine." M.A. thesis, University of Maryland at College Park, 1981.

71. **U. S. Department of the Interior:** *Size and Shape Characterization of Fibrous Zeolites by Electron Microscopy* by K. B. Shedd, R. L. Virta, and A. G. Wylie (U. S. Bureau of Mines Report of Investigations #8674). Washington, D.C.: United States Department of the Interior, Bureau of Mines, 1982.

72. **Pang, T.W.S., F.S. Schonfeld, and K. Patel:** The Precision and Accuracy of a Method for the Analysis of Amosite Asbestos. *Am. Ind. Hyg. Assoc. J. 49(7)*:351–356 (1988).

73. **Dodson, R.F., M.G. Williams, Jr., C.J. Corn, A. Brollo, and C. Bianchi:** Asbestos Content of Lung Tissue, Lymph Nodes and Pleural Plaques from Former Shipyard Workers. *Am. Rev. Respir. Dis. 142*:843–847 (1990).

74. **Wylie, A.G. and K.F. Bailey:** The Mineralogy and Size of Airborne Chrysotile and Rock Fragments: Ramifications of Using the NIOSH 7400 Method. *Am. Ind. Hyg. Assoc. J. 53*:442–447 (1992).

75. **Wylie, A.G. and P. Schweitzer:** The Effects of Sample Preparation and Measuring Techniques on the Shape and Shape Characterization of Mineral Particles: The Case of Wollastonite. *Environ. Res. 27*:52–73 (1982).

76. **Sebastien, P., X. Janson, G. Bonnand, G. Riba, R. Masse, and J. Bignon:** Translocation of Asbestos Fibers Through Respiratory Tract and Gastrointestinal Tract According to Fiber Type and Size. In *Dusts and Disease: Proceedings of the Conference on Occupational Exposures to Fibrous and Particulate Dust and Their Extension into the Environment*, R. Lemen and J. Dement, eds. Forest Park, Illinois: Pathotox Publishers, Inc., 1979. pp. 66–85.

77. **Langer, A.M., R.P. Nolan, J. Addison, J.C. Wagner:** Critique of the "Health Effects of Tremolite"; The Official Statement of the American Thoracic Society adopted by the ATS Board of Directors, June 1990. In *OSHA Docket H033d*, December 1990.

78. **Wylie, A.G.:** Discriminating Amphibole Cleavage Fragments from Asbestos: Rationale and Methodology. In *Proceedings of the VIIth International Pneumoconiosis Conference* (Department of Health and Human Services Pub. No. 90-108). Cincinnati, OH: National Institute for Occupational Safety and Health, 1990. pp. 1065–1069.

IC 8751

Bureau of Mines Information Circular/1977

Selected Silicate Minerals
and Their Asbestiform Varieties

Mineralogical Definitions
and Identification-Characterization

UNITED STATES DEPARTMENT OF THE INTERIOR

Selected Silicate Minerals
and Their Asbestiform Varieties

Mineralogical Definitions
and Identification-Characterization

By W. J. Campbell, R. L. Blake, L. L. Brown, E. E. Cather,
and J. J. Sjoberg

UNITED STATES DEPARTMENT OF THE INTERIOR
Cecil D. Andrus, Secretary

BUREAU OF MINES

CONTENTS

ILLUSTRATIONS--Continued

ILLUSTRATIONS--Continued

TABLES

SELECTED SILICATE MINERALS AND THEIR ASBESTIFORM VARIETIES

Mineralogical Definitions and Identification-Characterization

by

W. J. Campbell,[1] R. L. Blake,[2] L. L. Brown,[3] E. E. Cather,[4] and J. J. Sjoberg[5]

ABSTRACT

This report by the Federal Bureau of Mines Particulate Mineralogy Unit recommends mineralogical definitions and identification-characterization concepts for selected silicate minerals and their asbestiform varieties. Precise definitions acceptable to mineral analysts, regulatory personnel, and medical scientists are essential because of the present lack of conformity in terminology concerned with measuring and controlling asbestiform particulates and their related health effects. Because of the complexity and variability of crystal morphology in different mineral groups, the descriptive terms are generally explained by illustration rather than by numerical values. Applications and limitations of several analytical techniques for particulate identification and characterization are discussed.

INTRODUCTION

Concurrent with concerns within the Federal Government over future availability of minerals to meet our expanding needs is the requirement that minerals and mineral commodities be mined and processed with minimum environmental impact. Traditionally, matters related to "... inquiries and scientific and technologic investigations concerning mining, and the preparation, treatment, and utilization of mineral substances with a view to improving health conditions and increasing safety...." have been within the province of the Bureau of Mines as authorized in the amended Organic Act of 1913 (Public Law 62-386). Since its establishment by Congress, the Bureau of Mines has long been deeply involved in investigating the explosive characteristics of dusts in the mineral industries in its mining and metallurgy research centers, and has established analytical and mineralogical laboratories in seven metallurgy research centers. These laboratories are essential to solving the increasingly complex

[1]Program coordinator, Particulate Mineralogy Unit, College Park Metallurgy Research Center, College Park, Md.

[2]Supervisory geologist, Twin Cities Metallurgy Research Center, Twin Cities, Minn.

[3]Geologist, Albany Metallurgy Research Center, Albany, Oreg.

[4]Geologist, Salt Lake City Metallurgy Research Center, Salt Lake City, Utah.

[5]Geologist, Reno Metallurgy Research Center, Reno, Nev.

safety, health, and environmental problems posed by dusts within the mineral system.

Various legislative actions and public concerns within the past decade have had, and will continue to have, an impact upon the mineral industry. As a result, control of mineral particulates is becoming increasingly important, with much recent attention focused on asbestiform particulates in both air and water. Figure 1, from an Environmental Protection Agency report, shows the widespread occurrence of common amphibole and serpentine minerals that, according to existing regulatory definitions, may be classified as asbestiform minerals (16).[5] With such possibly overwhelming implications to both mineral producer and mineral consumer, it is essential that existing ambiguities regarding silicate minerals and their asbestiform varieties be resolved. Until recently, adverse health effects associated with asbestos were focused on occupational exposure in asbestos-related industries. Now there is inter-national concern regarding the effect on health from long-term low-level, or short-term high-level, exposure to mineral particulates by the general public (5, 28, 36). These particulates may include both the common and the asbestiform varieties of certain silicate minerals. In many instances, cleavage fragments of common amphibole minerals have been mistakenly identified as
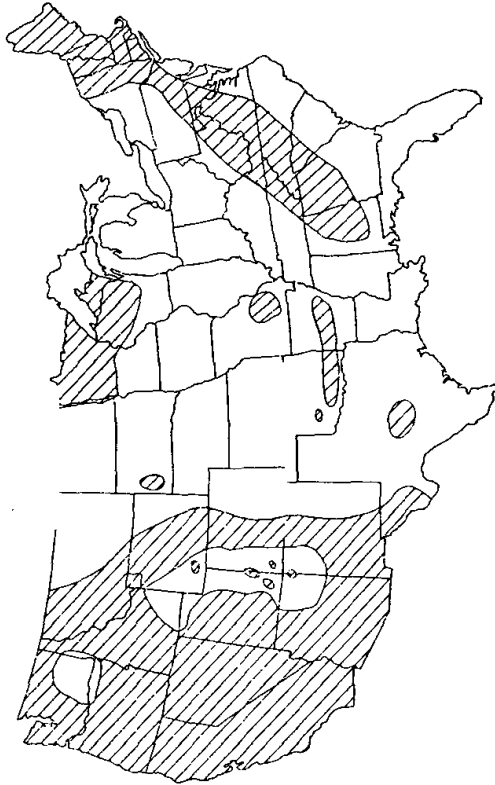
FIGURE 1.- Regions of the United States (shaded area) reported by the Environmental Protection Agency to contain asbestiform minerals in the bedrocks (16).

[5]Underlined numbers in parentheses refer to items in the list of references at the end of this report.

microscopic fibers of the related asbestiform variety. Such lack of precision in identifying these particulates is a handicap to scientific decisionmaking by regulatory agencies and medical researchers. The Particulate Mineralogy Unit was created to work on problems such as this.

The Particulate Mineralogy Unit

The Bureau of Mines established the Particulate Mineralogy Unit in September 1976. The College Park Metallurgy Research Center in College Park, Md.,[7] is the focal point for this unit, but substantial support will be supplied by the other Bureau of Mines metallurgy and mining research centers, which are located throughout the United States. The unit is to assist local, State, and Federal agencies in establishing precise and workable mineral definitions and to improve or develop methods of particulate identification and quantitative measurement. The unit is also providing characterized serpentine and amphibole minerals for use by Federal health agencies in their asbestos-related research programs.

Scope of Report

This Bureau of Mines report is intended to clarify some of the terminology used in identification and characterization of asbestiform minerals, and to sharpen the distinction between common rock minerals and their asbestiform varieties. It defines certain mineral terms related to asbestiform minerals and discusses mineral-characterization techniques on a strictly mineralogical basis. The report then discusses the identification of silicate particulates and suggests how to apply this information to asbestos-related problems. Suggested areas for further research are summarized at the end of this report.

[7]The research center is scheduled for relocation to Avondale, Md., in June 1978.

NOMENCLATURE OF SELECTED SILICATE MINERALS AND THEIR ASBESTIFORM VARIETIES[8]

Background

In August 1976, a preliminary paper (1) was presented from which the Bureau of Mines hoped to elicit suggestions from the mineralogical community for critically defining silicate minerals and their asbestiform varieties. Significant terms such as "asbestos," "asbestiform," and "fibers" have different meanings to the various concerned groups--mineralogists, regulatory agencies, medical scientists, and industry. This has resulted in situations where erroneous conclusions have been drawn. Thus, precise definitions are required that will be uniformly accepted and applied by all personnel involved with silicate minerals that have asbestiform varieties (4, 11, 24-25, 31, 39).

Mineralogical nomenclature recognizes the historical origin of terms, and changes are made only when they are proven incorrect by new information (10, 32). The science of mineralogy is constantly being advanced with newly examined mineral occurrences and with new and improved instruments and techniques that provide more details on chemical composition, crystal structure, and morphology. To prevent constant revision, nomenclature has to have a certain flexibility, yet must be definite enough to be scientifically useful. The objective of this part of the report is to summarize mineralogically acceptable terms that relate to asbestos.

There is no "group" of asbestos minerals. "Asbestos" is a general term applied to certain minerals (that are themselves classified under crystal-structure-based groups) when these minerals crystallize as the asbestiform variety. Table 1 lists some common silicate minerals and their asbestiform varieties, together with their relationships and formulas. Although discussion in this report is limited to these minerals, appropriate terms and statements also apply to other silicate minerals that have rare fibrous varieties such as talc, some clay minerals such as attapulgite, and other amphiboles such as arfvedsonite, eckermannite, and richterite.

TABLE 1. - Selected silicate minerals and their asbestiform varieties

Mineral	Asbestiform variety
AMPHIBOLE GROUP	
Anthophyllite: $(Mg,Fe^{+2})_7$ $Si_8O_{22}(OH,F)_2$.	Anthophyllite asbestos.
Cummingtonite-grunerite: $(Mg,Fe^{+2})_7$ $Si_8O_{22}(OH)_2$.	Cummingtonite-grunerite asbestos.
Tremolite-actinolite: $Ca_2(Mg,Fe^{+2})_5$ $Si_8O_{22}(OH,F)_2$.	Tremolite-actinolite asbestos.
Riebeckite: $Na_2Fe_3^{+2}$ Fe_2^{+3} $Si_8O_{22}(OH,F)_2$.	Crocidolite.
SERPENTINE GROUP	
Serpentine: Mg_6 $Si_4O_{10}(OH)_8$	Chrysotile.

Amphibole minerals and, to a lesser degree, serpentine minerals occur widely distributed in the earth's crust in many igneous or metamorphic rocks. In some rare instances, the mineralogical occurrences contain sufficient quantities of usable asbestiform minerals to be economically minable for commercial asbestos.[9] The soft, silky fibers of asbestos (sometimes called mineral silk) are so flexible that they can be spun into threads from which cloth can be woven. The resulting material is fireproof, is a good thermal and electrical insulator, and has moderate to good resistance to acids. It has been used from Roman times, and is most familiar in daily use in brake linings for automobiles and as the "asbestos" siding used in residential construction.

Only a very small quantity of the amphibole and serpentine minerals under particular geologic circumstances occur as the asbestiform variety of the mineral. The asbestiform varieties occur in veins or small veinlets within rock containing or composed of the common (nonasbestiform) variety of the same mineral. Macrophotographs of the minerals of table 1, both asbestiform and nonasbestiform varieties, are shown in figures 2 through 7.

The serpentine group of minerals is limited to serpentine as the common variety and to chrysotile as the asbestiform variety. Antigorite and lizardite are not listed as separate varieties, but are understood to be included in the term "serpentine" because they represent 2 frequently named polytypes of about 10 recognized polytypes of serpentine (20). The polytypes differ only in minor structural stacking of components and are not sufficiently different to have a separate mineral status. Chrysotile generally occurs segregated as parallel fibers in veins or veinlets, although a recent study (6) has shown fine chrysotile intimately intergrown with the lizardite polytype.

The minerals and mineral series of the amphibole group in table 1 have variable compositions with extensive elemental substitutions and are found in forms ranging from massive to blocky to very fibrous. Crocidolite is the varietal name given to the fibrous habit of the mineral riebeckite (fig. 7), as shown by at least one study (35). It is retained here as a useful and correctly identified term.

Cummingtonite-grunerite asbestos is the mineralogically proper terminology for the commercial material commonly known as "amosite." Amosite, implied to be a mineral variety, is really an acronym--Asbestos Mines of South Africa--for a fibrous mixture of minerals; namely, cummingtonite-grunerite with variable tremolite-actinolite. Amosite has been discredited as a mineral species (22), and its use as a mineralogical term should be discontinued; however, it is still useful as a commercial term.

Mineral compositional series such as cummingtonite-grunerite involve replacing one cation for another in a crystal structure without significantly altering the structure. There may be a gradation in the structure in some series, and minor changes in physical characteristics may occur with elemental substitution. Usually a series involves two named compositional end members with intermediate substitutional compounds being separately named (if the members were recognized by early mineralogists), given a varietal name (for similar reasons), or just qualified by being referred to as members of the series. Members of the tremolite-actinolite-ferroactinolite series are hydroxylated calcium-magnesium, magnesium-iron, and iron silicates, respectively. Their series is named in table 1 for two of its members, and when its composition is known, it should be called by the specific name, such as

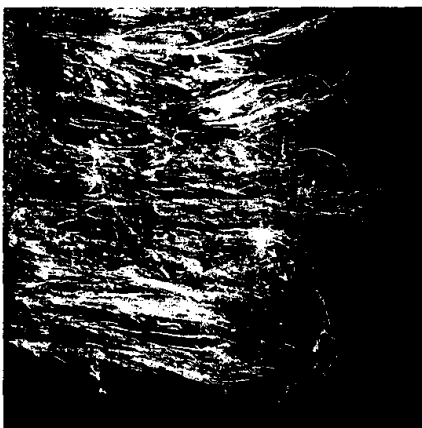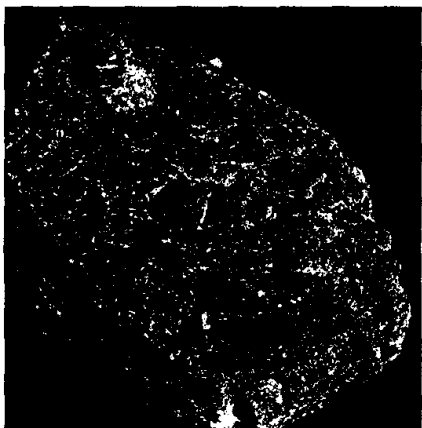[9]Clifton, R. A. Asbestos. BuMines MCP-6, in preparation, 1977.

FIGURE 2. - Macrophotographs of serpentine (top, X 1) and chrysotile (bottom, X 3).
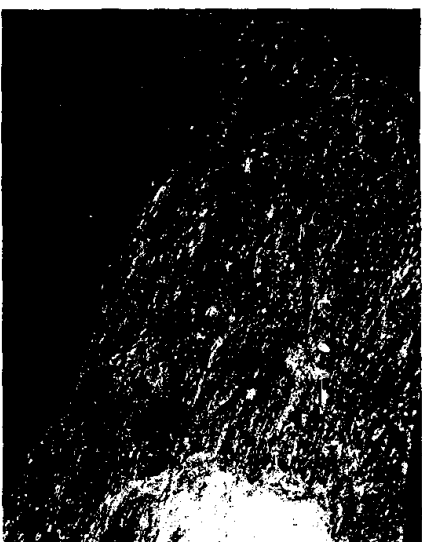

FIGURE 3. - Macrophotographs (X 3) of tremolite (top) and tremolite asbestos (bottom).
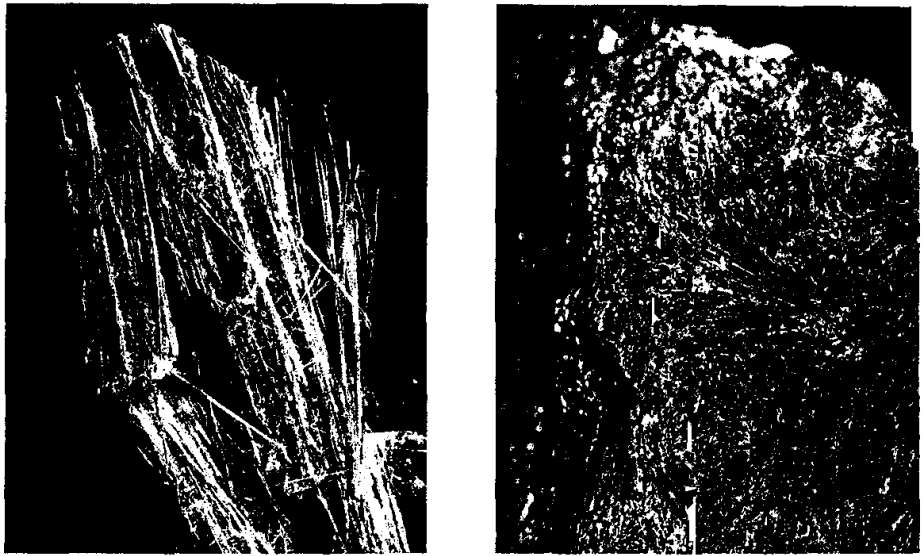
FIGURE 4. - Macrophotographs (X 3) of anthophyllite (top) and anthophyllite asbestos (bottom).
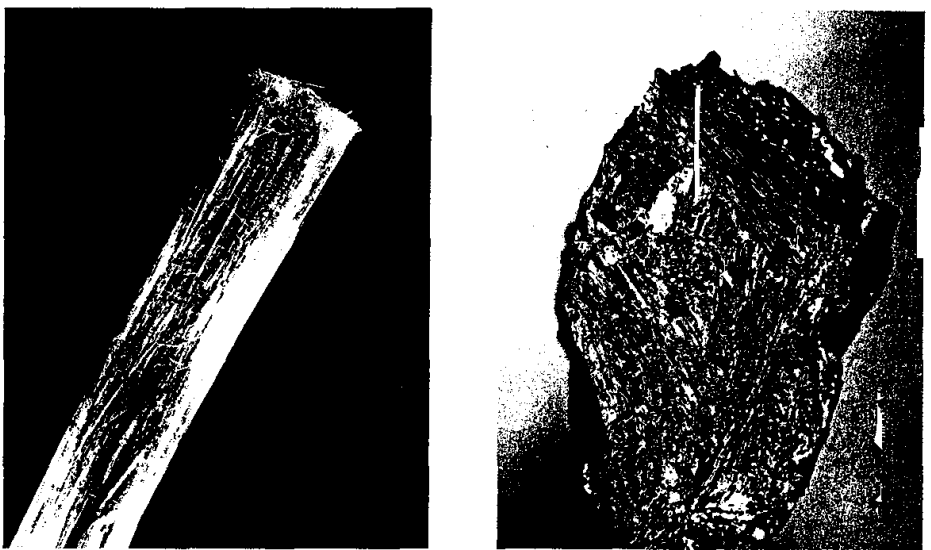

FIGURE 5. - Macrophotographs of actinolite (top, X 1) and actinolite asbestos (bottom, X 3).
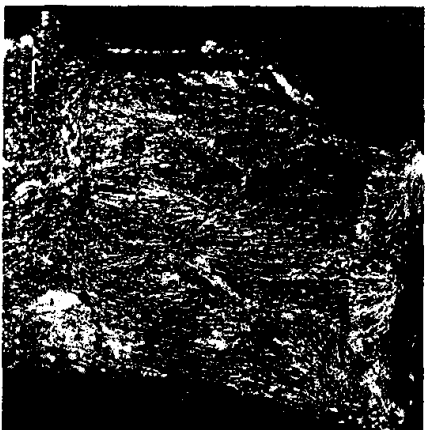
FIGURE 6. - Macrophotographs (X 3) of cumming-
tonite (top) and cummingtonite-
grunerite asbestos (bottom).

FIGURE 7. - Macrophotographs (X 3) of riebeckite (top) and
crocidolite (bottom).

tremolite. The following nomenclature for this series (7) is based on the mole ratio (in parentheses) of $\frac{Fe}{Fe + Mg}$ in the formula $Ca_2(Mg,Fe)_5Si_8O_{22}(OH)_2$: tremolite (0 to 0.2), actinolite (0.2 to 0.8), and ferroactinolite (0.8 to 1.0).

Definitions

Many mineralogical definitions apply to the entire mineral field, but the definitions in this report are restricted to those necessary to characterize the fibers and cleavage fragments related to asbestos identification-characterization. The terms to be defined are outlined in the following list:

Mineral terms:
Mineral
Mineral groups
Mineral series
Mineral varieties

Asbestos-related terms:
Asbestos
Fibrous
Mineral fiber
Fibril
Fibril structure
Asbestiform

Crystal terms:
Crystal structure
Crystalline
Crystal
Single crystal
Twinned crystal
Polycrystalline
Polymorphs
Polytypes
Crystal form
Crystal morphology:
Single crystals:
Equant
Prismatic
Acicular
Fiber
Fibril
Filliform
Bladed
Platy
Lamellar
Crystal aggregates:
Asbestiform
Columnar
Fibrous
Lamellar
Massive
Radiating
Reticulated

Breaking of minerals:
Cleavage:
Types:
Pinacoidal
Prismatic
Rhombohedral
Cubic
Octahedral
Quality:
Perfect
Good
Fair
Imperfect
Cleavage fragment
Fracture: Types:
Even
Uneven
Splintery
Conchoidal
Hackly
Parting

Mineral Terms

Mineral.--A homogeneous, naturally occurring, usually inorganic and crystalline substance. Minerals with distinct crystal structure types (including lack of crystal structure) and limited variation in chemical composition are given individual names.

The early concept of a mineral as a natural-history species was gradually abandoned and changed into a chemical and structural definition around the middle of the 19th century, long before crystal structures were understood. The term "species" persisted for a long time with this newer definition, but is now seldom used in mineralogy.

Mineral Group.--Minerals that have essentially the same (or comparable) structures, but have different cations in secondary structural position (for example, pyrites, feldspars, and amphiboles).

In silicates, most of the mineral groups have the same linkage patterns of the silica tetrahedra, like the characteristic double chains of amphiboles. However, the secondary atomic sites may be occupied by a relatively wide variety of cations or some may even be vacant in the actual structures of the members. In some silicate-mineral groups, the identity of the silica-tetrahedral frame is less restricted and may be limited to the similarities of some basic characteristics. For example, the silica-tetrahedral frames of the zeolite minerals are variable, but they are all characterized by large open channels.

All mineral groups have names. In some instances, this name is the universal name of a common or important member of the group (for example, serpentine group).

Mineral Series.--Two or more members of a mineral group in which the cations in secondary structural position are similar in properties and can be present in variable, although frequently limited, ratios (for example, cummingtonite-grunerite). Also known as an isomorphic series.

Some mineral series such as the plagioclases have unique names, but most are identified by the combined names of the end-member minerals, such as tremolite-actinolite. The current trend is to simplify long series names by using the mineral name of only one (end or intermediate) member.

Individual minerals in the series are either identified by the names given to compositional ranges (for example, bytownite or oligoclase in the plagioclases), or by the name of the series followed by a symbol expressing the mineral's position in the series or the ratios of the variable cations ($Ab_x An_{100-x}$% for plagioclases, where Ab and An designate the two end members, albite and anorthite).

Mineral Variety.--Minerals that are conspicuously different from those considered normal or common in crystallization habits, polytypes, and other structural variants, or other physical properties such as color. Varieties are named by mineralogists, miners, gemologists, manufacturers of industrial products, and mineral collectors.

Although mineral names are controlled by national and international mineralogical organizations, variety names are not. In practice, any variety name that becomes sufficiently popular is eventually recognized by these organizations as distinct enough to be used as a mineral-variety name. Typical of these are the various varieties of gypsum shown in figure 8. Figures 2 through 7 illustrate the massive and asbestiform varieties of serpentine and amphiboles.

FIGURE 8.- Four varieties of gypsum: (A) Selenite; (B) satin spar, fine fibrous; (C) satin spar, coarse fibrous; and (D) alabaster.

Asbestos-Related Terms

In the following discussion, asbestiform refers only to asbestos. The other terms, "fibrous," "mineral fiber," "fibril," and "fibril structure," apply to both asbestiform and nonasbestiform varieties.

Asbestos.--(1) A collective mineralogical term encompassing the asbestiform varieties of various minerals; (2) an industrial product obtained by mining and processing primarily asbestiform minerals.

The quality of asbestos depends on the mineralogy of the asbestiform variety, the degree of asbestiform development of the fibers, the ratio of asbestiform fibers to acicular crystals or other impurities, and the length and flexibility of the fibers. The major asbestiform varieties of minerals used for asbestos are chrysotile, tremolite-actinolite asbestos, cummingtonite-grunerite asbestos, anthophyllite asbestos, and crocidolite. Asbestos may be marketed by its mineral name such as anthophyllite asbestos, its variety name such as chrysotile or crocidolite, or a trade name such as Amosite or Montasite. Two types of commercial asbestos are shown in figures 9 and 10.

The term "asbestos" was first introduced by Plinius Secundus in 77 A.D. The term "amiant" was previously used for the same mineral by Dioscorides in 50 A.D., and this term was the more common one until the middle of the 17th century. After that until the 20th century, "asbestos" was more common, and "amiant" was reserved for the more silky and flexible asbestos. In the 18th century, asbestos was classified into five different species. Currently, all

asbestos is recognized as varieties of several individual minerals. Thus, in mineralogy, "asbestos" became a collective term, somewhat like "clays" or "gems." During the 20th century, asbestos developed into an important industrial material. Some asbestos products contain nonasbestiform minerals (for example, asbestos-cement and asbestos-magnesia); consequently, the mineralogical and the industrial definitions of asbestos do not always coincide.

Fibrous.--The occurrence of a mineral in bundles of fibers, resembling organic fibers in texture, from which the fibers can usually be separated (for example, satin-spar and chrysotile).

The term "fibrous" has been used during the last 200 years to describe all kinds of minerals that crystallized in habits resembling organic fibers, including asbestos minerals. However, the related

FIGURE 9.- Macrophotograph of tremolite asbestos (X 3).

FIGURE 10.- Macrophotograph of anthophyllite asbestos (X 3).

term "asbestiform" was never used for fibrous mineral habits other than asbestos. Accordingly, "fibrous" is the more general term, and asbestiform is a specific type of fibrosity. Figures 11, 12, and 13 show various types of fibrous mineral habits. Examples of fibrous minerals, both silicates and non-silicates, that are not classified as asbestiform are shown in figure 13.

Mineral Fiber.--The smallest elongated crystalline unit that can be separated from a bundle or appears to have grown individually in that shape, and that exhibits a resemblance to organic fibers. (Examples: fiber bundles, chryso-tile and crocidolite; individual fibers, epsomite and millerite.)

The term "fiber" is not limited to asbestos. However, it is distinct from "acicular" because it requires the resem-blance to organic fibers. Figures 14 and 15 illus-trate mineral fiber habits. Excellent photomicrographs of

FIGURE 12. - Photomicrograph illustrating the separation of a crocidolite fiber bundle into fibers (X 600).

organic fibers are illustrated in The Particle Atlas (18).

Fibril.--A single fiber, which cannot be separated into smaller compo-nents without losing its fibrous properties or appearances.

Most fibers are single structural entities, such as millerite and nickel sulfide, and some may be called fibrils. However, some fibers are composed of two or more fibrils that are less readily separable from each other than fibers are from bundles (for example, chrysotile and crocidolite). Figure 16 shows the high magnification necessary to resolve a fibril.

Fibril Structure.--A systematically deformed and/or defective crystal structure of a fibril. A defect structure would involve various types of dis-location. The fibril structure may be exhibited by a single crystal, a group of single crystals, or a twinned single crystal.
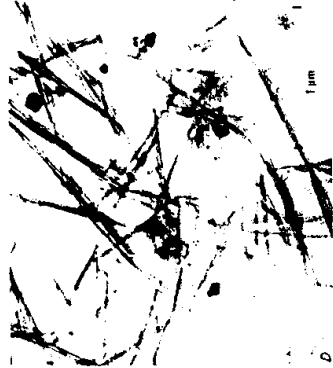

FIGURE 11. - Macrophotographs (X 3) of two fibrous amphiboles showing asbestiform habit: Byssolite (top) and richterite (bottom).

The scroll-like fibril structure of chrysotile (38), the twinned single-crystal fibrils of chrysotile (6), and the incompletely resolved fibril structure of an amphibole (9) are all examples illustrated in the literature.

Some acicular single crystals may have the appearance of fibers and fibrils, yet there is nothing unusual about their crystal structures. Other acicular single crystals may have significant structural deviations in addition to appearance that result in the display of certain properties usually found in fibers such as high tensile strength along the fiber axis. Thus, fibril structure is not limited to asbestiform structures, but may occur in a minor form in non-asbestiform structures.

Asbestiform.--A specific type of mineral fibrosity in which the fibers and fibrils possess high tensile strength and flexibility.

"Asbestiform" and "asbestos" are essentially synonymous in current usage. Some special properties of asbestiform varieties, including optical extinction and surface charge, are either not fully understood or are not uniformly applicable to all asbestiform fibers; consequently, they cannot be considered fundamental characteristics at this time. The prototype of the expression "asbestiform" was introduced by Werner in 1774. He recognized three subspecies of actinolite and of tremolite. One of these subspecies had the prefix "asbestartiger." Thus, the restriction of "asbestiform" to certain mineral varieties appears to
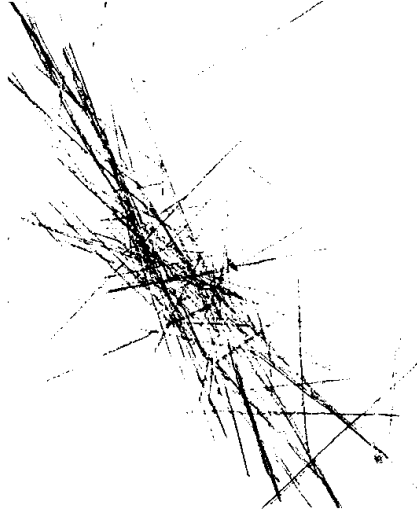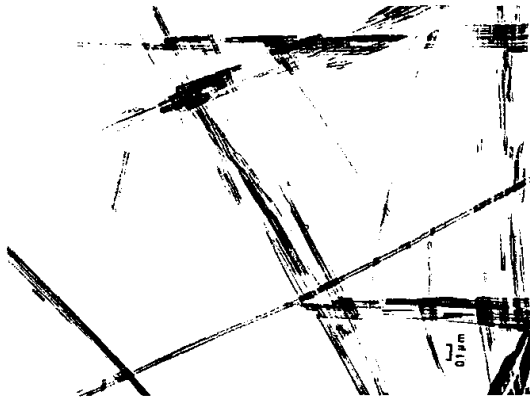

FIGURE 14. - Light optical photomicrograph of fibers from tremolite asbestos (X 115). A few particles are seen to be bundles of fibers.

FIGURE 15. - Fibers of epsomite (magnesium sulfate hydrate) (X 13).

FIGURE 13. - Four fibrous nonasbestiform mineral varieties: A, Fibrous talc (X 500); B, fibrous brucite (X 50); C, polygorskite (X 30,000); and D, attapulgite (X 30,000).

be justified on a historical as well as physical basis. Figures 17 to 20 show several asbestiform varieties of minerals.

Crystal Terms

Crystal Structure.--The pattern of the regular arrangement of atoms and ions in space. Usually refers to the basic (or average) structure of solids (and the ordered portions of liquids) without reference to minor, localized deviations.

Crystalline.--A substance possessing a reasonably well developed and long-range ordered crystal structure.

Crystal.--(1) Any single crystal; (2) a single crystal terminated by planar or nearly planar surfaces called crystal faces.

Single Crystal.--A crystal containing an uninterrrupted crystal structure in a single orientation.

Twinned Crystal.--A crystal composed of two or more single crystals where adjacent crystals share a plane that is an integral part of both orientations of the crystal structure.

Polycrystalline.--A substance composed of two or more single crystals.

Polymorphs.--Two crystals with identical chemical composition but different crystal structures.

FIGURE 17.- Crocidolite, showing a fiber bundle and fibers (X 300).

FIGURE 18.- Chrysotile by polarized light (X 100).

FIGURE 16.- Chrysotile, showing individual fibrils, at two magnifications: X 18,000 (top) and X 35,000 (bottom). The hollow-tube structure is visible at the higher magnification. (TEM microphotographs.)

FIGURE 20. - Chrysotile at two magnifications: X 1,960 (top) and X 2,800 (bottom).

Polytypes.--Polymorphs that contain essentially identical structural components, like layers, which are arranged in various patterns, like stacking of layers.

Crystal Form.--A set of symmetrically equivalent faces in a single crystal. A crystal may display several crystal forms.

Crystal Habit.--The actual shape assumed by a crystal or group of crystals as a result of the growth of dominant crystal forms (faces). Also known as crystal morphology.

Crystal Aggregate.--A cohesive mass of individual crystals or grains.

FIGURE 19. - Chrysotile (X 300).

Single crystals exhibit growth shapes, while crystal aggregates exhibit growth patterns or arrangements (fig. 21). Some habits imply minor deviation of the crystal structure (deformation of the structure, presence of defects, inclusions, or impurities). Most habits are limited to the appearance of single crystals (crystal forms, irregular terminations, dimensional development, texture) or the pattern of aggregation of single crystals (dimension, orientation of the crystals, and cohesion between them). Under the following heading of "Single Crystals," the growth shapes are arranged first as equant, followed by other shapes that can be thought of as being derived from equant by suppressing or extending one or two of the three space dimensions, thus conveying the gradational nature of various defined crystal shapes.

Single Crystals

Equant.--The shape of a single crystal or grain with three approximately equal space dimensions.
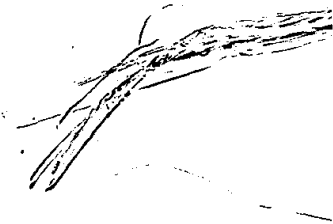
Prismatic.--The shape of a single crystal with one elongated dimension and two shorter, approximately equal, dimensions.

Prismatic shapes of various single crystals are shown in figures 22 to 25.

Acicular.--The shape shown by an extremely slender crystal with small cross-sectional dimensions (a special case of prismatic form). Acicular crystals may be blunt-ended or pointed. The term "needlelike" refers to an acicular crystal with pointed termination at one or both ends.

Figures 23 and 26 show acicular crystals or crystal shapes.

Fiber.--See definition under "Asbestos-Related Terms."

Fibril.--See definition under "Asbestos-Related Terms."

Filiform.--The shape of threadlike mineral fibers.

Bladed.--The bladelike shape of a crystal with one longer dimension and two unequal, much shorter, dimensions.

FIGURE 22.- Macrophotograph of spodumene ($LiAlSi_2O_6$) showing prismatic shape (X 1).

FIGURE 23.- Macrophotograph of tremolite showing prismatic and acicular crystal shapes (X 10).

SINGLE-CRYSTAL SHAPES

Equant

Prismatic

Acicular

Fiber

Fibril

Filiform

Bladed

Platy

Lamellar

CRYSTAL-AGGREGATE PATTERNS OR ARRANGEMENTS

Asbestiform

Columnar

See "Asbestiform" above.

Fibrous

Lamellar

Massive

Radiating

Reticulated

FIGURE 21.- Various shapes of single crystals, and patterns or arrangements of crystal aggregates.

Figure 25 shows the bladed prismatic habit of actinolite.

Platy.--The shape of a crystal with one short dimension and two longer, approximately equal, dimensions. Chlorite, micas, and talc usually crystallize into platy shapes.

The serpentines, although possessing layered structure similar to micas and talc, rarely grow in platy shapes. Talc is of interest here because some talc deposits have associated asbestiform and nonasbestiform minerals. Platy talc, when seen in thin sections or as fragments in oil, may occur in various orientations. Plates lying flat look like plates but, if standing on edge, could appear fibrous.

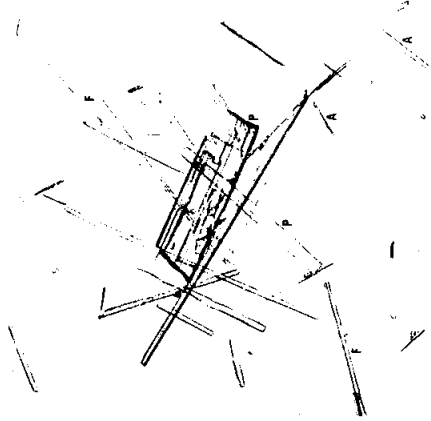Lamellar.--The shape of a very thin platy crystal.

FIGURE 26. - Tremolite cleavage fragments (X 130), showing acicular (A), fibrous (F), and prismatic (P) shapes.

Crystal Aggregates

Asbestiform.--See definition under "Asbestos-Related Terms."

Columnar.--The arrangement of a group of approximately parallel, prismatic, acicular, or bladed crystals.

Figure 27 shows columnar aggregates of coarse anthophyllite.

Fibrous.--See definition under "Asbestos-Related Terms."

FIGURE 24. - Riebeckite, showing prismatic shape (SEM photomicrograph at X 800).

FIGURE 25. - Actinolite, showing prismatic shape (SEM photomicrograph at X 20,000).

Lamellar.--The pattern exhibited by aggregates of very thin platy minerals.

Massive.--Homogeneous structure without stratification, flowbanding, foliation, or schistosity. Also, crystals or crystalline grains that are tightly packed and scarcely distinguishable.

Figure 2 (top) is a good example of massive serpentine.

Radiating.--An arrangement of prismatic, acicular, or bladed crystals that appear to be diverging from a common center.

Figure 28 shows radiating aggregates of pyrophyllite.

Reticulated.--The pattern of a crisscross network of acicular, prismatic, or bladed crystals.
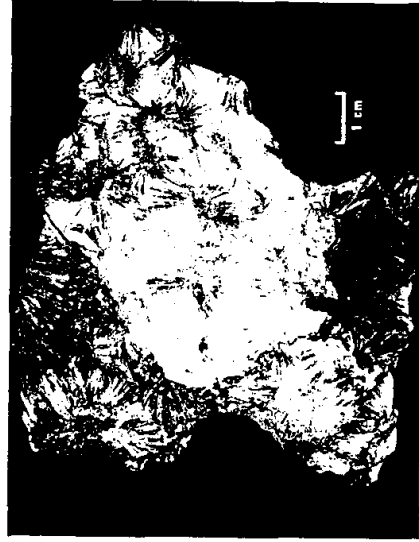
FIGURE 27.--Macrophotograph of columnar aggregates of coarse anthophyllite (X 1).

Breaking of Minerals

When a mineral crystal or grain is strained beyond its elastic and plastic limit, it will break in one of several characteristic modes described as cleavage, fracture, or parting.

Cleavage.--The tendency of a crystal to break in definite directions that are related to the crystal structure and are always parallel to possible crystal faces.

Cleavage Types

Pinacoidal Cleavage.--A crystal with only one cleavage plane that yields platy or lamellar fragments (for example, talc and the mica minerals). Also called platy, basal, or lamellar cleavage.

Prismatic Cleavage.--A crystal with two distinct cleavage planes that yield prismatic fragments (for example, the amphiboles and pyroxenes).

Rhombohedral Cleavage.--A hexagonal crystal with three distinct cleavage planes that yield rhombohedral fragments (such as calcite).

Figure 29 shows the excellent rhombohedral cleavage of calcite.

Cubic Cleavage.--An isometric crystal with three distinct cleavage planes that yield cubic fragments (for example, halite).

Octahedral Cleavage.--An isometric crystal with four distinct cleavage planes that yield octahedral cleavage fragments (for example, magnetite and fluorite).

Cleavage Quality

The quality or persistence of a cleavage is described as follows:

Perfect.--Difficult to break in any other direction; cleavage surfaces are extensive and smooth.

The cleavage of calcite in figure 29 is perfect.

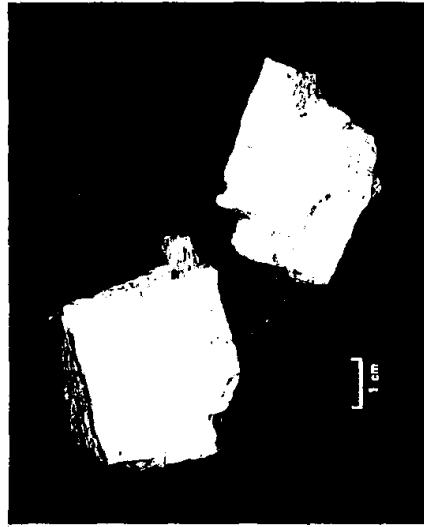Good.--Breaks readily along one direction, but can be broken in other directions; cleavage

FIGURE 28.--Macrophotograph of radiating aggregates of acicular pyrophyllite (X 1).

FIGURE 29.--Macrophotograph of calcite rhombohedral cleavage fragments (X 1.7).

surfaces are smooth but interrupted by other fractures.

Figures 30 and 31 show good cleavage of pyroxene and tremolite.

Fair.--Breaks most readily along cleavage but also fractures easily in other directions; cleavage surfaces are seldom large.

Imperfect.--Breaks about as easily by fracture as by cleavage; cleavage surfaces tend to be small and frequently interrupted.

Cleavage Fragment

Cleavage Fragment.--A fragment produced by the breaking of crystals in directions that are related to the crystal structure and are always parallel to possible crystal faces.

Minerals with perfect cleavage can produce perfect regular fragments. Amphiboles with prismatic cleavage will produce prismatic fragments (fig. 31). These fragments can be elongated and on superficial observation may resemble fibers (figs. 26 and 32). However, because they did not grow as fibers, they cannot have the characteristics of fibers. Consequently,

FIGURE 30. - Macrophotograph of pyroxene showing good cleavage interrupted by uneven fracture (X 1).
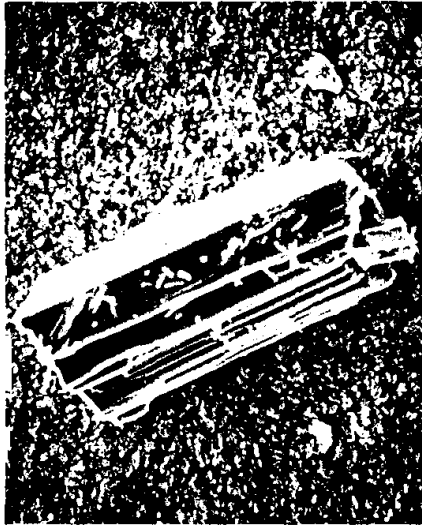
FIGURE 31. - Tremolite, showing good prismatic cleavage (SEM photomicrograph at X 560).

cleavage fragments cannot be called fibers. Minerals do not always break into the same shapes as their growth habits. For example, calcite has many growth habits, but usually breaks into rhombohedral cleavage fragments (fig. 29).

Fracture.--The tendency of a crystal or grain to break in an irregular manner apparently unrelated to crystallographic directions.

Fracture types are as follows:

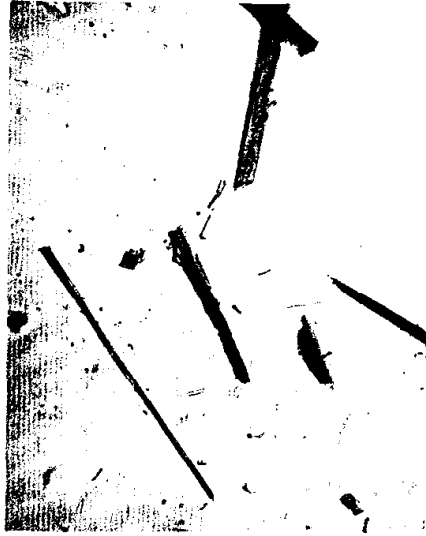Even.--Breaking along relatively smooth planes.

FIGURE 32. - Cleavage fragments of riebeckite (X 500). Particle F has a fibrous appearance.

Uneven.--Breaking along irregular planes.

Splintery.--Breaking into irregular, elongated fragments.

Conchoidal.--Breaking along spherical or conical surfaces.

Hackly.--Breaking with a jagged irregular surface.

Parting.--The tendency of a crystal or grain to break along crystallographic planes weakened by inclusions or structural defects. Different specimens of the same mineral may or may not exhibit parting. Twinned crystals often part along composition planes, which are lattice planes and, therefore, potential crystal faces. Parting is similar to cleavage.

MINERAL IDENTIFICATION AND CHARACTERIZATION

Until recently, emphasis in the United States was placed on occupational exposure of employees manufacturing or using asbestos products for insulation and other applications (29, 33). Regulatory procedures were adopted from those used in Great Britain. The industrial-hygiene identification procedures were acceptable to industry, health, and regulatory organizations because the concern was restricted to several mineral products known collectively as asbestos. Although light optical microscopic procedures counted only the larger particles collected on the air filters, the procedure was adequate for

amphibole minerals at the macroscopic level can be made by optical microscopy, elemental analysis, differential thermal analysis, and X-ray diffraction techniques. For essentially pure samples, these techniques should also be sufficient to identify the individual amphibole minerals based on the elemental composition corresponding to the various members of the solid solution series.

Many macroscopic samples of interest to the occupational and environmental health personnel may contain low percentages of asbestiform minerals (for example, chrysotile in serpentine and tremolite asbestos in talc). As a supplement to optical microscopy, the presence or absence of serpentine or amphibole minerals can be determined in 10- to 100-mg samples by instrumental techniques such as X-ray diffraction, differential thermal analysis, or infrared spectrophotometry. In general, the sensitivity of these instrumental methods is approximately 1.0 weight-percent. Sensitivity is significantly affected by the presence of other minerals that give a response at or near the response peak of the serpentine and amphibole minerals. It is important to note that these methods usually only distinguish between mineral groups; light optical or electron optical microscopy is required to obtain morphological characteristics necessary to identify varieties of the same material.

Chemical characterization is generally necessary to assign a specific mineral name to an amphibole whose structure is known. The amphiboles have been described ($\underline{8}$) using the structural formula $W_{0-1}X_2Y_5Z_8O_{22}(OH,O,F)_2$. Generally, W = Na, K; X = Na, Ca, Mg, Fe^{+2}, Mn; Y = Al, Fe^{+3}, Ti; and Z = Si, Al. In addition to the variation implied by the structural formula, a chemical analysis must take into account inclusions of other minerals that may be present. In contrast to the more formidable task of amphibole chemical characterization, the serpentine minerals generally show little deviation from the formula $Mg_3Si_2O_5(OH)_4$. For either structural or chemical characterization of a macroscopic sample, sufficient time must be spent in sample preparation to insure that relatively pure minerals are being examined.

Microscopic Samples

The petrographic microscope provides a general method by which particles larger than 5 um can be characterized. By observing the optical properties characteristic of the structure and chemistry of a mineral, an experienced microscopist can distinguish amphiboles from serpentines and, in some cases, distinguish individual minerals within these groups ($\underline{7}$). The refractive indices are sufficiently different for the serpentine and amphibole groups to make a distinction between groups by using the appropriate index oil (table 2). There is significant overlap in the range of the three refractive indices among the amphiboles, but a specific index (for example, α, β, or γ) can be determined to aid in identifying the amphibole species. Optical relationships can be confused, however, if the particle consists of fiber bundles or is some other form of crystalline aggregate. The well-known parallel extinction of the commercial asbestos known as Amosite can be used to distinguish that variety from the nonasbestiform varieties of cummingtonite and actinolite. A method of using extinction angles and cleavage directions to distinguish specific asbestiform and nonasbestiform amphiboles has been described ($\underline{37}$); however, this technique is limited to particles with diameters greater than about

correlating health effects to the number of fibers observed. Exact definitions for asbestos-related mineralogical terms were not essential since all three groups (industry, health, and regulatory) clearly understood what was being counted and regulated.

The light optical microscopic procedures used by industrial hygienists were designed for control of asbestos-processing operations in which the chrysotile and asbestiform amphiboles are present as bundles of fibers as well as individual fibers ($\underline{15}$). These bundles may have an average diameter of 0.75 to 1.5 um for chrysotile and 1.5 to 4.0 um for the amphibole asbestos ($\underline{3}$). Particulates of these sizes can be readily observed at a magnification of X 450 to X 500. In contrast, samples from ambient air and personnel air monitors may consist of individual fibrils or small bundles of chrysotile 0.02 to 0.1 um in diameter, and/or amphiboles 0.1 to 0.2 um in diameter ($\underline{3}$). Fibrils and small fibers in this size range are not visible using the conventional light optical microscopic procedures ($\underline{13}$, $\underline{34}$). Therefore, the identification procedures currently used for regulating the U.S. mineral producing and consuming industries must be reexamined to insure that they are both mineralogically correct and applicable to the size range of the particles being regulated.

This discussion will be limited to the selected silicate minerals and their asbestiform varieties listed in table 1. The objective is to point out the particle size at which the minerals can be identified and characterized by various analytical techniques ($\underline{12}$). Detailed descriptions of the various analytical and characterization techniques are available in numerous publications and textbooks and are therefore not included in this report.

A crystalline mineral is defined primarily by its crystal structure and by its definite composition or range of compositions. Therefore, any system of mineral identification should be based principally on crystal structure and chemical criteria. Additional characteristics have to be determined to distinguish varieties. These varieties have similar basic crystal structures and composition, but are usually differentiated macroscopically by the characteristic habits and/or other specific features of the varieties. The objective for this section of the report is to summarize the methodology for identifying the mineral first by mineral group (such as serpentine and amphibole), then by mineral (actinolite, anthophyllite, or chrysotile), and finally by mineral variety.

Macroscopic Samples

At the macroscopic level (easily visible by the unaided eye), the obvious feature of the asbestiform varieties is the presence of fibers that can be easily separated, while the nonasbestiform varieties have a massive, blocky, bladed, or columnar appearance (figs. 2-7). Although chrysotile does occur very rarely in a nonasbestiform habit, in general the distinction between chrysotile and serpentine can be based on the presence or absence of separable fibers. In some serpentine samples where an obvious asbestos texture is not displayed, the distinction between serpentine varieties may require more specialized techniques ($\underline{6}$, $\underline{19}$). The distinction between serpentine and

5 um and cannot be universally applied to all amphiboles. There are many other optical parameters such as pleochroism, sign of the elongation, and color that are easy to obtain. Other parameters such as optic axial angle, optical orientation, and optic sign are relatively more difficult to obtain.

TABLE 2. - Refractive indices for the serpentine group and selected amphibole minerals

	Refractive index	Range of values
Chrysotile...............	α	1.493-1.560
	β	1.504-1.550
	γ	1.517-1.562
Antigorite-lizardite...........	α	1.538-1.564
	γ	1.546-1.573
Anthophyllite...........	α	1.596-1.652
	β	1.605-1.662
	γ	1.615-1.676
Actinolite-tremolite...........	α	1.599-1.668
	β	1.612-1.680
	γ	1.622-1.688
Cummingtonite-grunerite...........	α	1.635-1.696
	β	1.644-1.709
	γ	1.655-1.729
Riebeckite...........	α	1.654-1.701
	β	1.662-1.711
	γ	1.668-1.717

Except for the asbestiform variety, serpentines are usually massive, while amphiboles range from fine-grained massive to columnar or radiating aggregates of prismatic or acicular crystals. Amphiboles in acicular habit may appear to grade into the asbestiform varieties. The characteristic features of this habit may still be seen by electron microscopy. Terms such as "acicular" or "prismatic" may still be applied when seen, but the term "asbestiform" begins to lose its usefulness. For example, how may flexibility be demonstrated in a 2-μm bundle of fibers? As particle size decreases, the inability to manipulate the mineral grains restricts the use of the term "asbestiform" without altering the original sense of the word. High magnification necessitates the use of strictly dimensional terms such as size and aspect ratios to accurately describe the morphology of the amphiboles and serpentines. The degree of morphologic characterization possibly will depend on the magnification being used. An asbestos particle being described as a single fiber at low magnification may be seen to be a bundle of fibers at some high magnification. Therefore, the magnification must be stated in the description. Morphologic characterization using light microscopy can be accomplished on particles as small as a few micrometers. Electron optics can

be used to characterize a wide range of sizes extending down to a few angstroms. Morphologic characterization alone will not identify a mineral without supplemental structural or chemical data.

Structural information on individual particulates can be obtained by use of a transmission electron microscope (TEM) in the selective area electron diffraction mode (SAED). The inclination of the single crystal fragments to the electron beam is very critical since a slight tilt of the crystal may change a relatively simple reciprocal lattice pattern into a very complex one. Consequently, a special goniometer or tilting stage is necessary to obtain easily interpretable diffraction patterns. For the identification of the mineral, a goniometer or tilting stage is even more essential since dependable conclusions cannot be made from measurements on one reciprocal lattice plane. The quality of the SAED pattern is a function of fiber diameter (fig. 33). The larger diameter fibers (>0.5 um) strongly absorb the 60- to 100-kev electrons used in a conventional TEM, while the very small-diameter fibers (<0.2 um) do not give sufficient electron-diffraction intensity. A second problem with small-diameter fibers is the degradation of the single-crystal pattern by diffraction lines from nearby particles. A higher energy TEM, with the resultant greater penetration of the electron beam, can be utilized for large-diameter particles. However, these costly instruments are not widely available.

Although the magnitude of the characteristic C, the distance between the conspicuous layer lines for chrysotile and the amphiboles, is similar in direct space ($d_{001} \sim 5.3A$), the chrysotile pattern has very prominent streaks on these layer lines compared with the spot pattern for the amphiboles (27). Researchers indicate the ability to distinguish between the fibrous and non-fibrous variety of amphiboles by SAED is still to be resolved.

At the very high magnification available with a TEM, chrysotile's hollow-tube (scroll-like) structure, approximately 50 A in diameter, is visible (fig. 16). This hollow-tube structure, together with chemical and structural data regarding the sample, is sufficient to identify the mineral variety. However, the hollow-tube structure is only visible for individual fibrils; fibers (composed of
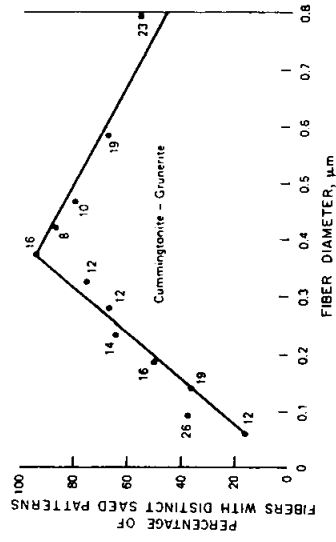

FIGURE 33. - Quality of SAED pattern as a function of amphibole fiber diameter. The values indicated on the graph are the number of fibers examined at each diameter. (Reprinted with permission of D. R. Beaman and D. M. File from Analytical Chemistry (2). Copyright by the American Chemical Society.)
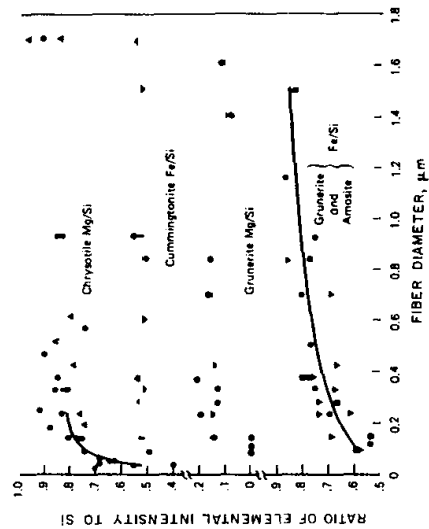
several fibrils) will not display this characteristic because of stacking of the fibrils.

The elemental composition of microscopic grains is determined by either wavelength or energy-dispersive X-ray spectrography in conjunction with scanning or transmission electron microscopy. Extreme care must be taken in the calculation of elemental concentrations from X-ray spectral intensities because the spectral line intensities (FeKα, MgKα, CaKα, relative to SiKα) are dependent on particle diameter for small fibers (2). The particle diameter becomes a significant variable in the spectral intensity-composition relationship below 0.2 um (fig. 34). Carbon contamination from diffusion pump oils must also be considered when analyzing small particles because the longer measuring times required to count sufficient numbers of X-ray photons allows time to build up a contamination layer. This carbon layer preferentially absorbs the lower energy X-ray photons.

Energy-dispersive X-ray spectral calibration data for each scanning or transmission electron microscope must be made using relatively pure standard minerals analyzed by accepted chemical-instrumental techniques. The analyst should be aware that other nearby grains may be contributing to the characteristic X-ray lines because of either penetration of the electron beam through the particles or secondary excitation of nearby particles from primary X-rays generated in the particle being measured. Modern electron optical instruments have electron beams diameters of approximately 0.1 um; however, the sphere of excitation can be several micrometers in diameter as a result of scattered electrons and primary X-rays generated in this particle (26). Conversion of intensity into concentration using accepted computer programs such as "MAGIC" is limited in accuracy because these programs are designed for use with grains or particles several micrometers in diameter or larger, whereas the average mineral fiber diameter is less than 0.5 um for amphiboles and less than 0.1 um for chrysotile. A good example is the diameter size distribution of chrysotile fibers in ambient air samples (table 3). The important point to note is that approximately 95 percent of these chrysotile fibers are 0.12 um or less in diameter. Therefore, quantitative correction procedures applicable to large particles will be of limited value in mineral-fiber identification because the relative X-ray spectral intensities are dependent on fiber diameter below 0.2 um.

FIGURE 34.- Intensity ratio of FeKα, MgKα, or CoKα relative to SiKα as a function of fiber diameter. (Reprinted with permission of D. R. Beaman and D. M. File from Analytical Chemistry (2). Copyright by the American Chemical Society.)

TABLE 3. - Frequency distribution of the width of chrysotile fibers in ambient-air samples,[1] percent

Diameter of chrysotile fibers, um	Sample 1	2	3	4	5	6
0.02-<0.04	10	70	57	17	15	6
.04-<.06	47	24	28	29	33	17
.06-<.08	24	5	8	28	20	49
.08-<.10	14	1	2	12	26	15
.10-<.12	2	0	1	7	3	6
.12-<.14	0	0	2	3	1	6
.14-<.16	0	0	2	1	1	1
.16-<.18	0	0	1	0	1	1
.18-<.20	0	0	0	1	0	1
.20-<.22	0	0	0	1	0	1
.22-<.24	1	0	1	0	0	1
>.24	1	0	0	1	0	1

[1]Samples were collected 1-2 miles from a serpentine rock quarry.

Another problem with the elemental characterization of very small particles is the poor signal-to-background ratio. Longer counting times will help to improve the reliability of the measurement, but the best approach is to minimize the continuum background resulting from the interaction of the electron beam and the same substrate. Figures 35 and 36 show the energy-dispersive X-ray spectra from chrysotile fibers mounted on beryllium oxide (BeO) and beryllium (Be) substrates, respectively. The lower effective atomic number of Be compared with that of BeO results in a reduced continuum, therefore
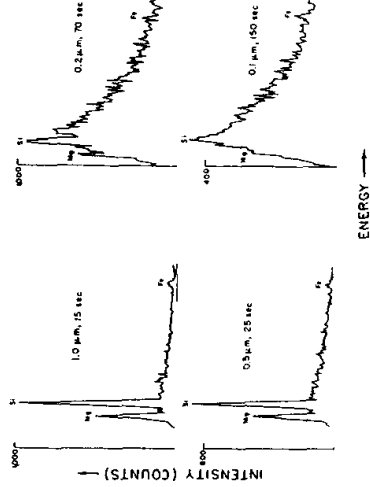
FIGURE 35.- Energy-dispersive X-ray spectra of chrysotile as a function of fiber diameter, BeO substrate (21).

giving an improved signal-to-background ratio.

APPLYING MINERAL TERMINOLOGY TO THE IDENTIFICATION AND CHARACTERIZATION OF PARTICULATES

This section addresses the practical considerations and limitations encountered when applying nomenclature and identification-characterization procedures to regulatory and environmental samples.

Applying Morphological Terminology

One of the obvious features of minerals and their particulates is their morphology or shape. The need for precise definitions of terms such as "asbestiform," "fiber," "cleavage fragment," and "fibril" was explained earlier. These definitions were carefully structured to eliminate ambiguity and to be technically correct. Applying the definitions to samples requires careful thought as to what limits must be placed on interpretations resulting from the use of these terms and other mineralogical concepts. The underlying problem, recognized by both medical and regulatory personnel, is classifying the mineral particle as the asbestiform or nonasbestiform variety. The classification should withstand the test of mineralogical logic and proof. In a mineralogical sense, the source of the mineral particulates must be considered, as explained in the following discussion.

Particulates From a Known Asbestiform Serpentine or Amphibole Source

The definition of asbestiform minerals includes three aspects: morphology, structure, and chemistry. Morphologically, asbestiform mineral varieties separate into flexible fibers or flexible bundles of fibers. Flexible fibers bend readily and only break across the fibers into distinct pieces with some difficulty. Structurally, the asbestiform minerals are limited, in this report and in common practice, to the serpentine and amphibole mineral groups. Chemically, these minerals are all hydroxylated silicates; the term "hydroxylated" is preferred over "hydrated" because these minerals contain OH ions rather than water of crystallization. The serpentines contain approximately 13 weight-percent water; the amphiboles, approximately 2.5 weight-percent water.
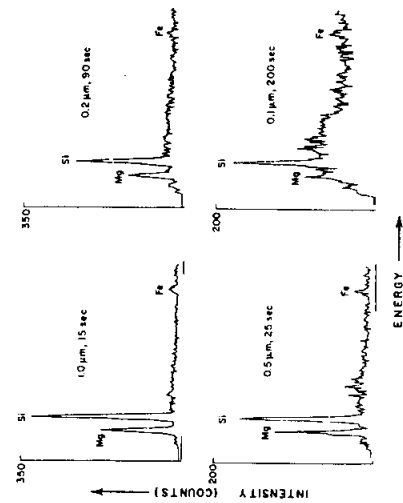

FIGURE 36. - Energy-dispersive X-ray spectra of chrysotile as a function of fiber diameter, Be substrate (21).

For the purpose of this discussion, assume that a hand specimen meeting these requirements is correctly identified as an asbestiform mineral. If this sample is crushed and its fragments examined at various magnifications, its fibrous nature would be apparent, as in figures 14 and 17 to 19. These elongated fragments would be termed "fibers" and "bundles of fibers," and with the other available information would be called asbestiform. As these asbestiform particles are examined at increasing magnification, smaller particles become visible, while the image of large fibers and fiber bundles may exceed the field of the microscope. At increasingly smaller sizes, while fibers or bundles of fibers are still the predominant shape, a few of the fibers are observed to have broken into shorter and shorter segments. (Several short fiber segments are visible in figures 14 and 16.) These very short fiber segments are no longer described as fibers, but would be classified as fragments of fibers, or cleavage fragments if one or more cleavage planes govern their shape. Therefore, a known asbestiform sample would show an increase in the ratio of fiber fragments to fibers with a decrease in particle size.

Particulates From a Known Nonasbestiform Serpentine or Amphibole Source

If the hand specimen discussed previously does not separate into flexible fibers or bundles of fibers, the mineral would not be considered asbestiform. However, the specimen would be classified as serpentine or amphibole if the specific mineral is identified on the basis of optical properties, chemistry, and structure.

If crushed fragments of this known nonasbestiform mineral are examined at various magnifications, the particles would be primarily cleavage fragments, or irregularly broken fragments if cleavage does not govern breakage. However, a few elongated particles may resemble a fiber in appearance to the degree that they may be indistinguishable morphologically from fibers derived from an asbestiform mineral sample. Figures 26 and 32 for tremolite and riebeckite, respectively, show cleavage fragments with fibrous shapes that could be incorrectly identified as fibers.

What can be stated morphologically about particles derived from crushing a known nonasbestiform mineral is that most of the particles are cleavage fragments with nonasbestiform texture; a few are fibrous in appearance, particularly at low magnification; and all of the particles are known to be derived from a nonasbestiform source.

Comparison of Particulates From Known Serpentine and Amphibole Minerals and Their Asbestiform Varieties

The appearance of particles generated by milling known serpentine and amphibole minerals and their asbestiform varieties is shown in figures 37 to 40. The samples shown in figures 37 to 39 were photographed using light optical microscopy at three magnifications to show that, at decreasing size (depicted by increasing magnification), the original habit generally persists. For the nonasbestiform amphibole minerals, there were a few elongated particles from the riebeckite and tremolite. Elongated particles of this type
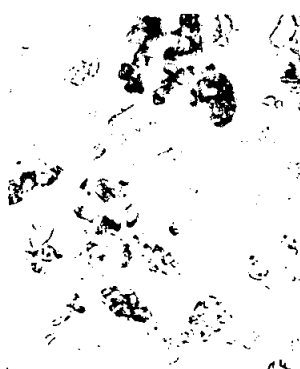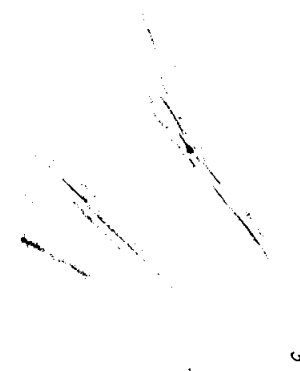
FIGURE 38. - Light optical photomicrographs of crocidolite and riebeckite at three magnifications; Crocidolite (left) at A, X 100; B, X 500; and C, X 950. Riebeckite (right) at D, X 100; E, X 500; and F, X 950.
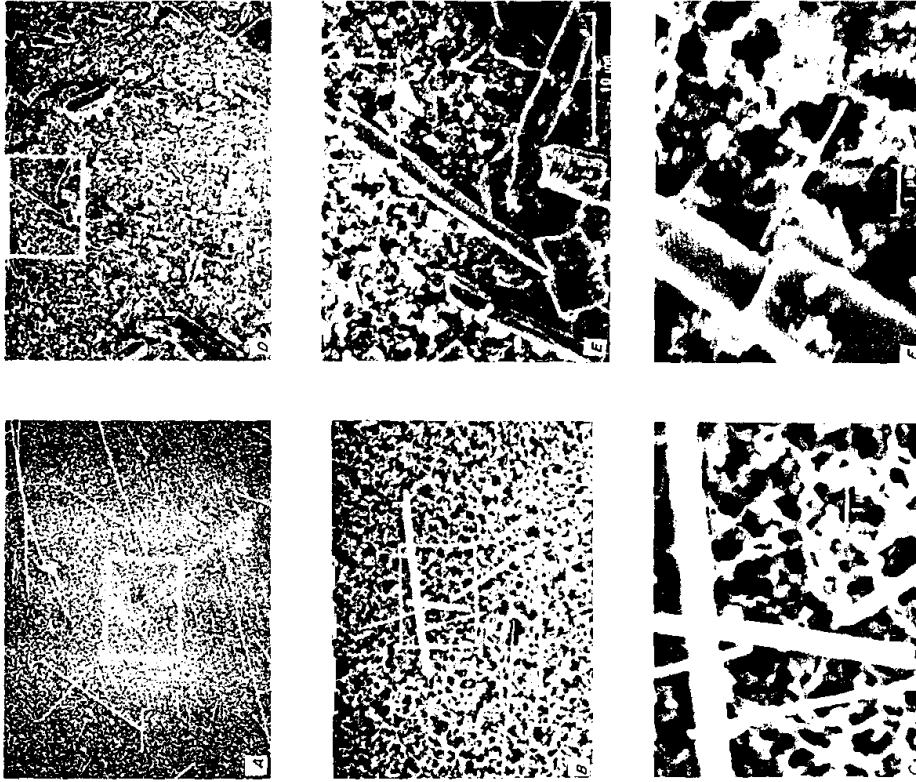

FIGURE 37. - Light optical photomicrographs of chrysotile and antigorite-lizardite at three magnifications. Chrysotile (left) at A, X 100; B, X 500; and C, X 950. Antigorite-lizardite (right) at D, X 100; E, X 500; and F, X 950.

FIGURE 40. - SEM photomicrographs of crocidolite and riebeckite at three magnifications: Crocidolite (left) at A, X 500; B, X 2,500; and C, X 10,000. Riebeckite (right) at D, X 500; E, X 2,500; and F, X 10,000. Rectangles indicate the area shown at the next higher magnification.
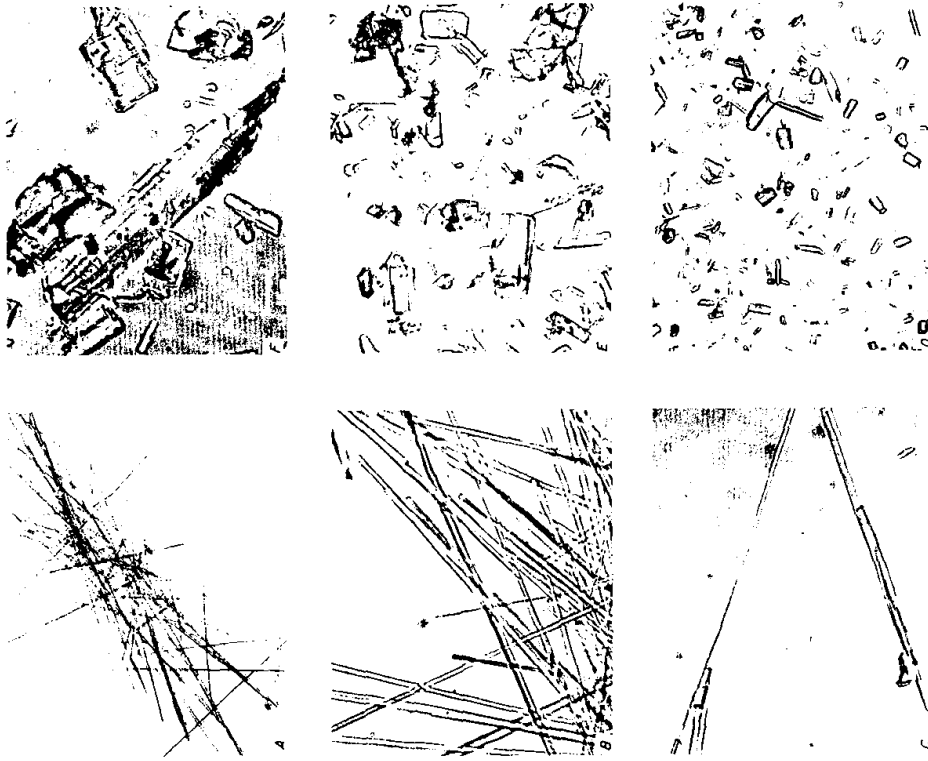
FIGURE 39. - Light optical photomicrographs of tremolite asbestos and tremolite at three magnifications. Tremolite asbestos (left) at A, X 100; B, X 500; and C, X 950. Tremolite (right) at D, X 100; E, X 500; and F, X 950.

are typical of the prismatic cleavage of amphiboles. To increase optical contrast, the serpentine group samples were dispersed in an immersion oil considerably below the refractive indices for the serpentine.

Riebeckite and crocidolite particles are compared at higher magnifications in figure 40. The outlined areas in the scanning electron micrographs indicate the area displayed at the next higher magnification. Again, note the presence of a few elongated cleavage fragments of riebeckite visible at the higher magnification. In contrast, the aspect ratio of the crocidolite will decrease with decreasing particle size because the individual fibers cannot cleave further along the fiber axis; they can only break into shorter segments.

Aspect Ratio

Existing regulatory standards are based on counting specific mineral particulates with aspect ratios of 3 to 1 or greater. This report emphasizes that the aspect ratio has little mineralogical significance for individual particulates but is applicable to a large number of particles. A few relatively long thin particles are produced as cleavage fragments from the crushing and grinding of many nonasbestiform minerals. Conversely, similar milling treatment will result in a few short segments of true fibers from the asbestiform varieties. However, statistically, the length-to-width characteristics of the milled amphiboles and serpentine and their asbestiform varieties are significantly distinct, as shown by the data in figures 41-44.

Figures 41, 42, and 43 show the frequency polygons of the aspect ratio distribution for milled samples of the normal nonasbestiform variety of three amphiboles--anthophyllite, tremolite, and hornblende, respectively. Note that in all three examples, approximately 70 percent of the particles have an
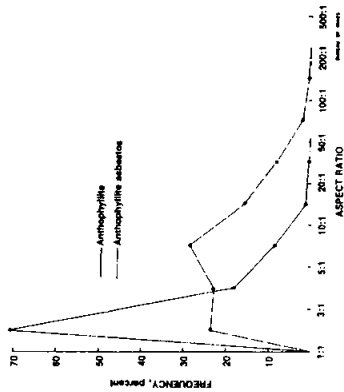
aspect ratio of less than 3 to 1, and 95 percent of the particles have a length-to-width ratio of less than 10 to 1. The frequency distribution maximums of the aspect ratios for milled anthophyllite asbestos and tremolite asbestos are significantly higher than those for the normal, nonasbestiform variety. Thirty to forty percent of the asbestiform particulates are in the 10-to-1-or-longer class, with a significant number of particles having an aspect ratio greater than 20 to 1.

Figure 44 shows the distribution frequencies for a milled commercial grade of chrysotile asbestos and for chrysotile particulates collected on ambient air filters in the vicinity of a serpentine rock quarry. For the commercial-grade chrysotile, over 50 percent of the particles have an aspect ratio greater than 50 to 1, whereas the frequency distribution for the ambient air sample has a maximum between 10 to 1 and 20 to 1. These results are anticipated because the higher aspect ratios for the commercial-grade chrysotile are characteristic of the significantly longer starting material.

All of the aforementioned samples except the ambient air were milled, then dispersed in water for collection on a suitable substrate. The samples were then measured using electron microscopy at magnifications

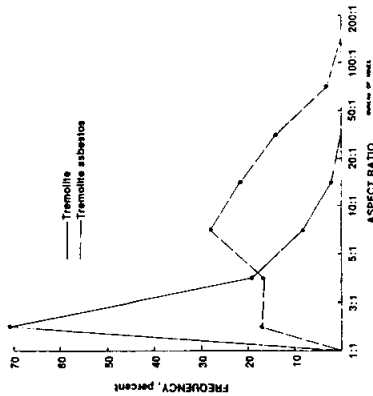FIGURE 41.- Frequency polygons for the aspect ratios of anthophyllite and anthophyllite asbestos.

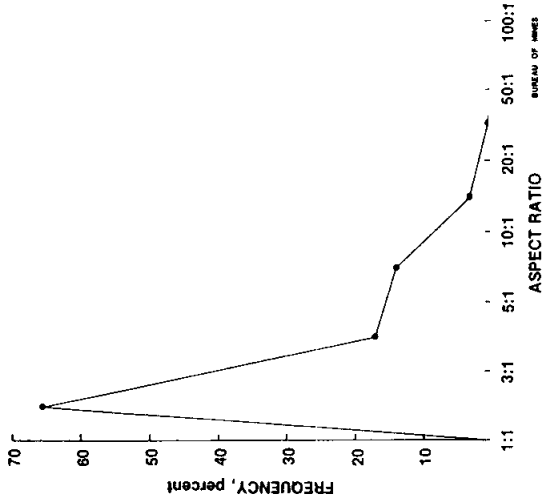FIGURE 42.- Frequency polygons for the aspect ratios of tremolite and tremolite asbestos.

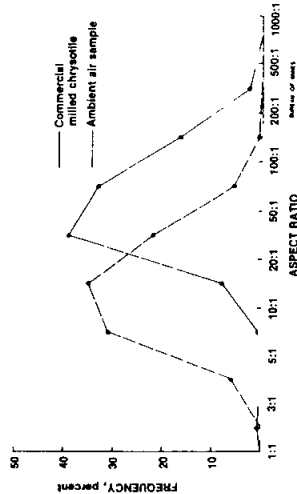FIGURE 43.- Frequency polygons for the aspect ratio of hornblende.

FIGURE 44.- Frequency polygons for the aspect ratios of commercial-grade chrysotile and chrysotile in ambient air.

of 5,000 to 10,000. The ambient air sample, collected near a serpentine rock quarry, was measured using a TEM with magnifications of X 5,000 to X 32,000.

Based on these data, one test for distinguishing the presence or absence of the asbestiform variety of a mineral could be an examination of the frequency distribution of the aspect ratio for that mineral. Assuming positive identification of the mineral type, then the designation of variety would be based both on particle morphology and the frequency maximum of the aspect ratio. Cleavage fragments will generally have a frequency maximum less than 3 to 1, whereas the asbestiform varieties will fall between 10 to 1 and 20 to 1 or higher, depending on the characteristics of the mineral and the history of the sample, particularly the type and degree of milling. If any shape or size limits are placed on characterizing mineral particulates, such limits should be based on medical evidence or on some limitation of the characterizing technique and so stated.

Particulates From Unknown Sources

Samples such as environmental airborne or waterborne mineral particulates collected at a considerable distance from a possible source are examples of particulates from an unknown source. The samples could have been collected at a location so distant from a known source that other mineral particulates originating from other sources compose most of the sample.

The source of the particulates in an environmental sample may be located by taking additional samples at selected intervals in the direction of, and closer to, the suspected source. However, several factors must be considered: The direction of air and water currents with respect to the suspected source, and the proximity to and direction of other sources with regard to the suspected source. One study found very low concentration of airborne chrysotile upwind from a source compared with a concentration two orders of magnitude greater downwind (14). Another important consideration is the level of natural or human disturbances of particulates; for example, strong versus weak winds, or heavy versus light vehicle traffic. In some instances, it may be possible to identify the source if the mineral particulates of interest have unique trace elements or combinations of elements that are specific to the probable mining or milling operation emitting the particulates. Detailed elemental analysis using the X-ray spectral capabilities of an SEM or TEM is required on both the suspected source and the particulates.

APPLICATIONS

The following examples illustrate the application of mineral terminology and identification-characterization procedures to three types of problems: (1) chrysotile determination in ambient-air samples collected near a serpentine rock quarry, (2) identification of asbestiform minerals in ceilings and walls of public buildings, and (3) characterization of a mineral product. These examples illustrate, in order, the need for higher magnification than available with the light optical microscope, the use of various characterization techniques to screen and identify asbestiform minerals, and the judgment of the analyst in distinguishing cleavage fragments and asbestiform particles.

Ambient-Air Samples Collected Near Serpentinite Rock Quarry

The Bureau of Mines is working with State and Federal officials to measure mineral particulates in ambient-air samples collected in the vicinity of a serpentine rock quarry. Optical microscopic procedures at about X 500 are limited to the identification of mineral particulates longer than 5 um with an aspect ratio of 3 to 1 or larger (criteria set by the Mining Enforcement and Safety Administration and the Occupational Safety and Health Administration). The mineralogist can further identify the particles as belonging to the serpentine, amphibole, or other mineral group with index oils (table 2).

FIGURE 45.- Macrophotograph showing chrysotile veins in serpentine rock (X 1).

The serpentine rock in the quarry is interlaced with small veins of chrysotile (fig. 45). Optical microscopic procedures used for industrial hygiene are adequate for the detection of large chrysotile fiber bundles. These fiber bundles of commercial-grade chrysotile can be several micrometers or larger in diameter (fig. 46). In contrast, the mining and crushing operations in the quarry plus transport of particulates over a distance breaks bundles of fibers down to fibers or fibrils with diameters of 250 to 1,000 A (table 3).
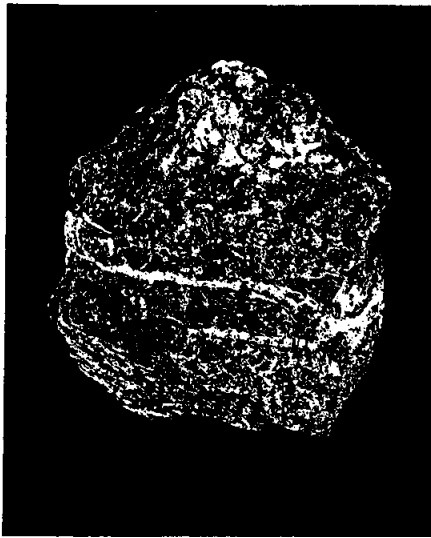

FIGURE 46.- Chrysotile bundle (SEM photomicrograph at X 5,000).

FIGURE 47. – Mixture of nonasbestiform serpentine and chrysotile at five magnifications: A, X 450; B, 2,250; C, X 9,000; D, 1,800; and E, X 18,000. Rectangles indicate the area shown in the next panel.

Figure 47 is a series of SEM photomicrographs of a mixture of chrysotile and nonasbestiform serpentine handpicked from a small vein in the serpentine rock quarry. Note that at X 450 (corresponding to the optical microscope magnification), only one or two bundles of chrysotile are faintly visible; the predominant particles are the nonasbestiform serpentine. As the magnification is increased, the high concentration of chrysotile fibers becomes readily visible. The fiber diameter size data in table 3 indicate that more than 95 percent of the chrysotile fibers in these ambient air samples are below the limit of resolution of the optical microscope. Although many other scientists have pointed out the limitation of the optical procedures for chrysotile in ambient air, there is a need for continuous emphasis that higher magnification techniques are necessary for environmental and regulatory samples.

Asbestos in Ceiling and Wall Materials

A possible environmental hazard is the release of asbestos from ceilings and walls in homes, churches, schools, and various other public and commercial buildings. Because of the very high number of potential samples to be examined by various State or Federal agencies, a rapid and reliable screening procedure is necessary to identify those samples that warrant further tests. Three complementary analytical methods for screening, identification, and semiquantitative estimate of the asbestiform mineral concentration are X-ray diffractometry, differential thermal analysis, and microscopy (light optical and scanning electron).

The screening identification procedures can be relatively simple because chrysotile is the principal asbestos mineral used for building insulation materials, with Amosite used to a much lesser extent. In 18 samples from a midwestern municipal health department, chrysotile was a major constituent (>50 weight-percent) in 2 samples, a minor constituent (1 to 10 weight-percent) in 12 samples, and not detected in 4 samples. Other minerals present in various concentrations in these samples were calcite, quartz, gypsum, and mica. Amosite was found as a major constituent in the ceiling of an older building located on a university campus.

The presence of either serpentine or amphibole minerals in the insulation materials can be used as a probable indication of asbestos. Therefore, screening tests are based on the presence or absence of characteristic differential thermal analysis or X-ray diffraction peaks of either serpentine or amphibole minerals. For the positive samples, confirmation of the presence of the asbestiform variety requires some type of microscopic examination because the thermal and X-ray diffraction methods do not identify the mineral variety.

Differential thermal analysis provides a detectable signal from chrysotile at 0.5 to 1.0 weight-percent, as indicated by the curves shown in figure 48. Note the increase in the endothermic (A) and exothermic peaks (B) upon addition of about 5 weight-percent chrysotile to a sample taken from a school ceiling. The sensitivity of differential thermal analysis for the amphibole minerals is significantly poorer because the H_2O content of amphiboles is approximately 2.5 percent compared with about 13 percent for chrysotile. The sensitivity of the X-ray diffraction method also ranges from 0.5 to
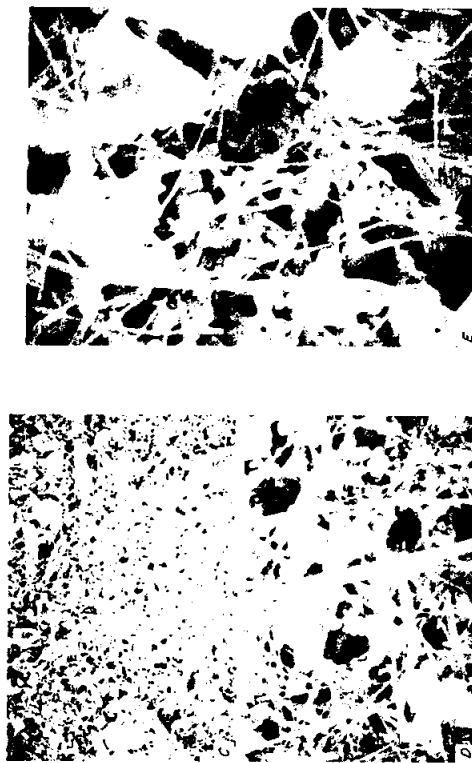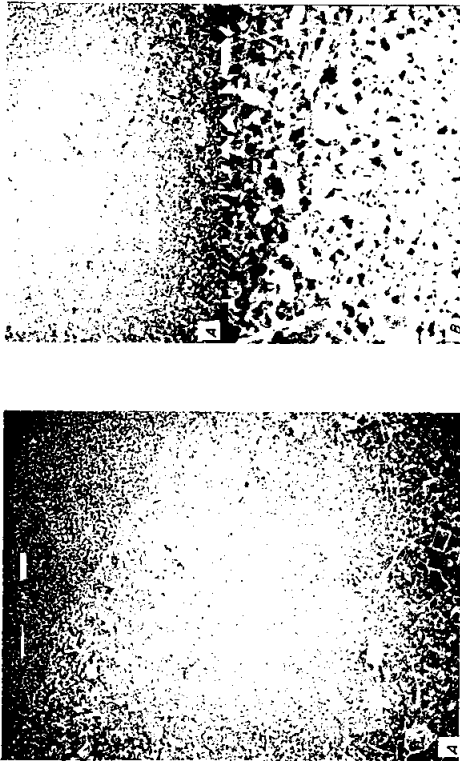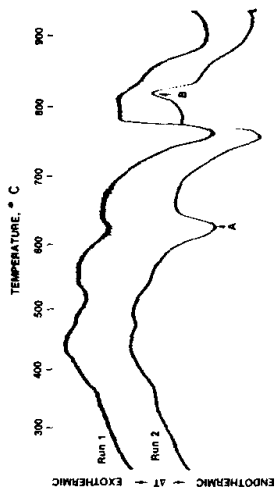
1.0 weight-percent. An X-ray diffractometer scan of the 2θ range for major serpentine peaks is shown in figure 49. The magnitude of the characteristic peaks for chrysotile are a function of several factors, including degree of fiber orientation and the type of milling or crushing used to process the sample. Also, the sensitivity of both methods is affected by the presence of other minerals that have characteristic thermal or diffraction peaks in the same region as those of the minerals of interest.

Some samples will be composed of a mixture of synthetic and natural fibers, such as the mixture of fiberglass and chrysotile shown in figure 50. Generally, it is not difficult to identify the synthetic fibers based on their larger diameter and the more uniform appearance.

Amphiboles and Talc

Asbestos-related health regulations are having a significant impact on the domestic talc industry from occupational exposure at the mines and mills and at various manufacturing plants that use talcs in their operations. Certification that the talc does or does not contain asbestiform minerals is important because the occupational health requirements are much more restrictive if the talc is designated as containing asbestiform serpentine or amphibole minerals.

FIGURE 48. - Differential thermal analysis of sample from school ceiling, showing endothermic (A) and exothermic (B) peaks of serpentine. Run 1 is the sample as received; run 2 is a mixture of 95 pct of the as-received sample and 5 pct chrysotile.
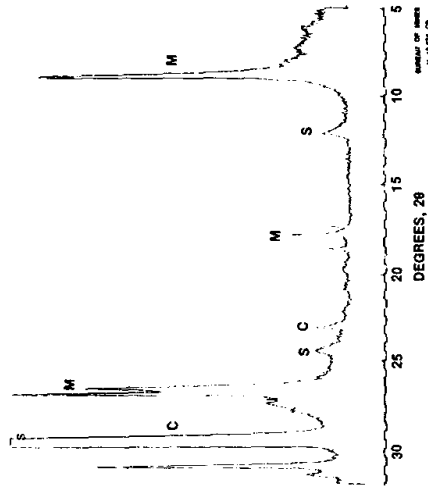

FIGURE 49. - X-ray diffractometer scan of sample from school ceiling, showing the presence of calcite (C), mica (M), and serpentine (S).

Talc is both the name of a specific mineral, $Mg_3Si_4O_{10}(OH)_2$, and a commercial term for a mixture of minerals ranging from essentially 100 percent talc to blends where the mineral talc is a minor constituent (12, 23). Semiquantitative estimation of the serpentine and/or amphibole mineral concentration, if present, can be obtained by X-ray diffraction and differential thermal analysis. Several talc deposits contain a variable amount of tremolite. Therefore, the essential question faced by the analyst is whether or not the tremolite is fibrous. Figure 51 shows the typical platy morphology of talc; no tremolite (amphibole) was detected in this sample by X-ray diffraction. Figure 52 illustrates the type of particles obtained from a mixture of tremolite and platy talc. The cleavage fragments of tremolite are typical of the nonasbestiform variety. Better judgment is required of the analyst
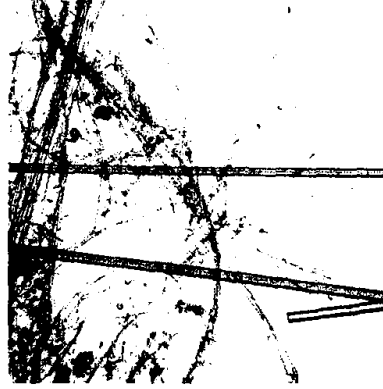

FIGURE 50. - Sample from university building, showing a mixture of chrysotile and fiberglass (X 140).

with the type of sample illustrated in figure 53. This sample consists of platy talc, cleavage fragments of tremolite, and minor to trace amounts of fibrous tremolite. For this latter sample, the 3-to-1 aspect-ratio criteria would greatly overestimate the number of fibrous tremolite particles collected on air filters or other monitors.

FIGURE 51. - Typical platy morphology of talc (X 600).

Fundamental studies should be conducted to determine if there are unique chemical and physical characteristics of a mineral fiber as compared to elongated cleavage fragments. For example, the surface properties of chrysotile are similar to those of magnesium hydroxide, whereas the nonasbestiform varieties of serpentine have the surface characteristics of a silicate (30). Variations in surface properties, if any, between asbestiform particles and cleavage fragments of amphiboles should be investigated. Surface characterization techniques to be considered should include Auger electron spectrography and low-energy X-ray spectrography. Research at the University of Minnesota indicates that asbestos fibers have an extensive surface charge over the whole surface, whereas cleavage fragments have a significantly lower surface charge (40). Extinction angle measurements are another possible approach to distinguishing asbestiform from the nonasbestiform varieties of amphiboles (37).

There is a critical need to reexamine the 3-to-1 aspect ratio as a criterion for a mineral fiber. The aspect ratio for fibers from asbestiform minerals were as much as 200 to 1 or higher, whereas the ratio for cleavage fragments is about 3 to 1, as illustrated by the data in this report. The 3-to-1 aspect ratio may be valid for the industrial hygiene control of asbestos-processing plants; however, its applicability to existing nonasbestos mining and ore processing plants requires critical evaluation. There is also need to evaluate the restriction of the mineral particulate measurements to light optical microscopy because many particulates of interest, especially chrysotile fibrils, are not visible by this technique. Low-cost scanning electron microscopes are in the same price range as research-grade petrographic microscopes, and the skill requirements for the operator are comparable for both instruments.

Particulate measurements by microscopic procedures are time consuming and expensive. Two possible approaches to reducing the time and cost are (1) automation of the particulate identification-characterization measurements using computerized image analyzers and (2) development of chemical reagents that give a specific response with either chrysotile or the various asbestiform amphibole minerals. Using the chemical-reagent approach, mass-concentration values could be obtained by measurement of some response such as color, ultraviolet fluorescence, X-ray spectral intensity, etc.

Health studies related to inhalation and ingestion of fibers have been essentially limited to well-defined commercial types of asbestos. The fundamental question to be resolved is the biological effects of cleavage fragments compared with those of true mineral fibers. If shape and size are the critical parameters, the analyst could establish and measure suitable analytical parameters to monitor the particulates of interest. Likewise, if the health scientists find a correlation between health and the amount of trace metals, adsorbed organics, surface area, etc., the analyst can respond accordingly. Therefore, there is a primary need for an adequate quantity of well-characterized amphiboles and serpentine of both the normal and asbestiform varieties for use in health-related studies.

RESEARCH NEEDS

There are several areas in particulate identification-characterization where further research is warranted. Areas of research that are immediately applicable to asbestos are briefly summarized.

Commercially available electron optical instruments are generally limited to morphological characterization for mineral particles with diameters less than 0.2 μm. As pointed out in the identification-characterization section, both the signal-to-background ratio for energy dispersive X-ray spectra and the SAED pattern are significantly degraded for elongated particles less than 0.2 um in diameter. Field emission electron optical microscopes with their higher vacuums and smaller beam diameter may have some advantages over conventional SEM instruments. Also, other microprobe techniques, in particular ion microprobe mass spectrographs and laser Raman microprobes, should be evaluated for particulate characterization.

Although electron microscopic methods can generally positively identify chrysotile in air and water samples, the quantitative aspects of the measurements need substantial improvement. Sample treatment and measurement errors need to be isolated from sampling variance.
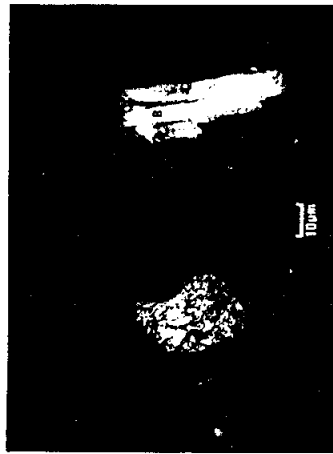

FIGURE 52. - Platy talc (A) and tremolite cleavage fragment (B) (X 640).

FIGURE 53. - Platy talc, tremolite cleavage fragments, and a fibrous tremolite particle (A) (X 400).

Because of the ambiguity of fiber counts, results should be reported both in mass equivalents and in fibers per unit volume.

REFERENCES

1. Ampian, S. G. Asbestos Minerals and Their Nonasbestos Analogs. Proc. Electron Microscopy of Microfibers, Pennsylvania State University, University Park, Pa., Aug. 23-25, 1976, 11 pp.; available from S. Ampian, Bureau of Mines, Washington, D.C.

2. Beaman, D. R., and D. M. File. Quantitative Determination of Asbestos Fiber Concentrations. Anal. Chem., v. 48, January 1976, pp. 101-110.

3. Berger, H. Asbestos Fundamentals. Chemical Publishing Co., New York, 1963, 171 pp.

4. Champness, P. E., G. Cliff, and G. W. Lorimer. The Identification of Asbestos. J. Microscopy, v. 108, December 1976, pp. 231-249.

5. Commission of the European Communities. Public Health Risks of Asbestos. Pergamon Press, New York, 1977, 149 pp.

6. Cressey, B. A., and J. Zussman. Electron Microscopic Studies of Ser-pentinites. Canadian Mineralogist, v. 14, 1976, pp. 307-313.

7. Deer, W. A., H. A. Howie, and J. Zussman. Rock Forming Minerals. John Wiley & Sons, Inc., New York, 1963, 5 v.

8. Ernst, W. G. Earth Materials. Prentice-Hall, Inc., New York, 1969, 149 pp.

9. Franco, M. A., J. L. Hutchison, D. A. Jefferson, and J. M. Thomas. Structural Imperfection and Morphology of Crocidolite (Blue Asbestos). Nature, v. 266, Apr. 7, 1977, pp. 520-521.

10. Gary, M., R. McAfee, Jr., and C. L. Wolf. Glossary of Geology and Related Sciences. American Geological Institute, Washington, D.C., 3d ed., 1972, 805 pp.

11. Goodwin, A. (comp.). Proceedings of the Symposium on Talc, Washington, D.C., May 8, 1973. BuMines IC 8639, 1974, 102 pp.

12. Hamer, D. H., F. R. Rolle, and J. P. Schelz. Characterization of Talc and Associated Minerals. J. American Industrial Hygiene Association, v. 37, May 1976, pp. 296-304.

13. Harwood, C. F., and G. Yamate. The Detection and Quantification of Asbestos Present in the Environment. Proc. 3d Internat. Conf. on the Physics and Chemistry of Asbestos Minerals, Aug. 17-21, 1975, Univer-sité Laval, Quebec, 1975, 21 pp.

14. John, W., A. Berner, G. Smith, and J. J. Wesolowski. Experimental Deter-mination of the Number and Size of Asbestos Fibers in Ambient Air. Calif. State Department of Health, Rept. AIHL/SP-1, January 1976, 36 pp.

15. Journal of the American Industrial Hygiene Association. Recommended Procedures for Sampling and Counting Asbestos Fibers. V. 36, February 1973, pp. 83-90.

16. Kuryvial, R. J., R. A. Wood, and R. E. Barrett. Identification and Assessment of Asbestos Emissions From Incidental Sources of Asbestos. Environmental Protection Agency Rept. EPA-650/2-74-087, 1974, 286 pp.

17. Langer, A. M. Approaches and Constraints to Identification and Quanti-fication of Asbestos Fibers. Environmental Health Perspectives, v. 9, 1974, pp. 133-136.

18. McCrone, W. C., and J. G. Delly. The Particle Atlas. Ann Arbor Science Publishers, Inc., Ann Arbor, Mich., 1973, 4 v.

19. Mumpton, F. A., and C. S. Thompson. Mineralogy and Origin of the Coalinga Asbestos Deposit. Clays and Clay Minerals, v. 23, 1975, pp. 131-143.

20. Page, N. J., and R. G. Coleman. Serpentine-Mineral Analyses and Physical Properties. U.S. Geol. Survey Prof. Paper 575-B, 1967, pp. B103-B107.

21. Pattnaik, A., and J. D. Meakin. Development of Scanning Electron Micros-copy for Measurment of Airborne Asbestos Concentrations. Environmental Protection Agency Rept. 650/2-75-029, January 1975, 84 pp.

22. Rabbitt, J. C. A New Study of the Anthophyllite Series. Am. Mineralo-gist, v. 33, 1948, pp. 263-323.

23. Rohl, A. N., A. M. Langer, I. J. Selikoff, A. Tordini, R. Klimentidis, D. R. Bowes, and D. L. Skinner. Consumer Talcums and Powders--Mineral and Chemical Characterization. J. Toxicology and Environmental Health, v. 2, 1976, pp. 255-284.

24. Ross, M. Geology, Asbestos, and Health. Environmental Health Perspec-tives, v. 9, 1974, pp. 123-124.

25. _____ The Problem of Defining and Characterizing "Asbestos." Paper pres. at Electron Microscopy of Microfibers Symp., Pennsylvania State University, University Park, Pa., Aug. 23-25, 1976; available from W. J. Campbell, Bureau of Mines, College Park, Md.

26. Rubin, I. B., and C. J. Maggiore. Elemental Analysis of Asbestos Fibers by Means of Electron Probe Techniques. Environmental Health Perspec-tives, v. 9, 1974, pp. 81-94.

27. Ruud, C. O., C. S. Barrett, P. A. Rissell, and R. L. Clark. Selected Area Electron Diffraction and Energy Dispersive X-Ray Analyses for the Identification of Asbestos Fibres, a Comparison. Micron, v. 7, 1976, pp. 115-132.

28. Saffiotti, U., and J. K. Wagoner, eds. Occupational Carcinogens. Annals of the New York Academy of Sciences, v. 271, 1976, 516 pp.

29. Shapiro, H. A. (ed.). Proceedings International Conference on Pneumoconiosis, Johannesburg, South Africa, April 24-May 2, 1969. Oxford University Press, London, 1970, 652 pp.

30. Speil, S., and J. P. Leineweber. Asbestos Minerals in Modern Technology. Environmental Research, v. 2, 1969, pp. 166-208.

31. Thompson, C. S. Asbestos in Your Future. Min. Cong. J., December 1976, pp. 35-40.

32. Thrush, P. W. A Dictionary of Mining, Mineral, and Related Terms. BuMines Special Pub. 2-68, 1968, 1269 pp.

33. U.S. Department of Health, Education, and Welfare. Criteria for a Recommended Standard—Occupational Exposure to Asbestos. HSM72-10267, 1972, 130 pp.

34. Wesolowski, J. J. Asbestos in the California Environment. California State Department of Health, Rept. AIHL 164-A, June 1975, 24 pp.

35. Whittaker, E. J. W. The Structure of Bolivian Crocidolite. Acta Cryst., v. 2, 1949, pp. 312-317.

36. World Health Organization. IARC Monographs on the Evaluation of the Carcinogenic Risk of Chemicals to Man: Asbestos. Albany, N.Y., v. 14, 1977, 106 pp.

37. Wylie, A. Optical Properties of Asbestiform Amphiboles and Their Nonasbestiform Analogs. Available from A. Wylie, Bureau of Mines, College Park, Md.

38. Yada, K. Study of Chrysotile Asbestos by a High Resolution Electron Microscope. Acta. Cryst., v. 23, 1967, pp. 704-707.

39. Zoltai, T., and J. H. Stout. Comments on Asbestiform and Mineral Fragments Relative to Reserve Mining Company Taconite Deposits. Minnesota Pollution Control Agency, Minneapolis-St. Paul, Minn., Mar. 24, 1976, 54 pp.

40. Zoltai, T., I. Veres, R. F. Hammer, and M. Y. Wagner. Surface Charges of Asbestiform Amphibole Fibers. 1977, 9 pp.; available from T. Zoltai, Bureau of Mines, College Park, Md.

968) "A Simple Dispenser
Reference Samples of As-

J A. M. Johnston (1981)
A Study of Its Causes,
Lungs of Rats," *Am. Ind.*

it Dust Particles," *Staub*

scope Eyepiece Graticule
ip. Hygiene 20:19.
h Concentrations of Small

ed Particles in Cylindrical

f Charged Particles from
.hannel by Image Force,"

CHAPTER 47

SIZE AND SHAPE CHARACTERISTICS OF AMPHIBOLE ASBESTOS (AMOSITE) AND AMPHIBOLE CLEAVAGE FRAGMENTS (ACTINOLITE, CUMMINGTONITE) COLLECTED ON OCCUPATIONAL AIR MONITORING FILTERS

Robert L. Virta, Kim B. Shedd, Ann G. Wylie and Janet G. Snyder

Avondale Research Center
Bureau of Mines
U.S. Department of the Interior
Avondale, Maryland

ABSTRACT

The objective of this study by the Bureau of Mines (BOM) was to determine if particle populations from asbestiform and nonasbestiform mineral sources can be distinguished through least-squares regression analyses using the relationship:

$$\log_{10} \text{width} = F \log_{10} \text{length} + b$$

where   F = fibrosity index, the slope of the regression line
        b = intercept on the $\log_{10}$ width axis

Amphibole particles on air monitoring filters from three mining and two industrial sites were characterized by scanning electron microscopy (SEM) and energy-dispersive X-ray spectroscopy (EDS) analysis. The data are evaluated using particle length and width summary statistics and compared with analyses by linear regression.

Conclusions based on comparison of data manipulation using these two techniques follow: The mining site particle populations are morphologically

similar, the industrial site particle populations are morphologically similar, and size and shape characteristics of mining site populations are statistically different from those of the industrial sites. Determination of either an asbestos or a nonasbestos source of amphiboles using linear regression techniques on data obtained from examination of air monitoring filters is a potential application of this technique.

INTRODUCTION

The purpose of this study by the BOM Particulate Mineralogy Unit, was to determine if particle populations collected on air monitoring filters from asbestiform and nonasbestiform amphibole mineral sources can be distinguished by the application of least-squares regression analysis to size and shape characteristics. Amphiboles collected on air monitoring filters from three mining sites where nonasbestiform amphiboles are major rock-forming minerals and two industrial sites employing commercial amphibole asbestos were characterized, and the data were statistically evaluated.

' Airborne amphibole particles at mining and industrial sites are of interest to health scientists and regulatory agencies because of adverse health effects resulting from exposure to airborne amphibole asbestos [Selikoff and Hammond, 1979]. To regulate asbestos exposure in the occupational environment, air monitoring filtration techniques are used to determine the amount of asbestos suspended in the air. At present, federal regulations define chrysotile, amosite, crocidolite, tremolite, actinolite and anthophyllite particles as asbestos if they are $\geqslant 5$ μm in length and $\leqslant 5$ μm in width, possess straight sides, and have aspect ratios $\geqslant 3:1$ [OSHA 1975]. This definition does not distinguish between amphibole asbestos fibers and cleavage fragments of nonfibrous amphiboles [Campbell et al. 1977].

Siegrist and Wylie [1980] characterized the size and shape of amphibole particles in monomineralic bulk samples and compared their populations using the linear regression relationship:

$$\log_{10} \text{width} = F \log_{10} \text{length} + b \qquad (1)$$

where   F = slope of the regression line = fibrosity index, a measure of the dependence
          of width on length
        b = intercept on the log width axis

As shown by Wylie [1979], F may be used to distinguish amphibole cleavage fragments, the widths of which increase with increasing length, from amphibole asbestos fibers, which display relatively constant widths.

In the present study, the linear least-squares regression of log width vs log length is applied to amphibole particles collected on air monitoring filters

morphologically similar,
ulations are statistically
:rmination of either an
 using linear regression
·f air monitoring filters

Mineralogy Unit, was to
monitoring filters from
al sources can be dis-
ion analysis to size and
monitoring filters from
are major rock-forming
:ial amphibole asbestos
lated.
·ial sites are of interest
· adverse health effects
sbestos [Selikoff and
 in the occupational
used to determine the
eral regulations define
e and anthophyllite
i μm in width, possess
975]. This definition
·rs and cleavage frag-

l shape of amphibole
ed their populations
 ·*·

(1)

isure of the dependence

ı amphibole cleavage
length, from amphi-
·hs.
 of log width vs log
r monitoring filters

and compared with values obtained by Siegrist and Wylie [1980] on bulk samples. A potential application of this technique is the determination of an asbestiform or nonasbestiform source of amphiboles collected on air monitoring filters from various mining and industrial sites. As with any characterization technique, the results are only as good as the samples. Extrapolation from bulk mineral characterizations to classification of particles on air filters must be done with caution, since the assumption is not always valid that the source of the particles is either asbestos or nonasbestos. Particles from veins of asbestos can be present in air samples from operations in essentially nonasbestiform mineral deposits. In addition, sorting may occur in air currents and result in selective deposition of particles. For these two reasons, air monitoring filter samples may not be representative of a whole deposit.

SAMPLES

Air monitoring filters were obtained from the Mine Safety and Health Administration (MSHA) and the Occupational Safety and Health Administration (OSHA), from mining operations in amphibole-bearing rocks and from industrial sites employing asbestos, respectively. Mine selection was based on geology and mineralogy reported in the literature. The criteria used were the presence of amphiboles, the absence of minerals that were difficult to distinguish from amphiboles on the basis of chemistry and morphology, and the importance of the products—iron ore, gold and crushed stone. The type of mining or industrial operation and the amphibole(s) present at each site are listed in Table I.

SAMPLE PREPARATION

The industrial site filters were prepared by cutting 5- X 5-mm portions from the air monitoring filters as received from OSHA and mounting the sections with double-stick tape on SEM stubs. Latex spheres, 1.099 μm in diameter, were placed on each SEM stub for magnification calibration. The samples were carbon-coated in a vacuum evaporator before analysis. Samples were prepared in this manner because the long asbestiform particles are easily observed on the textured substrate of the collection filters.

Mining site filters contained very small particles that were difficult to observe on the textured filter. Therefore, portions of each filter were ashed in a low-temperature asher. The resulting ash was suspended in 10 ml distilled filtered water containing approximately 0.5 ml Aerosol OT dispersing agent, agitated ultrasonically for 5 minutes, and then filtered through a 0.1-μm Nuclepore filter. A 5- X 5-mm section of the Nuclepore filter was cut and mounted on a SEM stub. Latex spheres were placed on each SEM stub for

Table I. Type of Operation and Amphibole Present at Each Site

Type of Operation	Site	Amphibole(s)	Composition
Mining	Homestake Gold Mine, SD[a]	Cummingtonite	$(Mg,Fe)_7Si_8O_{22}(OH)_2$
Mining	Peter Mitchell Iron Mine, MN[b]	Cummingtonite, hornblende, actinolite	$(Mg,Fe)_7Si_8O_{22}(OH)_2$ $(Ca,Na)_2(Mg,Fe,Al)_5Si_8O_{22}(OH,F)_2$ $Ca_2(Mg,Fe)_5Si_8O_{22}(OH)_2$
Mining	Charlottesville Stone Quarry, VA[c]	Actinolite	$Ca_2(Mg,Fe)_5Si_8O_{22}(OH)_2$
Industrial	Shipyard	Cummingtonite-grunerite asbestos (amosite)	$(Mg,Fe)_7Si_8O_{22}(OH)_2$
Industrial	Electric Company	Cummingtonite-grunerite asbestos (amosite)	$(Mg,Fe)_7Si_8O_{22}(OH)_2$

aNoble [1950].
bGundersen and Schwartz [1962].
cGiannini and Rector [1958].

$(Mg,Fe)_7Si_8O_{22}(OH)_2$

grunerite asbestos (amosite)

[a]Noble [1950].
[b]Gundersen and Schwartz [1962].
[c]Giannini and Rector [1958].

calibration of magnification, and the samples were carbon-coated. The Nuclepore filter substrate provided a smooth surface for observation of the very small particles present in these samples.

SAMPLE ANALYSIS

All samples were examined using SEM with EDS capability. The filters were scanned at 5000X, and particle measurements were made at 10,000X on the cathode ray screen of the SEM. When particles extended beyond the field of view, measurements were made at lower magnifications. A minimum of 250 particles with aspect ratio $\geqslant 2:1$ for the mining site samples and $\geqslant 3:1$ for the industrial site samples, straight sides, and suitable amphibole composition were measured. Most nonamphibole particles were eliminated by the use of the above criteria.

In all samples except those from the Peter Mitchell Mine, amphiboles could be distinguished from other minerals on the basis of particle morphology and chemistry (using EDS). In the Peter Mitchell samples, the pyroxenes hedenbergite $[(Ca,Fe)Si_2O_6]$ and hypersthene $[(Mg,Fe)_2Si_2O_6]$ could not be distinguished from hornblende and cummingtonite. However, pyroxenes are less abundant than amphiboles in the Peter Mitchell samples [Gundersen and Schwartz 1962] and should not represent a significant number of the particles measured. The length and width data for the amphiboles and pyroxenes on the Peter Mitchell Mine air filters were combined for the statistical analyses because of the similarities in their morphological characteristics,

Summary statistics including mean, minimum and maximum values were established for lengths and widths of each sample. Regression of the log width vs log length and standard error of estimate of log width based on log length were calculated for each particle population. The slope or "fibrosity index" of the regression equation was used to indicate the dependence of width on length for all samples. The summary statistics and aspect ratio distributions, commonly used to characterize particle size distributions, were used as the basis for evaluating the results of the regression analyses. These values were also compared with those obtained by Siegrist and Wylie [1980] on bulk mineral samples.

RESULTS

Particle Size Distribution

Results from the particle size distribution (Tables II and III) and regression analyses (Table IV and Figure 1) show two distinct sets of particle popula-

tions: one from the mining sites and one from the industrial sites. The particles from the mining sites are typically shorter and wider than those from the industrial sites. Length ranges for the particles from the mining sites are smaller than those from the industrial sites, while the ranges in widths are greater for the mining site particles.

Table II. Length and Width Characteristics of Airborne Amphibole Particles

Site	Number of Particles Counted	Length (μm)			Width (μm)		
		Mean	Min.	Max.	Mean	Min.	Max.
Mining							
Homestake Gold Mine	266	4.6	0.9	17.5	1.1	0.3	4.8
Peter Mitchell Iron Mine	464	5.5	1.0	32.4	1.2	0.2	5.0
Charlottesville Crushed Stone	605	5.3	0.8	36.0	1.4	0.2	12.0
Industrial							
Shipyard	698	8.2	0.9	93.5	0.4	0.1	2.6
Electric Company	285	15.6	1.3	181.0	0.5	0.1	1.7
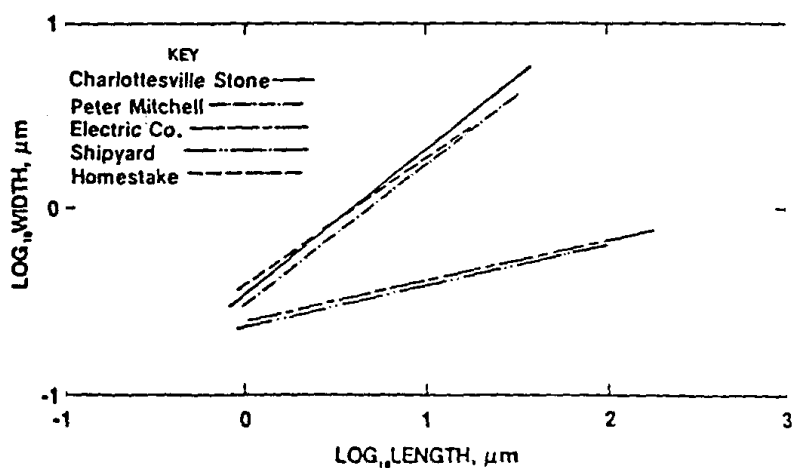
Figure 1. Regression lines summarizing length and width data collected for amphiboles on air monitoring filters from mining and industrial operations.

ıe industrial sites. The
: and wider than those
es from the mining sites
the ranges in widths are

Amphibole Particles

ı)	Width (μm)			
Max.	Mean	Min.	Max.
17.5	1.1	0.3	4.8
32.4	1.2	0.2	5.0
36.0	1.4	0.2	12.0
93.5	0.4	0.1	2.6
81.0	0.5	0.1	1.7

2   3

collected for amphiboles
ıs

Table III. Comparison of Aspect Ratios for Airborne Amphibole Particles

Site	Distribution of Particles, (%) for Aspect Ratio							Total Number of Particles
	2:1 to 2.9:1	3:1 to 4.9:1	5:1 to 9.9:1	10:1 to 19.9:1	20:1 to 49.9:1	50:1 to 99.9:1	>100:1	
Mining								
Homestake Gold Mine	22	46	28	4	0	0	0	265
Peter Mitchell Iron Mine	3	62	27	7	1	0	0	464
Charlottesville Crushed Stone	31	41	21	6	1	0	0	605
Industrial								
Shipyard	ND[a]	5	23	31	30	9	2	698
Electric Company	ND[a]	4	13	24	37	14	8	285

[a]ND = not determined.

Table IV. Fibrosity Index for Airborne Amphibole Particles

Site	Regression Analysis		Standard Error of Estimate
	Fibrosity Index (F)	Y Intercept (b)	
Mining			
Homestake Gold Mine	0.68	−0.43	0.17
Peter Mitchell Iron Mine	0.76	−0.52	0.18
Charlottesville Crushed Stone	0.78	−0.46	0.20
Industrial			
Shipyard	0.24	−0.64	0.26
Electric Company	0.21	−0.61	0.26

Aspect Ratio Distribution

The aspect ratio distributions (Table III) emphasize the significant differences between the mining and industrial site samples. The mining site populations have more particles in the lower-aspect-ratio categories than do the industrial site populations. Aspect ratios for 93% of the mining site particles are ≤10:1, while only 25% of the industrial site particles are ≤10:1. In terms of higher aspect ratios, only 1% of the mining site particles exceed 20:1 in aspect ratio, while >45% of the industrial site particles fall in this category. Long, thin amphibole particles (high aspect ratio) are the ones generally associated with adverse biological effects. These results for airborne particles are in general agreement with data on milled tremolite samples of various habits reported by Campbell et al. [1979].

Linear Regression Analysis

The linear least-squares regression of log width vs log length is another way of displaying the results described by the particle size and aspect ratio distributions (Table IV). The larger b values along with larger "fibrosity indices" indicate that the mining particles have greater widths than the industrial particles. The larger "fibrosity indices" for the mining samples also indicate a dependence of width on length, a characteristic typical of cleavage fragments [Siegrist and Wylie 1980]. In contrast to this, the low "fibrosity indices" of the industrial samples reflect the uniform width (independent of length) typical of asbestos fibers [Wylie 1979]. The fibrosity indices of each sample

nibole Particles

Intercept (b)	Standard Error of Estimate
-0.43	0.17
-0.52	0.18
-0.46	0.20
-0.64	0.26
-0.61	0.26

ize the significant differ-
mples. The mining site
-ratio categories than do
93% of the mining site
site particles are ≤10:1.
ing site particles exceed
site particles fall in this
)ect ratio) are the ones
hese results for airborne
'ed tremolite samples of

)g length is another way
: and aspect ratio distri-
rger "fibrosity indices"
ths than the industrial
; samples also indicate a
il of cleavage fragments
v "fibrosity indices" of
ndependent of length)
indices of each sample

were compared with those obtained by Siegrist and Wylie [1980] on bulk asbestos and nonasbestos amphibole samples (Table V). The fibrosity indices of the industrial site samples are similar to those obtained on bulk asbestos amphibole samples. The fibrosity indices of the mining sites are similar to those obtained on bulk nonasbestos amphibole samples.

Visual examination of the regression lines (Figure 1) provides a rapid morphological evaluation of the particle populations. The two distinct sets of particle populations described above can be easily seen. The mining site particle length range is smaller than the industrial site particle length range, and the industrial site particles have higher aspect ratios than do the mining site particles. The dependence of width on length and differences in particle widths for the five populations is also evident.

DISCUSSION

The differences in particle morphology can be attributed to the habits of the asbestos and nonasbestos amphiboles present in these samples. Asbestiform amphiboles, which are present in the industrial site samples, are composed of fibrils approximately 1000–1700 Å wide and up to several inches long. These fibrils can be easily separated from one another, but resist breakage across individual fibrils. Thus, long, thin, high-aspect-ratio particles are generated. Nonasbestiform amphiboles, like those present in the mining site samples, generally crystallize in a prismatic habit. These crystals have well-developed cleavage, which results in breakage both perpendicular and parallel to particle length. Consequently, short, prismatic, low-aspect-ratio cleavage fragments are produced as the particles are reduced in size.

Table V. Fibrosity Index for Bulk Amphibole Particles [Siegrist and Wylie 1980]

| Sample | Regression Analysis | | |
	Fibrosity Index (F)	Y Intercept (b)	Standard Error of Estimate
Prismatic			
Tremolite	0.67	-0.19	0.18
Riebeckite	0.56	-0.34	0.34
Asbestiform			
Amosite	0.18	-0.56	0.20
Crocidolite	0.14	-0.71	0.19

CONCLUSIONS

Three main conclusions are drawn from the calculations of length, width and aspect ratio distributions:

1. The three mining sites have similar particle populations.
2. The two industrial sites have similar particle populations.
3. The mining sample populations can be distinguished qualitatively from the industrial sample populations.

These conclusions are similar to the results obtained from linear regression analyses. Based on the fibrosity indices, the analyses indicate morphological similarities among the industrial site particle populations and among the mining site particle populations. The industrial site particle populations are different from the mining site particle populations. Correlation between fibrosity indices of airborne and bulk amphibole samples suggests that fibrosity indices can be used to determine whether an airborne amphibole population is from an asbestos or a nonasbestos source. Thus, the linear least-squares regression technique is suitable for quantitatively describing the morphology of particle populations as well as aiding in the identification of a predominantly asbestiform or nonasbestiform amphibole source for the airborne amphibole particles.

ACKNOWLEDGMENTS

REFERENCES

Campbell, W. J., R. L. Blake, L. L. Brown, E. E. Cather and J. J. Sjoberg (1977) "Selected Silicate Minerals and Their Asbestiform Varieties," U.S. BOM Information Circular 8751.

Campbell, W. J., E. B. Steel, R. L. Virta and M. H. Eisner (1979) "Relationship of Mineral Habit to Size Characteristics for Tremolite Cleavage Fragments and Fibers," U.S. BOM Report of Investigations 8367.

Giannini, W. F., and W. K. Rector, Jr. (1958) "Mineral Occurrence and Associations in the Albemarle Crushed Stone Quarry (Catoctin Formation) near Shadwell, Va.," *Virginia J. Sci.* 9(4):427.

Gundersen, J. N., and G. M. Schwartz (1976) "The Geology of the Metamorphosed Biwabik Iron Formation, Eastern Mesabi District, Minnesota," *Minn. Geol. Bull.* 43:139.

ɪlculations of length, width

ations.
ɟlations.
ɪshed qualitatively from the

ɪined from linear regression
ɣses indicate morphological
opulations and among the
ɪte particle populations are
tions. Correlation between
ɪole samples suggests that
ɪher an airborne amphibole
ɔs source. Thus, the linear
ɪuantitatively describing the
ɪng in the identification of a
ɪmphibole source for the

. Cather and J. J. Sjoberg
bestiform Varieties," U.S.

Eisner (1979) "Relation-
Tremolite Cleavage Frag-
ations 8367.
'Mineral Occurrence and
Quarry (Catoctin Forma-
27.
Geology of the Metamor-
ɪbi District, Minnesota,"

Noble, J. A. (1950) "Ore Mineralization in the Homestake Gold Mine, Lead, S.D.," *Geol. Soc. Am. Bull.* 61:221.

OSHA (1975) "Occupational Exposure to Asbestos," *Federal Register* (October 9), pp. 47652, 47660.

Selikoff, I. J. and E. C. Hammond, Eds. (1979) *Health Hazards of Asbestos Exposure, Ann. of the N.Y. Acad. Sci.* Vol. 330.

Siegrist, H. G., and A. G. Wylie (1980) "Characterizing and Discriminating the Shape of Asbestos Particles," *Environ. Res.* 23:348.

Wylie, A. G. (1979) "Fiber Length and Aspect Ratio of Some Selected Asbestos Samples," *Ann. N.Y. Acad. Sci.* 330:605.

Characteristics of asbestiform and non-asbestiform calcic amphiboles

MARIA DORLING and JACK ZUSSMAN

Department of Geology, University of Manchester, Manchester M13 9PL (Great Britain)

LITHOS
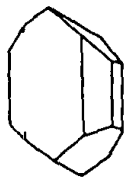
In terms of morphology there are four major types of calcic amphibole; massive, prismatic, finely acicular and asbestos. Representatives of each of these types have been examined by optical microscopy, X-ray diffraction, scanning and transmission electron microscopy, and electron probe microanalysis. Massive specimens (nephrite) consist of randomly oriented clusters of fine, roughly lath-shaped, sub-microscopic crystals; within each cluster the lath lengths (z) are approximately aligned but neighbouring laths are rotated with respect to one another. Finely acicular specimens ("byssolites") have well-formed crystals bounded mainly by $\{110\}$ (100) and (010) faces and characteristically have striations parallel to their lengths. Asbestiform varieties range from finer (flexible) to coarser (more brittle) specimens and many specimens contain a mixture of fine and coarse fibrils. The fibrils in a bundle are aligned parallel to z but are in a range of azimuthal orientations. It is inferred that they are formed by multiple independent nucleation and growth parallel to z rather than through parting or cleavage on $\{110\}$ planes, (100) defect or twin planes, or on (010) planar defects.

The $\{110\}$ cleavage in amphiboles is well reported but (100) features are rarely mentioned in the literature. Our observations reveal the importance of (100) as a cleavage or parting as well as the tendency in nephrites, byssolites and asbestos towards a lath-like (parallel to z) morphology with flattening on (100). In the latter varieties therefore, the y-direction is that of second fastest crystal growth, after z.

When subjected to moderate grinding, the comminution of asbestos fibres proceeds more by separation of fibrils and less by fracturing to shorter lengths as compared with prismatic and byssolite specimens. Prolonged grinding does, however, shorten lengths of even the least brittle asbestos.

Transmission electron microscopy revealed extensive sub-grain boundaries and dislocation networks (suggesting a deformation history) in all prismatic and nephrite specimens. Fine multiple (100) twinning was observed in asbestos but not in other varieties. Although chain-width defects [on (010)], with visibility enhanced by beam damage, were most abundant in nephrites and fibrous tremolites, there appears to be no completely consistent relationship between such features and morphological type.

Electron probe analyses showed that specimens that contain more than a very small amount of aluminium do not have asbestiform habit. Asbestos specimens also have lower contents of Mn, Na and K and have formulae closer to the ideal $Ca_2(Mg,Fe)_5Si_8O_{22}(OH)_2$. Small departures from this in asbestos involve Na in the A site compensated by Na for Ca rather than Al for Si whereas the reverse is true in byssolites. Chemical substitutions in prismatic specimens are much less constrained.

The characteristics of the four morphological sub-groups correlate reasonably well with what is known of their geological environments.

Introduction

During the past several years the amphibole and chrysotile varieties of asbestos have been increasingly studied, mainly because of the health hazards associated with them. Whether or not the non-asbestos amphibole counterparts possess equally harmful properties is not yet known, but there appears to be a tendency (perhaps with little justi-

cation) to associate the same hazards with all forms of amphibole.

The habits of amphibole minerals vary from stubby prismatic crystals of hornblende, through prismatic or acicular crystals of riebeckite, actinolite, tremolite and others, to fibrous forms of grünerite ("amosite"), anthophyllite, tremolite-actinolite and riebeckite ("crocidolite"). The prismatic and acicular crystal habits occur more commonly, and asbestiform habit is relatively rare. Some of the amphiboles, such as hornblendes, are not known to occur at all with asbestiform habit.

Processes which result in amphibole minerals being formed can be explained on the basis of chemical reactions, but the conditions of formation specifically of the asbestiform varieties are not well understood. Specimens of the tremolite-ferroactinolite series with almost identical chemistry, for example, can nevertheless exhibit very different morphological and physical properties.

The fact that asbestiform varieties are not very common may be an indication that asbestos requires very specific conditions for its development. Variations in chemical or physical properties of amphiboles may be responsible for differences in the morphology adopted. Alternatively, variations in morphology may be primarily a consequence of differences in conditions and mechanisms of crystal growth. But even in the latter case, chemical and/or physical differences may accompany, even if they do not cause, different morphologies. Either way it seemed important to investigate whether or not there are any fundamental differences between amphiboles of different habit.

Many investigations of amphibole asbestos have been carried out in recent years, mainly on cummingtonite-grünerite (amosite) and anthophyllite, but comparison has not usually been made with their prismatic counterparts. Exceptions to this were the studies by Ampian (1976), Campbell et al. (1977), Zoltai (1978) and Wylie (1979), but these were based almost entirely on optical properties, and in the case of Wylie (1979) on some X-ray diffraction in addition to optics. The aim of the present study was to determine the characteristics of both asbestos and non-asbestos varieties, but confining attention in the first instance to members of the tremolite-ferroactinolite series. A large number of specimens were examined by a variety of methods including optical and electron microscopy, chemical analysis

by electron microprobe, and X-ray and electron diffraction. Preliminary results were described by Dorling and Zussman (1980). More complete results are described here under three main headings: morphology and cleavage, internal sub-microscopic features and chemical composition. Specimens are listed in the latter section.

Useful reviews of the crystal chemistry of amphiboles have been given by Hawthorne (1981, 1983), and of the electron microscopy of asbestos by Chisholm (1983).

Morphology and cleavage

The amphiboles studied range from fine-grained massive, to blocky, bladed, prismatic or acicular crystals, the latter grading into asbestiform varieties. Most of the specimens studied had prismatic morphology. Three were of massive appearance but were crypto-crystalline; this variety is known commonly as nephrite jade. In this study, only specimens which occur as bundles of fibres (commonly having splayed ends), which readily split into still finer sub-microscopic units (fibrils), are referred to and are classed as asbestos. The remaining specimens exhibit very fine acicular or needle-like crystals and are not included in the group of asbestiform specimens. The name "byssolite" which was used by Dana (1922) and Hart (1927) for a fine acicular variety of actinolite and has also been used by Wylie (1979) will be used throughout this study to describe this habit. Their occurrence as clusters of individual crystals in cavities, e.g., in pegmatite veins in granite suggests that they have formed by different processes to those which give rise to asbestos.

Optical microscopy

Some specimens were prepared for optical study by crushing in an agate mortar; others were fine-grained and sufficiently friable to give suitable particles without crushing. As noted by Ampian (1976), Campbell et al. (1977) and Wylie (1979), asbestos specimens tended to separate on moderate crushing, mostly into long thin fibrils whereas others cleaved and fractured to produce particles most of which showed only moderate elongation.

A relatively simple observation which could be

made on large numbers of grains (100 for each specimen) was that of extinction angle. When such grains are scattered on a glass slide it is expected that the majority will lie on their predominant ($hk0$) face. This orientation can in principle at least be recognised by the measured extinction angle, the variation of which can be predicted by the Biot-Fresnel relationship. Results for the various morphological types of specimen were as follows:

Prismatic specimens. Some, when lightly crushed showed no dominance of {110}, (100) or any other ($hk0$) face. Others, which tended more towards acicular morphology have dominant surfaces approximating to {110}, indicating greater ease of {110} cleavage.

Byssolites. Most showed dominance of (100) implying a lath-like morphology.

Asbestos. For asbestos it has been suggested (e.g., Wylie, 1979) that one of its characteristics is straight extinction in all orientations in the [001] zone (despite monoclinic symmetry), due to either submicroscopic multiple twinning, or fibril structure with random azimuthal orientation. Most of the assumed asbestos specimens examined here yielded a fraction composed of tiny individual crystals, some of which showed oblique extinction, and only two specimens (Table 1c, sample Nos. 15 and 16) showed no oblique extinction at all.

For those specimens which showed straight extinction only, this could be due either to the morphology [flattening on (100)] of individual resolvable fibrils, or to the twinning or random orientations of sub-microscopic fibrils referred to above. Thus, when the "particle" size is very small, as in the case of asbestos specimens, the results of optical microscopy alone are ambiguous. Nevertheless, they are consistent with the detailed observations of individual particles by electron microscopy (see below), which can distinguish which of the above effects gives rise to straight extinction in any particular case.

Undulose extinction which was observed for asbestos bundles is probably due to twisting of fibres, i.e. an indication that fibres are not strictly parallel in the bundle (confirmed by SEM observations).

X-ray powder diffractometry and "single-crystal" diffraction

It might be expected (see, e.g., Ampian, 1976), that powdered specimens of asbestos varieties would be particularly strongly oriented and give fewer powder reflections than their non-fibrous counterparts. This distinction, at least for the Ca-amphiboles studied, is not as clear as predicted. The strongest observed reflections for both non-asbestos and asbestos specimens are those from 310 and 110; quite strong intensities are obtained for 240, 151, 330 and moderate intensities for 200, 040, 020. The 020 reflection certainly appears to be weaker for asbestos. However, even though it does not suppress many reflections completely, the orientation effect is more marked for asbestos varieties than for the prismatic specimens.

Since the specimens for powder diffractometry are finely crushed, the orientations produced are an indication largely of cleavage planes rather than natural faces in the case of prismatic specimens, but may still be an indication of natural faces in fibrous specimens, bearing in mind the widths of fibrils (< 1000–8000 Å).

We have used the relative intensities of X-ray powder reflections as another indication of the relative dominance of particular prism faces or cleavages, or parting planes. The well-known {110} cleavage is expected to enhance the 110 intensity, and indeed it does, but only by a factor of 2.4 for prismatic and 3.3 for fibrous tremolites as compared with intensity for a random powder. The 200 intensity however is enhanced far more, by factors of 9 and 21, for prismatic and fibrous tremolites, respectively. The surprising importance of the (100) cleavage, parting or natural faces, particularly in fibrous specimens is thus indicated.

X-ray "single-crystal" methods have been especially useful in studying byssolite specimens which might otherwise have been regarded as asbestos. Needle-like specimens ranging from 130 to 15 μm in diameter, gave diffraction patterns of single crystals. By comparison, asbestos fibres of similar thicknesses proved to be bundles of fibrils giving typical rotation photographs from an oscillating crystal.

Scanning electron microscopy (SEM)

Observations using a scanning electron microscope show a number of differences in the morphology and natural sizes of crystals or fibrils for different specimens of the tremolite-ferroactinolite series.

TABLE I

List of specimens in order of decreasing Mg/Fe ratio (localities, specimen numbers and/or donors, and chemical formulae, all on basis of 23 oxygen equivalents, are given)

(a) Prismatic and massive (nephrite) specimens:

(1) Tremolite   (Canaan, Conn., U.S.A.; JM 4173-7-4)
$Na_{0.03}(K_{0.08}Ca_{1.84}Na_{0.16})_{2.00}(Mg_{4.90}Fe_{0.03})_{4.93}Si_{8.04}O_{22}(OH)_2$

(2) Tremolite   (Nigeria; BM 1932, 207)
$Ca_{2.07}(Mg_{4.87}Fe_{0.03})_{4.90}Si_{8.02}O_{22}(OH)_2$

(3) Tremolite   (Przeworno, L. Silesia, Poland; Dr. B. Kwiecinska, Acad. Mining & Metall., Cracow, Poland)
$Na_{0.12}(Ca_{1.99}Na_{0.01})_{2.00}(Mg_{4.61}Fe_{0.05}Al_{0.28})_{4.94}Si_{7.73}Al_{0.27}O_{22}(OH)_2$

(4) Tremolite   (New York, U.S.A.; Colorado School of Mines, Golden, Colo., U.S.A.)
$(Ca_{1.83}Mn_{0.07}Mg_{0.07})_{1.97}(Mg_{4.92}Fe_{0.03}Al_{0.05})_{5.00}Si_{8.01}O_{22}(OH)_2$

(5) Tremolite   (Verla Irene, Sweetwater, Wyo., U.S.A.; Prof. T. Zoltai, Univ. of Minnesota, Minneapolis, Minn., U.S.A.)
$Ca_{2.04}(Mg_{4.67}Fe_{0.14})_{4.87}Si_{8.01}O_{22}(OH)_2$

(6) Tremolite   (Lander, U.S.A. (nephrite); Prof. W.S. MacKenzie, Univ. of Manchester, Manchester, U.K.)
$Ca_{1.97}(Mg_{4.85}Fe_{0.15})_{5.00}Si_{8.02}O_{22}(OH)_2$

(7) Tremolite   (Balmat, N.Y., U.S.A.; TN)
$Na_{0.09}(Ca_{1.75}Na_{0.19}Mn_{0.06})_{2.00}(Mg_{4.85}Mn_{0.09}Al_{0.06})_{5.00}Si_{8.01}O_{22}(OH)_2$

(8) Tremolite   (Italy, Cape Asbestos Fibres Ltd., Uxbridge, U.K.)
$Na_{0.08}(Ca_{1.88}Na_{0.09}Mg_{0.03})_{2.00}(Mg_{4.81}Fe_{0.15}Al_{0.04})Si_{8.00}O_{22}(OH)_2$

(9) Tremolite   (Perth, Ont., Canada; Jagiellonian Univ., Cracow, Poland)
$Na_{0.25}K_{0.08}Ca_{2.00}(Mg_{4.61}Fe_{0.19}Al_{0.08})_{4.88}Si_{7.83}Al_{0.17}O_{22}(OH)_2$

(10) Tremolite (nephrite) (Verla Irene, Wyo., U.S.A.; Prof. T. Zoltai, Univ. of Minnesota, Minneapolis, Minn., U.S.A.)
$(Ca_{1.98}Mg_{0.03})_{2.01}(Mg_{4.65}Fe_{0.25}Cr_{0.04}Al_{0.06})_{5.00}Si_{7.88}Al_{0.12}O_{22}(OH)_2$

(11) Tremolite   (Gouverneur, N.Y., U.S.A.; JM 4173-52-3)
$Na_{0.26}K_{0.13}(Ca_{1.76}Na_{0.24})_{2.00}(Mg_{4.62}Fe_{0.27}Al_{0.08})_{4.97}Si_{7.83}Al_{0.17}O_{22}(OH)_2$

(12) Tremolite   (Walliston, Ont., Canada; UM)
$Ca_{1.91}(Mg_{4.71}Fe_{0.29})_{5.00}Si_{8.04}O_{22}(OH)_2$

(13) Tremolite   (Greenland; BM 93371)
$Na_{0.16}(Ca_{1.88}Na_{0.07}Mg_{0.05})_{2.00}(Mg_{4.53}Fe_{0.41}Al_{0.06})_{5.00}Si_{7.75}Al_{0.25}O_{22}(OH)_2$

(14) Tremolite   (San Francisco, Calif., U.S.A.; BM 59400)
$Na_{0.14}(Ca_{1.78}Na_{0.18}Mg_{0.04})_{2.00}(Mg_{4.51}Fe_{0.44}Al_{0.05})_{5.00}Si_{8.01}O_{22}(OH)_2$

(15) Tremolite   (Tyrol, Austria; BM 31020)
$(Ca_{1.91}Na_{0.08}Mn_{0.01})_{2.00}(Mg_{4.55}Fe_{0.43}Mn_{0.02})_{5.00}Si_{8.02}O_{22}(OH)_2$

(16) Tremolite   (Sweden; BM 1939, 185; "actinolite")
$Na_{0.07}(Ca_{1.93}Na_{0.06}Mn_{0.01})_{2.00}(Mg_{4.49}Fe_{0.44}Mn_{0.03}Al_{0.04})_{5.00}Si_{7.96}Al_{0.04}O_{22}(OH)_2$

(17) Actinolite   (Loch Ailsh, Scotland, U.K.; Prof. R.A. Howie, Kings College, London, U.K.)
$Na_{0.08}(Ca_{1.81}Na_{0.03}Mn_{0.03}Mg_{0.13})_{2.00}(Mg_{4.42}Fe_{0.52}Al_{0.06})_{5.00}Si_{7.90}Al_{0.10}O_{22}(OH)_2$

(18) Actinolite   (unknown locality; Jagiellonian University, Cracow, Poland)
$Na_{0.03}(Ca_{1.78}Na_{0.09}Mn_{0.04}Mg_{0.09})_{2.00}(Mg_{4.44}Fe_{0.56})_{5.00}Si_{7.95}Al_{0.03}Fe_{0.02}O_{22}(OH)_2$

(19) Actinolite   (Zillertal, Austria; UM)
$Na_{0.03}(Ca_{1.82}Na_{0.07}Mg_{0.11})_{2.00}(Mg_{4.27}Fe_{0.6}Cr_{0.05}Al_{0.1})_{5.00}Si_{7.89}Al_{0.11}O_{22}(OH)_2$

(20) Actinolite   (Salzburg, Austria; UM)
$Na_{0.06}(Ca_{1.82}Na_{0.08}Mg_{0.10})_{2.00}(Mg_{4.31}Fe_{0.65}Al_{0.04})_{5.00}Si_{7.94}Al_{0.06}O_{22}(OH)_2$

(21) Actinolite   (Salzburg, Austria; JM 3647-152-10)
$Na_{0.07}(Ca_{1.73}Na_{0.13}Mg_{0.14})_{2.00}(Mg_{4.17}Fe_{0.70}Cr_{0.05}Al_{0.08})_{5.00}Si_{7.94}Al_{0.06}O_{22}(OH)_2$

(22) Actinolite   (Yancey Co., N.C., U.S.A.; UM)
$(Ca_{1.78}Mn_{0.05}Mg_{0.19})_{2.02}(Mg_{4.04}Fe_{0.70}Cr_{0.03}Al_{0.23})_{5.00}Si_{7.71}Al_{0.29}O_{22}(OH)_2$

(23) Actinolite   (Verla Irene, Wyo., U.S.A.; Prof. T. Zoltai, Univ. of Minnesota, Minneapolis, Minn., U.S.A.)
$Na_{0.03}(Ca_{1.93}Na_{0.04}Mg_{0.03})_{2.00}(Mg_{3.93}Fe_{0.74}Al_{0.33})_{5.00}Si_{7.46}Al_{0.54}O_{22}(OH)_2$

TABLE 1 (continued)

(a) Prismatic and massive (nephrite) specimens (cont.):

(24) Actinolite (Los Angeles, Calif., U.S.A.; Colorado School of Mines, Golden, Colo., U.S.A.)
$Na_{0.09}(Ca_{1.83}Na_{0.12}Mn_{0.05})_{2.00}(Mg_{4.08}Fe_{0.80}Mn_{0.01}Cr_{0.05}Al_{0.06})_{5.00}Si_{7.93}Al_{0.07}O_{22}(OH)_2$

(25) Actinolite (Habachtal, Austria; UM)
$Na_{0.14}(Ca_{1.81}Mn_{0.04}Mg_{0.28})_{2.13}(Mg_{3.74}Fe_{0.88}Al_{0.19})_{5.00}Si_{7.79}Al_{0.21}O_{22}(OH)_2$

(26) Actinolite (Telemark, Norway; UM)
$Na_{0.09}(Ca_{1.76}Na_{0.11}Mg_{0.13})_{2.00}(Mg_{3.93}Fe_{0.99}Al_{0.08})_{5.00}Si_{7.93}Al_{0.07}O_{22}(OH)_2$

(27) Actinolite (U.S.A.; BM 36209)
$Na_{0.13}(Ca_{1.91}Na_{0.02}Mn_{0.03}Mg_{0.04})_{2.00}(Mg_{3.91}Fe_{0.95}Al_{0.14})_{5.00}Si_{7.74}Al_{0.26}O_{22}(OH)_2$

(28) Actinolite (Wrightwood, Calif., U.S.A.; TN)
$Na_{0.17}(Ca_{1.84}Na_{0.10}Mn_{0.03}Mg_{0.03})_{2.00}(Mg_{3.83}Fe_{0.95}Cr_{0.03}Al_{0.19})_{5.00}Si_{7.68}Al_{0.32}O_{22}(OH)_2$

(29) Richterite (Warm Springs, Calif., U.S.A.; JM 4869-1-1)
$K_{0.14}Na_{0.50}(Ca_{1.24}Na_{0.76})_{2.00}(Mg_{4.98}Fe_{0.02})_{5.00}Si_{8.03}O_{22}(OH)_2$

(b) Byssolites:

(1) Actinolite (Doferthal, Tyrol, Austria; OUM 9250)
$Na_{0.19}(Ca_{1.99}Na_{0.01})_{2.00}(Mg_{3.68}Fe_{1.17}Mn_{0.03}Al_{0.12})_{5.00}Si_{7.69}Al_{0.31}O_{22}(OH)_2$

(2) Actinolite (Untersulzbachthal, Austria; OUM 13680)
$Na_{0.10}(Ca_{1.91}Mn_{0.04}Mg_{0.05})_{2.01}(Mg_{3.35}Fe_{1.46}Al_{0.19})_{5.00}Si_{7.51}Al_{0.49}O_{22}(OH)_2$

(3) Actinolite (Sulzbachtal, Austria; OUM 135149)
$Na_{0.16}Ca_{2.01}(Mg_{3.26}Fe_{1.48}Mn_{0.03}Al_{0.22})_{4.99}Si_{7.61}Al_{0.39}O_{22}(OH)_2$

(4) Actinolite (unknown locality; OUM 16175)
$Na_{0.27}(Ca_{1.84}Mn_{0.05}Mg_{0.07})_{2.00}(Mg_{3.24}Fe_{1.60}Al_{0.16})_{5.00}Si_{7.66}Al_{0.34}O_{22}(OH)_2$

(5) Actinolite (Nedre Erker, Norway, (Drammen granite); Dr. Rowbotham, Univ. of Keele, Keele, U.K.)
$Na_{0.06}(Ca_{1.99}Na_{0.01})_{2.00}(Mg_{2.94}Fe_{1.73}Mn_{0.05}Al_{0.22})_{4.94}Si_{7.76}Al_{0.24}O_{22}(OH)_2$

(6) Actinolite (unknown locality; H 109834 Harvard Mus., Cambridge, Mass., U.S.A.)
$Na_{0.16}(Ca_{1.98}Mg_{0.05})_{2.03}(Mg_{2.92}Fe_{2.07}Al_{0.01})_{5.00}Si_{7.80}Al_{0.20}O_{22}(OH)_2$

(7) Actinolite (St. Christopher, France; OUM 1819)
$Na_{0.15}(Ca_{2.02}Mn_{0.11})_{2.13}(Mg_{2.50}Fe_{2.25}Mn_{0.25})_{5.00}Si_{7.85}Al_{0.07}O_{22}(OH)_2$

(8) Ferroactinolite (unknown locality; OUM 1822)
$Na_{0.13}K_{0.03}Ca_{2.04}(Mg_{2.39}Fe_{2.51}Mn_{0.06}Al_{0.02})_{4.98}Si_{7.74}Al_{0.26}O_{22}(OH)_2$

(c) Asbestos specimens:

(1) Tremolite (Pennsylvania, U.S.A.; Prof. R.A. Howie, Kings College, London, U.K.)
$Na_{0.10}(Ca_{1.95}Na_{0.01}Mg_{0.04})_{2.00}(Mg_{4.97}Fe_{0.03})_{5.00}Si_{7.97}O_{22}(OH)_2$

(2) Tremolite (Korea; Cape Asbestos Fibres Ltd., Uxbridge, U.K.)
$Ca_{2.03}(Mg_{4.89}Fe_{0.09})_{4.98}Si_{8.00}O_{22}(OH)_2$

(3) Tremolite (Italy; BM 66130)
$Na_{0.02}(Ca_{1.97}Na_{0.03})_{2.00}(Mg_{4.87}Fe_{0.12})_{4.99}Si_{7.99}O_{22}(OH)_2$

(4) Tremolite (Piedmont, Italy; BM 406; pilolite)
$Na_{0.04}(Ca_{1.98}Mg_{0.03})_{2.01}(Mg_{4.84}Fe_{0.16})_{5.00}Si_{7.97}O_{22}(OH)_2$

(5) Tremolite (unknown locality; Dr. A. Wylie, Univ. of Maryland, College Park, Md., U.S.A.)
$(Ca_{2.00}Mg_{0.02})_{2.02}(Mg_{4.83}Fe_{0.17})_{5.00}Si_{8.00}O_{22}(OH)_2$

(6) Tremolite (Corsica, France; BM 59440)
$Ca_{1.97}(Mg_{4.81}Fe_{0.19})_{5.00}Si_{8.01}O_{22}(OH)_2$

(7) Tremolite (St. Gotthard, Switzerland; OUM 6806)
$Na_{0.16}Ca_{2.08}(Mg_{4.89}Fe_{0.20})_{4.89}Si_{7.94}Al_{0.05}O_{22}(OH)_2$

(8) Tremolite (Italy; TN)
$Na_{0.05}(Ca_{1.91}Na_{0.03}Mg_{0.05})_{2.00}(Mg_{4.70}Fe_{0.3})_{5.00}Si_{8.00}O_{22}(OH)_2$

(9) Tremolite (Baja Verepaz, Guatemala; U.S. Bureau of Mines, Washington, D.C., U.S.A.)
$Na_{0.18}(Ca_{1.98}Na_{0.01}Mg_{0.04})_{2.00}(Mg_{4.70}Fe_{0.30})_{5.00}Si_{7.98}O_{22}(OH)_2$

474

TABLE I *(continued)*

(c) Asbestos specimens (cont.):

(10) Tremolite   (Udaipur. India; Dr. A. Wylie, Maryland, College Park, Md., U.S.A.)

$(Ca_{1.90}Mn_{0.02}Mg_{0.11})_{2.03}(Mg_{4.71}Fe_{0.29})_{5.00}Si_{7.98}O_{22}(OH)_2$

(11) Tremolite   (St. Gotthard. Switzerland; OUM 1820)

$Na_{0.14}Ca_{2.10}(Mg_{4.4}Fe_{0.33})_{4.80}Si_{8.02}O_{22}(OH)_2$

(12) Tremolite   (Rajasthan. India; U.S. Bureau of Mines, Washington, D.C., U.S.A.)

$(Ca_{1.86}Mn_{0.04}Mg_{0.13})_{2.03}(Mg_{4.67}Fe_{0.33})_{5.00}Si_{7.98}O_{22}(OH)_2$

(13) Tremolite   (Jamestown. Calif., U.S.A.; JM 4173-70-1)

$Ca_{2.06}(Mg_{4.44}Fe_{0.43}Mn_{0.04})_{4.91}Si_{8.01}O_{22}(OH)_2$

(14) Tremolite   (Kobuk River. N.W. Alaska, U.S.A.; Colorado School of Mines, Golden, Colo., U.S.A.)

$Ca_{1.93}Mg_{0.01}(Mg_{4.43}Fe_{0.57})_{5.00}Si_{8.02}O_{22}(OH)_2$

(15) Actinolite   (Mexico; JM 4869-2-6)

$Na_{0.05}(Ca_{1.82}Na_{0.09}Mn_{0.05}Mg_{0.04})_{2.00}(Mg_{3.07}Fe_{1.89}Al_{0.04})_{5.00}Si_{7.99}Al_{0.01}O_{22}(OH)_2$

(16) Ferroactinolite   ("prieskaite") (Ex Mine, Prieska, South Africa; Dr. Rowbotham, Univ. of Keele, Keele, U.K.)

$(Ca_{1.80}Na_{0.11}Mn_{0.05}Mg_{0.01})_{1.97}(Mg_{1.12}Fe_{3.88})_{5.00}Si_{8.05}O_{22}(OH)_2$

Key to donors: BM = British Museum (Natural History); JM = Johns Manville Co. Ltd.; TN = Turner and Newall Ltd.; UM = University of Manchester. Department of Geology; OUM = University of Oxford Museum.

The morphology of coarse prismatic crystals is close to that generally regarded as typical for amphiboles i.e. with major {110} and smaller (010) and (100) faces. The topography of a cleavage surface is clearly different from that of a growth face. Growth surfaces (Fig. 1a) are usually roughened and striated due to the presence of vicinal faces and small irregularities, and often have adhering particles giving a "dusty" appearance. Cleavage planes (Fig. 1b) appear as clean and smoother surfaces but are broken up by steps in the {110} cleavage plane.

The massive variety of nephrite is fine-grained and exhibits near-random polycrystalline texture (Fig. 2).

Byssolite crystals appear as thin laths, bounded by crystallographic planes striated parallel to their length (Fig. 3). These striations represent vicinal faces which are normally associated with rapid growth and metastability. Stepped faces observed by transmission electron microscopy (TEM) on asbestos fibres see p. 476) were found to be a combination of {110} and (100) planes. It is possible that the steps observed on byssolite needles are of a similar character.
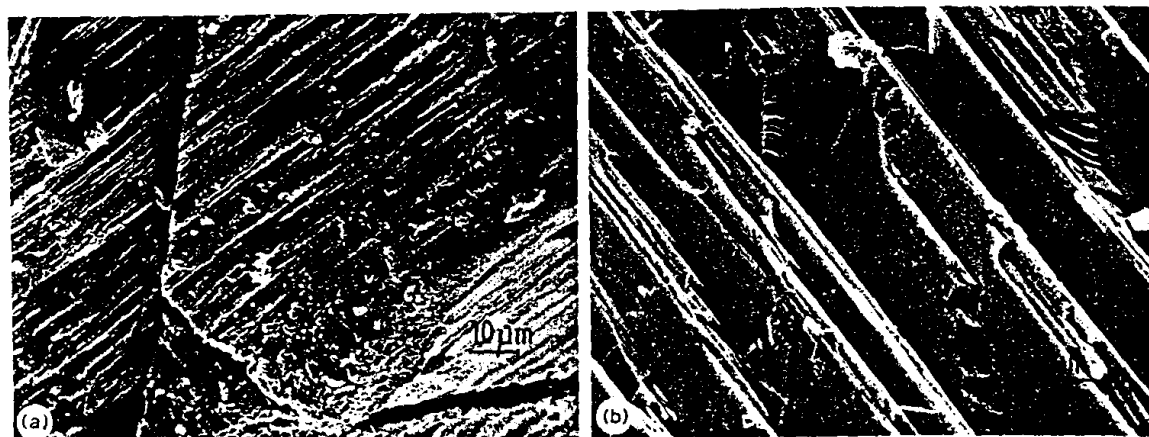

Fig. 1. Scanning electron micrograph of: (a) growth surface (actinolite — Italy); and (b) cleavage surface (actinolite — Habachtal. Austria).

Fig. 2. Scanning electron micrograph of fracture surface of massive variety (nephrite jade. Warm Springs, Calif., U.S.A.) exhibiting texture of randomly oriented crystals.

A common feature was observed for asbestos fibres and byssolite crystals, i.e. flattening of crystals on (100). No cleavage cracks were observed on the surfaces perpendicular to the z-axis of asbestos fibres or byssolite crystals.

It appears that the morphologies observed for asbestos specimens and byssolites depart from the morphologies predicted for the tremolite-actinolite series by Chisholm (1980) based on estimates of surface energy derived from electrostatic bond strengths. The morphology predicted is such that the forms (010) and {110} are prominent and more or less equally developed, yielding a cross-section perpendicular to z which would be slightly elongated in the direction perpendicular to y rather than the elongation parallel to y observed.

It is generally thought that rounded and other non-

Fig. 3. Scanning electron micrograph of "byssolite" (13680) showing striations parallel to the crystal's length.

planar surfaces, also vicinal faces, form on crystals as metastable features, occurring during the first stages of crystallization and transforming into flat faces if growth continues (Chojnacki, 1973). Those observed on natural asbestos are consistent with the conclusion from laboratory experiments (e.g., Makarova et al., 1970) that asbestos forms as a result of rapid growth from a supersaturated medium, conditions applicable to fluid-filled vugs and veins. Experiments also showed that prolonged favourable conditions lead to the coarsening of fibres; the presence of some coarse fibres within a natural asbestos bundle may be explained in a similar fashion.

Transmission electron microscopy (TEM)

The method of TEM has been particularly useful in our study of: (1) the morphological features of asbestiform specimens; and (2) internal defects in each of the morphological groups. In general ion-thinned specimens and dispersions were examined, but for asbestiform specimens cross-sections produced by ultramicrotomy were particularly useful.

In electron microscopic studies the surprising importance of (100) development revealed by optical observations is again evident. In asbestos, byssolites and in the crystallites of nephrites there is a tendency towards a lath-like morphology ($y > x$ dimension). For asbestos, lath widths varied from 500 to 3000 Å in most specimens but fibrils up to 8000 Å wide were observed.

The sizes of fragments of asbestos fibres are of course greatly influenced by the treatment during sample preparation. Experiments carried out on asbestos showed that prolonged ultrasonic dispersion leads to reduction in fibres' widths and thicknesses, and not so much to reduction in lengths, whereas prolonged grinding in a mortar prior to dispersion causes fibres to break into shorter fragments.

Observations of cross-sections and dispersions indicate that most fibrils are produced by separation along interfibrillar boundaries and not by cleavage or parting of unit fibrils. It has been suggested (Chisholm, 1973; Veblen, 1980) that the fibrous nature of amphibole asbestos might be a consequence of breakage on (010), the plane on which Wadsley defects (chain-width errors) occur. Although we observe beam damage to occur readily on such planes, they do not appear to act as planes of cleavage or fracture. The possibility of fibrils

Fig. 4. Actinolite asbestos (Mexico). Low-magnification electron micrograph of ion-thinned cross-section. X =areas with fibres tightly packed in a bundle.

breaking longitudinally along (100) faults and {110} planes cannot be ruled out however, and it may be an especially active mechanism in coarse fibres, although some of the observed separation on {110} may have been induced during the sample preparation by ultramicrotome.

If fibrils were indeed primarily derived from the fracture of larger units on such planes as (100), (010) or {110}, then one would expect to find that fibrils are in similar orientations. In fact TEM studies of cross-sections of fibres (see below for detail) show that even within small clusters the individuals are in a variety of azimuthal orientations. It is perhaps surprising that the {110} cleavage of amphiboles does not feature more prominently in TEM studies. The cleavage property may therefore diminish in prominence with decreasing crystal size.

The relative orientations of asbestos fibrils and the boundaries between them were most clearly revealed in cross-sections. A low-magnification electron micrograph of ion-thinned actinolite (Table 1c, No. 15) fibres cross-section is shown in Fig. 4. Many fibrils, even very small ones, were separated by the resin during embedding, so the natural boundaries between these fibrils were not observable. However, in some regions (e.g., X in Fig. 4), fibrils were less separated, showing the actual arrangement of fibrils within a bundle, fibrils fitting tightly like a jigsaw puzzle. A number of fibrils are partially bounded by what seem to be {110} planes.

Various fibril morphologies have been observed; those of irregular outline, but nevertheless flattened in one direction; some with unusual morphology (Fig. 5a) bounded by {110}, and (010) and (100) crystallographic planes; and fibrils approaching an "ideal" crystal shape. In Fig. 5b the fibril, although only 0.1 μm wide, is bounded by low index crystallographic planes {110}, (100) and very small (010) faces. For some fibrils (Fig. 5c) high-resolution electron micrographs show that parts of the (100) and {110} faces consist of a series of very fine steps, sometimes only a few lattice planes deep.

Cross-sections of ferroactinolite asbestos (Table 1c, No. 16) were examined only by means of ultramicrotome sections with approximate thickness of 300 Å. Its fibrils were seen to be smaller than those of actinolite (Table 1c, No. 15) and were often 1000 Å wide. They were found also to have more irregular morphology. The most commonly observed outline of fibrils, still held together in a bundle, is illustrated by Fig. 6. This specimen did, however, also contain some fibrils partially bounded by straight faces. Fibrils are randomly oriented in the bundle; in the example shown fibrils are rotated around the z crystallographic axis with respect to one another by up to 40°.

"Massive" varieties of amphibole commonly known as nephrite jade, and one specimen which proved to be of richterite composition, have been examined by TEM using the dispersion and ion-beam thinning techniques to prepare specimens. Detailed results were given in Dorling and Zussman (1985) and only a brief summary is given here. The specimens were found to contain clusters of very small lath-like crystallites with z-axes approximately parallel but in a range of azimuthal orientations (Fig. 7). It is suggested that these clusters, which are themselves in varied orientations, are the result of post-tectonic re-crystallization of strained amphibole crystals, the new crystals inheriting the z-axis orientations of the old. The extreme toughness of nephrite jade is attributed to a number of the sub-microscopic features observed including the sizes, habits and orientations of its crystallites and the nature of its grain boundaries. These observations on nephrite are consistent with those obtained using the polarizing microscope and the scanning electron microscope.
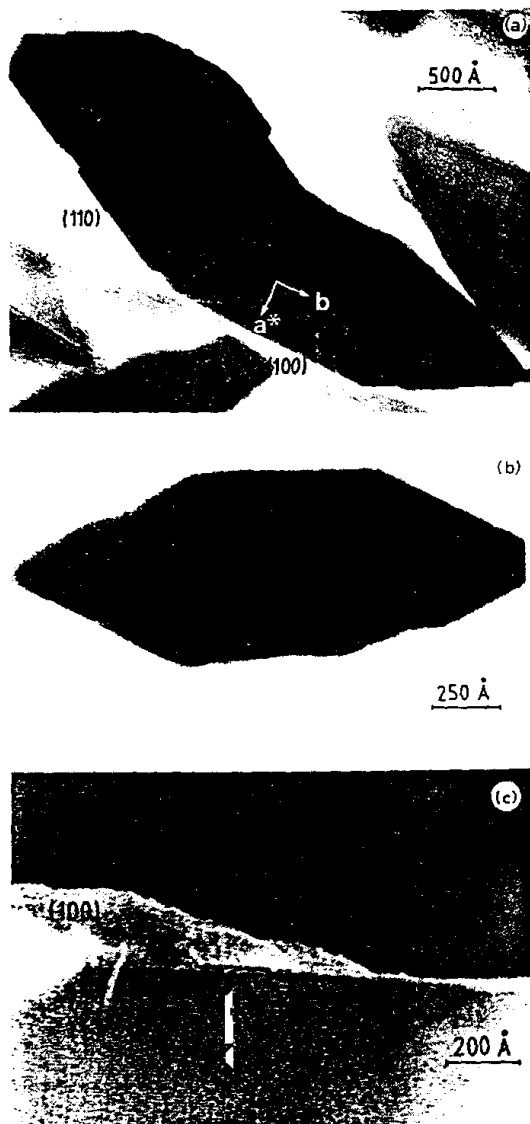
Fig. 6. Ferroactinolite asbestos (Prieska, South Africa). High-resolution electron micrograph of microtomed cross-section perpendicular to z. Note irregular outline of fibrils, and varying orientations in the bundle.

features as grain boundaries, exsolution lamellae, multiple-chain defects (010), twinning on (100), dislocation networks and alteration margins.

Prismatic varieties

Many of the features mentioned above were observed in the prismatic actinolite from Habachtal (Table 1a, sample No. 25) and for this a fairly full

Fig. 5. Actinolite asbestos (Mexico). Electron micrographs of:
a. Single fibril (cross-section) with unusual morphology, bounded by straight crystallographic planes, i.e. (100), {110}, (010).
b. Single fibril approaching an "ideal" crystal shape.
c. High-resolution image of part of a fibril with {110} lattice planes resolved. Note the stepped nature of the (100) face.

Internal sub-microscopic features

In this study similarities and differences have been noted as between different morphological varieties of amphibole with regard to such fine-scale
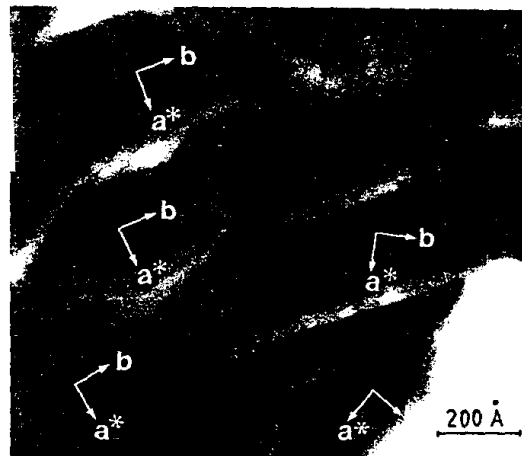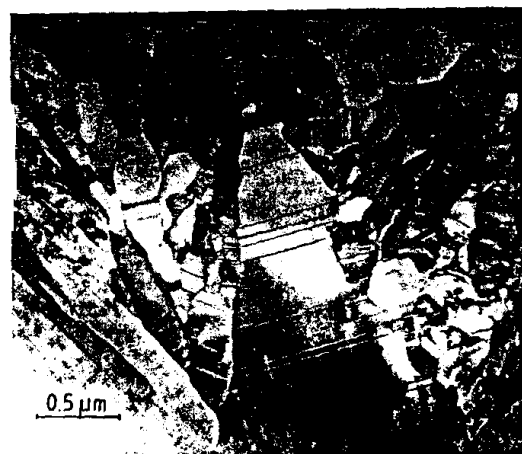

Fig. 7. Nephrite jade (Verla Irene, Sweetwater, Wyo., U.S.A.). Electron micrograph of cross-sections of crystallites exhibiting approximately random orientation. The directions of y-axes of individual crystallites are indicated by the (010) defects.

description is given. For other prismatic specimens only additional features are reported. In hand specimen, the actinolite appears as dark-green, coarse prismatic crystals. Electron microscopic studies revealed that it contains abundant defects on (010), (i.e. chain-width defects), dislocations and an extensive grain boundary network characteristic of deformation structure.

A typical area of this actinolite is shown in Fig. 8a. The specimen was tilted slightly away from the [100] zone axis to obtain contrast from the (010) defects, visible as linear features running parallel to the z-axis. An extinction contour running across the crystal is slightly displaced at the defects. Sometimes Wadsley defects appeared at low magnification to be non-parallel, as for example shown in Fig. 8b, where defect I continues along the same plane through a considerable distance, whereas defect II is displaced through the crystal in step fashion towards I. This is because defect II consists of several defects, each extending through a relatively short distance and then being offset by a few planes at the fault which is visible by fringe contrast. Fringe contrast indicates that the fault plane at which the termination occurs is inclined to the projection plane and that there is a certain amount of strain associated with the termination. Terminations of defects can be seen in Fig. 8c (e.g., at A and B) where the fault plane is edge-on.

Where dense chain-width defects were observed, these gave rise to streaking along b^* in the diffraction patterns, an effect expected due to the considerable structural disorder involved.

Chain-width defects have been examined by the one-dimensional lattice imaging technique, tilting the specimen in the electron microscope to bring the [100] direction, or indeed any other zone axis perpendicular to y, parallel to the electron beam. At high resolution, chain-width defects appear as wider spacings among approximately 9 Å (020) lattice fringes corresponding to the normal amphibole double chain width (see, e.g., Fig. 14). The best results were obtained from areas close to a thin crystal edge, but the edge itself was often beam-damaged. Beam-damage also occurred along chain-width defects. This was observed frequently and in most cases it causes the defects to appear to be wider than they really are. Decomposition, probably by dehydration, usually appears to progress along defects from the edge of the specimen. This must indicate
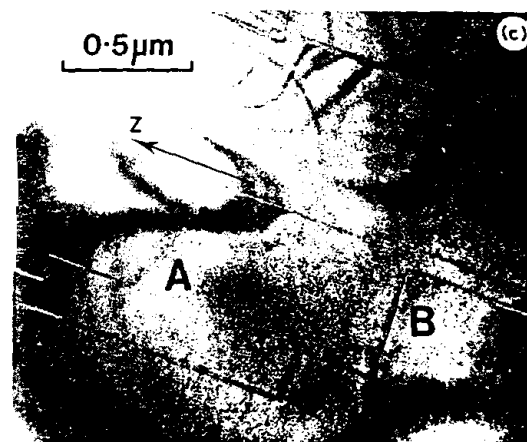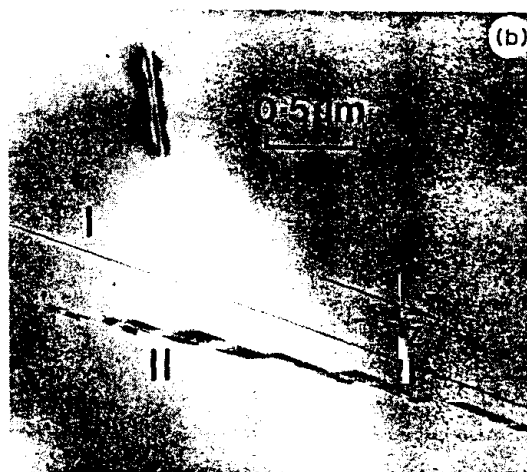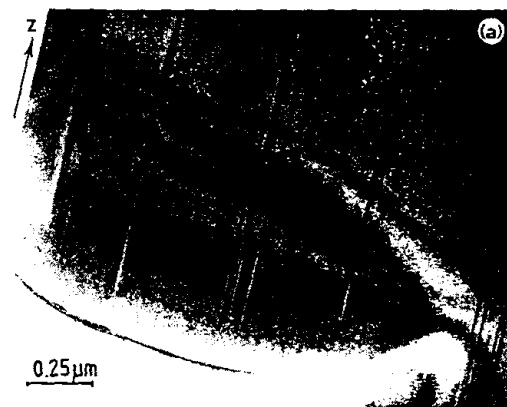
Fig. 8. Prismatic actinolite (Habachtal, Austria) ion-thinned specimen:
a. A low-magnification electron micrograph showing abundant defects on (010).
b. Defects on (010) *I* and *II*. Defect *II* crosses the crystal in step-wise fashion via faults.
c. Terminations of (010) defects at faults, e.g. A and B seen edge-on.
d. Microstructure showing dislocations in mostly curved sub-grain boundaries.

some different property of the defect lamellae compared with the double-chain matrix, possibly a difference in chemical composition. Beam damage appeared to be most evident in regions where there are higher multiples (4-chain and above) of chain width, or a higher density of chain-width errors of all kinds.

Other typical microstructures are illustrated in Fig. 8d. At sufficiently high magnification it could be seen that sub-grain boundaries consist of a series of dislocations, roughly parallel to [001]. The sub-grain boundaries in general were slightly curved and did not follow any particular crystallographic direction.

Planar arrays of dislocations were commonly observed. Isolated individual dislocations frequently present in this specimen were studied by contrast experiments, and the Burgers vector b was deduced to be parallel to [001]. Where dislocations with Burgers vector parallel to z have been described in pyroxenes, it was suggested (Christie and Ardell, 1976) that their formation took place by translation of the layers of chains involving breaking of only metal-oxygen bonds between the chains rather than the Si-O bonds in the chains. Similar mechanisms

probably apply here to amphiboles. Lorimer (1974) suggested that the sub-grain networks probably form during a recovery and recrystallization process, while the planar arrays of dislocations and individual dislocation networks are primary deformation structures. Rearrangement of dislocations into boundaries is one of the mechanisms for releasing strain energy accumulated during deformation (Hull, 1975). Further imperfections occurring in this actinolite were stacking faults on (100).

Another prismatic actinolite (Table 1a, sample No. 26) exhibited exsolution lamellae, on (100), of a Ca-free phase which were identified as grünerite using the analytical mode of the Philips 400T electron microscope.

A prismatic tremolite from Nigeria (Table 1a, No. 2) and another from New York (Table 1a, No. 4) showed regions of alteration to talc, the margins of which appear to be associated with either faults or low-angle sub-grain boundaries. In Fig. 9, talc appears to be eroding tremolite along (020) planes. By contrast, in another prismatic specimen there is a sharp talc-actinolite interface (Fig. 10) for which the diffraction pattern suggests coincidence of c^* (talc) with $[110]^*$ (actinolite). The relationship a (talc) $=c$ (tremolite), as observed by Stemple and Brindley (1960) possibly occurs also in this case. These relationships suggest parallel growth rather than alteration.

The specimens of tremolite and actinolite of prismatic habit studied here by electron microscopy have been shown to contain highly deformed areas (i.e. with dense dislocations and boundaries) as well as homogeneous, almost defect-free regions. This indicates the need to examine several sections of a specimen before drawing conclusions as to the abundance of defects.

Fine acicular varieties of actinolite (byssolites), and nephrites

Individual needle-like crystals of three byssolite specimens were mounted directly across brass rings and ion-thinned. Observations revealed the presence of faults on (100), dislocations and multiple-chain defects, but in general byssolites are free of defects as compared with prismatic specimens. An unusual effect was observed in some specimens of byssolite and is illustrated in Fig. 11. These are thought to be fluid inclusions with large strain fields

Fig. 9. Prismatic tremolite (New York, U.S.A.). Electron micrograph showing:
a. The alteration of tremolite to talc (with large pores). Inset: SAED pattern from tremolite on either side of the alteration "river" of talc (beam parallel to [101]). Slight rotation at the boundary is indicated by split reflections.
b. Enlargement of the boundary area between talc and tremolite showing alteration developed along (010) planes.
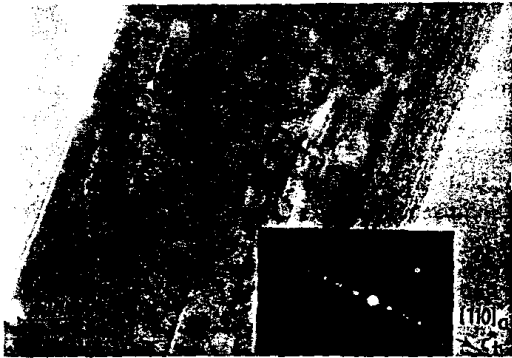

Fig. 10. Prismatic actinolite (unknown locality). Direct lattice resolution of talc with numerous faults. Inset: SAED across the interface talc-actinolite; c^* of talc coincides with $[110]^*$ of actinolite.

Fig. 11. Actinolite (variety byssolite). Electron micrograph showing faults or sub-boundaries decorated with void-like features.

around them, but attempts to identify the nature of these tiny inclusions were unsuccessful. In the three nephrite specimens examined, chain-width errors on (010); some isolated and some regularly repeating, are more abundant than in other amphibole specimens. Beam damage occurs preferentially along
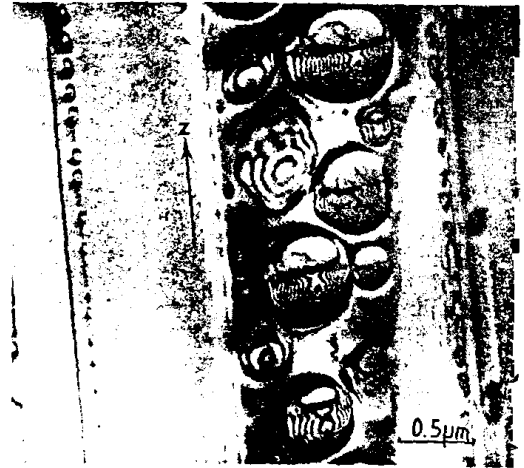
these defects (as well as at grain boundaries) and helps to reveal them even at relatively low magnification.

Asbestos

Asbestos specimens were prepared by ion-thinning of doubly polished thin-sections, by ion-thinning of fibres directly mounted longitudinally on a specimen grid, by the dispersion method or by ultramicrotomy of cross-sections. A common problem encountered with the ion-thinned specimens was overlap of fibrils. Whereas such specimens were useful for the observations of defects, they did not readily provide information about sizes and orientation of fibrils. Lamellar features often present in such sections would seem to indicate twinning but electron diffraction patterns are complex and are similar to those produced by fibrils in random azimuthal orientations as well as twinning.

Observations on ultrasonically dispersed fibres of actinolite asbestos (Table 1c, sample No. 15) show well-separated units which are believed to represent naturally occurring individual fibrils. Not all fibrils show smooth parallel sides. Features as arrowed on Fig. 12a are thought to be "impressions" of other fibrils growing in different directions. In some specimens, boundaries running across fibres, i.e. roughly perpendicular to their lengths, were observed where the (020) lattice fringes show rotation of approximately 10° across the boundary.

Multiple twinning is frequently present. Fibrils showing twinning by diffraction contrast are lying approximately on (010). Evidence of twinning was observed also on b^* c^* diffraction patterns, i.e. with the electron beam perpendicular to the twin plane. These frequently exhibited anomalous features, i.e. they appeared to contain 0k0 and 0kl reflections with k odd which are not allowed by the space group C2/m. This can be explained by the superimposition of the two orientations; in most cases the electron beam was parallel to [100] in one part of the twin and to [101] in the other part. (The additional reflections were too intense to be explained by double diffraction.) Multiple (100) twinning in asbestos (Table 1c, No. 15) seen in longitudinal sections was observed also by diffraction contrast in cross-sections, e.g. Fig. 12b.

Changes, most likely due to beam damage, occurred in some specimens, forming "amorphous" rims on fibrils, as shown for example in Fig. 13; similar changes were found to occur at the defects and fibril boundaries. Crawford (1980), in his studies on crocidolite asbestos in human tissue, showed a similar effect, which was described as a "grey layer" and its presence was explained by erosion which had occurred as a result of biological activities of lung tissue and blood serum. There could
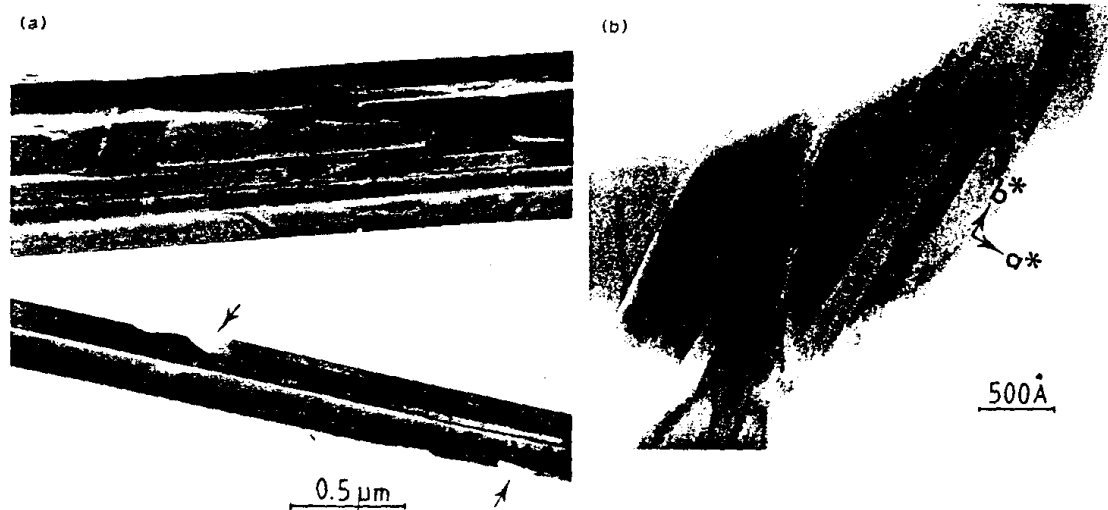

Fig. 12. Actinolite asbestos (Mexico):
a. Electron micrograph showing morphology of fibrils dispersed without grinding. "Impression" features are arrowed.
b. Section of fibrils approximately perpendicular to z-axis, slightly tilted, giving rise to diffraction contrast in multiple twinned fibrils.
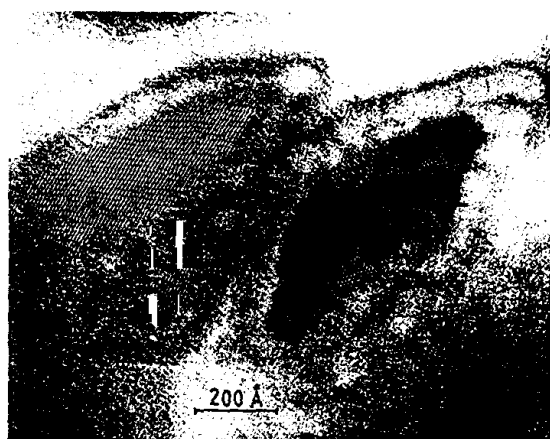
Fig. 13. Electron micrograph showing beam damage occurring at the outer rims of fibrils sectioned perpendicular to z-axis.

Fig. 14. Tremolite asbestos (Jamestown, Calif., U.S.A.). High-resolution lattice image of fibril showing chain-width defects on (010).

be difficulty in distinguishing possible effects of this kind from those which arise purely from electron beam damage.

Multiple twinning was shown also by ferroactinolite asbestos (Table 1c, No. 16), the twin lamellae having thicknesses of approximately 200 Å. Selected-area diffraction patterns from such fibres show elongation of reflections along a^* due to the very fine-scale twinning. The a^* direction is common for both parts of the twin.

Chain-width defects were particularly abundant (Fig. 14) in fibrils of tremolite asbestos (Table 1c, No. 13). Streaking parallel to b^* was frequently observed in diffraction patterns. In other studies (e.g., Hutchison et al., 1975) it was reported that such defects in tremolite asbestos did not cause streaking, but this may be dependent upon the density of defects, which can vary considerably from fibril to fibril even within one specimen. Cross-sections of this asbestos confirmed the presence of chain-width defects and showed that some of them terminated at a fibril's surface and others within a fibril. Chain-width defects were common also in other specimens of fibrous tremolite but very few were observed in the two specimens of actinolite asbestos (Table 1c, Nos. 15,16).

Chemical composition

Throughout the present study the nomenclature recommended by the IMA Commission (Leake,
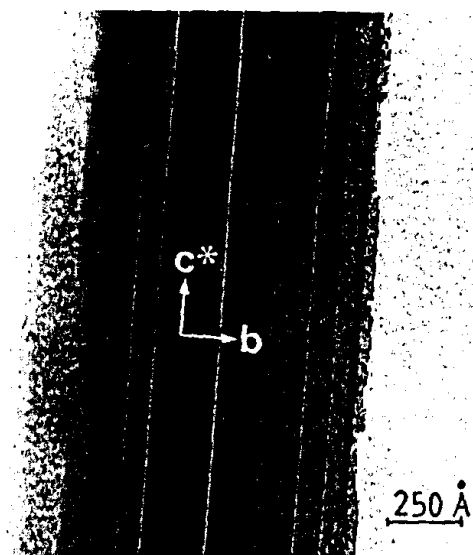
1978) is used, according to which all amphiboles with $(Ca+Na)_x > 1.34$ and $Na_x < 0.67$ on the basis of $22(O)$ and $2(OH)$ per formula unit are members of the calcic amphibole group. The name tremolite is used for specimens for which $(Ca+Na)_x > 1.34$, $Na_x < 0.67$, $(Na+K)_{A\text{-}site} < 0.5$, $Si > 7.50$ and $Mg/(Mg+Fe) > 0.90$. The name actinolite is used when $Mg/(Mg+Fe)$ is between 0.50 and 0.90, while other factors are the same as for the definition of tremolite. End-member tremolite has the formula $Ca_2Mg_5Si_8O_{22}(OH)_2$. Assignment of the cations to the various sites was made following the recommendations in Leake (1978).

Electron microprobe analyses

The specimens of the tremolite-ferroactinolite series we have studied are listed in Table 1 with localities, catalogue numbers and chemical formulae. The formulae were calculated from the electron probe analyses which are tabulated in order of decreasing $Mg/(Mg+Fe)$ ratio in Table 2a, b and c. In all cases the results represent mean values obtained from each specimen by analysing several spots. In electron microprobe analyses there is no distinction between the two oxidation states of iron; total Fe was used for calculating the ratio $Mg/(Mg+Fe)$. In ad-

dition to the major elements of the tremolite-ferroactinolite series, i.e. Ca, Mg, Fe, Si, specimens were analysed for Al, Mn, Ti, Cr, Na and K. Because the water content has not been determined, the numbers of atoms per formula unit were calculated on the basis of 23 oxygen equivalents.

In the case of asbestos and asbestiform specimens, the results can be regarded as average compositions for a bundle of fibrils since the beam size is approximately ten times larger than the average fibril diameter (0.1 μm). In all, 54 specimens were analysed; 26 prismatic, 3 nephrites, 8 byssolites and 17 asbestiform amphiboles. The analyses were carried out using a Cambridge Geoscan instrument

with Link Systems energy dispersive spectrometer. Accelerating voltage was 15 kV, specimen current 3 nA, and counting time 100 s. ZAF corrections were applied. The accuracy of the method and details of procedures were discussed by Dunham and Wilkinson (1978). Standards were: Si wollastonite; Al corundum; Mg periclase; Fe fayalite; Ti rutile; Mn tephroite; Cr metal; Ca wollastonite; Na jadeite; K orthoclase.

The totals of analyses presented in Table 2 fall mostly between 97% and 98%. This would be expected since constitutional "water" (H_2O^+, normally about 2%) and adsorbed water (H_2O^-, normally between 0 and 1%) are not detected by

TABLE 2a

Electron microprobe analyses of prismatic and massive (nephrite) specimens of the tremolite-ferroactinolite series

	1	2	3	4	5	6	7	8	9	10
SiO_2	58.88	58.72	57.48	58.97	58.04	58.86	58.77	58.59	56.74	58.27
Al_2O_3	—	—	3.48	0.30	0.39	—	0.37	0.28	1.51	1.13
Cr_2O_3	—	—	—	—	—	—	—	—	—	0.36
FeO	0.21	0.25	0.46	0.27	1.23	1.35	—	1.20	1.62	2.19
MnO	—	—	—	0.59	—	—	1.33	—	—	—
MgO	24.06	23.94	22.98	24.65	22.66	23.89	23.87	23.53	22.38	23.24
CaO	12.57	14.14	13.83	12.58	13.78	13.48	12.00	12.57	13.55	13.67
Na_2O	0.73	—	0.50	—	—	—	1.05	0.83	0.92	—
K_2O	0.46	—	—	—	—	—	—	—	0.47	—
Total	96.91	97.05	98.73	97.36	96.10	97.58	97.39	97.00	97.19	98.86

	11	12	13	14	15	16	17	18	19	
SiO_2	57.29	59.03	56.56	58.00	57.86	57.43	58.06	57.51	57.00	
Al_2O_3	1.55	—	1.97	0.27	—	0.50	0.98	0.46	1.27	
Cr_2O_3	—	—	—	—	—	—	—	—	0.44	
FeO	2.35	2.53	3.54	3.78	3.72	3.79	4.58	5.01	5.20	
MnO	—	—	—	—	0.26	0.30	0.21	0.30	—	
MgO	22.66	23.22	22.43	22.10	22.04	21.74	21.41	21.96	21.22	
CaO	11.98	13.12	12.73	12.00	12.86	13.03	12.42	12.01	12.27	
Na_2O	1.88	—	0.88	1.20	0.31	0.51	0.42	0.46	0.36	
K_2O	0.76	—	—	—	—	—	—	—	—	
Total	98.47	97.90	98.11	97.35	97.05	97.30	98.08	97.71	97.76	

	20	21	22	23	24	25	26	27	28	29
SiO_2	57.57	57.55	55.61	53.27	56.72	56.16	56.59	55.56	55.03	58.69
Al_2O_3	0.60	0.84	3.16	5.26	0.79	2.46	0.91	2.45	3.08	—
Cr_2O_3	—	0.46	0.27	—	0.40	—	—	—	0.28	—
FeO	5.66	6.04	6.02	6.32	6.84	7.59	8.41	8.11	8.17	0.24
MnO	—	—	0.45	—	0.50	0.32	—	0.32	0.29	—
MgO	21.48	20.97	20.46	18.96	19.57	19.41	19.44	19.00	18.57	24.39
CaO	12.33	11.70	11.95	12.88	12.24	12.15	11.71	12.76	12.31	8.42
Na_2O	0.69	0.75	—	1.01	0.79	0.53	0.73	0.55	1.00	4.73
K_2O	—	—	—	—	—	—	—	—	—	0.82
Total	98.33	98.31	97.92	97.70	97.85	98.62	97.79	98.75	98.73	97.29

Specimen Nos. 6, 10 and 29 are nephrites; the latter is a richterite with nephrite texture.

TABLE 2b

Electron microprobe analyses of byssolite-type specimens of the tremolite-ferroactinolite series

	1	2	3	4	5	6	7	8
SiO_2	53.07	51.98	52.10	53.07	53.35	53.43	52.12	51.75
Al_2O_3	2.52	4.01	3.55	2.91	2.39	1.21	0.68	1.59
Cr_2O_3	—	—	—	—	—	—	—	—
FeO	9.65	12.04	12.10	13.24	13.98	16.96	18.36	20.08
MnO	0.24	0.29	0.23	0.38	0.28	—	2.95	0.48
MgO	17.05	15.81	14.96	15.37	13.96	13.66	10.39	10.73
CaO	12.84	12.31	12.86	11.93	12.48	12.63	12.54	12.73
Na_2O	—	1.06	0.56	1.09	0.29	0.51	0.42	0.46
K_2O	—	—	0.19	—	—	—	—	0.18
Total	95.37	97.50	96.55	97.99	96.73	98.40	97.46	98.00

TABLE 2c

Electron microprobe analyses of asbestiform and asbestos specimens of the tremolite-ferroactinolite series

	1	2	3	4	5	6	7	8
SiO_2	58.53	58.20	57.88	58.04	58.03	58.33	57.72	55.63
Al_2O_3	—	—	—	—	—	—	0.32	—
Cr_2O_3	—	—	—	—	—	—	—	—
FeO	0.30	0.70	1.06	1.42	1.45	1.62	1.73	2.48
MnO	—	—	—	—	—	—	—	—
MgO	24.65	23.81	23.68	23.80	23.60	23.42	22.87	22.15
CaO	13.36	13.05	13.34	13.47	13.53	13.26	13.98	12.41
Na_2O	0.42	—	0.36	0.35	—	—	0.59	0.32
K_2O	—	—	—	—	—	—	—	—
Total	97.26	95.76	96.32	97.08	96.61	96.63	97.21	92.99

	9	10	11	12	13	14	15	16
SiO_2	57.47	57.76	54.45	58.39	58.45	58.03	41.30	52.18
Al_2O_3	—	—	—	—	—	—	0.25	—
Cr_2O_3	—	—	—	—	—	—	—	—
FeO	2.56	2.49	2.66	2.88	3.82	4.96	11.65	30.25
MnO	—	0.24	—	0.36	0.37	—	0.28	0.29
MgO	22.94	23.40	20.34	23.56	21.72	21.56	10.80	4.54
CaO	13.12	12.86	13.27	12.68	14.03	13.08	8.78	10.95
Na_2O	0.72	—	0.49	—	—	—	0.37	—
K_2O	—	—	—	—	—	—	—	—
Total	96.81	96.75	91.21	97.87	98.39	97.63	73.43	98.21

electron probe analysis. In a few cases (Table 1b, No. 1 and c, Nos. 2, 8 and 15) totals are exceptionally low since for these the specimens analysed were appreciably narrower than the probe size and the quality of the polished surfaces were poor. Even for these however, the estimates of the relative amounts of elements present are expected to be meaningful and a formula has therefore been calculated.

Compositional trends

The specimens in this study were chosen to be near to tremolite-ferroactinolite in composition, but it can be seen from the chemical analyses, that most (34 out of 54) specimens depart significantly from the idealized formula, $Ca_2(Mg,Fe)_5Si_8O_{22}(OH)_2$, of the series. Substitutions of Al^{3+} for Si^{4+}, Al^{3+} for $(Mg,Fe)^{2+}$ and Na^+ for Ca^{2+} are found, and

the A-site has some content of Na^+, or Na^+ plus K^+. These are all possible within the limits of the general amphibole formula $A_{0-1}X_2Y_5Z_8O_{22}(OH)_2$.

Observed deviations from the ideal tremolite-actinolite formula can be assigned to compositional trends toward other amphibole end-members as illustrated graphically in Fig. 15. Considering the way that the main morphological varieties of tremolite-ferroactinolite plot on the compositional diagram, some systematic chemical features can be discerned.

The asbestos specimens show zero or very slight departures from the ideal tremolite-actinolite formula, and when they do divert they tend to fall on the plane tremolite-richterite-winchite, i.e. they have Na in the X- and A-sites but little or no Al in Z. For 14 of the 16 asbestos specimens the content of aluminium is below the limit of detection (<0.01 atoms per formula unit), and the remaining two have 0.01 and 0.05 Al. In the latter case 0.01 Al is in substitution for Si.

For 6 of the 8 byssolite specimens the X-site is full without the need to allocate Na to it, and for the remaining two only 0.01 Na is needed. Substitution of Na in the A-site is however appreciable, as also is Al for Si and Mg. Byssolites thus plot close to the base plane of Fig. 15, with $Na(X) = 0$.

The 26 prismatic specimens of tremolite-actinolite show a wide range of compositions including some which have the restrictions referred to above. It should be clearly understood therefore that the

conclusion that asbestos cannot have significant Al content does not imply that it will necessarily form if Al is absent. A similar caveat applies to byssolites and their lack of Na(X).

Of the massive (nephrite) specimens examined, two were close to richterite and tremolite respectively and the other showed a tschermakitic trend, but too few specimens were available for any general conclusion to be drawn.

Additional variations of chemistry with morphology are evident from the probe analyses. Potassium is not present in any of the asbestos specimens but it is present in some of the prismatic and byssolite specimens. Sodium is observed in fewer of the asbestos specimens and when present shows a narrower range of contents. Manganese occurs in fewer asbestos specimens than in byssolites, and when present is in lower concentrations.

According to published accounts, Fe^{3+} is present only in relatively small amounts (<0.2 at./formula unit) in the more Mg-rich members of the tremolite-actinolite series, but in the more Fe-rich actinolites the amount of Fe as Fe^{3+} can be appreciable (Deer et al., 1963). The total FeO content determined by means of electron microprobe was recalculated for Fe^{2+} and Fe^{3+} for 22 of our specimens (14 prismatic, 5 byssolites and 3 asbestos), using the method of Papike et al. (1973). Most of the tremolites, i.e. specimens containing 0–10% $Fe/(Mg+Fe)$ do not appear to have Fe as Fe^{3+}. Al-
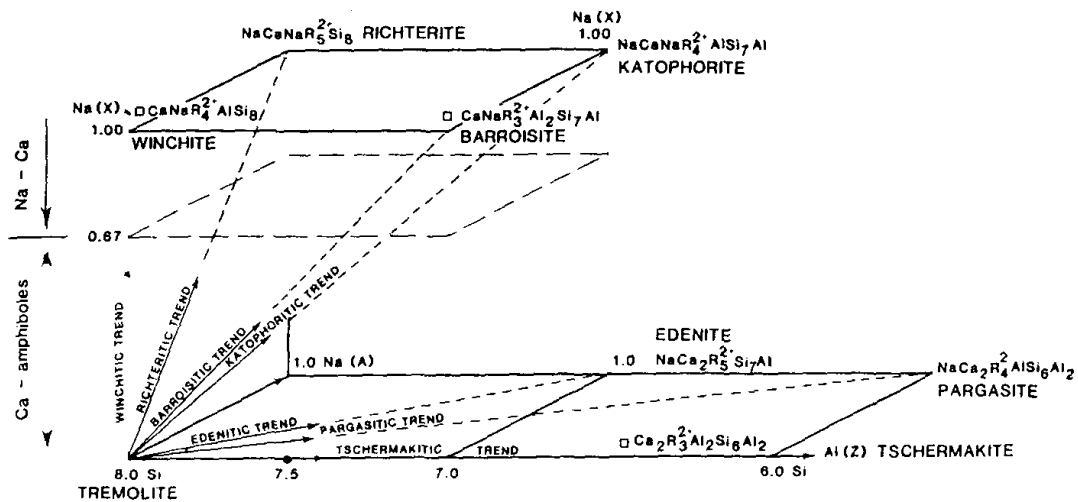

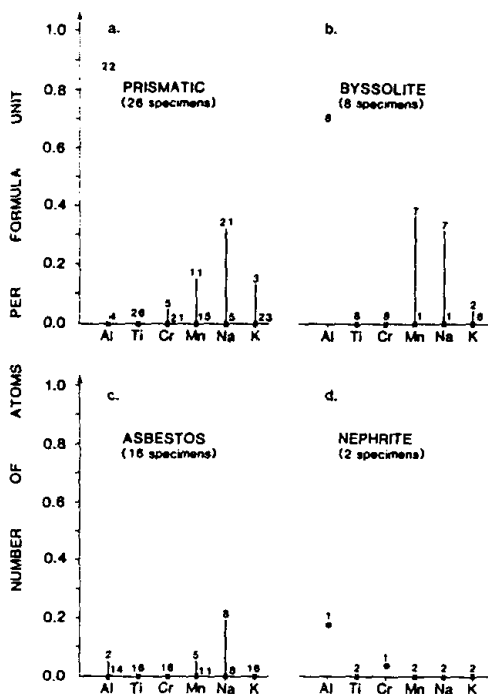Fig. 15. Types of substitution and chemical trends in calcium-rich amphiboles.

486

a.

1.0

22

0.8   PRISMATIC
      (26 specimens)

0.6

0.4
                      21

0.2   11
                          3
0.0 4 20 5   21 19 5 23
     Al Ti Cr Mn Na K

b.

BYSSOLITE
(8 specimens)
8
                  7
                      7

                          2
     8   8   1   1   8
     Al Ti Cr Mn Na K

c.

ASBESTOS
(15 specimens)

                  8

     2   5
     14 15 15 11 8 15
     Al Ti Cr Mn Na K

d.

NEPHRITE
(2 specimens)

      1

     2   1   2   2   2
     Al Ti Cr Mn Na K

(y-axis labels: NUMBER OF ATOMS PER FORMULA UNIT)

Fig. 16. The minor-element ranges in tremolite specimens for: (a) prismatic; (b) byssolite; (c) asbestos; and (d) massive (nephrite) habit. Number of specimens in range and number below detection limit (×) are indicated.

though total Fe and Fe^{3+} content is variable across the range of specimens examined, it was found that Fe^{3+} is either absent or is a very small proportion of the whole Fe content in byssolite and asbestos-type actinolites, despite the fact that they are Fe-rich.

The minor-element contents of Al, Ti, Cr, Mn, Na and K are summarized for the four morphological groups in Fig. 16. The asbestiform group shows lower maximum contents of all the above-mentioned elements and moreover these are present in a relatively small proportion of the asbestos specimens. Viewing the overall chemical composition, the asbestiform specimens appear to have compositions closer to the ideal for the tremolite-actinolite series.

The most striking chemical feature of asbestos specimens, their lack of aluminium, is discussed in greater detail below.

All the main amphibole groups which are known to occur sometimes in asbestiform habit, e.g., grünerite, anthophyllite, riebeckite, tremolite, actinolite and richterite, are Si-rich and have end-member ideal formulae with $[Si_8O_{22}]$, i.e. with no tetrahedral Al, whereas common hornblendes, pargasites, hastingsites, tschermakites and edenites all have appreciable tetrahedral Al content and do not occur with asbestiform habit.

The amounts of Al present in analyses of tremolite-actinolite compiled by Leake (1968) varies from 1.0 to 6.0 wt.% which is equivalent roughly to 0.16–1.00 atoms per formula unit, the maximum allowed by definition in his classification of amphiboles. Unfortunately from our point of view, crystal morphological descriptions were not given in the above work. Our observations show that, within the range of Al content permitted by definition, truly asbestiform specimens are restricted to those at the Al-free end-member composition, or very near to it. Thus it appears from the analyses of natural specimens that there is a link between asbestos formation and lack of aluminium.

Published experimental studies also give useful information about the growth of amphibole fibres. Asbestiform amphiboles have been synthesized (e.g., Fedoseev et al., 1970; Kalinin et al., 1975) using a wide range of compositions including some with major components (e.g., Ni, Co, Zn, Cu) not normally found in natural specimens*, but as emphasized by Grigorieva et al. (1975), compositions including Al did not yield a fibrous amphibole.

The above-mentioned workers also demonstrated that fibrous amphiboles are formed at relatively low temperatures and so temperature of formation may be another factor as well as Al content which correlates with morphology (see also Kostyuk and Sobolev, 1969). Since higher temperatures usually favour higher $[Al]^{IV}$ content, the two factors are mutually consistent. It may be suggested that if appreciable Al is present asbestos will not form even at the right temperatures for its formation, and that if Al is absent, asbestos forms at lower,

*One natural specimen (zincian actinolite, Franklin, New Jersey) studied by us contains 6% ZnO and is asbestiform. Further details are given in Dorling and Zussman (1984).

rather than higher, temperatures of crystallization. Alternatively (but rather unlikely), it may be that fibres form at such low temperatures that even very small amounts of Al are excluded, even from an Al-rich environment. The association of asbestos formation with lower temperatures as shown by experimental work is also indicated by its natural occurrence in veins, the latter being of secondary (lower temperature) formation.

Theoretical reasons for.the correlation of fibrous morphology with Al content have been alluded to by Harry (1950) and DeVore (1953, 1955, 1957), and are developed further here. Harry (1950) suggested that low values for Si replacement by Al common in the actinolitic amphiboles may result in weaker bonding between chains of tetrahedra, thereby favouring asbestiform development. Conversely, a high degree of Al substitution for Si, as in the hornblendes, favours strong links between chains and therefore a stumpy prismatic habit. DeVore (1953) also noted that Al for Si substitution weakened the bonding within the chains.

The substitution of Al for Si increases the Z-Ò bond distances (Papike and Clark, 1968; Litvin, 1977) and therefore reduces the strength of bonding within and parallel to the length of the amphibole chains. This in itself would argue for a lesser tendency to fibrous habit, and this effect will be enhanced by the necessary compensating substitution of Al in Y-sites. Whereas Al in M1 or M3 would strengthen each amphibole ribbon, Al in M2 (strongly preferred) should decrease M2-O4 distances and thus strengthen lateral bonding between neighbouring chains.* The alternative compensation by Na entering the otherwise vacant A-site will also serve to strengthen lateral bonding but there is no indication from our observations or from the literature that specimens of asbestos have lower A-site contents than non-asbestos varieties.

While the effects of a large amount of Al substitution on bonding and crystal growth can be readily visualized, our observation that even very small amounts of Al can be effective is surprising. A possible explanation can be offered as follows. At the structural sites where Al atoms occur in the amphibole chain, development of a lateral growth step will be favoured through stronger lateral bonding. Once formed, however, the step could act as a nucleus for rapid growth parallel to the chain length. The process of lateral steps at Al atoms and z-direction growth could be repeated. It must be admitted, however, that there is no direct evidence for the mechanism having operated.

Conclusions

The physical and chemical features that can be assigned broadly to each of the four morphologi-

---

*Standard M site labelling (see, e.g., Hawthorne, 1981).

TABLE 3

Morphology and properties of tremolite-actinolites; a general comparison

Properties Morphology	Crystal units	Multiple twinning	Well-developed crystal faces	Multiple chain (010) defects	Dislocation networks and sub-grain boundaries	Exsolution	Chemical substitutions		
							Na in A	Na for Ca	Al for Si
Prismatic	large crystals	none	common	abundant in one specimen; few in others	common	some specimens	varied	varied	varied
Acicular ("byssolite")	slender needles or laths	none	common	rare	none	none	appreciable	very little	appreciable
Massive ("nephrite")	submicro-scopic short laths	none	rare	abundant	sub-grain bounda-ries common	none	(*)	(*)	(*)
Asbestos	submicro-scopic fibrils	common	rare	abundant in tre-molites; few in actinolites	none	none	varied	little	almost zero

*Insufficient samples for generalization.

cally different kinds of calcic amphibole are summarized in Table 3. Caution is needed however in its interpretation for two main reasons: (1) asbestiform varieties range from finer (flexible) to coarser (more brittle) specimens and many specimens contain a mixture of fine and coarse fibrils; and (2) there can be some variability in properties [e.g., density of (010) defects] even within an apparently homogeneous specimen.

The characteristics of the four morphological subgroups correlate reasonably well with what is known of their geological environments. For asbestos specimens, their low level of substituting cations (particularly Al), lack of exsolution, lack of dislocations and sub-grain boundaries and generally poorly developed crystal faces are all compatible with relatively rapid multiple nucleation and growth in a low-temperature stress-free environment. Multiple twinning on (100) also seems favoured by these conditions. The opposite properties and conditions apply to most prismatic specimens. The nephrites, with massive fine-grained texture, derive from recrystallization of pre-existing coarser-grained amphibole. The features of the finely acicular byssolites, reminiscent of "whiskers", are consistent with stress-free growth from fluids or vapour in cavities, perhaps at moderate growth rates and temperatures. There appears to be no consistent relationship between abundance of chain-width defects and morphological type.

With regard to the question of health hazards, it seems unlikely, though not impossible, that some of the distinguishing features enumerated above (e.g., twinning or Al content) would confer different biological activity on the different varieties. We are left then with the widely accepted view that morphology itself is the important factor, small particles with high length/breadth ratios being the most hazardous. Our studies allow us to conclude qualitatively that although crushed non-asbestos specimens produce some small highly elongated particles the proportion of these is far lower than for dispersed or crushed asbestos. This is because asbestos is comminuted mainly by the separation of fibrils whereas the others break across prism, lath or needle length, as well as by {110} and (100) cleavages and partings.

The prominent {110} cleavages are always emphasized in textbook discussions of amphiboles. Our observations on the macro-, micro- and sub-micro-scopic scale show the surprising importance of (100) cleavage or parting as well as the tendency of a lath-like (parallel to z) growth morphology with flattening on (100).

Acknowledgements

References

Ampian, S.G., 1976. Asbestos minerals and their nonasbestos analogs. Proc. Symp. on Electron Microscopy of Microfibres. Pennsylvania State Univ., University Park, Pa.

Campbell, W.J., Blake, R.L., Brown, L.L., Cather, E.E. and Sjöberg, J.J., 1977. Selected silicate minerals and their asbestiform varieties. U.S. Bur. Mines, Info. Circ., No. 8751.

Chisholm, J.E., 1973. Planar defects in fibrous amphiboles. J. Mater. Sci., 8: 475–483.

Chisholm, J.E., 1980. Attempted prediction of the morphology of amphiboles from their crystal structures. Proc. 4th Int. Conf. on Asbestos, Turin, 1: 301–316.

Chisholm, J.E., 1983. Transmission electron microscopy of asbestos. In: S.S. Chissick and R. Derricott (Editors), Asbestos. Vol. 2. Wiley, New York, N.Y., pp. 85–167.

Chojnacki, J., 1973. Elementy krystalografii chemicznej i fizycznej. Państwowe Wydawnictwo Naukowe, Warsaw, 465 pp.

Christie, J.M. and Ardell, A.J., 1976. Deformation structures in minerals. In: H.-R. Wenk (Editor), Electron Microscopy in Mineralogy. Springer, New York, N.Y., pp. 374–403.

Crawford, D., 1980. Electron microscopy applied to studies of the biological significance of defects in crocidolite asbestos. J. Microsc. (Oxford), 120: 181–192.

Dana, E.S., 1922. A Text-book of Mineralogy with an Extended Treatise on Crystallography and Physical Mineralogy. Revised and enlarged by W.E. Ford. Wiley, New York, N.Y., 3rd ed.

DeVore, G.W., 1953. Compositional control of dimensional properties of crystals. Am. Mineral., 38: 334–335.

Deer, W.A., Howie, R.A. and Zussman, J., 1963. Rock Forming Minerals, Vol. 2, Chain Silicates. Longmans, London, 250 pp.

DeVore, G.W., 1955. Crystal growth and the distribution of elements. J. Geol., 63: 471–494.

DeVore, G.W., 1957. The association of strongly polarizing cations with weakly polarizing cations as a major influence in element distribution, mineral composition and crystal growth. J. Geol., 65: 178–195.

Dorling, M. and Zussman, J., 1980. Comparative studies of asbestiform and non-asbestiform calcium-rich amphi-

boles. Proc. 4th Int. Conf. on Asbestos, Turin, pp. 317-333.

Dorling, M. and Zussman, J., 1984. Zincian actinolite asbestos. Mineral. Pol., 15: 11-19.

Dorling, M. and Zussman, J., 1985. An investigation of nephrite jade by electron microscopy Mineral. Mag., 49: 31-36.

Dunham, A.C. and Wilkinson, F.C.F., 1978. Accuracy, precision and detection limits of energy dispersive electron-microprobe analyses of silicates. X-ray Spectrom., 7: 50-56.

Fedoseev, A.D., Grigorieva, L.F., Chigarieva, O.G. and Romanov, D.P., 1970. Synthetic fibrous fluoramphiboles and their properties. Am. Mineral., 55: 854-863.

Grigorieva, L.F., Makarova, T.A., Koritkova, E.N. and Chigarieva, O.G., 1975. Synthetic Amphibole Asbestos. Nauka, Leningrad, 250 pp. (in Russian).

Harry, W.T., 1950. Aluminium replacing silicon in some silicate lattices. Mineral. Mag., 29: 142-149.

Hart, G., 1927. The nomenclature of silica. Am. Mineral., 12: 388.

Hawthorne, F.C., 1981. Crystal chemistry of the amphiboles. Rev. Mineral., Mineral. Soc. Am., 9A: 1-102.

Hawthorne, F.C., 1983. The crystal chemistry of the amphiboles; a review. Can. Mineral., 21: 173-480.

Hull, D., 1975. Introduction to Dislocations. Pergamon, Oxford, 2nd ed., 271 pp.

Hutchison, J.L., Irusteta, M.C. and Whittaker, E.J.W., 1975. High resolution electron microscopy and diffraction studies of fibrous amphiboles. Acta Crystallogr., Sect. A, 31: 794-801.

Kalinin, D.V., Deniskina, N.D. and Lokhova, G.G., 1975. Amphibole Asbestos. In: V.S. Sobolev (Editor), Synthesis and Genesis in Nature. Acad. Nauk U.S.S.R., Novosibirsk, No. 193 (in Russian).

Kostyuk, E.A. and Sobolev, V.S., 1969. Paragenetic types of calciferous amphiboles of metamorphic rocks. Lithos, 2: 67-81.

Leake, B.E., 1968. A catalog of analyzed calciferous and sub-calciferous amphiboles together with their nomenclatures and associated minerals. Geol. Soc. Am., Spec. Pap. No. 98, 210 pp.

Leake, B.E., 1978. Nomenclature of amphiboles. Mineral. Mag., 42: 533-563.

Litvin, A.L., 1977. Crystallochemistry and Structural Typomorphism of Amphiboles. Naukova Dumka, Kiev, 235 pp. (in Russian).

Lorimer, G.W., 1974. The plastic deformation of minerals. In: R.G.J. Strens, The Physics and Chemistry of Minerals and Rocks. Wiley, London, pp. 3-17.

Makarova, T.A., Nestierchuk, N.I., Koritkova, E.N., Pivovarova, L.N. and Kosulina, G.V., 1970. Synthetic asbestos type silicates and their properties. Izv. Akad. Nauk S.S.S.R., Neorg. Mater., 6(8): 1513-1517 (in Russian).

Papike, J.J. and Clark, J.R., 1968. The crystal structure and cation distribution of glaucophane. Am. Mineral., 53: 1156-1173.

Papike, J.J., Cameron, K.L. and Baldwin, K., 1973. Amphiboles and pyroxenes: Characterization of other than quadrilateral components and estimates of ferric iron from microprobe data. Geol. Soc. Am., Abstr. Progr., 6: 1053-1054 (abstract).

Stemple, I.S. and Brindley, G.W., 1960. A structural study of talc and talc tremolite relations. J. Am. Ceram. Soc., 43: 34-42.

Veblen, D.R., 1980. Anthophyllite asbestos: microstructures, intergrown sheet silicates, and mechanisms of fiber formation. Am. Mineral., 65: 1075-1086.

Wylie, A.G., 1979. Optical properties of the fibrous amphiboles. Ann. N.Y. Acad. Sci., 330: 611-619.

Zoltai, T., 1978. History of asbestos-related mineralogical terminology. (U.S.). Natl. Bur. Stand., Spec. Pap., 506: 1-18.

FIBER LENGTH AND ASPECT RATIO OF SOME SELECTED ASBESTOS SAMPLES*

Ann G. Wylie

*Department of Geology
University of Maryland
College Park, Maryland 20742*

The primary diagnostic characteristics of asbestos used by most microscopists studying environmental air and water samples are mineral identity and aspect ratio (length/width). These indices are used primarily because other asbestos characteristics, such as tensile strength, surface charge, and flexibility, are not practically demonstrable under the microscope for such samples. Therefore, microscopists rely heavily, and sometimes exclusively, on morphologic features. However, the choice of a 3:1 aspect ratio as the definition of a fiber[1] is an unfortunate one. Many minerals, including the amphiboles, pyroxenes, and alumino silicates, such as sillimanite, readily cleave into fragments with this aspect ratio. It is especially inappropriate for distinguishing between fibrous and nonfibrous amphibole fibers.

Yet, the constraints of phase-contrast microscopy for particle counting require a reasonable aspect ratio criterion for asbestos. To help establish such an aspect ratio, we have characterized four samples of commercial asbestos by size distribution analysis and mineralogy. These data suggest that the choice of an aspect ratio on the order of 20:1 would ensure that most asbestos particles are counted. This aspect ratio would probably preclude the misidentification of nonfibrous silicates. However, aspect ratio cannot be used as the only criterion for the identification of asbestos.

SAMPLES

Four samples of asbestos were characterized in this study: a short-fiber chrysotile from the New Idria Serpentinite Body, Diablo Range, California (COF-25); a long-fiber chrysotile from the Jeffrey Mine, Asbestos, Quebec, Canada (Plastibest 20); an amosite sample that consists of about 95% grunerite asbestos and 5% actinolite asbestos from Africa (S-33); and a crocidolite sample (blue asbestos), also from Africa (ML 6). The two chrysotile samples had not been milled but had been processed to remove impurities. The amosite and crocidolite samples were both air-jet milled to reduce the average particles length.

ANALYSIS

Sample Preparation

All samples were prepared for observation in the scanning electron microscope (SEM) in the following manner. A few milligrams of the mineral were agitated in distilled water with a small amount of detergent added to aid in dispersion. This suspension was filtered onto a 0.1 μm Nucleopore® filter and washed several times with distilled water to remove the soap. Segments of the filter were then mounted

605

directly on aluminum specimen tabs, and a drop of a suspension that contained 1.1 μm latex spheres was added and allowed to dry. These spheres served as the internal standard for size calibration for all measurements. The tabs were then coated with either copper or carbon before being placed in the SEM.

Data Collection

To obtain data that would describe the samples in terms of number of particles, only the length and width of particles whose center fell closest to the center of the field of view as the specimen tab was moved in increments were recorded. This technique essentially reduces all particles to points and ensures that the data are not skewed to favor the longer-sized fractions. Length and widths were measured directly on the cathode ray tube by a ruler calibrated to the 1.1 μm latex spheres. It should be noticed that in most cases, the width measured was the intermediate dimension, because most particles will settle out of suspension with their minimum dimension perpendicular to the surface on which they settle. Generally, morphologic features alone were sufficient to ensure that only asbestos particles were being counted. However, when the aspect ratio of a particle was small, energy-dispersive x-ray analysis was performed to confirm the mineral's identity. This procedure was necessary since all of the bulk samples contained small but significant mineral impurities. The data for each mineral represent between 1200 and 2000 individual particle measurements taken from 12–20 separate sample preparations. All data were collected with a Cambridge Mark IIa SEM located at the Institute for Physical Sciences and Technology, University of Maryland, or an AMR 1400 SEM located at the Bureau of Mines, College Park.

RESULTS

FIGURES 1–4 summarize the results of these experiments. The raw data are presented as the percentage of particles in each length class that have a given aspect ratio. Also shown for each sample are the frequencies of each aspect ratio class.

It is clear from these Figures that there is a linear relationship between aspect ratio and length. The linear equations derived from a regression analysis of the mean aspect ratio of each length class and the mean length in each length class are as follows (see FIGURE 5):

1) long-fiber chrysotile

$$\log_{10} \text{aspect ratio} = 1.01 (\log_{10} \text{length}) + 0.77 \tag{1}$$

2) short-fiber chrysotile (SEM)

$$\log_{10} \text{aspect ratio} = 0.99 (\log_{10} \text{length}) + 0.83 \tag{2}$$

3) crocidolite

$$\log_{10} \text{aspect ratio} = 0.88 (\log_{10} \text{length}) + 0.62 \tag{3}$$

4) amosite

$$\log_{10} \text{aspect ratio} = 0.77 (\log_{10} \text{length}) + 0.59 \tag{4}$$

The data fit linear models exceptionally well. The R^2 values, or "percent explained,"[2] by the four linear models given above are: long-fiber chrysotile, 97.1%; short-fiber chrysotile, 98.2%; crocidolite, 99.2%; and amosite, 98.9%.

Equations 1–4 can be written in a general form as follows:

$$\log l/w = M \log l + B, \tag{5}$$

FIGURE 1. Frequencies are aspect ratios f...

FIGURE 2. Frequency ratio frequencies are expre... of aspect ratios found in th...
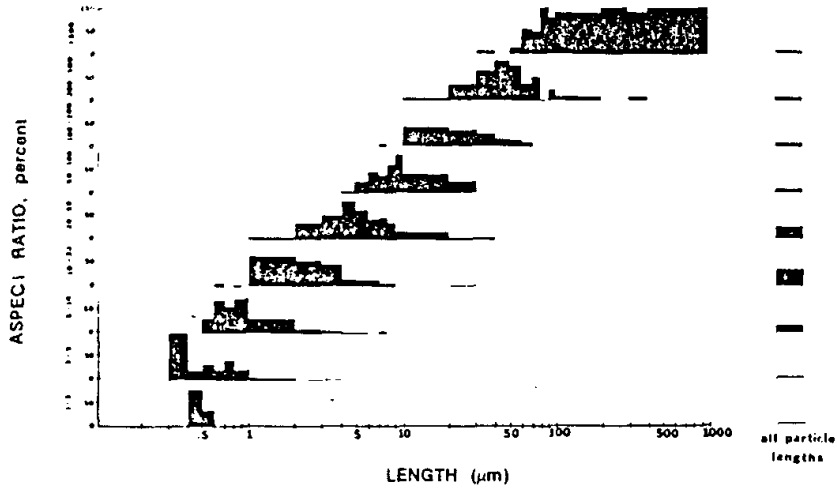
FIGURE 1. Frequency of aspect ratios in each length class of long-fiber chrysotile. Aspect ratio frequencies are expressed as percentages; lengths are given in micrometers. The frequencies of aspect ratios found in the sample as a whole (all particle lengths) are also indicated.
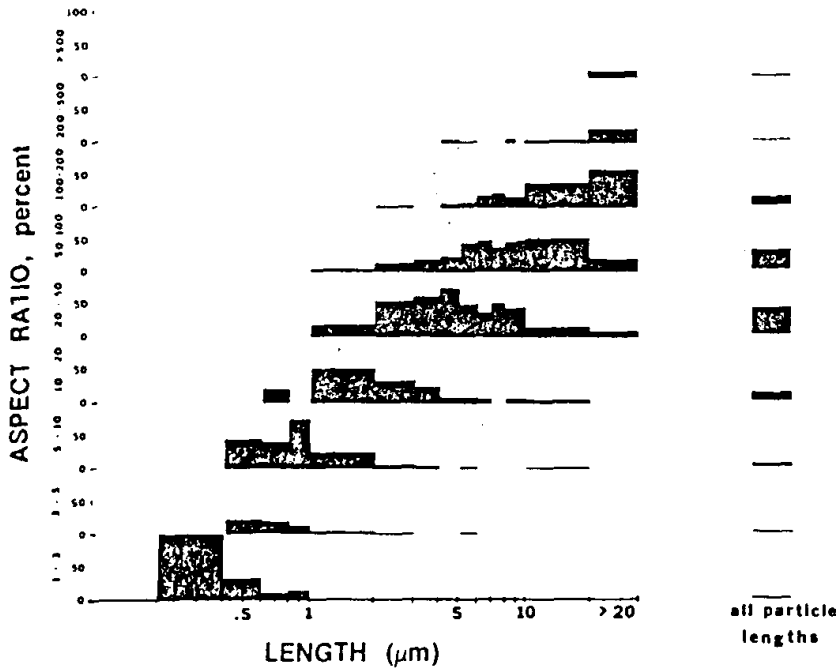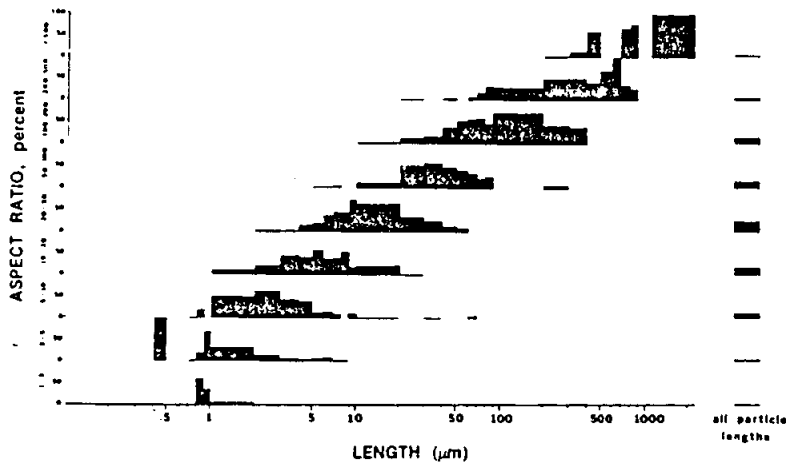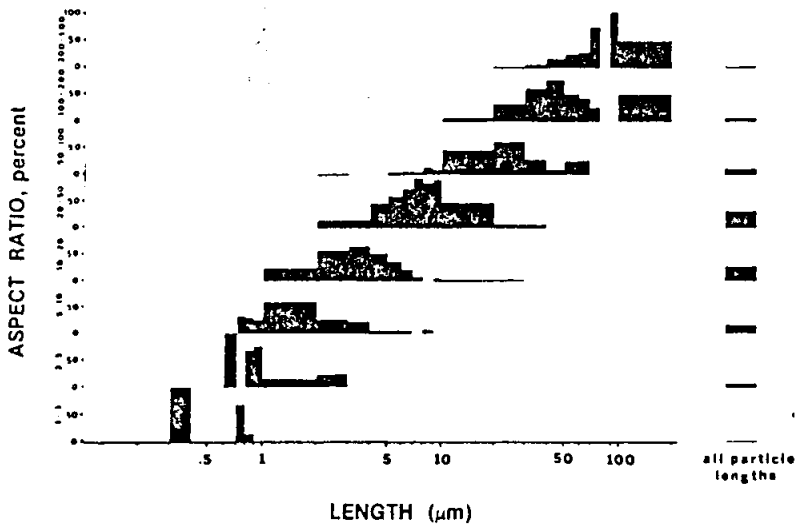

FIGURE 2. Frequency of aspect ratios in each length class of short-fiber chrysotile. Aspect ratio frequencies are expressed as percentages; lengths are given in micrometers. The frequencies of aspect ratios found in the sample as a whole (all particle lengths) are also indicated.

FIGURE 3. Frequency of aspect ratios in each length class of amosite. Aspect ratio frequencies are expressed as percentages; lengths are given in micrometers. The frequencies of aspect ratios found in the sample as a whole (all particle lengths) are also indicated.

where l is the length, w is the width, and M and B are constants.

Rearranging Equation 5, we have:

$$- \log w = \log l (M-1) + B. \tag{6}$$

From this equation, it is evident that when $M = 1$, width remains constant throughout all length classes. This relation holds for both samples of chrysotile. There is a slight

FIGURE 4. Frequency of aspect ratios in each length class of crocidolite. Aspect ratio frequencies are expressed as percentages; lengths are given in micrometers. The frequencies of aspect ratios found in the sample as a whole (all particle lengths) are also indicated.

FIGURE 5. ...
straight lines ...
class.

increase in width ...
pronounced for ...

The widths of ...
because asbestos ...
fibers may be ...
tubular structure, ...
more inter- and ...
fibrils ranging from ...
has fibril widths less than ...
Å. More work is needed ...
fibrils.

The value of M (Equation ...
measure of the dependence ...
fibrils, such as chrysotile, ...
asbestos types that exhibit ...
amosite, will be slightly ...
suggest that M values ...

ASPECT RATIO FREQUEN...

Long-fiber chrysotile
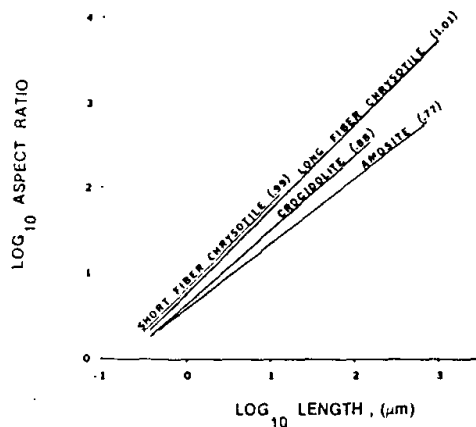Short-fiber chrysotile
Amosite
Crocidolite

FIGURE 5. Linear models show aspect ratio dependency on length. The equations for the straight lines were derived from regression analyses of the mean aspect ratio in each length class.

increase in width as length increases for crocidolite ($M = 0.88$); the effect is more pronounced for amosite ($M = 0.77$).

CONCLUSIONS

The widths of asbestos fibers show very little variation with length, probably because asbestos is composed of fibrils, unit single or twinned crystals.[3-5] Individual fibers may be composed of one or more fibrils. The chrysotile fibril has a distinct tubular structure, with a diameter of 250–500 Å.[5] Amphibole fibril widths exhibit more inter- and intrasample variations. Franco *et al.*[4] have reported finding crocidolite fibrils ranging from 500 to about 1500 Å in diameter. The crocidolite described here has fibril widths less than 3500 Å; the amosite fibril widths are less than about 5000 Å. More work is needed to describe more accurately the shape and size of these fibrils.

The value of M (Equation 5) may be a good "fibrosity index." It is essentially a measure of the dependency of width on length. Asbestos with well-developed uniform fibrils, such as chrysotile, will have M values close to unity. The values of M for asbestos types that exhibit more variation in fibril shape, such as crocidolite or amosite, will be slightly less. Preliminary results from a study of massive tremolite suggest that M values characteristic of nonfibrous amphiboles are less than 0.5.

TABLE 1

ASPECT RATIO FREQUENCY FOR ASBESTOS PARTICLES LONGER THAN 5 μm

	Particles with Aspect Ratios Greater Than or Equal to 10:1 (%)	Particles with Aspect Ratios Greater Than or Equal to 20:1 (%)	Particles with Aspect Ratios Greater Than or Equal to 50:1 (%)
Long-fiber chrysotile	99.5	96.2	76.6
Short-fiber chrysotile	99.2	95.7	59.0
Amosite	96.8	83.9	59.6
Crocidolite	99.0	89.0	37.8

Further testing of this model is required before its validity as a reliable measure of fibrosity can be established.

The aspect ratios predicted by Equations 1–4 are very large for long particles, but for particles less than 1 μm, they approach ratios typical of many nonfibrous silicates (less than 5:1). But 5 μm is usually given as the practical working microscopic limit for asbestos particle measurement.[6] TABLE 1 shows that more than 96% of all measured particles longer than 5 μm have aspect ratios in excess of 10:1; many have aspect ratios in excess of 50:1. Aspect ratios of this magnitude and frequency are uncharacteristic of most rock-forming mineral fragments and are probably unique to asbestos. This observation does not mean, however, that a single mineral particle with an aspect ratio of this magnitude is necessarily an asbestos fiber. Only the prevalence of high aspect ratios in a population of particles of a mineral known from hand samples to occur in an asbestiform habit should be used as a criterion for asbestos identification.

Since the preferred index of asbestos exposure is the presence of fibers longer than 5 μm counted on membrane filters at 430× by phase-contrast microscopy,[7] the data suggest that once the presence of asbestos has been established, if only particles with aspect ratios in excess of 20:1 are counted, most asbestos particles would be included; most nonfibrous mineral fragments probably would not be counted.

The choice of 10:1 as the aspect ratio used would increase the probability of including *all* asbestos fibers, but, in this case, some nonfibrous acicular cleavage fragments might also be counted as asbestos. The exact aspect ratio criterion might be designed to fit the particular circumstances of each individual case. In any event, the use of 3:1 is not justified on mineralogic grounds and should be abandoned.

Summary

Four samples of asbestos: short fiber chrysotile, long fiber chrysotile, amosite and crocidolite, have been characterized by particle length and aspect ratio on the scanning electron microscope. A linear model expressed by $\log l/w = M \log l + B$ (or, $-\log w = \log l(M-1) + B$) approximates the data very well. It is proposed that M be considered as a "fibrosity index." The data indicate that most asbestos fibers longer than 5 μm in length are characterized by aspect ratios in excess of 20:1.

Acknowledgments

References

1. NATIONAL INSTITUTE FOR OCCUPATIONAL SAFETY AND HEALTH. 1972. Criteria for a recommended standard for occupational exposure to asbestos. Washington, D.C.
2. DAVIS, J. C. 1973. Statistics and Data Analysis in Geology. John Wiley & Sons, Inc. New York, N.Y.
3. HEINRICH, E. WM. 1965. Microscopic Identification of Minerals. McGraw-Hill Book Company. New York, N.Y.
4. FRANCO, M. A., J. L. HUTCHISON, D. A. JEFFERSON & J. R. THOMAS. 1977. Structural imperfections and morphology of crocidolite (blue asbestos). Nature (London) 266(7): 520–521.
5. YADA, K. 1967. Study of chrysotile asbestos by a high resolution electron microscope. Acta Crystallogr. 23: 704–707.
6. ADDINGLEY, C. F. 1966. Asbestos dust and its measurement. Ann. Occup. Hyg. 9: 73–82.
7. LYNCH, J. R., H. E. AYER & JOHNSON. 1970. The interrelationships of selected asbestos exposure indices. Amer. Ind. Hyg. Ass. J. 31(5): 598–604.

Characterizing and Discriminating Airborne Amphibole Cleavage Fragments and Amosite Fibers: Implications for the NIOSH Method

ANN G. WYLIE,[A,B] ROBERT L. VIRTA[A] and ESTELLE RUSSEK[C]

[A]Bureau of Mines, Avondale Research Center, Avondale, MD 20782; [B]Department of Geology, University of Maryland, College Park, MD 20742; [C]Department of Animal Science, University of Maryland, College Park, MD 20742

The NIOSH method for determining asbestos exposure in the mining environment involves using phase contrast microscopy to examine mineral particulates collected on air monitor filters. Particles are classified as asbestiform or non-asbestiform based on their size and length-to-width (aspect) ratio. The procedure works well when only fibers are present. In most non-asbestos mining operations, however, cleavage fragments are the most abundant airborne particulates. In this research, discriminate function analysis was applied to morphological data for airborne amphibole particulates to show that dimensional criteria could distinguish between amphibole asbestos and amphibole cleavage fragments. The particulates for this research were collected from industrial sites where amosite alone was in use and from mining sites where amphiboles are major rock-forming minerals. The results suggest that cleavage fragments can be differentiated from asbestos fibers based on dimensional criteria alone, but only if the current working definition of a fiber is modified. The data suggest that an appropriate definition of a regulatory fiber would be a particle longer than $5\mu m$ with a width less than $3\mu m$ and an aspect ratio of 20:1 or greater. Adoption of the 20:1 aspect ratio would greatly increase the precision of the NIOSH method. However, a new aspect ratio criterion must be coupled with a lower exposure index in order to prevent an increase in worker exposure to asbestos.

Introduction

The membrane filter method is specified as the method of test by the Occupational Safety and Health Administration (OSHA) Federal Standard for asbestos in industrial air (29 CFR Part 1910.1001) and in the Mine Safety and Health Administration (MSHA) regulations (30 CFR 55.5-1(b), 56.5-1(b), 57.5-1(b) and 71.202) governing mining air. The federal standards define asbestos as chrysotile, amosite, crocidolite, tremolite, anthophyllite and actinolite. The membrane filter method (NIOSH analytical method #P&CAM 239) defines an asbestos fiber as "a particulate which has a physical dimension longer than five micrometers and with a length to diameter ratio of three to one or greater."[1] Futhermore, it specifies that "in an atmosphere known to contain asbestos, all particulates with a length to diameter ratio of three to one or greater, and a length greater than five micrometers should, in the absence of other information, be considered to be asbestos fibers."[1] The five micrometer length is the most practical minimum fiber length measurable by phase contrast microscopy for fiber counting.[2-4] The choice of an elongated aspect ratio was made to eliminate most confounding mineral particles such as dirt and rock fragments, but the lower bound of three was arbitrary.[5] As long as the asbestos fiber definition is applied to an industrial environment in which only asbestos is being used, it provides a useful basis for exposure monitoring. However, in the mining environment, where many non-fibrous particles may fit the definition of a fiber, it may not be appropriate. The problem is especially acute when amphibole minerals are abundant.

Of the six minerals regulated as asbestos in the United States, all but chrysotile belong to a group of silicate minerals known as the amphiboles. Amphiboles are extremely common in the earth's crust. Approximately 30% of the rocks found in the continental United States contain amphiboles as major constituents.[6] Amphiboles are characterized structurally by a double chain of silicon-oxygen tetrahedra and they form prismatic crystals. When crushed, they form prismatic cleavage fragments which frequently have aspect ratios in excess of 3:1. Only rarely do the amphiboles grow with the extreme elongation and narrow widths typical of asbestos. This rare habit is characterized by flexibility and high tensile strength. A more extensive discussion of the asbestiform habit is presented elsewhere.[7,8] Because of the unique physical properties of asbestos, the distinction between asbestiform and other amphibole habits is readily apparent in hand specimens, but these macroscopic properties often cannot be observed on small discrete particles such as those collected on air monitoring filters. In many mining operations amphiboles are a common constituent of the rock while amphibole asbestos is present in trace amounts or absent entirely. In these environments, elongated cleavage fragments are classified as amphibole asbestos fibers according to the existing regulatory criteria and the membrane filter method.

The Bureau of Mines undertook this study in an attempt to provide criteria for discriminating between airborne amphibole cleavage fragments and amphibole asbestos fibers. Specific questions addressed were:

1. What are the dimensional characteristics of both populations?
2. What particle dimensions are common to both populations and how abundant are these particles?
3. How can the populations be best distinguished?

This type of study is necessary because amphibole cleavage fragments are often abundant in the mining environment and because, where comprehensive epidemiological studies have been made, no association between amphibole cleavage fragments and cancer has been demonstrated.[9-11]

Samples

Sixteen air-monitoring filters from two industrial sites where amosite (grunerite-asbestos) alone was being used were provided by OSHA, and eleven air-monitoring filters collected from three mine sites where amphiboles are major constituents of the country rock were provided by MSHA. These are: the Homestake Gold Mine, South Dakota; Peter Mitchell Iron Mine, Minnesota; and the Charlottesville Stone Quarry, Virginia.

For this study, we have assumed that the particles collected from the industrial sites are fibers of amosite, not cleavage fragments of grunerite. While the mining of amosite may produce cleavage fragments in the raw ore, during processing the fibers are separated from the gangue. This separation results in a commercial product which is essentially free of cleaved fragments of country rock. We have also assumed that the particles collected at the three mines are cleavage fragments. This assumption is based on the fact that the geology of the deposits has been described in detail in the literature and significant amounts of asbestos have not been noted.[12-14] On the other hand, the country rocks are known to contain large quantities of nonasbestiform amphibole: cummingtonite at the Homestake Gold Mine; grunerite, hornblende and actinolite at the Peter Mitchell Iron Mine; and actinolite at the Charlottesville Stone Quarry.[12-14] At all three mines, the country rock is crushed during mining and processing, producing large quantities of amphibole cleavage fragments. Futhermore, in preliminary studies of the mine particles collected in the same air filters, Virta et al.[15] have shown that the regression coefficients F and b, derived from a least-squares linear regression analysis of the form: log width = F log length + b, are similar to those derived from the same analysis of bulk samples of amphibole cleavage fragments and are markedly different from those of bulk asbestos.[15,16] While we recognize that, because we are dealing with real-world samples, we can not rule out the possibility that there could be an asbestos fiber among the cleavage fragments and cleavage fragments among the asbestos fibers. However, the approach that we have used is one that evaluates population characteristics, and the presence of a few anomalous particles would not affect the results and conclusions of this study.

Approximately 1000 particles were measured from each environment on the scanning electron microscope. All particles have aspect ratios of 3:1 or greater. Energy dispersive x-ray analysis was used to confirm the identity of every particle measured. Details of sample preparation and measurement have been presented elsewhere.[15]

Discriminant Function Analysis

In discriminant function analysis, the objective is to find the linear function of the variables — in this case, log width and log length — that most efficiently discriminates between two previously defined groups. The data were transformed into log values so that their distributions would more closely approximate normality. The analysis defines a linear function which, when computed for each particle in the two sample types, maximizes the variance between the groups relative to the variance within the groups.[17] Discriminant function analysis depends upon a prior knowledge that there are, in fact, two distinct populations. In this study the two populations from which the discriminant function was derived are the amosite asbestos fibers collected from the industrial sites and the amphibole cleavage fragments collected from the mine sites. The discriminant function that divides the two populations is of the form

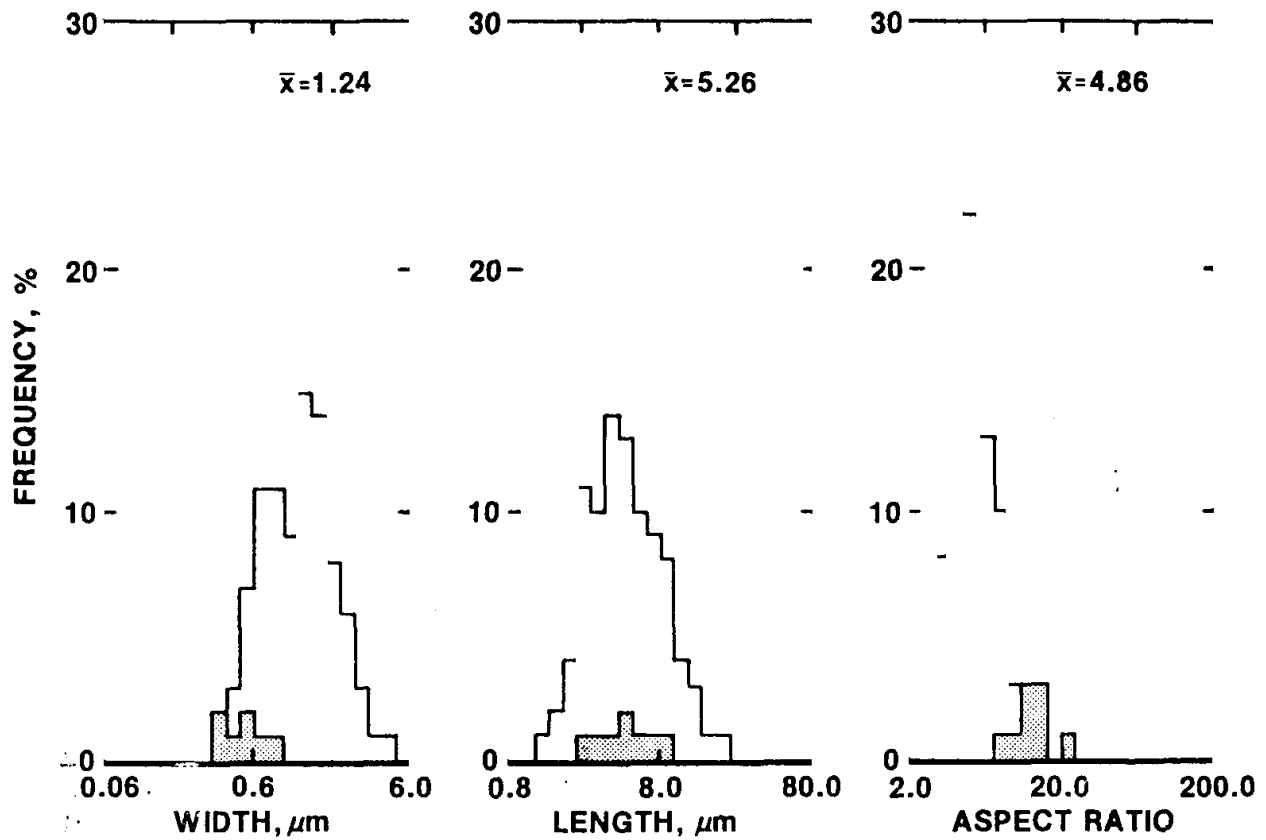$$Y = 5.9 \log \text{length} - 9.2 \log \text{width} - 6.63 \qquad (1)$$

A particle is classified as a "Group A" particle if its value of Y is greater than 0 and as a "Group B" particle if Y is less than 0. By using equation (1), 81% of the asbestos fibers were assigned to Group A and 91% of the cleavage fragments were assigned to Group B. We will call the particles in Group A "fiber-like" and those in Group B "cleavage-like."

The frequency distributions of width, aspect ratio, and length for the cleavage fragments and asbestos fiber populations are shown in Figure 1. Also shown are the frequency distributions of the cleavage fragments that were classified by equation (1) as "fiber-like" and the asbestos fibers that were classified as "cleavage-like." Several characteristics of the populations are evident from the distributions shown in Figure 1. First, the distribution of length of the cleavage fragments is similar to that of the asbestos fibers while the distributions of width and aspect ratio are different. Second, while the cleavage-like asbestos fibers are wider and shorter (60% are less than 5μm) than the asbestos population as a whole, their most notable characteristics are that they have low aspect ratios (93% have aspect ratios less than 10:1) and large widths (80% are wider than 0.6μm). The distributions of aspect ratio and width of the cleavage-like asbestos fibers are very similar to that of the cleavage fragments. Third, the particles from the mine which were classified as fiber-like are distinguished from the other cleavage fragments by their narrower widths and higher aspect ratios. Seventy-six percent have aspect ratios in excess of 10:1 and 71% have widths less than 0.6μm. However, their lengths are only slightly less than those of the cleavage fragment population as a whole; approximately half are less than 5μm long.

Discussion

We do not consider it practical to use the specific discriminant function we have derived as a basis for the regulation of asbestos fiber exposure. The magnitudes of the coeffecients are too sensitive to slight changes in the populations. However, it is possible to make some general observations from the analysis which might form the basis for formulating alternative dimensional criteria. First, there are dimensions that are common to populations of airborne amphibole cleavage fragments and amosite asbestos fibers. Amosite fibers which are wide and have low aspect ratios look like

198

Am. Ind. Hyg. Assoc. J (46)   April, 1985

MINE SAMPLES (n = 1,069)

$\bar{x}$=1.24

$\bar{x}$=5.26

$\bar{x}$=4.86

FREQUENCY, %

WIDTH, μm

LENGTH, μm

ASPECT RATIO

KEY

INDUSTRIAL SAMPLES (n = 976)

Group A   Group B

$\bar{x}$=0.44

$\bar{x}$=10.33

$\bar{x}$=28.95

FREQUENCY, %

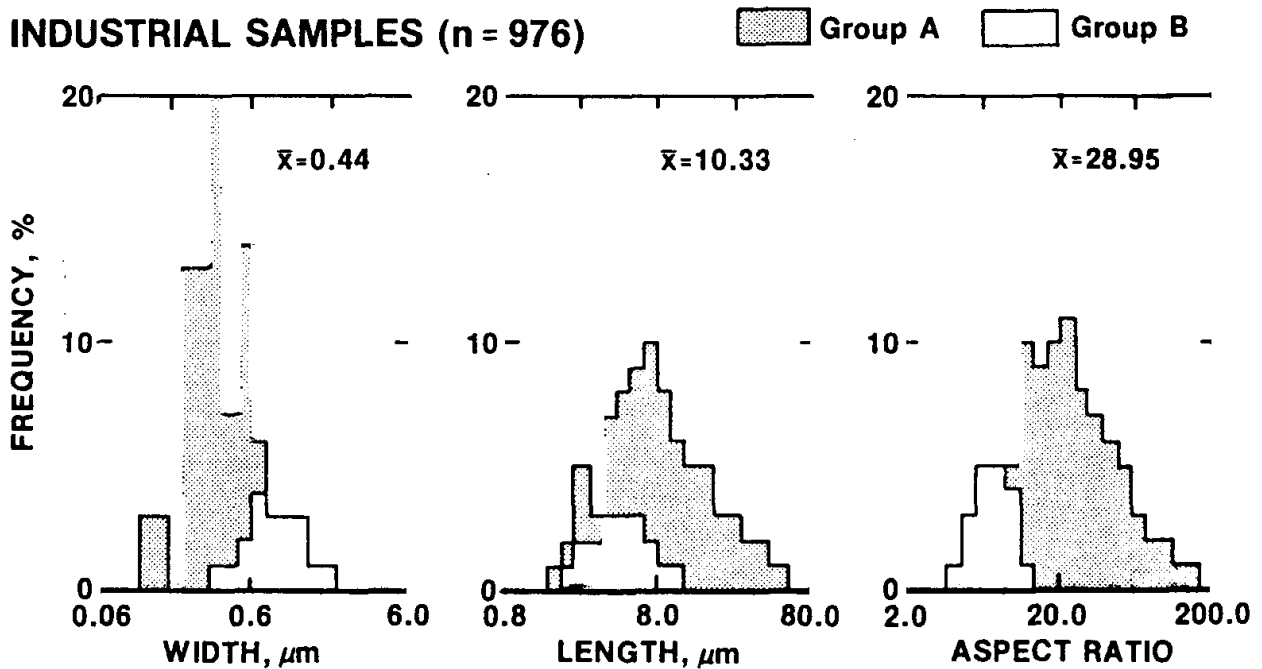WIDTH, μm

LENGTH, μm

ASPECT RATIO

Figure 1 — Frequency distributions of width, length and aspect ratio of the amphibole cleavage fragments (Mine Samples) and amosite asbestos (Industrial Samples). Group A and Group B are the two populations defined by the discriminant function analysis.

cleavage fragments and cleavage fragments which have narrow widths and high aspect ratios look like amosite fibers. Second, particles which cannot be differentiated based on dimensions comprise a fairly small percentage of the total airborne particle population. Futhermore, amosite fibers are generally wider and have lower aspect ratios than other forms of commercial asbestos, crocidolite and chrysotile. Yet only 19% of the airborne amosite fibers could not be differentiated from cleavage fragments. These results imply that the definition of a fiber could be based on dimensions, and, if carefully chosen, could include enough asbestos fibers to provide a reasonable basis for an exposure standard while it would exclude most cleavage fragments and alleviate the problem the mineral industries face under current definitions. Third, if dimensional criteria are to be used to define a fiber, they should be chosen to describe and include long, thin particles of high aspect ratio. These are the dimensions which are most characteristic of asbestos fibers and least common in a population of cleavage fragments.

In Table I we have examined the effectiveness of six dimensional criteria for differentiating the two populations. Three of the criteria have been cited in the literature as having biological relevance. Two were chosen because they were generally consistent with our findings from the discriminant function analysis. The sixth is the criteria employed in the membrane filter method (NIOSH criteria). It is evident from the data that both the industrial and the mine populations are composed of significant amounts of "fibers" if the

NIOSH criteria are applied. According to these criteria, the two populations appear similar; in both populations close to half of the elongated particles meet the regulatory criteria for fibers. It is evident that the NIOSH criteria do not dicriminate between cleavage fragments and fibers. The dimensions suggested by Stanton et al.[18] and Pott[19] include a very small number of the airborne amosite fibers, and it would appear that it would be impractical to base an exposure standard for amosite on them. On the other hand, if other dimensional criteria are applied, the populations can be distinguished fairly well. For example, an aspect ratio of 20 and length greater than or equal to 5μm would include 41% of the amosite fibers while it would eliminate almost all of the cleavage fragments. Similar results are obtained by using the dimensional criteria suggested by Spurney et al.[20]

The NIOSH method uses phase contrast microscopy for monitoring asbestos exposure. By examining only particles with widths greater than or equal to 0.25μm, it is possible to evaluate the effects of the use of the optical microscope in conjunction with various dimensional criteria for fiber counting. A value of 0.25μm was chosen as the lower limit of visibility of fibers in the optical microscope. This is somewhat lower than the theoretical resolution of the optical conditions normally employed in air filter analysis but probably is a good approximation of the width of a visible fiber.[21] The effects of an upper width limit of 3μm, the maximum width of a respirable particle, are also given in Table I.

From Table I it is evident that the optical microscope and the SEM provide essentially identical data from the mine samples. This agreement is a result of the large widths of amphibole cleavage fragments. On the other hand, for the airborne amosite population the use of the optical microscope results in a reduction in the number of particles in all dimensional categories, especially in those of higher aspect ratio. For example, while 41% of all the amosite fibers are longer than or equal to 5μm and have aspect ratios greater than or equal to 20:1, only 27% of the visible fibers fall in this category. These data reflect the mineralogical reality that asbestos fibers have narrow widths and that many airborne fibers are not visible by optical microscopy. If the same analyses were made for crocidolite or chrysotile, the effect would be much more striking. These minerals have significantly smaller widths than amosite and considerably fewer would be visible by optical microscopy. For example, in one study it was shown that only 15% of the crocidolite fibers longer than 5μm can be seen by optical microscopy.[22] Under the present regulatory procedures and definitions, the difference in the widths of cleavage fragments and asbestos fibers has the effect of allowing higher total exposures to asbestos fibers, a designated carcinogen, than to cleavage fragments for which no carcinogenic potential has been established.

TABLE I
Percentage of Amphibole Cleavage Fragments and Amosite Asbestos Fibers that Conform to Several Dimensional Criteria

Dimensional Criteria		Percent of Total Particles	
Length and Aspect Ratio	Width (w)	Cleavage Fragments	Amosite Asbestos Fibers
Length ≥ 5μm[A]	all widths	41	64
Aspect ratio ≥ 3	w ≥ 0.25μm	41	50
	3μm ≥ w ≥ 0.25μ	39	50
Length ≥ 5μm	all widths	6	57
Aspect ratio ≥ 10	w ≥ 0.25μm	6	43
	3μm ≥ w ≥ 0.25μm	6	43
Length ≥ 5μm	all widths	1	41
Aspect ratio ≥ 20	w ≥ 0.25μm	1	27
	3μm ≥ w ≥ 0.25μm	1	27
Length ≥ 10μm	w ≤ 0.25μm[B]	0	5
Length ≥ 5μm	w ≤ 0.5μm[C]	2	42
Length ≥ 8μm	w ≤ 0.25μm[D]	0	7

[A]NIOSH membrane filter method criteria for a "fiber."

[B]Suggested by Pott (1978)[19] as having a high probability of being carcinogenic.

[C]Suggested by Spurney et al. (1979)[20] as having a high probability of being carcinogenic.

[D]Suggested by Stanton et al. (1981)[18] as having a high probability of being carcinogenic.

Recommendation

The existing regulatory criteria for counting asbestos "fibers" are useful for industrial monitoring during the processing and utilization of asbestos. These criteria have been in place for many years and are used worldwide to evaluate exposure

in such an industrial environment. In contrast, there are many mining operations in the United States and elsewhere where employees are exposed to airborne amphibole cleavage fragments for which there are no biological or epidemiological data to support the exposure limitations required for asbestos. The critical problem is that the existing regulatory definition does not distinguish between amphibole cleavage fragments and asbestos fibers.

This research indicates that the two classes of particulates can be distinguished statistically using the following criteria for an amphibole fiber: length greater than or equal to $5\mu m$ and aspect ratio greater than or equal to 20:1 This definition includes approximately 50% of airborne amosite amphibole fibers and eliminates most amphibole cleavage fragments. For airborne particulates, these dimensions would include only fibers with widths less than $3\mu m$, the upper limit of the size of respirable dust.

If this definition were adopted, other changes would have to follow. The 20:1 aspect ratio would include approximately 50% of the amosite particles presently counted using the 3:1 aspect ratio criterion and the optical microscope. This suggests that the occupational exposure index must be lowered so that no change in total occupational exposure would occur. If the exposure index was reduced from two fibers/mL to one fiber/mL and the 20:1 criterion was used, then those working with amosite would have a slightly reduced total exposure limit. For the other types of amphibole asbestos, especially crocidolite, these numbers would be somewhat different. Crocidolite fibers in general are much narrower than amosite fibers, and a higher percentage of the fibers longer than $5\mu m$ have aspect ratios in excess of 20:1. Approximately 75% of the optically visible airborne crocidolite fibers longer than $5\mu m$ have aspect ratios in excess of 20:1.[22] These data suggest that an exposure standard for crocidolite of two fibers/mL based on a 3:1 aspect ratio would be equivalent to 1.5 fibers/mL based on a 20:1 aspect ratio if only optically visible fibers were considered.

The adoption of new fiber criteria would bring with it other changes. The allowable levels of occupational exposure would have to be revised to insure that there were no increases in the exposure to total fiber (*i.e.*, all lengths and widths). If such a change were forthcoming, the instrumentation used for fiber counting might also be re-evaluated. The data show that the ratio of optically visible to total fiber varies dramatically among the asbestos minerals.[22] In view of this fact, electron microscopy might be more appropriate. The undertaking would be complicated. However, the alternative of ignoring the facts and leaving the existing regulations in place puts an unnecessary burden on our domestic mining industry without any obvious benefits for their employees, customers, or the general public.

References

1. Leidel, N.A., S.G. Bayer, R.D. Zumwalde and K. A. Busch:*USPHS/NIOSH Membrane Filter Method for Evaluating Airborne Asbestos Fibers*, U.S. Dept of Health, Education and Welfare, NIOSH, Technical Report No. 79-127, Cincinnati. OH (1979).

2. Addingley, C.F.: Asbestos Dust and Its Measurements. *Ann. Occup. Hyg. 9*:73-82 (1966).

3. Lynch, J.R., H.E. Ayer and D.L. Johnson: The Interrelationships of Selected Asbestos Exposure Indices. *Am. Ind. Hyg. Assoc. J. 31*:598-604 (1970).

4. Winer, A.A. and M. Cossette: The Effect of Aspect Ratio on Fiber Counts: A Preliminary Study. *Ann. N.Y. Acad. Sci. 330*:661-672 (1979).

5. Cossette, M. and A.A. Winer: The Standard for Occupational Exposure to Asbestos Being Considered by ASTM Committee E-34, in *Workshop on Asbestos: Definition and Measurement Methods*, pp. 381-386, NBS Special Publication 506, Washington, DC (1978).

6. Kuryvial, R.J., R.A. Wood and R.E. Barrett: *Identification and Assessment of Asbestos Emissions From Incidental Sources of Asbestos*, U.S. Environ. Prot. Agency Publ. EPA 650/2-74-087, Washington, DC (1974).

7. Campbell, W.J., R.L. Blake, L.L Brown, E.E. Cather and J.J. Sjoberg: *Selected Silicate Minerals and Their Asbestiform Varieties*. U.S. Bur. Mines Inf. Cir. 8751, Washington, DC (1977).

8. Steel, E. and A.G. Wylie: Mineralogical Characteristics of Asbestos, in *Geology of Asbestos Deposits*, pp. 93-100. Edwards Brothers, Inc., Ann Arbor, MI (1981).

9. McDonald, J.C., G.W. Gibbs, F.O.K. Liddell and A.D. McDonald: Mortality After Long Exposure to Cummingtonite-Grunerite. *Am. Rev. Respir. Dis. 118*:271-277 (1978).

10. Higgins, I.T.T., J.H. Glassman, M.S. Oh and R.G. Cornell: Mortality of Reserve Mining Company Employees in Relation to Taconite Dust Exposure, *Am. J. Epidemiol, 118*:710-719. (1983).

11. Selikoff, I.J.: Carcinogenic Potential of Silica Compounds, in *Biochemistry of Silicon and Related Problems*, (G. Bendy and I. Lindquist, eds.), Plenum Publishing Corp. New York, NY (1978).

12. Giannini, W.F. and W.K. Rector, Jr.: Mineral Occurrence and Associations in the Albemarle Crushed Stone Quarry (Catoctin Formation) near Shadwell, Va. *Va. J. Sci. 9*:4:427 (1958).

13. Gundersen, J.N. and G.M. Schwartz: The Geology of the Metamorphosed Biwabik Iron Formation, Eastern Mesabi District, Minnesota. *Minn. Geol. Bull. 43*:76-101 (1962).

14. Noble, J.A.: Ore Mineralization in the Homestake Gold Mine, Lead, S.D. *Geol. Soc. Amer. Bull. 61*:221-251 (1950).

15. Virta, R.L., K.B. Shedd, A.G. Wylie and J.G. Snyder: Size and Shape Characteristics of Amphibole Asbestos (Amosite) and Amphibole Cleavage Fragments (Actinolite, Cummingtonite) Collected on Occupational Air Monitoring Filters, in *Aerosols in the Mining and Industrial Work Environment*, pp. 633-643. Ann Arbor Sci. Publ., Ann Arbor, MI (1983).

16. Siegrist, H.G., and A.G. Wylie: Characterizing and Discriminating the Shape of Asbestos Particles. *Environ. Res. 23*:348-361 (1980).

17. Kleinbaum, D.G. and L.L. Kupper: *Applied Regression Analysis and Other Multivariable Methods*. Duxbury Press, North Scituate, MA (1978).

18. Stanton, M.F., M. Layard, A. Tegeris, E. Miller, M. May, E. Morgan and A. Smith: Relation of Particle Dimension to Carcinogenicity in Amphibole Asbestos and Other Fibrous Minerals. *J. Nat. Cancer Inst. 67*:965-975 (1981).

19. Pott, F.: Some Aspects on the Dosimetry of the Carcinogenic Potency of Asbestos and Other Fibrous Dusts. *Staub-Reinhalt Luft 38*:12:486-490 (1978).

20. Spurney, K., W. Stober, H. Oprela and G. Weiss: Size Selective Preparation of Inorganic Fibers for Biological Experiments. *Am. Ind. Hyg. Assoc. J. 40*:20-38 (1979).

21. ASTM: *Test Method for Respirable Airborne Asbestos Concentration in Workplace Atmospheres*. Am. Soc. Test. Mater. D 4240, Philadelphia, PA (1983).

22. Gibbs, G.W. and C.Y. Hwang: Dimensions of Airborne Asbestos Fibers, in *Biological Effects of Mineral Fibers*, *IARC Sci. Pub. 30*:69-78 (1980).

REVIEW

Asbestos Exposure Indices[1]

MORTON LIPPMANN

*Institute of Environmental Medicine, New York University Medical Center,
Tuxedo, New York 10987*

Received July 18, 1987

The ability of inhaled asbestos to produce asbestosis, lung cancer, and mesothelioma in both humans and animals is well established, and asbestos exposures in the occupational and general community environment are recognized as significant hazards. However, it has not been possible to establish realistic and credible dose–response relationships, primarily because of our inability to define which constituents of the aerosols produce or initiate the pathological responses. It is generally acknowledged that the responses are associated with the fibers rather than the nonfibrous silicate mineral of the same chemical composition. Available data from experimental studies in animals exposed by injection and inhalation to fibers of defined size distributions are reviewed, along with data from studies of fiber distributions in lungs of exposed humans in relation to the effects associated with the retained fibers. It is concluded that asbestosis is most closely related to the surface area of retained fibers, that mesothelioma is most closely associated with numbers of fibers longer than ~5 μm and thinner than ~0.1 μm, and that lung cancer is most closely associated with fibers longer than ~10 μm and thicker than ~0.15 μm. The implications of these conclusions on methods for fiber sampling and analyses are discussed. © 1988 Academic Press, Inc.

INTRODUCTION

The evidence from both human epidemiology and experimental animal inhalation studies is clear and consistent. Inhaled asbestos fibers cause (1) asbestosis, a diffuse fibrosis in the nonciliated portion of the lung; (2) lung cancer; and (3) mesothelioma, a cancer of the pleura and peritoneum. However, the exposure–response relationships for these diseases are much less clear and consistent.

There are three different types of concentration indices which have been used for airborne asbestos. Initially, the most widely used index was the number of particles per unit volume of air, expressed in millions of particles per cubic foot (MPPCF), and determined from impinger samples analyzed by the old USPHS standard dust counting technique using a 10× objective lens. Since there was no discrimination between fibrous and non fibrous particles, and since fibers are a very variable fraction of the total dust in most cases, dust counting for occupational exposure evaluations was replaced by a technique which counts fibers only. At the time the fiber counting technique was first adopted in the UK, it was already clear that long fibers were of most concern. This, combined with the

---

[1] Presented at the Eighth Annual Scientific Meeting, Universities Occupational Safety and Health Educational Resource Center, New York, New York, April 2, 1987.

practical limitation that fibers shorter than ~5 μm could not be reliably identified by light microscopy, led to the adoption of a counting procedure which uses a 45× phase-contrast objective to count the fibers collected on a membrane filter having a length/diameter (aspect) ratio >3 and longer than 5 μm (ACGIH-AIHA Aerosol Comm., 1975). The phase-contrast optical method (PCOM) is specified in the OSHA occupational health standard for asbestos. Table 1 summarizes recommended occupational exposure limits and standards used in the United States over the last 40 years.

The third type of concentration index is based on the mass concentration of asbestos, or on the mass concentration passing a pre-collector meeting the British Medical Research Council (BMRC) or American Conference of Governmental Industrial Hygienists (ACGIH) sampler acceptance criteria. Some of the recent animal inhalation studies report the chamber concentrations in terms of the "respirable" mass based on samples collected using samplers which meet the BMRC criteria.

Environmental exposures have been measured either in terms of fiber count or fiber mass. Fiber counts have been made using both phase-contrast optical and electron microscopy. The reported concentrations have differed according to the size distributions of the fibers, the resolving power of the microscope, and whether there was any discrimination in the analyses according to fiber type. The fiber mass index was developed by Selikoff et al. (1972) at Mt. Sinai School of Medicine. The fibers in the sample are mechanically reduced to fibrils, which are then identified and measured by electron microscopy. Mass concentrations in nanograms per cubic meter are calculated from the numbers of fibrils and their dimensions.

Use of these various exposure indices has sometimes led to the development of a site- or industry-specific exposure–response relationship for one or more of the asbestos-related diseases, but it has not been possible to develop any generic relationships. This demonstrates the inadequacy of our current indices of exposure.

TABLE 1
RECOMMENDED AIR CONCENTRATION LIMITS AND STANDARDS FOR ASBESTOS

Group	Year	Limit
ACGIH	1946	5×10^6 particles/ft^3
ACGIH	1968[a]	12 fibers[c]/ml or 2×10^6 particles/ft^3
ACGIH	1970,[a] 1974[b]	5 fibers/ml
OSHA	1972	5 fibers/ml
OSHA	1976	2 fibers/ml
NIOSH	1976	0.1 fiber/ml
ACGIH	1978,[a] 1980[b]	0.2 fiber/ml for crocidolite
		0.5 fiber/ml for amosite
		2.0 fiber/ml for chrysotile and other forms
OSHA	1986	0.2 fiber/ml

[a] Notice of Intent.

[b] Adopted as threshold limit value (TLV).

[c] All fiber limits based on phase-contrast optical determination at 400–450× magnification.

sition by interception at or near the carinal edge. To the extent that a fiber is entrained in the secondary flow streams which form at bifurcations, its deposition probability by interception should be further enhanced.

Deposition in Nonciliated Airways and Effects at Deposition Sites

Deposition patterns within the nonciliated airways distal to the terminal bronchioles may be quite varied. Brody *et al.* (1981) have studied the deposition of chrysotile asbestos in lung peripheral airways. They exposed rats for 1 hr to 4.3 mg/m^3 of respirable chrysotile. The animals were killed in groups of 3 at 0, 5, and 24 hr and at 4 and 8 days after the end of the exposure. The pattern of asbestos fiber retention on the epithelial surfaces was examined by scanning electron microscopy of lung sections cut to reveal terminal bronchiolar surfaces and adjacent airspaces. The rat does not have recognizable respiratory bronchioles, and the airways distal to the terminal bronchioles are the alveolar ducts. In rats killed immediately after exposure, asbestos fibers were rarely seen in alveolar spaces or on alveolar duct surfaces, except at alveolar duct bifurcations. There were relatively high concentrations on bifurcations nearest the terminal bronchioles, and lesser concentrations on more distal duct bifurcations. In rats killed at 5 hr, the patterns were similar, but the concentrations were reduced. Similar deposition patterns were seen in rats exposed for 1 hr to an aerosol of crocidolite asbestos by Roggli *et al.* (1987).

The sudden enlargement in air path cross section at the junction of the terminal bronchiole and alveolar duct may play a role in the relatively high deposition efficiency at the first alveolar duct bifurcation. Little is known about the flow profiles in this region of the lung.

Johnson (1987) exposed rats to UICC crocidolite aerosols at 10 mg/m^3 for 6 hr/day, 5 days/week for periods ranging from 1 day to 12 months, and examined cells in structures distal to the terminal bronchioles. Alterations in the distribution of cells were seen within 3 months. Airway bifurcations were the initial sites where evidence of cell damage and collagen deposition was seen. By 12 months, there was substantial thickening of the epithelial lining of the bifurcations. Type II cell hyperplasia was evident without apparent damage to Type I cells.

For rats receiving inhalation exposures to chrysotile at 11 mg/m^3 for 7 hr/day, 5 days/week for 12 months, Pinkerton *et al.* (1986) found that fiber accumulation in the airways immediately distal to terminal bronchioles was inversely related to airway pathlength and, to an even greater extent, to the number of bifurcations along each conductive airway path. Fiber concentrations were much higher in the cranial region of the left lung than in the costolateral, which had higher concentrations than the caudal. The differences increased with increasing fiber length, with the ratios increasing to 9:2:1 for fibers >20 μm in length. In addition, fiber burden within each region was strongly correlated with the degree of tissue injury present. The authors concluded that focal irregularities of pulmonary asbestosis of the type characteristic in exposed workers may be due to regional differences in the deposition and retention of asbestos fibers.

Fiber Clearance and Translocation

The fate of fibers deposited on surfaces within the lungs depends on both the

interstitium of the lung parenchyma. Roggli *et al.* (1987) subsequently performed essentially the same study with a crocidolite aerosol. For the crocidolite, there was a progressive increase in mean fiber length with increasing time postexposure, but the change was less pronounced than that for chrysotile. In addition, there was no change in fiber diameter with time for the crocidolite. In contrast, the longitudinal splitting of the chrysotile into fibrils had caused a marked reduction of diameter with time.

Accumulation of fibers in distal lung airways may, by itself, slow the clearance of fibers and other particles from the lung. Ferin and Leach (1976) exposed rats by inhalation to 10, 5, or 1 mg/m^3 of UICC amosite or Canadian chrysotile for periods ranging from 1 hr to 22 days. Exposures at 10 mg/m^3 for 1–3 hr, or for >11 days at 1 mg/m^3 suppressed the pulmonary clearance of TiO$_2$ particles.

REVIEW OF BIOLOGICAL EFFECTS OF SIZE-CLASSIFIED FIBERS

The pathological effects produced by fibers depend upon both the characteristics of the fibers and their persistence at sensitive sites. A number of carefully designed studies have been performed in which the size distributions of fiber suspensions have been well characterized as well as their persistence and/or effects.

King *et al.* (1946) instilled 100 mg of Rhodesian chrysotile into rabbit lungs at monthly intervals. One group received fibers microtomed to a length of 15 μm, and another group received fibers cut to 2.5 μm in length. At this huge dosage level, both groups showed foreign body reactions in the lungs. The long fiber produced a nodular reticulinosis, while the short fiber produced a diffuse interstitial reticulinosis.

Wright and Kuschner (1977) used short and long asbestos and manmade mineral fibers in intratracheal instillation studies in guinea pigs. With suspensions containing an appreciable number of fibers longer than ~10 μm, all of the materials produced lung fibrosis, although the yields varied with the materials used. However, with equal masses of short fibers of equivalent fiber diameters, none produced any fibrosis. The yields were lower for the long glass fibers than for the long asbestos, and this was attributed to their lesser durability within the lungs.

For fibers injected intraperitoneally (Davis, 1976; Pott *et al.,* 1976; Wagner *et al.,* 1976) or placed in a pledget against the lung pleura (Stanton and Wrench, 1972), a similar kind of fiber size and composition dependence was observed. The yield of mesotheliomas varied with both fiber diameter and length, and with dose, with very little response when long, thin fibers were not included. Asbestos fibers were more effective than glass in these studies also. At a dose of 2 mg of chrysotile, crocidolite, or glass fiber, Pott *et al.* (1976) found only slight degrees of fibrosis, but tumor yields of from 16 to 38% in rats. When the chrysotile was milled to the extent that 99.8% of the fibers were shorter than 5 μm, the dose required to produce a comparable tumor yield (32%) was 50 times greater (100mg).

Various hypotheses have been proposed to account for the pathological effects produced by asbestos. One was the contamination of the surface by trace metal and/or organic carcinogens. However, the studies of Stanton and Wrench (1972) found that surface contaminants played no role in mesothelioma yield, and con-

TABLE 2

SUMMARY OF RESULTS OF MINERAL FIBER INHALATION STUDIES IN RATS

Reference	Fiber type	Resp. Conc. (mg/m³)	d_m (μm)	Length—% > 5 μm	Length—% > 10 μm	No. rats	Mesothelioma	Adenoma	Adeno-CA	Squam. CA	Score[a]	%[b]
Wagner et al. (1974)	UICC											
	Amosite	10	NR	NR	NR	146	1(0.7)	19(13)	5(3.4)	6(4.1)	4.3	
	Anthophyllite	10	NR	NR	NR	145	2(1.4)	22(15)	8(5.5)	8(5.5)	6.2	
	Crocidolite	10	NR	NR	NR	141	4(2.8)	26(18)	7(5.0)	9(6.4)	4.8	
	Chrysotile											
	Canadian	10	NR	NR	NR	137	4(2.9)	20(15)	11(8.0)	6(4.4)	6.0	
	Rhodesian	10	NR	NR	NR	144	0	19(13)	19(13)	11(7.6)	5.8	
Davis et al. (1978)	UICC											
	Amosite	10	0.38	16	2.7	43	0	2(4.7)	0	0		2.6
	Crocidolite	10	0.38	12	4	40	0	1(2.5)	0	0		1.4
	Crocidolite	5	0.38	12	4	43	0	2(4.7)	0	0		0.8
	Chrysotile	10	0.42	30	16	40	0	7(18)	6(15)	2(5.0)		9.2
	Chrysotile	2	0.42	30	16	42	1(2.4)	6(14)	1(2.4)	1(2.4)		3.5
Davis et al. (1985)	Tremolite	10	0.25	28	7	39	2(5.1)	2(5.1)	8(21)	8(21)		14.5
Davis et al. (1986)	Amosite—short	10	0.32	1.7	0.1	42	1(2.4)	0	0	0		0.15
	Amosite—long	10	0.37	30	10	40	3(7.5)	3(7.5)	3(7.5)	4(10)		11.0
Wagner et al. (1985)	UICC crocidolite	10	0.30	53	12	28	0	0	0	1(3.6)		
	Erionite	10	0.22	44	7	28	27(96)	0	0	0		
Davis et al. (1987)	Chrysotile—short	10	0.17	5	0.7	40	1(2.5)	1(2.5)	6(15)	0		2.4
	Chrysotile—long	10	0.18	12	2	40	3(7.5)	8(20)	6(15)	5(13)		12.6

Note. NR, not reported.

[a] Relative scale where 1-nil; 2 = minimal; 4 = slight; 6 = moderate; 8 = severe—at 24 months.
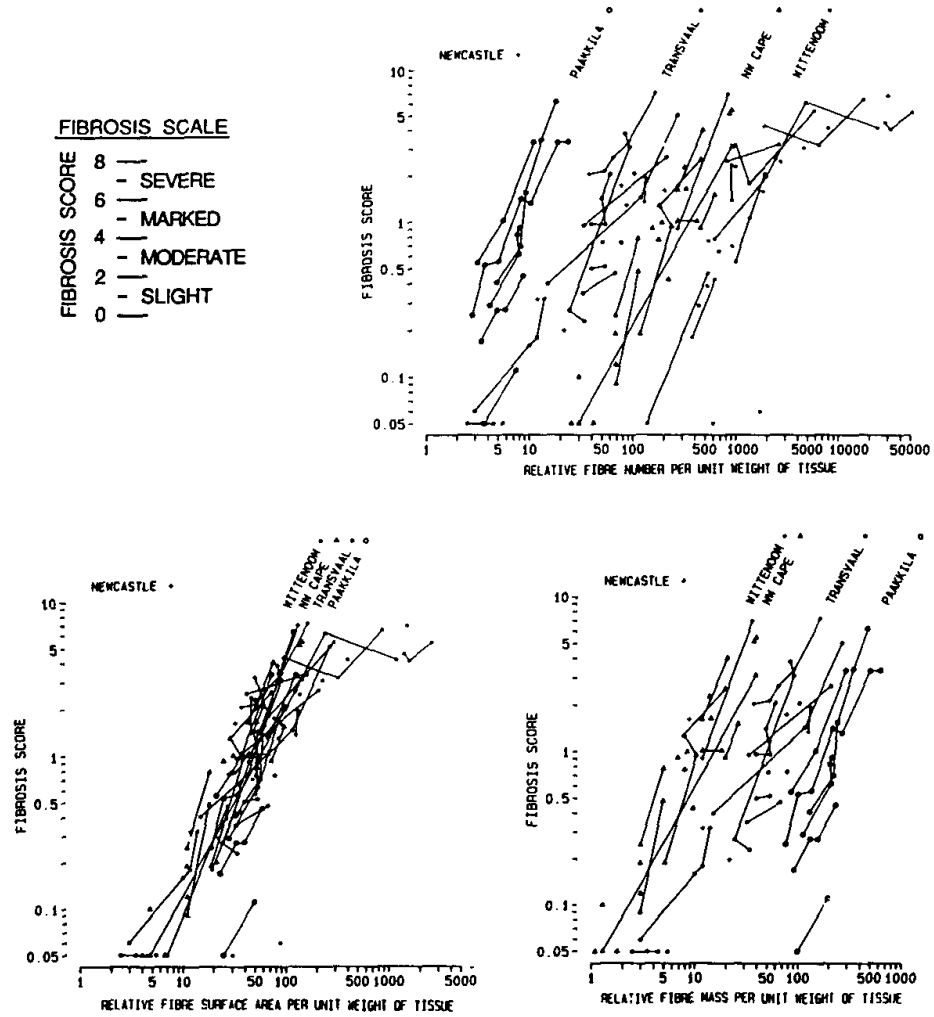
[b] % of tissue with fibrosis—at 27–29 months.

FIG. 1. Relationships between fibrosis scale and relative concentrations of fibers per unit weight of dry lung tissue. The lines connect data points from the same subject. The relative fiber surface area normalizes the data better than either the relative fiber number concentration or the fiber mass concentration (illustrations courtesy Dr. Vernon Timbrell).

the chrysotile fibers into fibrils, to give them a ratio of total surface area to mass resembling that of the particularly fine Wittenoom fibers. The result indicates that the fibrogenicity of the retained chrysotile per unit of surface area within the lungs was similar to that of the amphiboles.

Timbrell et al. (1987) also reported that amphibole mineworkers with a given fiber mass concentration in their lungs showed much higher degrees of fibrosis than goldminers with roughly the same mass concentration of retained quartz grains. The amphibole and quartz produced about the same fibrogenicity per unit

tion, he developed a model for the retention of fibers as a function of length and diameter (Fig. 2—right panel). As shown in this panel, fiber retention rises rapidly with fiber lengths between 2 and 5 μm, and peaks at ~10 μm. Fiber retention also rises rapidly with fiber diameters between 0.15 and 0.3 μm, peaks at ~0.5 μm, and drops rapidly between 0.8 and 2 μm. The utility of the model was demonstrated by applying it to predict the lung retention of Cape crocidolite and Transvaal amosite workers on the basis of the measured length and diameter distributions of airborne fibers. The predicted lung distribution did, in fact, closely match those measured in lung samples from a Cape worker (Timbrell, 1984) and, as shown in Fig. 3, from a Transvaal worker (Timbrell, 1983). Thus, fibrosis is most closely related to the surface area of fibers with diameters between 0.15 and 2 μm, and lengths greater than ~2 μm. The work of King et al. (1946), showing that chrysotile with lengths = 2.5 μm produced interstitial fibrosis in rabbits following multiple intratracheal instillations, is consistent with the retention shown in Fig. 2 and a critical fiber length of ~2 μm.

Critical Fiber Parameters for Mesothelioma

A National Research Council study (NRC, 1984) summarized mortality data for
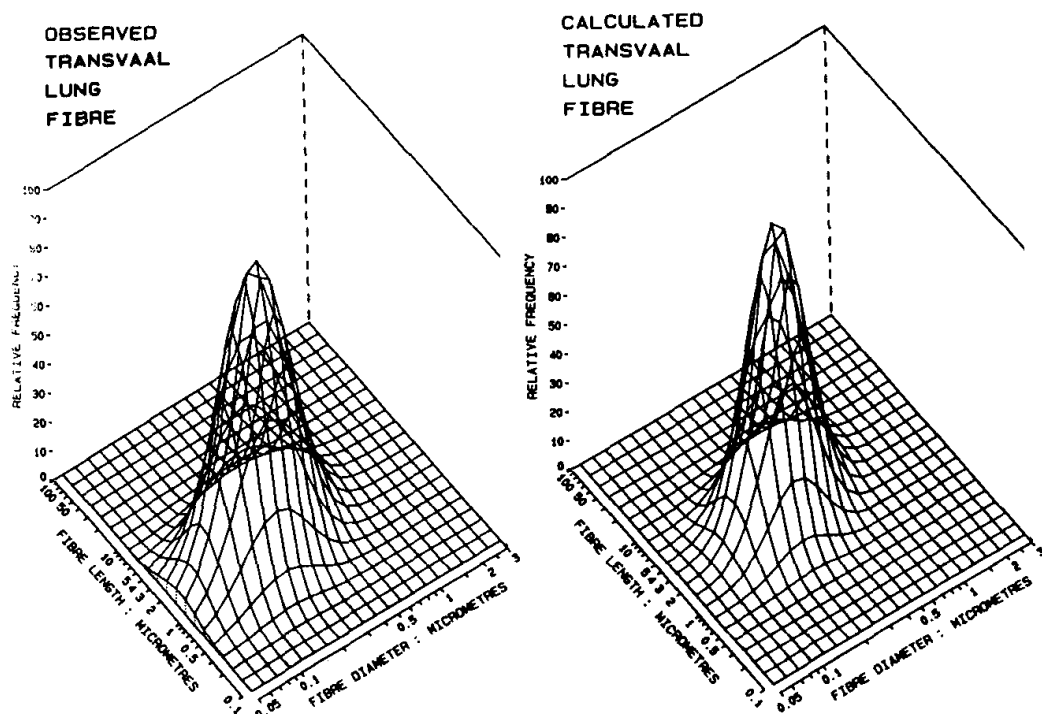
FIG. 3. Distributions of fiber lengths and diameters of amosite asbestos in the lungs of a Transvaal worker. The predicted distribution at the left is based on the lengths and diameters of the airborne fibers, and on the lung retention as a function of length and diameter from the right panel of Fig. 2. This corresponds closely to the distribution in the right panel, which was measured in samples from worker's lung (illustrations courtesy Dr. Vernon Timbrell).

of fibers in the 0.5- to 3-μm diameter range, should have produced many mesotheliomas as well as excesses in fibrosis and lung cancer. As noted earlier, an average of 38% of the excess lung cancer plus mesothelioma in working populations exposed to asbestos was expressed as mesothelima. Despite the very high exposures of the Paakkila population, no mesotheliomas were observed. Timbrell's (1983) examination of the size distributions and mesothelioma incidence at Paakkila and other asbestos mines world-wide led him to conclude that a good correlation was obtained if the threshold diameter was reduced to 0.1 μm. The mesotheliomas which Paakkila fiber has produced in animals were, most likely, due to the use of excessive doses, 10,000 times that observed in man. Paakkila asbestos contains only 1% of fibers with diameters below 0.1 μm, but with such a large dose this represents an enormous absolute number. Harington (1981) noted that the data for the northwest Cape in South Africa, where numerous mesotheliomas have been reported, and for the northeastern Transvaal, where mesotheliomas are rare, are consistent with a low fiber diameter limit. In the NW Cape, about 60% of the fibers have diameters <0.1 μm, while for the Transvaal, only about 1% have diameters < 0.1μm, comparable to Paakkila.

Timbrell (1983) also noted that the length distributions at Paakkila and the NW Cape point to a need to reduce the 10-μm threshold in Stanton's criteria. Paakkila had a high percentage of fibers longer than 10 μm, while the NW Cape had virtually none. And yet the NW Cape has been the major source of mesothelioma. Attributing potential carcinogenicity to shorter fibers by lowering the length threshold brings the estimated levels of significant fibers into closer line with the observed mesothelioma rates.

Combining the findings of Timbrell with the results of experiments reported by Davis et al. (1986b) leads to the conclusion that the critical fibers for mesothelioma induction have lengths between 5 and 10 μm. Davis et al. reported that intraperitoneal injections of short amosite (1.7% > 5 μm) produced only 1 mesothelioma among 24 rats (after 837 days), while UICC amosite (11% > 5 μm, 2.5% > 10 μm) produced 30 mesotheliomas among 32 rats, and long amosite (30% > 5 μm, 10% > 10 μm) produced 20 mesotheliomas among 21 rats. Thus, fibers shorter than 5 μm appear to be ineffective, while an appreciable fraction longer than 10 μm appears to be unnecessary.

Critical Fiber Parameters for Lung Cancer

Excess incidence of lung cancer has been reported for workers exposed to amphiboles (amosite, anthophyllite, and crocidolite), to chrysotile, and to mixtures of these fibers (NRC, 1984), but these studies have been uninformative with respect to the fiber parameters affecting the incidence. The series of rat inhalation studies performed by Davis et al. (1978, 1985, 1986, 1987), which have also produced lung cancers, have provided the most relevant evidence on the importance of fiber length on carcinogenicity in the lung.

The Wagner et al. (1974) study found that the yield of squamous cell carcinoma and adenocarcinoma was greatest with Rhodesian chrysotile, with decreasing yields for Canadian chrysotile, crocidolite, anthopyllite, and amosite, respective-

7.4% > 10 μm, median diameter of 0.22 μm). The UICC crocidolite produced 1 squamous carcinoma in 28 rats (but no mesotheliomas), while the erionite produced no carcinomas in 28 rats, but did produce 27 mesotheliomas.

In summary, Table 2 shows that 10 mg/m³ of short amosite (~0.1% > 10 μm), UICC amosite (~2.5% > 10 μm), UICC crocidolite (~3% > 10 μm), and Oregon erionite (7.4% > 10 μm) failed to produce malignant lung cancers, while 10 mg/m³ of UICC chrysotile, long amosite, and tremolite (all with ⩾ 10% > 10 μm) all produced malignant lung tumors. While there was no clear-cut influence of fiber diameter on tumor yield, the results suggest that carcinogenesis incidence increases with both fiber length and diameter. Since Timbrell (1983) has shown that fiber retention in the lungs peaks between 0.3 and 0.8 μm in diameter, it is likely that the thinner fibers, which are more readily translocated to the pleura and peritoneium, play relatively little role in lung carcinogenesis. Therefore, it appears that the risk of lung cancer is associated with long fibers, especially those with diameters between ~0.3 and 0.8 μm, and that substantial numbers of fibers >10 μm in length are needed.

One reason that short fibers may be less damaging could be the fact that they can be fully ingested by macrophages (Beck et al., 1971), and can therefore be more rapidly cleared from the lung. The fibrogenic response to long fibers could result from the release of tissue digesting enzymes from alveolar macrophages whose membranes are pierced by the fibers they are attempting to engulf (Allison, 1977). The fibers may also cause direct physical injury to the alveolar membrane. A positive association between asbestosis and lung tumors has been demonstrated by Wagner et al. (1974). The induction of fibrosis would impair clearance of deposited fibers, increasing the persistence of fibers in the lung.

The preceding implies that short fibers will have a low order of toxicity within the lung, comparable to that of nonfibrous silicate minerals. Within this concept, the critical fiber length would most likely be on the order of the diameter of an alveolar macrophage, i.e., about 10 to 15 μm. This line of reasoning leads to the same conclusion reached on the basis of the incidence of lung cancer in rats exposed to fibrous aerosols, i.e., that the hazard is related to the number of fibers longer than ~10 μm deposited and retained in the lungs. The Timbrell (1983) model predicts alveolar retention of deposited fibers approaching 100% for 10-μm-long fibers in the 0.3- to 0.8-μm-diameter range. Airborne fibers longer than ~100 μm may be much less harzardous than those in the 10- to 100-μm range because they do not penetrate deeply into the airways as interception increases with fiber length.

DISCUSSION

The various hazards associated with the inhalation of mineral fibers, i.e., asbestosis, mesothelioma, and lung cancer, are all associated with fibers with lengths which exceed critical values. However, it now appears that the critical length is different for each disease, i.e., 2 μm for asbestosis, 5 μm for mesothelioma, and 10 μm for lung cancer. There are also different critical values of fiber diameter for the different diseases. For asbestosis and lung cancer, which are related to fibers retained in the lungs, only fibers with diameters >0.15 μm need

is impractical for routine exposure assessments. The only practical surface analysis method currently available for membrane filter samples is MALS (Timbrell, 1982).

The applicability of this new index of asbestosis hazard for chrysotile is less well established than for the amphiboles. The long amphibole fibers clear very slowly from the lungs and do not dissolve, so the ratio of inhaled fiber surface area to lung retained fiber surface area remains relatively constant. The chrysotile fibers dissolve and clear more rapidly, reducing the ratio of retained fiber surface to airborne surface. On the other hand, the fibers split longitudinally within the lung, increasing the surface area of retained fibers. Another factor contributing to the uncertainty of the applicability of this index for chrysotile is that the calibration of MALS for chrysotile is less well established than for the amphiboles. These issues need to be addressed in further experimental studies.

A better index of mesothelioma hazard is the number of fibers longer than 5 μm and thinner than 0.1 μm. Since fibers with diameters less than 0.1 μm cannot be resolved by optical microscopy, analyses of relevant fiber counts must be done by electron microscopy or MALS. The differences in fiber retention between chrysotile and the amphiboles may necessitate different concentration limits for the different fiber types.

A tentative proposal for a better index of lung cancer hazard is the number of fibers longer than 10 μm which are retained within the lungs. Lung retention rises rapidly for diameters greater that about 0.15 μm. Thus, the relevant fibers have diameters >0.15 μm and lengths >10 μm. The current phase-contrast optical method of analysis of membrane filter samples is recommended for fibers with diameters between 0.25 and 3 μm (WHO, 1986). Since lung retention of fibers with diameters between 0.15 and 0.25 μm is relatively low (Fig. 2), PCOM analysis may provide an adequate index of hazard if the length limit is adjusted to 10 μm. Alternatively, analyses can be done by scanning electron microscope or MALS. Once again, the differences in fiber retention between chrysotile and the amphiboles may necessitate different concentration limits for the different fiber types.

Even if there were convenient and economical methods of sampling and analysis available for each of the three different asbestos hazards, it would undoubtedly be impractical to make three different kinds of exposure assessments at each potential exposure of concern. One option is to use the MALS analysis method, since the fiber size distributions data it generates can be used to determine quantitative values for each of the three separate indices. Another option is to do a limited amount of detailed analyses of fiber size distribution initially by electron microscopy to determine if one or more of the potential hazards can be considered to be de minimus. For example, if there is negligable potential for exposure to fibers longer than 5 μm, there would be virtually no risk of either mesothelioma or lung cancer. For most nonoccupational exposures, there is virtually no risk of asbestosis, since prolonged exposure to high dust concentrations are needed to produce evidence of this disease.

If there were appreciable concentrations of fibers >5 μm in length, but with essentially all having fiber diameters larger than ~0.1 μm, there would be virtually

Davis, J. M. G. (1987). Experimental data relating to the importance of fibre type, size, deposition, dissolution and migration. *In* "Proceedings of 1987 Mineral Fiber Symposium, Lyon, France, Sept. 1987."

Ferin, J., and Leach, L. J. (1976). The effect of amosite and chrysotile asbestos on the clearance of TiO_2 particles from the lung. *Environ. Res.* 12, 250–254.

Gylseth, B., Mowe, B., and Wannag, A. (1983). Fiber type and concentration in the lungs of workers in an asbestos cement factory. *Brit. J. Ind. Med.* 40, 375–379.

Harington, J. S. (1981). Fiber carcinogenesis: Epidemiologic observations and the Stanton hypothesis. *J. Natl. Cancer Inst.* 67, 977–989.

Hiett, D. M. (1978). Experimental asbestosis: An investigation of functional and pathological disturbances. *Brit. J. Ind. Med.* 35, 129–145.

Holt, P. F., Mills, J., and Young, K. K. (1965). Experimental asbestosis with four types of fibers. *Ann. N.Y. Acad. Sci.* 132, 87–97.

Johnson, N. F. (1987). Asbestos-induced changes in rat lung parenchyma. *J. Toxicol. Environ. Health* 21, 193–203.

Jones, J. S. P., Pooley, F. D., Sawle, G. W., Madeley, R. J., Smith, P. G., Berry, G., Wignall, B. K., and Aggarwal, A. (1980). The consequences of exposure to asbestos dust in a wartime gas-mask factory. *In* "Biological Effects of Mineral Fibres," (J. C. Wagner, Ed.), Vol. 2, pp. 637–653. IARC Scientific Publ. No. 30. International Agency for Research on Cancer, Lyon.

King, E. J., Clegg, J. W., and Rae, V. M. (1946). The effect of asbestos, and of asbestos and aluminum, on the lung of rabbits. *Thorax* 1, 188–197.

McConnochie, K., Simonato, L., Mavrides, P., Christofides, P., Pooley, F. D., and Wagner, J. C. (1987). Mesothelioma in Cyprus: The role of tremolite. *Thorax* 42, 342–347.

Meurman, L. O., Kiviluoto, R., and Hakama, M.(1974). Mortality and morbidity among the working population of anthophyllite asbestos miners in Finland. *Brit. J. Ind. Med.* 31, 105–112.

Meurman, L. O., Kiviluoto, R., and Hakama, M. (1979). Combined effects of asbestos exposure and tobacco smoking on Finnish anthophyllite miners and millers. *Ann. N.Y. Acad. Sci.* 330, 491–495.

Newhouse, M. L., Berry, G., and Skidmore, J. W. (1982). A mortality study of workers manufacturing friction materials with chrysotile asbestos. *Ann. Occup. Hyg.* 26, 899–909.

NRC (1984). "Asbesiform Fibers—Nonoccupational Health Risks." National Academy Press, Washington.

Pinkerton, K. E., Plopper, C. G., Mercer, R. R., Roggli, V. L., Patra, A. L., Brody, A. R. and Crapo, J. D. (1986). Airway branching patterns influence asbestos fiber location and the extent of tissue injury in the pulmonary parenchyma. *Lab. Invest.* 55, 688–695.

Pooley, F. D. (1976). An examination of the fibrous mineral content of asbestos lung tissue from the Canadian chrysotile mining industry. *Environ. Res.* 12, 281–298.

Pott, F., Friedrichs, K. H., and Huth, F. (1976). Results of animal experiments concerning the carcinogenic effect of fibrous dusts and their penetration with regard to the carcinogenesis in humans. *Zbl. Bakt. Hyg.* 162, 467–505.

Pott, F., Huth, F., and Friedrichs, K. H. (1976). Results of animal carcinogenesis studies after application of fibrous glass and their implications regarding human exposure. *In* "Occupational Exposure to Fibrous Glass," pp. 183–191. HEW Publ. No. (NIOSH) 76-151.

Roggli, V. L., and Brody, A. R. (1984). Changes in numbers and dimensions of chrysotile asbestos fibers in lungs of rats following short-term exposure. *Exp. Lung Res.* 7, 133–147.

Roggli, V. L., George, M. H., and Brody, A. R. (1987). Clearance and dimensional changes of crocidolite asbestos fibers isolated from lungs of rats following short-term exposure. *Environ. Res.* 42, 94–105.

Rossiter, C. F., and Coles, R. M. (1980). H.M. Dockyard, Devonport: 1947 mortality study. "Biological Effects of Mineral Fibres" (J. C. Wagner, Ed.), pp.713–721. IARC Scientific Publ. No. 30. International Agency for Research on Cancer, Lyon.

Sebastien, P., Bignon, J., Baris, Y. I., Awad, L., and Petit, G. (1984). Ferruginous bodies in sputum as an indication of exposure to airborne mineral fibers in the mesothelioma villages of Cappadocia. *Arch. Environ. Health* 39, 18–23.

Selikoff, I. J., Nicholson, W. J., and Langer, A. M. (1972). Asbestos air pollution. *Arch. Environ. Health* 25, 1–13.

The Sizes, Shapes, and Mineralogy of Asbestos Structures that Induce Lung Tumors or Mesothelioma in AF/HAN Rats Following Inhalation[1]

D. Wayne Berman,[2] Kenny S. Crump,[3] Eric J. Chatfield,[4] John M.G. Davis,[5] and Alan D. Jones[5]

Data from inhalation studies in which AF/HAN rats were exposed to nine different types of asbestos dusts (in 13 separate experiments) are employed in a statistical analysis to determine if a measure of asbestos exposure (expressed as concentrations of structures with defined sizes, shapes and mineralogy) can be identified that satisfactorily predicts the observed lung tumor or mesothelioma incidence in the experiments. Due to limitations in the characterization of asbestos structures in the original studies, new exposure measures were developed from samples of the original dusts that were re-generated and analyzed by transmission electron microscopy using a direct transfer technique. This analysis provided detailed information on the mineralogy (i.e., chrysotile, amosite, crocidolite or tremolite), type (i.e., fiber, bundle, cluster, or matrix), size (length and width) and complexity (i.e., number of identifiable components of a cluster or matrix) of each individual structure.

No univariate measure of exposure was found to provide an adequate description of the lung tumor responses observed among the inhalation studies, although the measure most highly correlated with tumor incidence is the concentration of structures ≥ 20 μm in length. Multivariate measures of exposure were identified that do adequately describe the lung tumor responses. Structures contributing to lung tumor risk appear to be long (≥ 5 μm) thin (0.4 μm) fibers and bundles, with a possible contribution by long and very thick (≥ 5 μm) complex clusters and matrices. Potency appears to increase with increasing length, with structures longer than 40 μm being about 500 times more potent than structures between 5 and 40 μm in length. Structures <5 μm in length do not appear to make any contribution to lung tumor risk. This analysis did not find a difference in the potency of chrysotile and amphibole toward the induction of lung tumors. However, mineralogy appears to be important in the induction of mesothelioma with chrysotile being less potent than amphibole.

KEY WORDS: Asbestos; tumorigenicity; lung tumors; mesothelioma; inhalation; dose/response; AF/HAN rats.

INTRODUCTION

Inhalation of asbestos dust has been clearly linked to lung cancer and mesothelioma in a broad range of human exposure settings; more than 50 positive epidemiology studies have now been published.[1] However, a quantitative dose-response relationship that applies across exposure environments has not been established for either disease; potency estimates derived from dif-

[2] ICF Kaiser Engineers, Oakland, California.
[3] ICF Kaiser Engineers, Ruston, Louisiana.
[4] Chatfield Technical Consulting Limited, Mississauga, Ontario, Canada
[5] Institute of Occupational Medicine, Edinburgh, United Kingdom

ferent epidemiological studies differ by up to 600-fold for lung cancer (Table 6-10 of an HEI-AR report[11]) and potency estimates reported for mesothelioma induction are also quite variable.

Although there are many features of epidemiological studies that may contribute to the variability observed in dose-response relationships, a major component may be the inadequate characterization of the asbestos dusts to which individuals are exposed in the epidemiological studies. In most epidemiological studies, asbestos dust concentrations were measured (if at all) by phase contrast microscopy (PCM) or by midget impinger.[2] The impingers produce a count of total dust particles that are frequently converted to PCM-equivalent counts when comparison data are available, although the correlations are generally poor.[2] PCM measurements may not be useful for distinguishing among exposure environments that differ in their potential to induce disease because (1) PCM is not capable of distinguishing asbestos from non-asbestos structures[3] and (2) existing animal studies suggest that asbestos structures outside the range of sizes visible by PCM may contribute to risk.[1]

Because of the limitations in the characterization of asbestos exposures in epidemiological studies, the best information regarding the effects of size and mineralogy on the relative potency of asbestos structures has come from animal studies. Injection and implantation experiments (in which asbestos or other fibrous material is either injected or implanted into the pleura or peritonea of rats) generally indicate that long, thin fibers exhibit the greatest tendency to induce mesothelioma.[4-31] However, injection and implantation experiments bypass the processes associated with inhalation, retention in the lungs, and transport from the lungs, which may be important in modulating the effects of airborne exposure. Thus, results obtained from animal inhalation studies are likely to be more relevant for evaluating human risk than injection and implantation experiments.

A number of inhalation studies have been conducted in which animals (generally rats) have been exposed to varying concentrations of asbestos dusts of various types and the incidence of tumors observed in the animals recorded.[7-13,26,28,32-36] In addition to verifying that different types of asbestos can cause lung cancer and mesothelioma when inhaled by animals, these studies generally indicate that longer fibers tend to be more carcinogenic than shorter ones. However, no measure of asbestos exposure that satisfactorily predicts tumor incidence is identified in these studies.

In this study, data on tumor incidence in AF/HAN rats from 13 inhalation experiments reported in a series

of studies conducted by Davis et al.[7-13] are combined in a statistical analysis to determine if a measure of exposure can be identified that satisfactorily predicts lung tumor or mesothelioma incidence. Because of limitations in the characterization of asbestos exposures in the original Davis et al. studies (use of scanning electron microscopy precluded observation of structures thinner than 0.2 μm; only SEM visible fibers and bundles were included in the characterized size distributions while clusters and matrices may also contribute to tumorigenicity in a unique way; and lack of bivariate characterization of the size distributions precluded evaluation of the combined effects of structure length and width), archived samples of the original stock samples were used to regenerate asbestos dust clouds that were collected on filters and characterized in detail by transmission electron microscopy (TEM). TEM is capable of detecting and identifying even the thinnest asbestos structures.

DATABASE AND METHODS

The Animal Inhalation Database

The series of animal studies by Davis et al.[7-11,13] all employed a common protocol, utilized the same strain of rat, and were conducted in the same laboratory by the same group of investigators. In these studies, groups of 40 male AF/HAN rats, aged 3 months at the beginning of the experiment, were exposed by inhalation for 7 hours per day, 5 days per week for 224 days over one year and then observed for a minimum of an additional year. These studies involved UICC crocidolite, Korean tremolite, four types of chrysotile and three types of amosite (Table 1). Several of the samples were also studied at two doses or on multiple occasions. Details of the experimental procedures used in these studies (along with the sources of the asbestos samples employed) are reported in the studies cited in Table 1. Due to the small number of mesotheliomas observed, the present evaluation was limited primarily to lung tumors. Benign and malignant lung tumors were pooled for this evaluation. Also, control groups from the various studies were combined into a single group.

Regeneration and Analysis of Dusts from the Animal Studies

To obtain more definitive characterization of the asbestos dusts used in the Davis et al. studies, dusts were

Table 1. Summary Data for Animal Inhalation Experiments Conducted by Davis and Coworkers[a]

Fiber type	Description	Abbre-viations	Mass concen-tration (mg/m³)	PCM f/ml	Number of animals	Number of benign pulmonary tumors	Number of malignant pulmonary tumors	Total number of pulmonary tumors	Mesothe-liomas	Reference
Chrysotile	UICC-A	UC	2	390	42	6	2	8	1	(7)
Chrysotile	UICC-A	UC	10	1,950	40	7	8	15	0	(7)
Chrysotile	Long	LC	10	5,510	40	8	12	20	3	(13)
Chrysotile	Short	SC	10	1,170	40	1	6	7	1	(13)
Chrysotile	UICC-A	UC	9.9	2,560	36	6	8	14	0	(12)
Chrysotile	UICC-A (Discharged)[b]	DC	9.9	2,670	39	4	6	10	1	(12)
Chrysotile	WDC Yarn[c]	WC	3.6	679	41	5	13	18	0	(11)
Amosite	UICC	UA	10	550	43	2	0	2	0	(7)
Amosite	Long	LA	10	2,060	40	3	8	11	3	(10)
Amosite	Short	SA	10	70	42	0	0	0	1	(10)
Crocidolite	UICC	UR	4.9	430	43	2	0	2	1	(7)
Crocidolite	UICC	UR	10	860	40	1	0	1	0	(7)
Tremolite	Korean	KT	10	1,600	39	2	16	18	2	(9)
None	Control	C	0		20	0	0	0	0	(7)
None	Control	C	0		36	0	0	0	0	(9)
None	Control	C	0		61	1	1	2	0	(10)
None	Control	C	0		64	1	1	2	0	(11)
None	Control	C	0		47	1	1	2	0	(13)

[a] Exposure occurred for 7 hours a day, 5 days a week for 1 year
[b] UICC-A Chrysotile in this experiment was treated with mixed polarity air (produced with a source of beta radiation) following generation to reduce the surface charge on individual particles within the dust
[c] Chrysotile samples used for dust generation in this experiment were obtained from material treated by a commercial wet dispersion process

regenerated from samples archived from the original studies using the same equipment, procedures, and personnel as in the original studies. For each asbestos sample type, three or four sets of filters at three different particle loadings were collected at regular time intervals over approximately one hour during which the rate of dust generation was kept constant. The set of optimally-loaded filters (one from each time interval) was then prepared and analyzed and the results from the individual filters were combined. A separate set of filters was also collected for PCM analysis at the same time as the filters collected for analysis by TEM. A detailed discussion of the preparation and analysis of samples for this study and a characterization of the samples based on this analysis is currently in preparation (Berman et al., Journal article in preparation).

The regenerated dusts were analyzed by TEM using the counting criteria from the Interim Superfund Method for the Determination of Asbestos in Air.[37] These criteria provide that, in addition to examination of a portion of each filter in which all asbestos structures present are identified, a separate examination of a different portion of each filter is performed at lower magnification, during

which only structures ≥ 5 μm in length are evaluated. The stopping rules in the Superfund method were modified for this study to assure that a minimum of 200 structures derived from total structure examination and, separately, 200 structures derived from examination for long structures (≥ 5 μm in length) would be evaluated for each sample. By using a separate examination for long structures, the present study achieves a level of precision for the determination of long structures that could otherwise require the counting of thousands of structures when all sizes are evaluated simultaneously.[35]

In the data base developed from the regenerated dusts, fibers, bundles, clusters and matrices (as defined in the literature[37]) are characterized separately along with measurements of the length and width of each such structure. Up to five fibers and bundles that are components of clusters or matrices are also characterized for those complex structures (i.e., clusters and matrices) where individual fibers or bundles can be characterized.[38] In the analyses reported herein, two methods of utilizing information on complex structures are applied. In one set of analyses, only the primary structures enter the analysis. In a second set of analyses, whenever com-

ponent fibers or bundles in a cluster or matrix are characterized, these components are included as if they are independent structures and the parent cluster or matrix is not included.

Estimation of Exposure Concentrations

Concentrations of asbestos structures in each regenerated dust that exhibit specific characteristics based on size or type were calculated by multiplying the number of structures in a particular sample displaying the characteristic(s) of interest by the total area of the filters exposed during air sample collection and dividing by the product of the area of the portion of the filters examined during the analysis and the volume of air passed through the filters during air sample collection. The concentrations of structures in the original dusts to which the animals were exposed were estimated by multiplying the corresponding concentration in the regenerated dust by the ratio of the concentration measured by PCM in the original dust to the PCM concentration in the regenerated dust.

Statistical Methods

Once the re-generated dusts were characterized, a statistical analysis was performed to test for relationships between the size, shape, and mineral type of an asbestos structure and its relative potency for inducing lung tumors. In the statistical methods employed, the probability of a lung tumor (benign or malignant) response in an animal is assumed to be of the form:

$$P = 1 - \exp(-\alpha - \beta * WC) \qquad (1)$$

where α specifies the response probability in unexposed animals (*i.e.*, the probability of a response in unexposed animals is $1 - \exp[-\alpha]$), β represents the absolute potency of a dust for producing a tumor response, and WC is a weighted sum of the concentrations of structures in different structure categories. A structure category is defined by restrictions on structure sizes (*e.g.*, a defined range of lengths, widths, and/or aspect ratios) and structure types (*e.g.*, fibers, bundles, clusters, and/or matrices). The weights in the weighted sum are estimates of the relative potencies of structures in the different structure categories. Thus,

$$WC = q_1 * x_1 + q_2 * x_2 + ... + q_k * x_k = \Sigma q_j x_j \qquad (2)$$

where x_j is the concentration of airborne asbestos structures in the jth structure category and q_j represents the

potency of structures in the jth structure category relative to the potency of structures in other categories.

The q_js are constrained to be non-negative ($q_j \geq 0$ for $j = 1, ..., k$) and to sum to one ($q_1 + ... + q_j = 1$). The latter constraint makes each q_j a measure of relative potency rather than absolute potency. The non-negativity constraint implies that no category of structures is capable of reducing the probability of a tumor response.

In a few of the analyses the model is expanded to permit the probability of response to depend upon the chemical composition (mineralogy) of the structures (*e.g.*, chrysotile or amphibole). This expanded version of the model is of the form:

$$P_i = 1 - \exp(-\alpha - \beta_i * WC) \qquad (3)$$

where P_i is the probability of tumor response in animals exposed exclusively to material of type i, and β_i a measure of the absolute potency of this material. Thus, in this more general model, a different absolute potency is assumed for materials of differing mineralogy but the relative potencies of structures in different structure categories are assumed to be independent of mineralogy.

In still other analyses, the tumorigenic potential of a structure is assumed to be embodied in a single quantitative measure (*e.g.*, the surface area of the structure). In these analyses the probability of a tumor response in an animal is assumed to be of the form:

$$P = 1 - \exp(-\alpha - \beta * SM) \qquad (4)$$

where SM is the sum of the quantitative measures over the structures contained in a specified volume of air. For example, if the quantitative measure is surface area, then SM is the total surface area of structures per milliliter of air.

The parameters of these models (α, β and q_j) are estimated using maximum likelihood methods and likelihood ratio tests are used for testing hypotheses.[39] Confidence intervals for individual parameters are constructed using the "profile likelihood method."[39] The goodness-of-fit of each model to the data is assessed by applying a chi-square distribution to the deviance statistic.[40] The p-value of the chi-square statistic is approximated using the chi-square distribution with degrees of freedom equal to the [number of dose groups] − [number of q_j's estimated as being non-zero] − 1.

The non-negativity constraints imposed on these models make this approach very different from ordinary (unconstrained) regression. In ordinary regression, a perfect fit of a model is guaranteed whenever the number of parameters equals or exceeds the number of data points. However, in the constrained model described above, typically all but a few of the q_j's are estimated
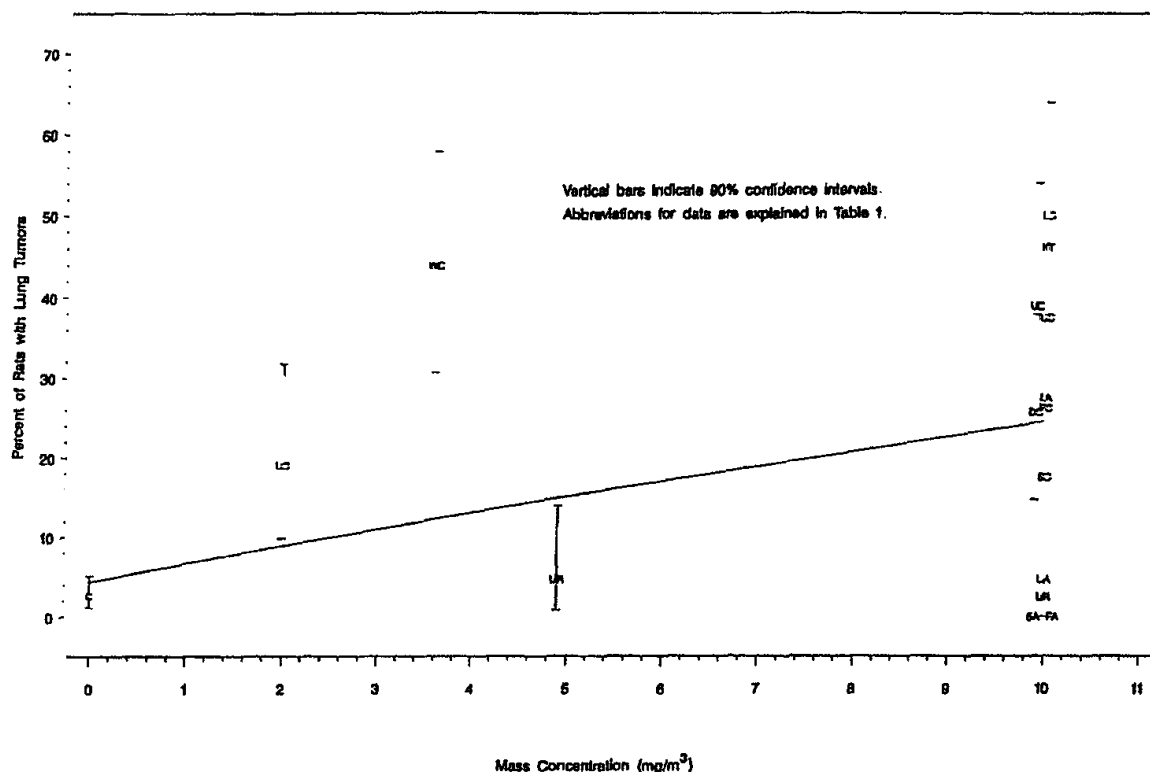
Fig. 1. Fit of model Tumor incidence versus mass concentration from animal study.

to be zero so that the estimation results are the same as if these q_j's had not been included in the estimation procedure. Consequently these models may legitimately include more categories of asbestos structures than there are animal exposure groups.

Evaluation of Mesothelioma Incidence

Although there were too few mesotheliomas observed in the animal inhalation studies to perform an extensive analysis similar to that conducted for lung tumors, a test was conducted of whether the risk of mesothelioma was proportional to the risk development of lung tumors. If this test cannot be rejected, it suggests that any fiber size distribution that describes the lung tumor responses also describes the mesothelioma responses. The specific test conducted was a likelihood ratio test of whether the probability of mesothelioma could be expressed as

$$P_{meso} = cP_{lt}$$

where P_{meso} is the probability of developing mesothelioma following exposure; P_{lt} is the probability of developing lung tumors following exposure; and c is the constant of porpotionality between the probability of developing a mesothelioma and the probability of developing a lung tumor.

This test was applied to the total data set and to the chrysotile and amphibole studies separately.

RESULTS

Univariate Measures of Exposure

Figure 1 is a plot of the percentage of animals with lung tumors versus the mass concentrations (mg/m³) of total dust reported in the original Davis et al. studies. The curve in the figure represents the maximum likelihood fit of the dose-response model represented by Equation 4, where SM is the measured dust mass for each experiment reported in Table 1.

It is clear from Figure 1 that mass concentration of total dust does not provide a consistent dose-response

Length Categories: 5μm−40μm, ≥ 40μm
Width Categories: < 0.3μm and ≥5μm
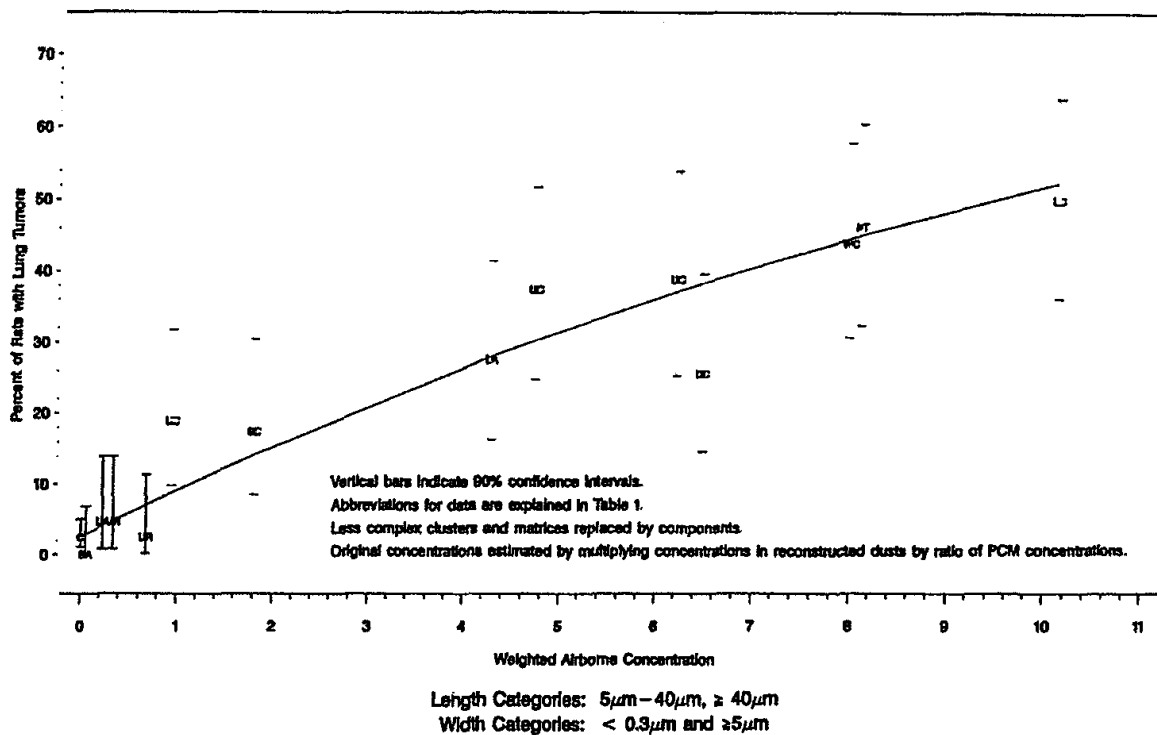
Fig. 2. Fit of model. Tumor incidence versus PCM concentration from animal study

for these studies. Several of the Davis et al. studies employed a target mass concentration of 10 mg/m³ (Table 1) and results of these studies appear grouped together on the right side of the figure. Despite having been exposed to similar dust mass concentrations, responses in these animal groups are quite variable, ranging from 0 pct (0/42 animals) for short amosite to 50 pct (20/40 animals) for long chrysotile. Moreover, even though the experiment involving wet dispersed chrysotile involved exposure to a total dust mass concentration of only 3.5 mg/m³, the tumor response was 44 pct (18/41), which is considerably greater than that of several of the experiments employing a total mass concentration of 10 mg/m³.

Figure 2 is similar to Figure 1, except that the concentration of fibers measured by PCM (f/cc) in the original study replaces mass concentration as the measure of exposure. This figure likewise exhibits no consistent dose-response pattern. Thus, neither of the two measures of exposure reported in the original Davis et al. studies (total dust concentration and PCM fiber concentration) relate to lung tumor risk in a consistent manner.

Table 2 is a summary of the tests of goodness-of-fit for the exposure-response models presented in Fig-

ures 1 and 2 and similar models based on other univariate measures of exposure that are derived from TEM measurements of the re-generated dusts. For each univariate measure of exposure, the table contains the correlation coefficient (R^2) for the relationship between the airborne asbestos concentration (defined by the univariate measure) and the negative logarithm of the probability of remaining tumor-free [-Ln(1-P)]. The table also contains the deviance of the maximum likelihood fit of the univariate dose-response model (defined using Equation 4) and the p-value for the goodness-of-fit test associated with that deviance. Large deviances and, correspondingly, small p-values (i.e., p ≤ 0.05) indicate a poor description of the lung tumor response by a particular univariate measure of exposure.

Both total dust mass and PCM concentrations give very large deviances and corresponding, highly significant lack of fit, 138.0 (p ≤ 0.0001) and 56.1 (p ≤ 0.0001), respectively (Table 2), which is consistent with the visual impressions from Figures 1 and 2. Likewise, the concentrations of total asbestos structures measured by TEM, of TEM structures longer than 5 μm, and of TEM structures longer than 20 μm all give poor fits to the data, although the deviance statistic decreases as the

Table II. Summary of Fits of Univariate Concentrations to Lung Tumor Data

Dose measure	R^2	Deviance	df	p-value[a]
Total dust mass concentration	0.05	116.0	12	<0.0001
PCM structure concentration	0.50	56.1	12	<0.0001
Total TEM structure concentration[b]	0.32	112.1	12	<0.0001
Concentration of structure longer than 5 μm[b]	0.39	87.7	12	<0.0001
Concentration of structure longer than 10 μm[b]	0.50	51.4	12	<0.0001
Concentration of structure longer than 20 μm[b]	0.72	31.4	12	0.0017
Concentration of structure longer than 30 μm[b]	0.71	41.7	12	<0.0001
Concentration of structure longer than 20 μm and thinner than 0.4 μm[b]	0.60	37.41	12	0.0002
Concentration of structure longer than 20 μm and thinner than 0.2 μm[b]	0.29	92.9	12	<0.0001
Concentration of structure longer than 20 μm and thicker than 0.4 μm[b]	0.71	38.0	12	0.0002
Total structure surface area per air volume[c]	0.65	38.4	12	0.0001
Total structure volume per air volume[c]	0.54	50.2	12	<0.0001
Sum of aspect ratios per air volume[b]	0.32	108.8	12	<0.0001
Sum of (aspect ratio)[1.8] per air volume[b]	0.35	100.3	12	<0.0001
Stanton Index[b,d]	0.38	79.85	12	<0.0001

[a] P-values ≤0.05 indicate a significant lack of fit of model to lung tumor data, based on chi-square distribution for the defiance with 12 degrees of freedom (14 data sets and two parameters).

[b] Concentrations derived counting components of less complex structures as individual structures and ignoring the parent structure.

[c] Concentrations derived counting only primary structures.

[d] The index proposed by Stanton et al [24] is the concentration of all fibers ≥ 8 μm in length and < 0.25 μm in width.

structures are restricted to increasing lengths in this series, which indicates an improving fit. However, restricting the analysis to even longer structures (≥ 30 μm), restricting the widths of structures longer than 20 μm to thinner structures (< 0.4 μm or < 0.2 μm) or to thicker structures (≥ 0.4 μm) all make the fit worse.

Several other measures evaluated in Table 2 are similar to exposure measures found by other investigators to be significantly correlated with tumor incidence: structures longer than 8 μm and thinner than 0.25 μm,[24] total surface area of the asbestos structures per unit volume of air (implied by Lippman,[41] assuming a relationship between tumor induction and fibrosis as described by Davis and Cowie[42]); total volume of asbestos per unit volume of air (which is proportional to the total mass concentration of asbestos[43]), the concentration of aspect ratios (sum of aspect ratios of structures per unit volume of air[29]); and the concentration of aspect ratios raised to the 1.8 power.[30]

All measures reported in Table 2 are significantly correlated (p ≤ 0.05, based on the slope of the regression line) with lung tumor incidence. Nevertheless, all of these measures provide a poor fit to the lung tumor data (p ≤ 0.0017, based on the deviance statistic) despite a significant correlation coefficient.

The results in Table 2 suggest that the tumorigenicity of the asbestos dusts studied by Davis et al. are more closely related to the concentration of longer structures than to the concentration of shorter structures. As previously suggested by Wylie et al.,[31] however, the fact that none of the exposure measures listed in Table 2 provide an adequate description of the database suggests that the features of asbestos that relate to risk are too complex to be represented by a single univariate exposure measure and that multivariate measures may be required to adequately describe lung tumor response to asbestos.

Multivariate Measures of Exposure

To gain an understanding of the combinations of structure categories that relate best to potency, more than 100 statistical analyses were conducted in which relative potencies were estimated for various combinations of length and width categories. The results of these exploratory analyses are summarized by an analysis that incorporates a matrix of five length categories (< 5 μm, 5–10 μm, 10–20 μm, 20–40 μm, and ≥ 40 μm in length) in combination with five categories of width (< 0.15 μm, 0.15–0.3 μm, 0.3–1.0 μm, 1.0–5.0 μm, and ≥ 5.0 μm in width), for a total of 25 categories of structures that potentially contribute independently to potency. In this analysis, the relationship between exposure and response was modeled using Equation 1 with WC consisting of a 25-term function that is the sum of the product of each size category multiplied by a relative potency for that size category (Equation 2). Table 3 indicates the maximum likelihood estimates of the relative

Table III. Relative Potencies for Inducing Lung Cancer[*]

	Width (μm)	Length (μm)					Total
		< 5	5-10	10-20	20-40	> 40	
A: Analysis based on primary structures	< 0.15		0.0055	0.42	X	X	0.42
	0.15-0.3			0.040			0.040
	0.3-1.0						0
	1.0-5.0						0
	> 5.0	X		0.043	0.074	0.42	0.54
	Total	0	0.0055	0.50	0.074	0.42	1.0
	Deviance = 13.33 (7 df)						
	p = 0.06						
B: Less complex clusters and matrices replaced by components	< 0.15			0.033	0.10	X	0.13
	0.15-0.3		0.0018			0.72	0.72
	0.3-1.0						0
	1.0-5.0						0
	> 5.0	X			0.02	0.13	0.15
	Total	0	0.0018	0.033	0.12	0.85	1.0
	Deviance = 12.03 (7 df)						
	p = 0.10						

[*] Entries represent an estimate of the relative potency assigned to structures in that size category by the model defined by Equation (1). An "X" indicates a category that contains no structures. A blank indicates zero potency estimated for that category. P-value is for fit of model to lung tumor data in Table 1, based on chi-square distribution for the deviance (small p-values indicate poor fits).

potencies (i.e., the q_j's from the model) of the structures in each of the 25 size categories.

Table 3A presents results in which only primary structures are included, whereas Table 3B presents results in which parent clusters and matrices (for which component structures were characterized) are replaced by their components. The statistical analysis in which complex structures are resolved into components (Table 3B) provides the best fit to the data and the resulting model provides an overall adequate description of the data based on goodness-of-fit (deviance = 12.03 [7 df], p = 0.10). The fit is also marginally acceptable from the analysis (Table 3A) that includes only primary structures (deviance = 13.33 [7 df], p = 0.06). These two analyses exhibit several common features. Both of the analyses attribute zero potency to structures shorter than 5 μm. Positive potencies are confined to structures that are either thin (< 0.3 μm) or very thick (≥ 5 μm). For both thin and thick structures, potency tends to increase with increasing length, although the observed relationships are not entirely monotone.

Resolution of complex structures into component fibers and bundles significantly increases the precision with which fibers and bundles can be categorized, since roughly 50 pct of the fibers and bundles characterized in the re-generated dusts are components of complex structures. Consequently, from this point on, only analyses that resolve clusters and matrices into components are considered.

Although the statistical analysis reported in Table 3B adequately describes the data, the relative potencies assigned to the two narrowest categories of structures seems somewhat unrealistic; one expects dose-response relationships to vary smoothly with size. Positive potencies are assigned to structures thinner than 0.15 μm in combination with one long and one short length category (5-10 μm and ≥ 40 μm) and to structures between 0.15 and 0.3 μm in width in combination with two intermediate length categories (10-20 μm and 20-40 μm). This suggests that the potencies of structures in these two width categories cannot be distinguished using this database.

To test this hypothesis, these two categories were combined into a single category (width < 0.3 μm). The results of this analysis are presented in Table 4A. Combining these width categories only slightly increases the deviance (from 12.03 to 12.15), so that the hypothesis that structures in the two width categories are equally potent cannot be rejected. Moreover, the fit of the model actually improves somewhat (the p-value increases from 0.10 to 0.14), due to a reduction in the number of degrees of freedom.

Because the pattern of potencies observed among the length categories of the model presented in Table 4A

Table IV. Additional Analyses Performed to Obtain an "Optimum Exposure Index"[a]

	Width (μm)	Length (μm)					
		< 5	5–10	10–20	20–40	> 40	Total
A: Intermediate analysis	< 0.3		0 0012	0 0054		0 84	0.847
	0 3–1.0						0
	1.0–5.0						0
	> 5.0	X			0 012	0 14	0 152
	Total	0	0 0012	0 0054	0 012	0.98	1.0
	Deviance = 12.15 (8df)						
	p = 0.14						
B: Optimum exposure index	< 0.30		0 0017			0 853	0 855
	> 5.0					0 145	0 145
	Total		0 0017			0.998	1.0
	Deviance = 12.66 (10 df)						
	p = 0.24						

[a] Entries represent an estimate of the relative potency assigned to structures in that size category by the model defined by Equation (1) An "X" indicates a category that contains no structures. A blank indicates zero potency estimated for that category. P-value is for fit of model to lung tumor data in Table 1, based on chi-squared distribution for the deviance (Small p-values indicate poor fits).

also appear somewhat unrealistic, this model was simplified by reducing the number of length categories in the same manner that the number of width categories was reduced for the model described above. Therefore, structures between 5 μm and 40 μm in length were combined into a single length category. Also, structures shorter than 5 μm were removed from the analysis because, even with the reduced number of length categories, the short structures were assigned zero potency. Structures between 0.3 and 5.0 μm in width were also removed because these too were assigned zero potency in the reduced model.

The model resulting from the maximum likelihood fit of the remaining size categories (referred to as the "optimum exposure index") is shown in Table 4B. The deviance of 12.66 obtained from this analysis is only slightly larger than that of the full model (12.03) and the goodness-of-fit p-value from the reduced model is 0.24 (10 df), which indicates a better statistical fit than was obtained using the original model (Table 3B) or the intermediate model (Table 4A).

The "optimum exposure index" assigns a relative potency of:

- 0.0017 for structures < 0.3 μm in width and between 5 and 40 μm in length;
- 0.853 for structures < 0.3 μm in width and ≥ 40 μm in length; and
- 0.145 for structures ≥ 5.0 μm in width and ≥ 40 μm in length.

All other structures are assigned a potency of zero in the optimum exposure index. Interestingly, whereas the lat-

ter size category is composed completely of complex structures, the two categories of thin structures are composed almost totally of fibers and bundles (including many that are components of complex structures).

The fit to the experimental data obtained by the "optimum exposure index" is presented in Figure 3. The x-axis of this plot is exposure expressed as the weighted airborne concentration formed by the sum of the relative potencies from this analysis times the concentrations of structures in the corresponding categories (WC in Equation 2). Unlike Figures 1 and 2, this graph indicates a consistent dose-response relationship.

Table 5 contains 90 pct confidence intervals for the three structure categories that are assigned positive potency by the optimum exposure index. The fact that none of these three confidence intervals contains zero potency implies that none of these three structure categories can be removed from the model without significantly degrading the fit (i.e. the hypothesis that one of these categories has zero potency can be rejected). Thus, to obtain adequate fits to the lung tumor incidence data within the framework of this analysis, it is necessary to assign positive potencies to all three of the size categories of structures that contribute to the optimum exposure index.

Table 5 also contains 90 pct confidence intervals for two categories of structures assigned zero potency in the optimum exposure index: structures < 5 μm in length and structures 5–40 μm in length and ≥ 5 μm in thickness. The upper 95 pct confidence bound for the relative potency of structures shorter than 5 μm is estimated as 0.00008. This upper bound is 0.00008/0.0017
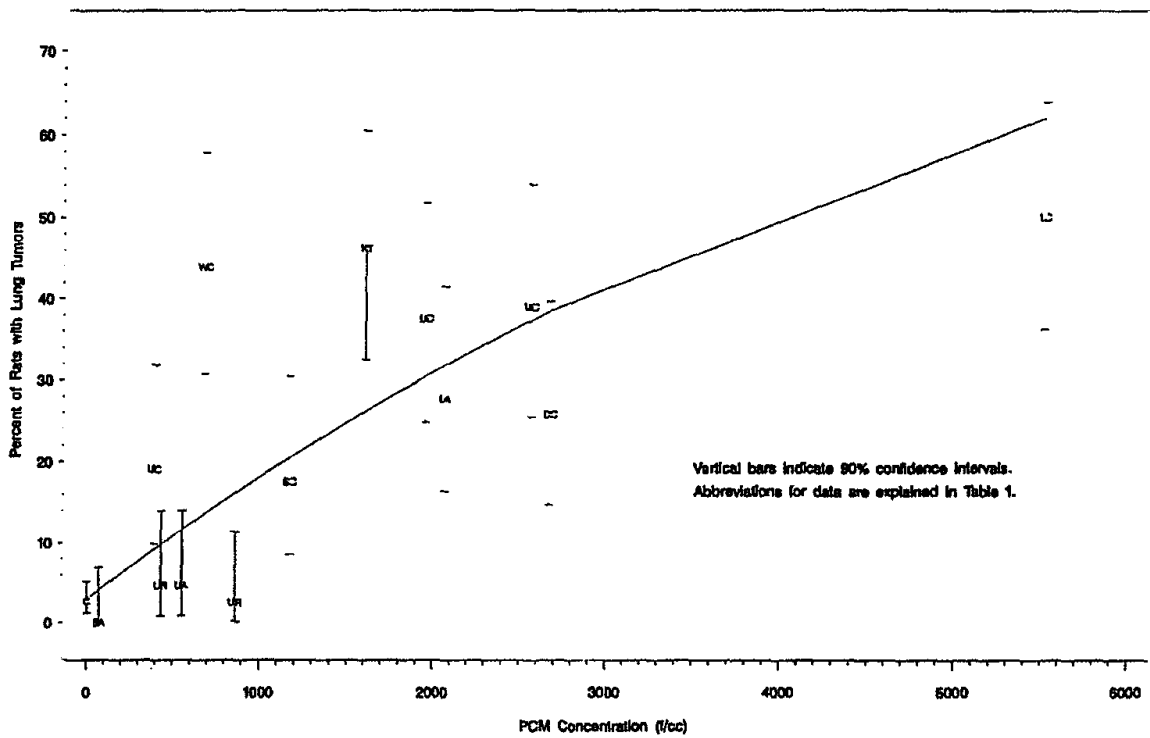
Fig. 3. Fit of model. Tumor incidence versus structure concentration by TEM.

Table V. Relative Potency Estimates Derived from the "Optimum Exposure Index" with 90% Confidence Intervals

Category (units in μm)	Relative potency estimate	90% confidence interval
length < 5	0	[0, 0.00008][a]
5 ≤ length < 40 width ≤ 0 3	0.0017	[0 0010, 0.0032]
5 ≤ length < 40 width ≥ 5 0	0	[0, 0 030][a]
length ≥ 40 width < 0.3	0.85	[0 67, 0.95]
length ≥ 40 width ≥ 5.0	0.15	[0 04, 0 32]

[a] The size category is assigned zero potency in the model derived from the maximum likelihood fit and therefore does not contribute to the "optimum exposure index."

= 1/20 as large as the estimated relative potency of structures between 5 and 40 μm in length and thinner than 0.3 μm, and only 0.00008/0.85 = 1/10,000 as large as the estimated relative potency of structures longer than 40 μm and thinner than 0.3 μm.

Results of various additional hypothesis tests are presented in Table 6. All of the analyses presented indicate a zero potency for all categories of structures shorter than 5 μm. Since this is the outcome most favorable to the hypothesis that such structures are nonpotent, $p = 1.0$ is the p-value associated with a test of this hypothesis. Although some analyses reported herein assign a positive potency to structures 5–10 μm in length, the hypothesis that structures shorter than 10 microns in length are non-potent cannot be rejected either ($p = 0.09$).

Results of hypothesis tests for a difference between the potency of chrysotile and amphibole, conducted within the framework of the optimum exposure index, are also presented in Table 6. This test was performed by estimating different absolute potencies (i.e., different values for β; in the model) for chrysotile and amphibole, but assuming that the relative potencies of structures in different size categories (i.e., the q_i's) are the same for chrysotile and amphibole (Equation 3). The resulting p-value for this test is 0.72 (non-significant), indicating no detectable difference between the potency of chrysotile and amphibole. It is also *not* possible to reject the com-

pound hypothesis that chrysotile and amphibole have the same relative potencies *and* that the relative contributions to potency from different size fractions are the same for chrysotile and amphibole.

The optimum exposure index assigns positive potency to thin (< 0.3 μm) and very thick (> 5 μm) structures but not to structures of intermediate thickness. Although a potency for very thick structures could be due to thin structures imbedded within complex structures (see discussion), this result could also be an artifact caused by limitations in the data base and the specific cutpoints used to create the optimum exposure index. Additional analyses taken to further explore this issue identified a slightly different index that also provides an adequate fit to the data (p = 0.09) and which does not result in a positive potency for very thick structures. This index assigns a relative potency of:

- 0.0024 for structures < 0.4 μm in width and between 5 and 40 μm in length; and
- 0.9976 for structures < 0.4 μm in width and ≥ 40 μm in length.

Statistical Analyses of Mesothelioma Data

Results in Table 7 indicate that the hypothesis that mesothelioma incidence is proportional to lung tumor incidence for all sample types combined can be rejected. However, the hypotheses that mesothelioma incidence is proportional to lung tumor incidence either for chrysotile sample types or amphibole sample types (considered separately) cannot be rejected.

The best indication (i.e., maximum likelihood) is that the probability of a chrysotile (amphibole) exposure inducing mesothelioma is 0.058 (0.20) times the probability that the same exposure induces lung tumors. These two values are significantly different (p = 0.032). Since the analyses of the lung tumor data indicate that there is no difference between chrysotile and amphibole in their ability to induce lung tumors, these results suggest that amphibole is 0.20/0.058 = 3.4 times more potent than chrysotile for causing mesothelioma in rats (assuming that the relative potencies of structures in different size categories are approximately the same for mesothelioma and lung tumors.

DISCUSSION

Results from this study indicate that the induction of lung tumors in rats following inhalation of asbestos

Table VI. Hypothesis Test Results for Lung Tumor Incidence

	Decrease in deviance	P-value of Hypothesis test[a]	
Structures shorter than 5 μm are non-potent	0	1	(NS)[b]
Structures shorter than 10 μm are non-potent[c]	1.76	0.09	(NS)
Structures shorter than 40 μm are non-potent[d]	74.6	<0.0001	(S)[e]
Structures longer than 40 μm are non-potent[d]	73.1	<0.0001	(S)
Structures thicker than 5 μm are non-potent[d]	10.0	0.007	(S)
Structures thinner than 0.3 μm are non-potent[d]	54.4	<0.0001	(S)
Amphibole and chrysotile structures are equally potent[d,f]	0.12	0.72	(NS)
Fibers and bundles are equally potent[d]	0.78	0.68	(NS)

[a] A P-value less than 0.05 indicates that the hypothesis can be rejected.
[b] NS - not significant (hypothesis cannot be rejected).
[c] Based on analysis of data in Table 5A.
[d] Based on analysis of data in Table 5B.
[e] S - significant (hypothesis can be rejected).
[f] Due to a limitation in the computer program used to perform these calculations, the value of the background parameter, α, was fixed at the value that provides a perfect fit to the control data

is a function of the size and shape of asbestos structures within the inhaled dusts. Structures contributing to lung tumor risk appear to be long (≥ 5 μm) thin (< 0.3 or 0.4 μm) fibers and bundles, with a possible contribution by long and very thick (≥ 5 μm) complex clusters and matrices. Potency appears to increase with increasing length, with structures longer than 40 μm being about 500 times more potent than structures between 5 and 40 μm in length. Fibers and bundles of similar dimensions appear to contribute equally to potency.

For all types of asbestos structures, results of this study suggest that a minimum length (between 5 and 10 μm) exists such that the best estimate of the potency of structures shorter than this minimum is zero. This analysis also indicates that, as a worst case, a 95% upper limit to the potency of individual structures shorter 5 μm is no more than about 1/20 of the potency estimated for individual fibers or bundles between 5 and 40 μm in length and no more than about 1/10,000 of that estimated for individual fibers or bundles ≥40 μm in length and <0.3 μm in width. In contrast, the evidence suggesting a range of widths within which structures can be considered non-potent is less compelling.

Table VII. Hypothesis Test Results for Comparing Mesothelioma and Lung Tumor Incidence

Hypothesis tested	Increase in deviance	P-value of hypothesis test[a]
The relative probability of inducing mesotheliomas and lung tumors are the same for all dusts tested ($P_{meso} = cP_{lu}$)[b]	20.9	0.028
The relative probability of inducing mesotheliomas and lung tumors are the same for all chrysotile dusts tested. ($P_{meso} = c_1 P_{lu}$)[c]	9.97	0.20
The relative probability of inducing mesotheliomas and lung tumors are the same for all amphibole dusts tested. ($P_{meso} = c_2 P_{lu}$)[d]	6.30	0.28
The proportionality constant relating mesothelioma incidence to lung tumors incidence is the same for chrysotile and the amphiboles. ($c_1 = c_2$)	4.62	0.032

[a] A P-value less than 0.05 indicates that P is significant and the hypothesis can be rejected

[b] The best estimate for the constant of proportionality between mesothelioma and lung tumor incidence is $c = 0.094$ when all dusts are considered.

[c] The best estimate for the constant of proportionality betwen mesothelioma and lung tumor incidence is $c_1 = 0.058$ when chrysotile dusts are considered separately.

[d] The best estimate for the constant of proportionality between mesothelioma and lung tumor incidence is $c_2 = 0.20$ when amphibole dusts are considered separately.

For mesothelioma, it appears that mineralogy is an important determinant of the relative potency of inhaled dusts, with chrysotile being less potent toward the induction of mesotheliomas than the amphiboles in comparison to their relative potency for inducing lung tumors.

Despite the special emphasis placed on the characterization of long structures, the data base employed in this study contains only a limited number of very long structures (e.g., ≥40 μm in length). This contributes uncertainty to the specific quantitative estimates of relative potency for long structures, the most potent structures identified. Our statistical analysis does not address this type of uncertainty; fiber concentrations were assumed to be known with certainty. Additional uncertainties in the exposure estimates result from the reliance on regenerated dusts in this study rather than the actual dusts to which the experimental animals were exposed. This problem was mitigated by having the dusts regenerated by the same personnel using the same stock material, equipment, and procedures that were employed in the original studies.

Despite the above considerations, we know of no other set of experimental data that is more suitable for quantitative determination of relative potencies of asbestos structures of different types and dimensions that are apt to be relevant to conditions of human exposure. Our study involves inhalation, which is more relevant to human exposures than injection or implantation studies. Our data base contains data on a variety of different types of asbestos including crocidolite, tremolite, chrysotile, and amosite. It includes four different samples of chrysotile and three different samples of amosite, which were chosen to represent a range of asbestos structure size dimensions. It also involves a more detailed char-

acterization of long structures and complex structures than those available from other experimental settings.

The only other studies in which the relationship between structure size and shape and tumor response has been examined formally (using some type of statistical analysis) are the studies by Stanton et al.[23,24] and other statistical studies employing the database reported by Stanton et al.[29,30] or employing a re-analysis of the samples studied by Stanton and coworkers.[31] However, these studies all incorporate a statistical procedure that differs radically from that employed in the present study. While the earlier studies only identify exposure measures that are significantly correlated with tumor incidence, the present study identifies an exposure measure that satisfactorily describes the tumor incidence (i.e., provides an acceptable fit to all of the data).[e] In fact, it

[e] The methodology utilized in this study avoids several methodological problems associated with the analysis by Stanton et al and the others who re-evaluated their data and conclusions Stanton et al. computed a correlation between the logarithm of the concentration of fibers in specific dimensional ranges and the logit of the probability of a tumor A number of exposure categories for individual fiber types investigated by Stanton et al. contained no fibers, which implies that the logarithm of the fiber concentration for these categories is undefined Stanton et al. assigned a zero in place of the logarithm of concentration in these cases However, this decision is entirely arbitrary and the value selected could have had a large impact upon the correlation coefficient Similarly, no tumors were detected in several experimental groups investigated by Stanton et al and the logit is undefined whenever no tumors occur Although it is not clear how Stanton et al. handled this problem, it seems likely that such groups were omitted from their analysis Note that, because of these problems, the correlation coefficients presented in Table 2 (which are calculated based on a linear relationship that is not undefined at zero) may not be directly comparable to those calculated by Stanton et al

is apparent from Text Figure 2 of Stanton et al.[24] that the exposure measure they identify as being most highly correlated with tumor incidence (fibers longer than 8 μm and thinner than 0.25 μm) does not provide an acceptable fit to the observed tumor incidence. Similarly, although all of the univariate measures considered in the present study (Table 2) are highly correlated with tumor incidence, none of them adequately describe lung tumor incidence.

In contrast, when asbestos exposure is expressed as the weighted sum of the concentrations of structures in the three size categories of structures defined in this study by the optimum exposure index, this exposure index provides a statistically adequate fit to the lung tumor response data reported in the studies by Davis et al. (Table 1). Consequently, the hypothesis that the model determined by the optimum exposure index completely characterizes the potency of asbestos structures in the induction of lung tumors in AF/HAN rats cannot be rejected. This implies that this model can potentially provide adequate descriptions of risk in a broader range of exposure settings.

Stanton et al.[24] found that fibers longer than 8 μm appear to correlate best with mesothelioma incidence, which parallels the findings in this study that structures longer than some minimum length (between 5 and 10 μm) tend to contribute to the induction of lung tumors following inhalation and that potency tends to increase with increasing length. However, our analysis indicates that the potency of structures increases with length up to lengths of at least 40 μm, whereas Stanton et al. did not explicitly consider the contribution to potency by such long structures.

The maximum thickness for potent fibers and bundles found in this study (< 0.3 or 0.4 μm) is comparable to the maximum thickness reported by Stanton et al.[24] of 0.25 μm. Stanton et al. did not report information on complex structures in their data base and, indeed, the meaning of complex structures in a gel suspension (which they used for implantation) is not clear. Consequently, their study provided no information on the effects of thick clusters. Complex asbestos structures do occur as isolated species in the air, however, and results in this study indicate that clusters longer than 40 μm and thicker than 5 μm may contribute to the potency of an asbestos dust.

That long, thick clusters (structure for structure) may contribute about one-sixth as much to total potency as long, thin fibers or bundles (Table 5B) suggests a mechanism in which some of these may break down and liberate long fibers or bundles that may then contribute to the induction of tumors. The structures longer than

40 μm and thicker than 5 μm that are evaluated in this study are open structures with settling velocities that are likely comparable to their component fibers or bundles. Thus, it is likely that they are respirable and can penetrate the deep lung. Once in the deep lung, however, when such structures impact a wall, some may liberate component fibers or bundles and the longest and thinnest of those may then contribute to the induction of tumors.

Although neither Stanton et al.[23,24] nor Bertrand and Pezerat[29] concluded that mesothelioma induction following injection or implantation is a strong function of fiber mineralogy, such a conclusion was reached by Bonneau et al.[30] In our study, there is no evidence that mineralogy is a determinant of potency toward the induction of lung tumors. However, assuming the size range that induces lung tumors and mesothelioma are similar, results in this study suggest that for inhaled dusts that exhibit comparable potency toward lung tumor induction, amphibole dusts are approximately three times as likely to induce mesothelioma as chrysotile dusts.

Implications for Human Exposure

For human exposures, potency estimates obtained from different epidemiological studies, which are based upon PCM measurements, have been found to differ by large factors.[1] This study likewise demonstrates that PCM measurements do not provide a consistent dose response in the animal inhalation studies either. However, more complex exposure measures based upon TEM measurements are shown to provide a consistent dose-response relationship for the animal data. This suggests that the observed lack of a consistent dose response across epidemiological studies is due at least partially to the fact that the features of asbestos important to determining potency are not adequately represented by PCM measurements.

Regarding mineralogy, human epidemiology studies (taken as a whole) suggest that mineralogy is important at least for determining potency toward the induction of mesothelioma.[1] Our results likewise indicate that amphibole dusts are more likely (by a factor of about three) to induce mesothelioma than chrysotile dusts whenever their potential to induce lung tumors are comparable.

The importance of mineralogy in determining the relative potency of a dust toward the induction of lung tumors in human exposure is less clear.[1] Results from this study suggest that, when the relative size distribution of structures in a dust is taken into account, the miner-

alogy of a structure does not contribute to the determination of potency toward the induction of lung tumors. However, this finding may not be applicable to humans because chrysotile degrades more rapidly than amphibole *in vivo*. Since humans live much longer than the animal species typically used in experiments, the relative persistence of chrysotile and amphibole *in vivo*[1] may have a much larger impact on the induction of lung tumors in humans while remaining unimportant in animals.

Implications for Asbestos Measurement

Results from this study indicate strongly that methods for the measurement of asbestos should be modified to include better characterization of longer structures and that such characterization should be performed using TEM (as opposed to PCM), due to the need to include thin structures (and the need to distinguish asbestos structures from non-asbestos structures). Better characterization of longer structures can be achieved, just as in our reanalysis of the data from the animal experiments, by examination of grid specimens at lower magnifications in which only structures exceeding some minimum length are recorded. At a minimum, we recommend that separate examinations be made for structures ≥ 5 µm in length. However, because of the indication in this study that very long structures (≥ 40 µm in length) are highly potent relative to shorter structures, we also recommend that a separate examination of still longer structures (e.g., structures ≥ 20 µm in length) be included in the routine analysis of asbestos. Similarly, to obtain exposure measures that relate more closely to risk without unduly increasing the cost of the analysis, characterization of structures shorter than 5 µm can be deemphasized.

ACKNOWLEDGMENTS

REFERENCES

1 HEI-AR (Health Effects Institute-Asbestos Research), *"Asbestos in Public and Commercial Buildings: A Literature Review and Synthesis of Current Knowledge"* (HEI-AR, 141 Portland St, Suite 7100, Cambridge, Massachusetts, 1991)
2. USEPA (United States Environmental Protection Agency), *Airborne Asbestos Health Assessment Update* (Office of Health Effects Assessment, Washington, D.C., Report 600/8-84-003F, 1986).
3. W.H. Walton, *"The Nature, Hazards and Assessment of Occupational Exposure to Airborne Dust: A Review"* Annals of Occupational Hygiene 26, 115–247.
4. R.E. Bolton, J.M.G. Davis, K. Donaldson, and A. Wright, "Variation in the Carcinogenicity of Mineral Fibres," *Annals of Occupational Hygiene*, 26, 569-582 (1982).
5. R.E. Bolton, J.M.G. Davis, B.G. Miller, K. Donaldson, and A. Wright, "The Effect of Dose of Asbestos on Mesothelioma Production in the Laboratory Rat," *Proceedings of the VIth International Pneumoconiosis Conference*, 2, 1028-1035 (1984).
6. R.E. Bolton, J. Addison, J.M.G. Davis, K. Donaldson, A.D. Jones, B.G. Miller, and A. Wright, "Effects of the Inhalation of Dusts from Calcium Silicate Insulation Materials in Laboratory Rats," *Environmental Research*, 39, 26-43 (1986).
7. J.M.G Davis, S.T. Beckett, R.E. Bolton, P. Collings, and A.P. Middleton, "Mass and Number of Fibres in the Pathogenesis of Asbestos-Related Lung Disease in Rats," *British Journal of Cancer*, 37, 673-688 (1978).
8. J.M.G. Davis, S.T. Beckett, R.E. Bolton, and K. Donaldson, "A Comparison of the Pathological Effects in Rats of the UICC Reference Samples of Amosite and Chrysotile with Those of Amosite and Chrysotile Collected from the Factory Environment" (J.C. Wagner, ed, *Biological Effects of Mineral Fibres*, IARC Scientific Publications, 288-292, 1980).
9. J.M.G Davis, J. Addison, R.E. Bolton, K. Donaldson, A.D. Jones, and R.G. Miller, "Inhalation Studies on the Effects of Tremolite and Brucite Dust in Rats," *Carcinogenesis*, 6, 667-674 (1985).
10. J.M.G. Davis, J. Addison, R.E. Bolton, K. Donaldson, A.D. Jones, and T. Smith, "The Pathogenicity of Long Versus Short Fibre Samples of Amosite Asbestos Administered to Rats by Inhalation and Intraperitoneal Injection," *British Journal of Experimental Pathology*, 67, 415-430 (1986).
11. J.M.G. Davis, J. Addison, R.E. Bolton, K. Donaldson, and A.D. Jones, "Inhalation and Injection Studies in Rats Using Dust Samples from Chrysotile Asbestos Prepared by a Wet Dispersion Process," *British Journal of Pathology*, 67, 113-129 (1986)
12. J.M.G. Davis, R.E. Bolton, A.N. Douglas, A.D. Jones, and T. Smith, "Effects of Electrostatic Charge on the Pathogenicity of Chrysotile Asbestos," *British Journal of Industrial Medicine*, 45, 292-309 (1988).
13. J.M.G Davis, and A.D. Jones, "Comparisons of the Pathogenicity of Long and Short Fibres of Chrysotile Asbestos in Rats," *British Journal of Exposure Pathology*, 69, 171-738 (1988).
14. E.J. King, J.W. Clegg, V.M. Rae, "The Effects of Asbestos, and of Asbestos and Aluminum, on the Lungs of Rabbits," *Thorax*, 1, 188-197 (1946)

15. H. Muhle, B. Bellmann, S. Takenata, and U. Ziem, "Inhalation and Injection in Rats to Test the Carcinogenicity of MMMF," *Annals Occupational Hygiene*, 31, 755-764 (1987).

16. F. Pott, F. Huth, and K.H. Friedrichs, "Tumorigenic Effect of Fibrous Dust in Experimental Animals," *Environmental Health Perspectives*, 9, 313-315 (1974).

17. F. Pott, F. Huth, and K.H. Friedrichs, "Results of Animal Carcinogenesis Studies After Application of Fibrous Glass and Their Implications Regarding Human Exposure" (*Occupational Exposure to Fibrous Glass*, U.S. HEW Publication No 76-151, pp. 183-191, 1976)

18. F. Pott, "Some Aspects on the Dosimetry of the Carcinogenic Potency of Asbestos and Other Fibrous Dusts," *Staub-Reinhalt*, 38, 486-490 (1978)

19. F. Pott and H. Muhle, "Animal Experiments with Mineral Fibres" Proceedings from a symposium, *Short and Thin Mineral Fibres Identification, Exposure, and Health Effects*, National Board of Occ Safety and Health, Solnic, Sweden pp. 133-161, 1982)

20. F. Pott, U. Ziem, and U. Mohr, "Lung Carcinomas and Mesotheliomas Following Intratracheal Instillation of Glass Fibres and Asbestos" (*Proceedings of the 6th Pneumoconiosis Conference*, pp. 747-756, 1983)

21. F. Pott, U. Ziem, R.J. Reiffer, F. Huth, H. Ernst, and U. Mohr, "Carcinogenicity Studies on Fibres, Metal Compounds, and Some Other Dusts in Rats," *Experimental Pathology*, 32, 129-152 (1987).

22. M. Stanton, and C. Wrench, "Mechanisms of Mesothelioma Induction with Asbestos and Fibrous Glass," *Journal of the National Cancer Institute*, 48, 797-821 (1972)

23. M. Stanton, M. Layard, A. Tegeris, E. Miller, M. May, and E Kent, "Carcinogenicity of Fibrous Glass: Pleural Response in the Rat in Relation to Fiber Dimension," *Journal of the National Cancer Institute*, 58, 587-597 (1977).

24. M. Stanton, M. Layard, A. Tegeris, E. Miller, M. May, and E Morgan, "Relation of Particle Dimension to Carcinogenicity in Amphibole Asbestos and Other Fibrous Minerals," *Journal of the National Cancer Institute*, 67, 965-975 (1981)

25. J.C. Wagner, G. Berry, and J.W. Skidmore, "Studies of the Carcinogenic Effects of Fiber Glass of Different Diameters Following Intrapleural Inoculation in Experimental Animals" (*NIOSH 76-151*, pp. 193-197, 1976).

26. J.C. Wagner, G. Berry, R.J. Hill, D. Munday, and J.W. Skidmore, "Animal Experiments with MMM(V)F-Effects of Inhalation and Intrapleural Inoculation in Rats. Biological Effects of Man-made Fibres" (*Proceedings of a WHO/IARC Conference*, Copenhagen, pp. 209-233, 1982).

27. M.M.F. Wagner, J.C. Wagner, R. Davies, and D.M. Griffith, "Silica-Induced Malignant Histiocytic Lymphoma: Incidence Linked with Strain of Rat and Type of Silica," *British Journal of Cancer*, 41, 908-917 (1980).

28. J.C. Wagner, J.W. Skidmore, R.J. Hill, and D.M. Griffith, "Erionite Exposure and Mesotheliomas in Rats," *British Journal of Cancer*, 51, 727-730 (1985).

29. R. Bertrand and H. Pezerat, "Fibrous Glass: Carcinogenicity and Dimensional Characteristics *Biological Effects of Mineral Fibres*" (J.C Wagner, ed., *IARC Scientific Publications*, 901-911, 1980).

30. L. Bonneau, C. Malard, and H. Pezerat, "Studies on Surface Properties of Asbestos," *Environmental Research* 41, 268-275 (1986).

31. A.G Wylie, R.L. Virta, and J.M. Segretti, "Characterization of Mineral Population by Index Particle: Implications for the Stanton Hypothesis," *Environmental Research*, 43, 427-439 (1987)

32. K.P. Lee, C.E. Barras, R.S. Griffith, R.S. Waritz, and C.A. Lapin, "Comparative Pulmonary Responses to Inhaled Inorganic Fibers with Asbestos and Fiberglass," *Environmental Research*, 24, 167-191 (1981).

33. E. McConnell, J.C. Wagner, J.W. Skidmore, and J. Moore, "A Comparative Study of the Fibrogenic and Carcinogenic Effects of UICC Canadian Chrysotile B Asbestos and Glass Microfibre (JM 100)" (*Biological Effects of Man-made Fibres*, Proceedings of a WHO/IARC Conference, pp. 234-252, 1982).

34. D.M. Smith, L.W. Oritiz, R.F. Archuleta, and N.F. Johnson, "Long-Term Health Effects in Hamsters and Rats Exposed Chronically to Man-Made Vitreous Fibres," *Annals of Occupational Hygiene*, 34, 731-754 (1987).

35. J.W. Wagner, G. Berry, J.W. Skidmore, and V. Timbrell, "The Effects of the Inhalation of Asbestos in Rats," *British Journal of Cancer*, 29, 252-269 (1974).

36. J.C. Wagner, D.M. Griffiths, and D.E. Munday, "Experimental Studies with Palygorskite Dusts," *British Journal of Industrial Medicine*, 44, 749-763 (1987)

37. E.J. Chatfield, and D.W. Berman, "*Interim Superfund Method for the Determination of Asbestos in Ambient Environments, Part 1: Method*" (USEPA publication: 540/2-90/005a, May 1990)

38. D.W. Berman and E.J. Chatfield, "*Interim Superfund Method for the Determination of Asbestos in Ambient Environments. Part 2: Technical Background Document*" (USEPA publication: 540/2-90/005b, May, 1990).

39. D. Cox and D. Lindley, *Theoretical Statistics* (Chapman and Hall, London, 1974)

40. National Research Council, *Health Effects of Exposure to Low Levels of Ionizing Radiation BEIR V. Committee on the Biological Effects of Ionizing Radiations* (National Academy Press, Washington, D.C., 1990)

41. M. Lippman, "Review: Asbestos Exposure Indices," *Environmental Research*, 46, 86-106 (1988).

42. J.M.G Davis, and H. Cowie, "The Relationship Between Fibrosis and Cancer in Experimental Animals Exposed to Asbestos and Other Fibers," *Environmental Health Perspectives*, 88, 305-309 (1990).

43. W.J. Nicholson, *Airborne Levels of Mineral Fibres in the Non-Occupational Environment* (Division of Environmental and Occupational Medicine, Mt Sinai School of Medicine, City University of New York, 1988)

Particle Loading in the Human Lung— Human Experience and Implications for Exposure Limits

MORTON LIPPMANN,[1] VERNON TIMBRELL,[2]

*[1]New York University Medical Center,
Institute of Environmental Medicine,
Tuxedo, NY 10987
[2]Medical Research Council,
Epidemiology Unit (South Wales)
Cardiff, South Glamorgan CF2 3AS, UK*

ABSTRACT

Timbrell's analyses of fiber burdens in the post-mortem lungs of workers with long-term inhalation exposures to a variety of amphiboles have shown that the clearance of fibers is strongly dependent on lung burden and its associated lung fibrosis, with a small percentage of very heavily exposed workers having little, if any clearance from parts of the lung. The extent of lung fibrosis is proportional to the total surface of retained mineral particles for both fibers and more compact particles. The human data base from the asbestos workers can provide a sound basis for the development of more generic models describing the influence of lung burden of mineral dust on particle deposition in, and clearance from, human lungs. The implications of the results obtained to the pathogenesis of chronic lung diseases and the evaluation and/or establishment of exposure limits are also discussed, along with some research needs to facilitate interspecies extrapolation of fiber toxicity data.

INTRODUCTION

Our assignment for this Symposium paper was to discuss the following The following issues:

- What evidence, if any, do we have from human epidemiology data that would tend to validate or argue against the rat data with respect to lung overloading?

- What are the implications of lung overloading with respect to environmental health standards?

With respect to the first issue, we have interpreted epidemiology broadly, and will include a review of data from a variety of studies of human lung tissue

Key Words
    Particle retention
    Fiber burdens
    Post-mortem human lungs
    Lung fibrosis
    Occupational & environmental exposure limits
    Critical fiber dimensions
    Particle surface

oz occupationally exposed workers by one of us (V.T.) in association with numerous colleagues (Timbrell, 1982, 1983, Timbrell et.al., 1988, 1990). Our review of other human exposure-response literature will be brief, since little of it provides quantitative information on lung dust retention in relation to exposure duration or intensity.

The human data base, while limited, shows evidence that overloading of clearance mechanisms is a major determinant of lung fibrosis among workers in the dusty trades. However, it remains inadequate for valid intercomparisons with the results of controlled exposure studies in rats and other laboratory animals. Furthermore, some of the critical determinants of disease potential established in the human studies have not been measured or reported in the results of the animal studies, e.g. particle surface areas, and, for fibers, fiber length and diameter distributions. These critical fiber dimensions differ for the three different diseases associated with asbestos exposure as discussed previously (Lippmann, 1988). The critical fiber dimensions are summarized in Table 1. We will discuss the research needs that we have identified to achieve a more definitive resolution of interspecies differences in response to inhaled mineral dusts.

With respect to the second question, it is already clear that so-called "inert" or "nuisance" dusts can produce adverse effects when clearance mechanisms become overloaded, and that the current occupational exposure limits deserve a careful re-examination. We also review recent evidence that current non-specific ambient air quality standards may not fully protect the more sensitive segments of the population from adverse health effects. This suggests the presence of a threshold for response, analogous to the particle clearance overload phenomenon that has been observed at higher exposure levels in chronic animal exposure studies, as discussed later in this paper.

TABLE 1

·Summary of Recommendations on Asbestos Exposure Indices*

Disease	Relevant exposure index
Asbestosis	Surface area of fibers with: Length > 2 μm; diameter > 0.15 μm
Mesothelioma	Number of fibers with: Length > 5 μm; diameter < 0.1 μm
Lung cancer	Number of fibers with: Length > 10 μm; diameter > 0.15 μm

* Reprinted by permission from Lippmann (1988).

Evidence for Dust Overload in Human Epidemiology

Snipes (1989) has estimated that a lung burden of 10 to 20 g in humans corresponds to 10-20 mg particles per gram of wet lung, which is similar to the lung burden of Diesel soot in rats after 24 months of exposure to 3.5 or 7.0 mg soot/m^3. These soot concentrations are clearly "overload" doses in the rat. Thus, evidence of coal workers pneumoconiosis (CWP) among miners who accumulate 10-40 g in British coal mines (Rossiter et al., 1967, Davis et al., 1983, Ruckley et al., 1984, Soutar et al., 1986) or 25 to 50 g in German coal miners (Stöber et al., 1967) is quite consistent with the overload hypothesis. The prevalence of CWP varies with coal rank and other factors for reasons that remain elusive. Data on other potentially important exposure variables, such as particle size distribution and specific surface area are not generally available to separate the effects of mass loading from those associated with surface properties or chemical-specific interactions with epithelial cells.

For community air data, the enhanced response due to overloading may not be comparable to that in the dusty trades. There is however, some epidemiologic
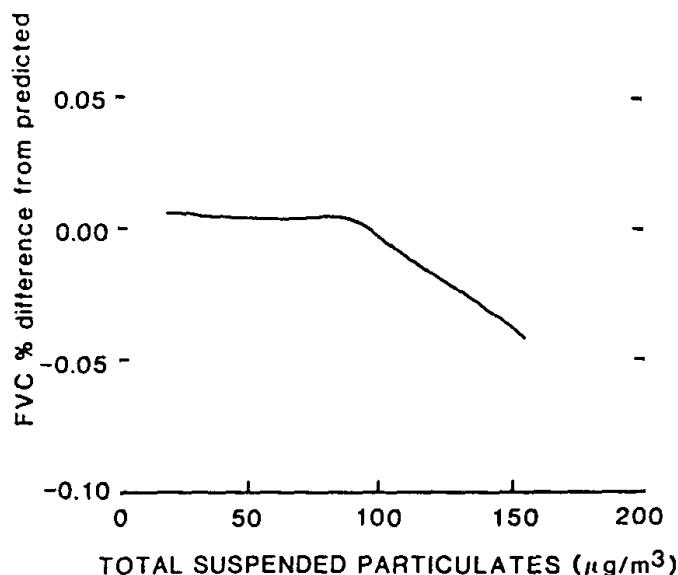
FIGURE 1. The line shown represents a nonparametric fit of the percentage
difference between the observed FVC and the FVC predicted by a regres-
sion controlling for the effects of standing height, sitting height,
age, race, sex, body mass index, smoking, and respiratory conditions
smoothed against TSP ($\mu g/m^3$). Reprinted by permission from Schwartz
(1989).

evidence for a threshold type of response for total suspended particulates (TSP)
in relation to morbidity indices. Schwartz (1989) examined lung function in 4300
representative children and young adults (ages 6-24) in relation to TSP in their
communities, using data collected during the second National Health and Nutrition
Examination Survey (NHANES II) conducted in the period 1976-1980 throughout the
U.S. He found highly significant associations between forced vital capacity (FVC)
and peak flow rates and TSP. As shown in Figure 1, there appeared to be a thres-
hold of response at about 90 $\mu g/m^3$ daily average TSP.

In another use of secondary data sources for studies of the health effects
of air pollutants, Ostro and Rothschild (1989) regressed data on respiratory-
related restricted activity days (RRAD) from the 1976-81 Health Interview Survey
(HIS) against the daily average concentration of fine particulate matter (FP),
i.e., mass concentration of aerosol $\leq$ 2.5 μm in aerodynamic diameter. The HIS is
a national (U.S.) multistage probability survey of working individuals, aged 18-
65 in 50,000 households. Respondents were asked to report RRAD in the prior 2-
week period, such as days of work loss or bed disability as well as more minor
restrictions associated with an acute respiratory condition. They found the best
estimate for the effect of FP on RRAD to be a 1.58% increase for each 1 $\mu g/m^3$ of
FP.

Ozkaynak and Thurston (1987) reported on associations between 1980 U.S. mor-
tality rates in 98 Standard Metropolitan Statistical Areas (SMSAs) and four
measures of particulate air pollution. These were total suspended particulate
matter (TSP); inhalable particulate matter, i.e., particulate < 15 μm in aero-
dynamic median diameter (IHP); fine particulate matter, i.e., particulate < 2.5
μm in aerodynamic median diameter (FP); and sulfate (SO_4^{2-}), a major component of
FP. They found that FP and SO_4^{2-} were most consistently and significantly asso-
ciated with the reported SMSA-specific total annual mortality rates, whereas TSP
and IP were often nonsignificant predictors of mortality.

The analyses of Ostro and Rothschild (1989) and Ozkaynak and Thurston (1987)
did not consider a threshold model. Furthermore, their results suggest that the
FP associated responses are due to the acidic nature of the small particle frac-
tion and not the mineral dust in the coarse particles that dominate the IHP and
TSP measures. Thus, the threshold type of response reported by Schwartz (1989)

Evidence for Dust Overload in Human Lung Studies

Timbrell (1982) developed a model for fiber deposition in human lungs based upon his analysis of the bivariate diameter and length distributions found in air and lung samples collected at an anthophyllite mine at Paakkila in Finland. At this particular mine, the length and diameter distributions of the airborne dust were exceptionally broad, and historic exposures were very high. He observed that, for workers with the highest exposure and most severe lung fibrosis (Ashcroft et al., 1988), the lung fiber distributions in some tissue segments approached those of the airborne fibers. Adjacent tissue, analyzed for extent of fibrosis, showed severe fibrotic lesions. He concluded that long-term retention was essentially equal to deposition in such segments, and that the fibrosis in the tissue had not affected deposition. His deposition model, illustrated in Figure 2, is based upon the bivariate size distribution differences between airborne dust samples and the dust in the most heavily fibrosed lung tissue. Figure 3 shows a series of retention curves for different degrees of lung fibrosis. These curves were determined by comparing the fiber size distributions in other tissue samples from the same lung with the distribution in the sample for which all fibers deposited were retained.
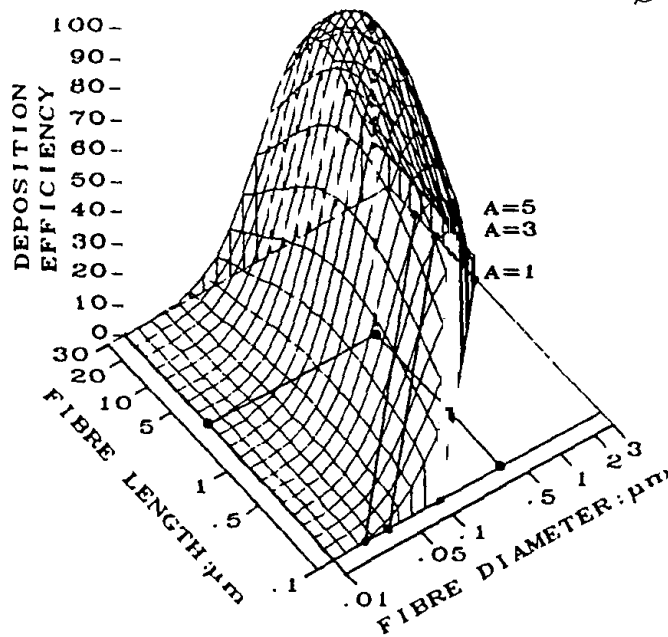
FIGURE 2. Bivariate plot of deposition efficiency model for the gas-exchange region of the human lung as a function of fiber length and fiber diameter. Limits are shown for aspect ratios (A) equal to 1, 3, and 5. The model is based on differences between airborne fiber distributions and distributions measured in very severely fibrosed lung tissue.

The deposition model was tested by comparing the fiber retention found in the lungs of much less heavily exposed asbestos workers at Paakkila and other locations to that predicted by applying the deposition model to the specific airborne dust distributions. Figure 4 shows the bivariate size distributions for airborne fibers at the Transvaal in South Africa (crocidolite and amosite), at the Northwest Cape in South Africa (crocidolite) and at Wittenoom in Australia
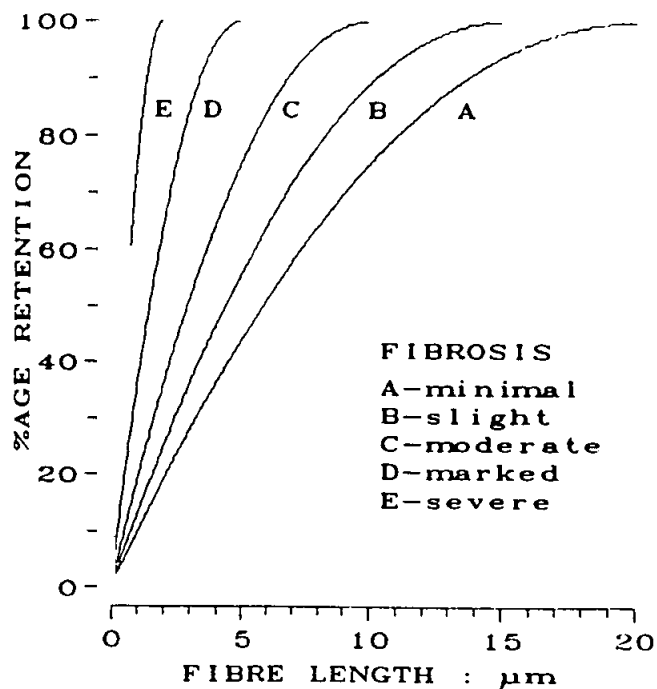
FIGURE 3. Effect of lung fibrosis on fiber retention in human lungs as a function of fiber length. The model is based on retention in lung segments from the same lung used to develop the model illustrated in Figure 2, but with various lesser degrees of fibrosis.

(crocidolite). Figure 4 also shows the distributions of fiber lengths for specific fiber diameter intervals. This is a particularly useful form of presentation for studies of the influence of fiber diameter on mesothelioma. It is clear that as one goes from Paakkila to the Transvaal, to the NW Cape, to Wittenoom, both the lengths and diameters shift downward substantially.

Figure 5 shows the predicted bivariate size distributions based on combining the data used to develop Figure 2 with the data from Figure 4 for workers at Paakkila and Transvaal, with relatively light occupational exposures, as well as the observed bivariate lung distribution data from these regions. It is apparent that the model fits the observations satisfactorily.

Figures 6 and 7 show the influence of fiber size and degree of lung fibrosis on fiber retention and clearance for the fiber size extremes represented by Paakkila and Wittenoom respectively. Paakkila, with virtually no fibers with diameters less than 0.1 μm, produced many cases of lung cancer and asbestosis, but no mesothelioma. Wittenoom, with virtually all of the fibers having diameters less than 0.1μm and lengths less than 5μm, produced a very high yield of mesothelioma and lung fibrosis, as well as an excess in lung cancer (SMR=1.57) (Hobbs, et al., 1980). These figures also show the great differences in the fibers retained in and cleared from the gas exchange region of the lung at Paakkila and Wittenoom. The cleared fibers represent the longest capable of reaching the pleural surfaces where mesotheliomas are found. The modal values for both fiber length and diameter are also shown in Figures 6 and 7. The differences between retained and cleared fibers' modes are much greater for both the minimal and severe fibrosis cases for the longer, thicker fibers at Paakkila than for the shorter, thinner fibers at Wittenoom. The data indicate the need to review the critical dimensions of fibers for mesothelium production. Long fibers may be more carcinogenic than shorter fibers. The fibers at Wittenoom were almost all shorter than five μm, but were present in enormous numbers. In fact, Rogers (1990) reported on reanalyses of thermal precipitator slides from Wittenoom using currently used analytical techniques, and reported about 300 fibers/mL greater than 5 μm in length.

Lung fibrosis is associated with increased fiber retention, and fiber retention is clearly associated with fiber length and diameter. More precise descrip-
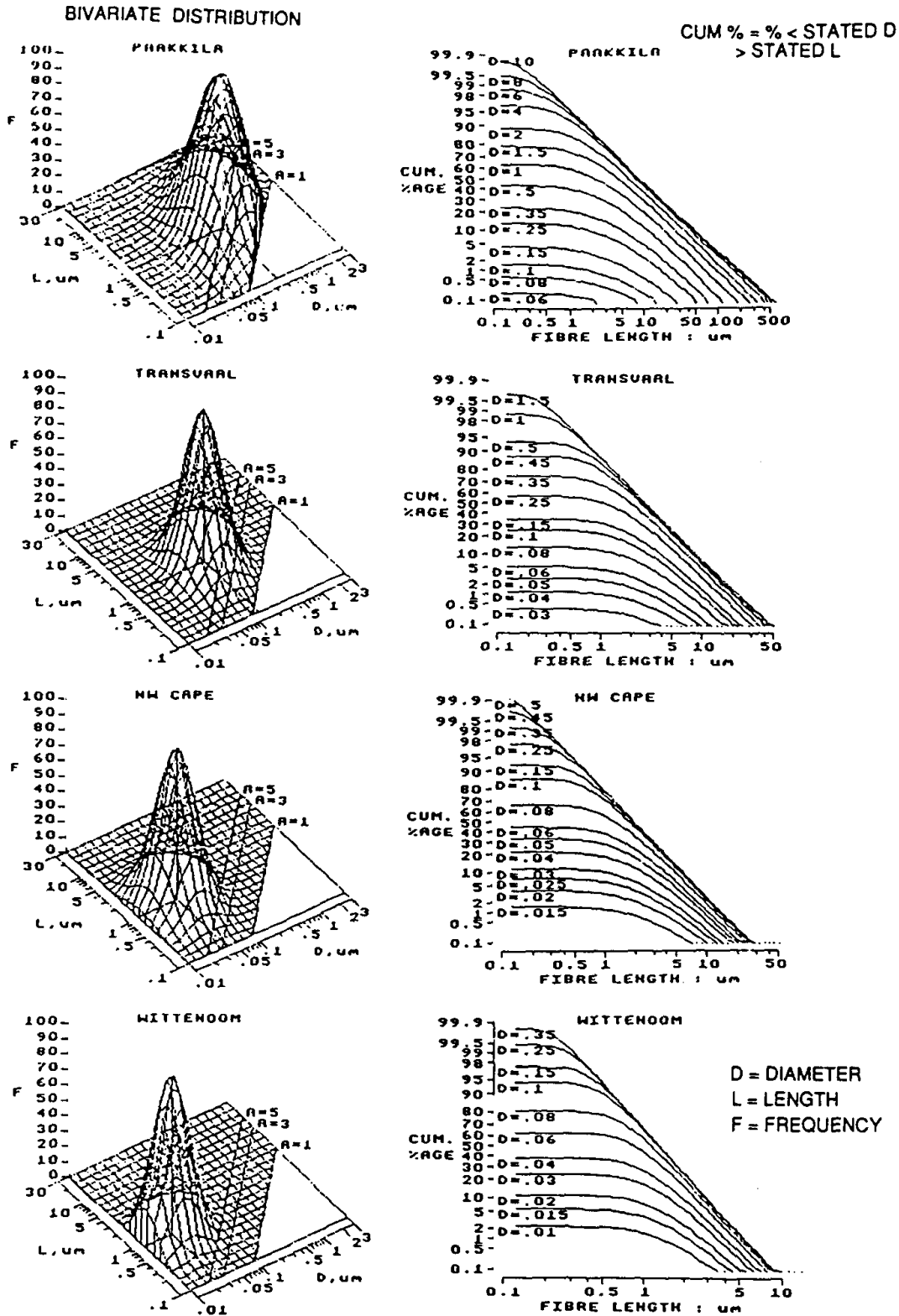
FIGURE 4. Size distributions of airborne fibers collected at asbestos mines   and mills at Paakkila, Finland, The Transvaal and Northwest Cape in South Africa, and at Wittenoom in Australia. The left side shows bivariate frequency distributions by length and diameter. The right side shows the cumulative percentages less than the stated diameter that are longer than the indicated length.
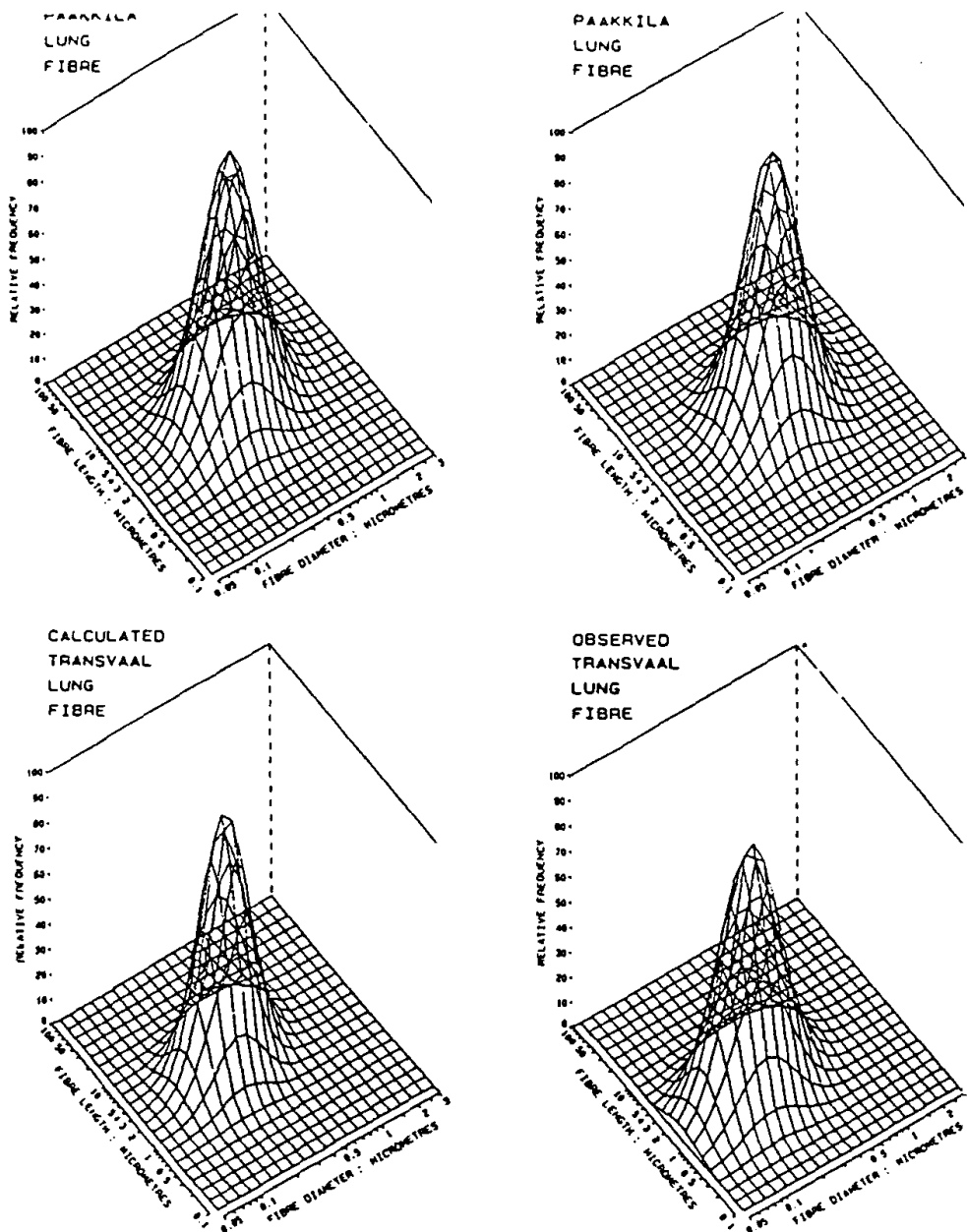
FIGURE 5. The left side shows bivariate fiber length and diameter distributions calculated for retention in Paakkila and Transvaal miners' lungs based upon Timbrell's deposition and retention model as applied to measured airborne fiber distributions. The right side shows the bivariate size distributions measured in miners' lungs at these locations.

tions of the effect of fiber loading in the lung on fibrosis need to be based on the use of the most appropriate index of fiber loading. Figure 8 clearly shows that the only fiber concentration index that normalizes the diverse data from the various asbestos mining regions is the total fiber surface of the aerosol. When fiber number concentration or total fiber mass concentration is used, each mining region exhibits a quite different exposure-response relationship.

Timbrell (1989) next asked the question of whether the clear association between particle surface concentration and lung fibrosis was limited to fibers. Lung samples were collected from 39 dust exposed workers from a variety of locations including gold mines, shipyards, etc. and bivariate size distributions were analyzed from tissue adjacent to that used to determine the extent of lung
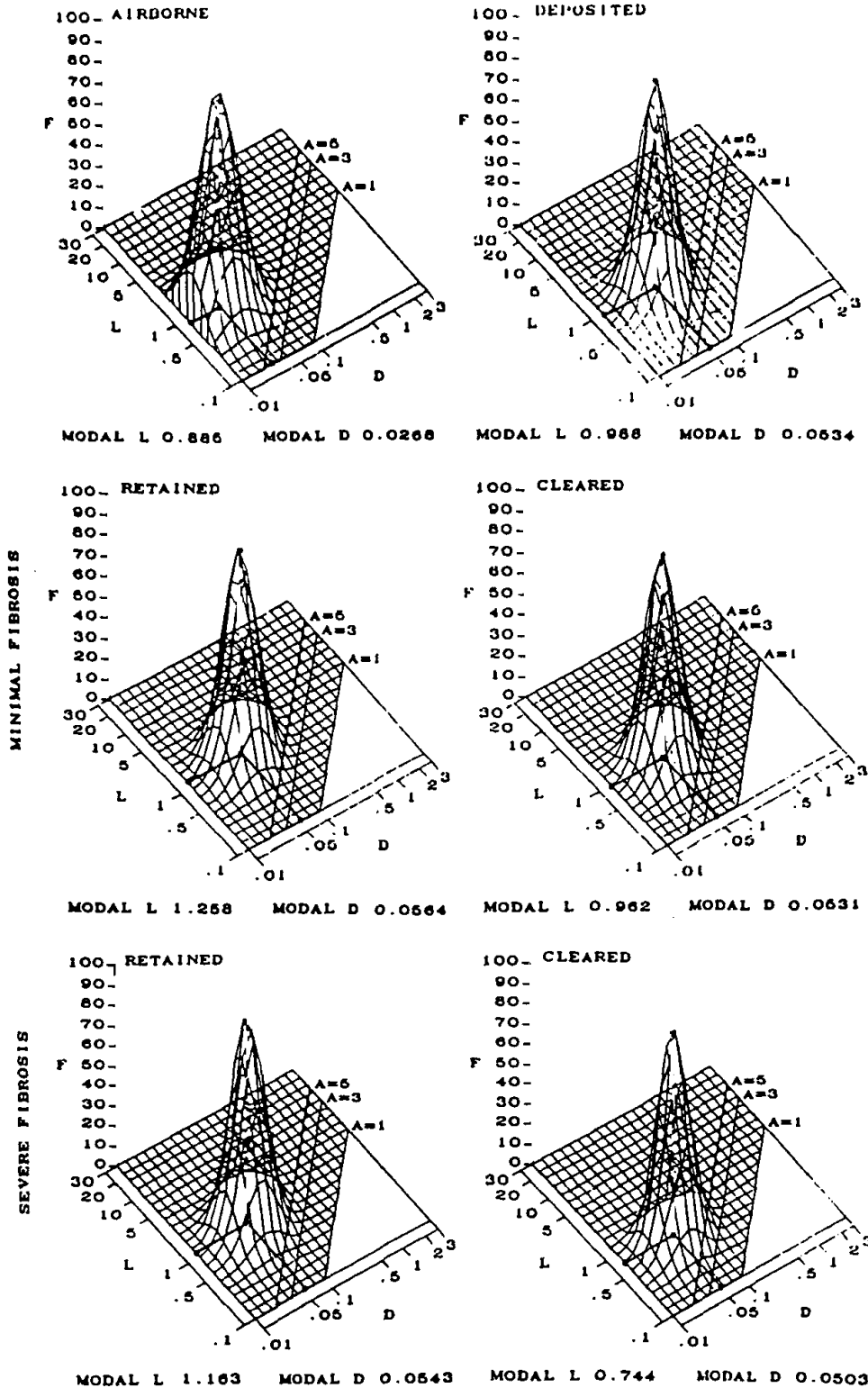
FIGURE 6. Bivariate distributions of asbestos fibers at Wittenoom that were: 1) airborne; 2) deposited in the deep lung; 3) retained in a part of the lung with minimal fibrosis; 4) cleared from lung tissue with minimal fibrosis; 5) retained in a part of the lung with severe fibrosis; and 6) cleared from lung tissue with severe fibrosis.
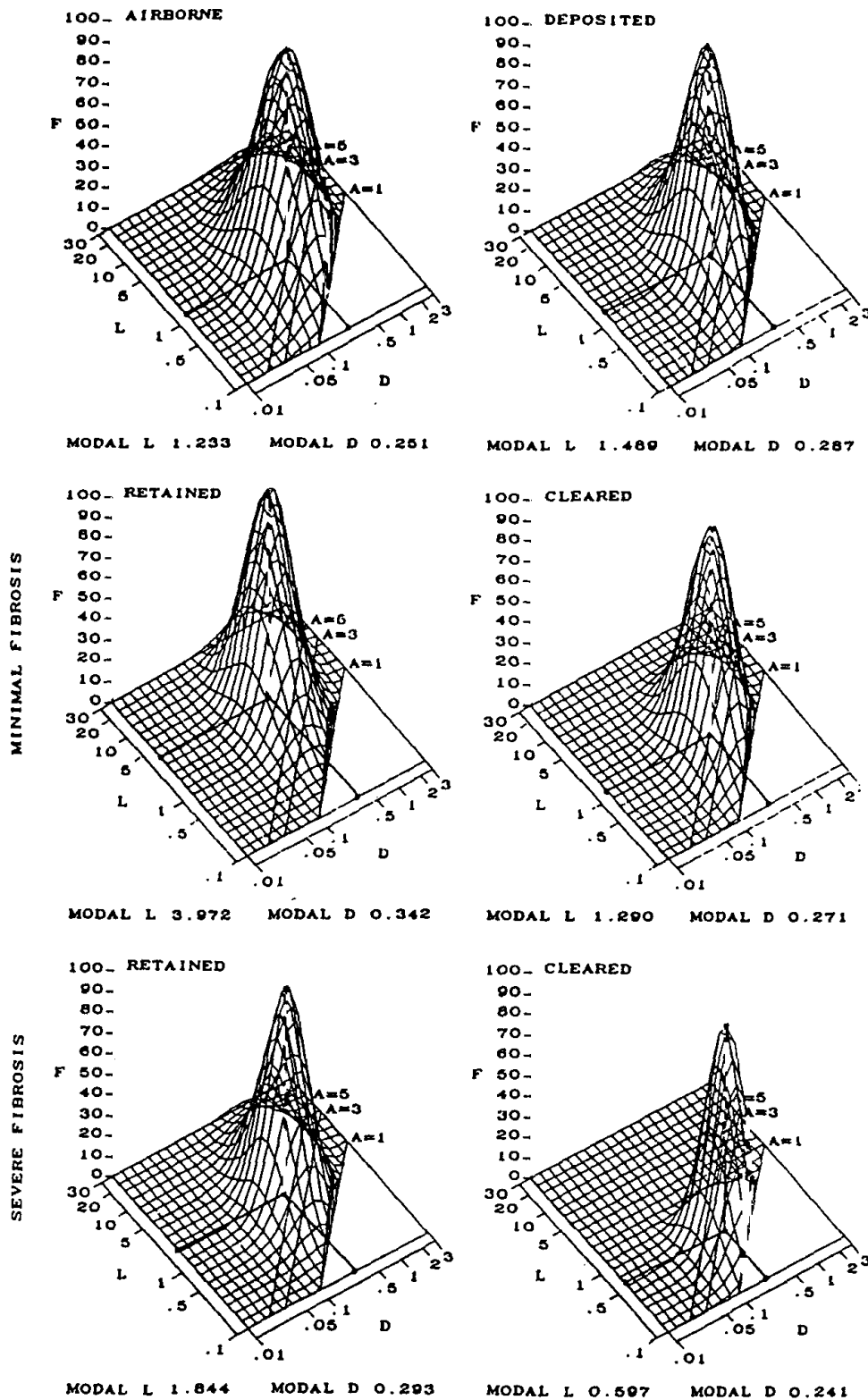
FIGURE 7. Bivariate distributions of asbestos fibers at Paakkila that were: 1) airborne; 2) deposited in the deep lung; 3) retained in a part of the lung with minimal fibrosis; 4) cleared from lung tissue with minimal fibrosis; 5) retained in a part of the lung with severe fibrosis; and 6) cleared from lung tissue with severe fibrosis.
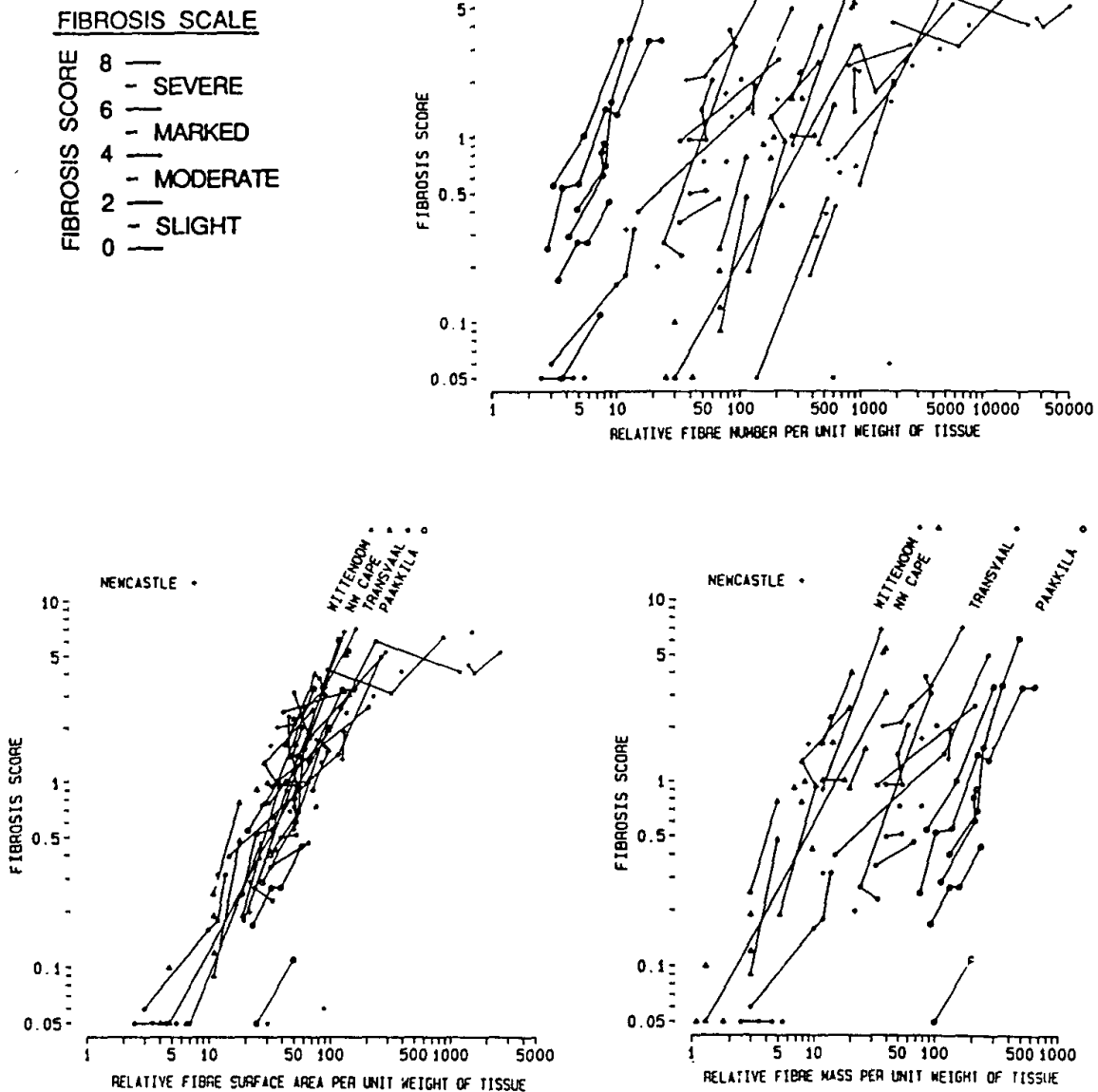
FIGURE 8. Relationships between fibrosis scale and relative concentrations of fibers per unit weight of dry lung tissue. The lines connect data points from the same subject. The relative fiber surface area normalizes the data better than either the relative fiber number concentration or the fiber mass concentration. Reprinted by permission from Lippmann (1988).

fibrosis. As shown in Figure 9, the correlation between dust surface area and the degree of fibrosis was much better (r=0.80) than for particle number concentration (r=0.50). He then analyzed whether different components of the dust mixtures in these lungs contributed disproportionately to the fibrotic response. The results are summarized in Table 2 in terms of the asbestos alone, the asbestos plus quartz, and the other constituents generally considered much less fibrogenic than asbestos or quartz. The fibrogenicity coefficient of 2.38 units for the category "other then asbestos and quartz" is not substantially different from those for the more "fibrogenic" dusts, suggesting that its components, including talc, mica, various other silicates and iron are as fibrogenic as asbestos and quartz when expressed in terms of particle surface area. The table also shows
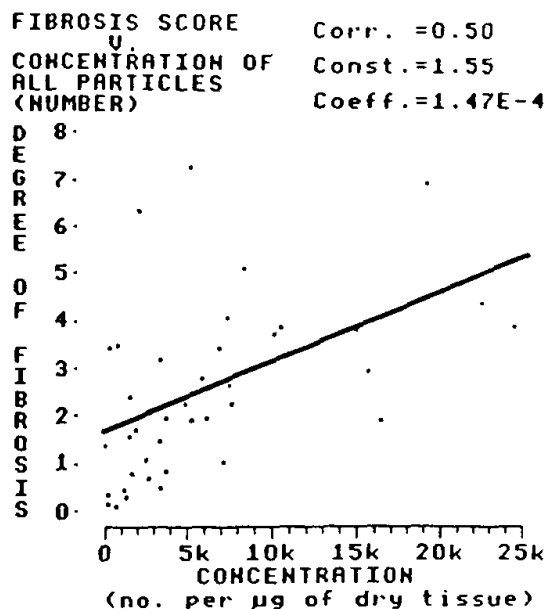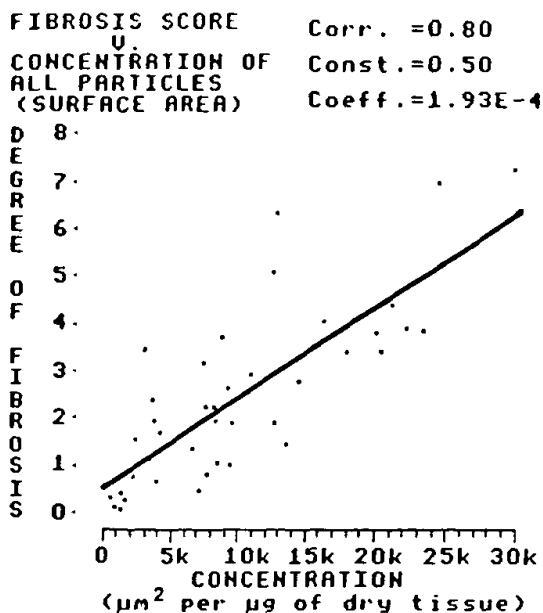
FIGURE 9. The left panel shows the relationship between fibrosis scale and concentrations of total particulate surface per unit weight of dry lung tissue for workers in a variety of dusty trades. The right panel shows the results for the same tissue samples when expressed as particle number concentration.

that concentrations expressed as particle volume had correlation coefficients somewhat lower than those for particle surface, but much higher than those for particle number concentration. Thus, respirable mass concentrations, as conventionally measured for dust exposed workers, are better surrogate measures of fibrogenicity hazard than particle counts for the dusty occupations represented in this limited study.

TABLE 2

Fibrogenicity (and Correlation) Coefficients for Fibrosis
Score vs. Particle Concentration for 39 Lung Samples of
Workers with Various Mineral Dust Exposures*

| Types of particles included in analysis | Concentration index[+] | | |
	Surface	Volume	Number
All measured particles	1.93^a (0.80)	1.26^b (0.69)	1.47^c (0.50)
Asbestos only	2.70^a (0.72)	2.07^b (0.64)	2.22^c (0.49)
Asbestos & quartz	2.03^a (0.71)	1.57^b (0.65)	1.47^c (0.49)
Other than asbestos & quartz[†]	2.38^a (0.43)	1.43^b (0.44)	2.65^c (0.33)

* Specimens obtained from long-term workers at asbestos mines and factories,
    gold mines, a platinum mine, British shipyards and other work.
[+] Derived from high resolution transmission electron microscopy by
    Finnish Acad. Sci.
[†] Includes talc, mica, kaolinite, iron, etc.
[a] Degree of fibrosis/μm^2/μg dry tissue X 10^{-4}.
[b] Degree of fibrosis/μm^3/μg dry tissue X 10^{-4}.
[c] Degree of fibrosis/no./μg dry tissue X 10^{-4}.
Note: Comparison across rows is invalid for fibrogenicity coefficients,
       since the fibrogenicity units differ.

Overloading of particles in the lung can be operationally defined as a marked reduction in lung clearance, and the evidence is clear from both the animal and human studies reviewed at this Symposium that such reductions in clearance are threshold phenomena. If we had definable thresholds it would be relatively easy to set occupational and environmental exposure limits for airborne particles. We would need only define the particle properties to be measured and the exposure-response relationships for the health endpoints of interest. It would not be necessary to wait for a full mechanistic understanding at the cellular and molecular level. In any case, based upon the presentations and discussions at this Symposium, such an understanding is not likely to be available in the near future.

Furthermore, for the specific case of "insoluble" particles that deposit in lung airways and airspaces, it is not at all clear that the fascinating and complex biochemical events occurring at the cellular and molecular level are as important as determinants of disease potential as the biophysical processes that determine deposition patterns, translocation pathways, and retention times at critical target sites. Perhaps this Symposium needed one more half-day session devoted to issues such as: 1) the implications of the highly concentrated surface deposition at airway bifurcations in both large and small airways, and the virtual absence of deposition in the peripheral alveoli; 2) the influence of particle dimensions on clearance rates and pathways, e.g., the relatively rapid migration of ultrafine particles and fibers with diameters <0.1 μm into the interstitium, and the lack of migration of fibers longer than $-$ 10 μm from their initial deposition sites; 3) the critical role of the total surface area of retained particles in the formation of fibrotic lesions; and 4) the relative unimportance of chemical composition in the fibrotic response to durable mineral particles retained in the lungs.

While we know how, in principle, to approach the setting of exposure standards for insoluble mineral particles, it does not follow that we have all of the data we need to set good standards. We will need to more firmly establish which particle properties are to be measured, and how they are to be analyzed. We also need to establish and/or verify that we can relate the defined exposure parameters to the health outcomes measured in the human studies and/or extrapolated from the animal studies. These tasks are formidable, but not impossible. The critical first step is to get the interested parties in the research community and the regulatory authorities to commit the necessary resources to this undertaking.

RESEARCH NEEDS

The lack of biophysical perspectives has inhibited the effective integration of the results of the fairly extensive data bases from the animal and human studies. We strongly suspect that the apparent differences in the toxicity rankings of the various asbestos minerals between the animal and human studies would disappear if the data were adjusted for the different lengths and diameter distributions of the inhaled fibers. As demonstrated by the recent work of Davis et al (1986, 1988) with long and short amosite and chrysotile, the UICC reference samples were much less toxic than the raw materials that many of the mine and mill workers exposed to. The grinding and blending processes used to make the UICC reference materials uniform made them much less suitable for realistic toxicity testing.

To the extent that the bivariate fiber size distributions of the test materials used in the animal toxicity studies can be determined retrospectively, it may be possible to reanalyze the exposure-response relationships from these studies and gain valuable new perspectives. It would also be extremely desirable to do bivariate fiber size distribution analyses on the dust retained in the lungs of the animals that were chronically exposed to durable fibers, and to compare the retention to the degree of fibrosis. This would permit a valid interspecies comparison with Timbrell's data on the lungs of chronically exposed asbestos workers.

REFERENCES

Ashcroft, T., Simpson, J. M., and Timbrell, V. (1988). Simple Method of Estimating Severity of Pulmonary Fibrosis on a Numerical Scale. J. Clin. Pathol. 41, 467-470.

Davis, J. M. G., Chapman, J., Collings, P., Douglas, A. N., Fernie, J., Lamb, D., and Ruckley, V.A. (1983). Variations in the Histological Patterns of the Lesions of Coal Workers' Pneumoconiosis in Britain and Their Relationship to Lung Dust Content. Am. Rev. Respir. Dis. 128, 118.

Davis, J. M. G., Addison, J., Bolton, R. E., Donaldson, J., Jones, A. D. and Smith, T. (1986). The pathogenicity of long versus short fibres of amosite asbestos administered to rats by inhalation and intraperitoneal injection. Brit. J. Exp. Pathol. 67, 415-430.

Davis, J. M. G. and Jones, A. D. (1988). Comparisons of the pathogenicity of long and short fibers of chrysotile asbestos in rats. Brit. J. Exp. Pathol. 69, 717-737.

Hobbs, M. S. T., Woodward, S. D., Murphy, B., Musk, A. W., and Elder, J. E. (1980). The Incidence of Pneumoconiosis, Mesothelioma and Other Respiratory Cancer in Men Engaged in Mining and Milling Crocidolite in Western Australia. In: Biological Effects of Mineral Fibres, Wagner, J. C., Ed., IARC Sci. Publ. #30, IARC, Lyon, pp. 615-625.

Lippmann, M. (1988). Asbestos Exposure Indices. Environ. Res. 46, 86-100.

Ostro, B. D., and Rothschild, S. (1989). Air Pollution and Acute Respiratory Morbidity: An Observational Study of Multiple Pollutants. Environ. Res. 50, 238-47.

Ozkaynak, H., and Thurston, G. D. (1987). Associations Between 1980 U.S. Mortality Rates and Alternative Measures of Airborne Particle Concentration. Risk Anal. 7, 449-461.

Rogers, A. (1990). Cancer mortality and exposure to crocidolite. Brit. J. Indust. Med. 47, 286.

Rossiter, C. E., Rivers, D., Bergman, I., Casswell, C., and Nagelschmidt, G. (1967). Dust Content, Radiology and Pathology, In Simple Pneumoconiosis of Coal Workers. In: Inhaled Particles and Vapours II, Davies, C. N., Ed., Pergramon Press, Oxford, UK, p. 419.

Ruckley, V. A., Gauld, S. J., Chapman, J. S., Davis, J. M. G., Douglas, A. N., Fernie, J. M., Jacobsen, M., and Lamb, D. (1984). Emphysema and Dust Exposure in a Group of Coal Workers. Am. Rev. Respir. Dis. 129, 528.

Snipes, M. B. (1989). Long-term Retention and Clearance of Particles Inhaled by Mammalian Species. Crit. Rev. Toxicol. 20, 175-211.

Soutar, C. A., and Hurley, J. F. (1986). Relation Between Dust Exposure and Lung Function in Miners and Ex-miners. Br. J. Ind. Med. 43, 307.

Stober, W., Einbrodt, H. J., and Klosterkotter, W. (1967). Quantitative Studies

of Dust Retention in Animal and Human Lungs After Chronic Inhalation. In: Inhalation Particles and Vapours II, Davies, C. N., Ed., Pergamon Press, Oxford, UK, p. 409.

Schwartz, J. (1989). Lung Function and Chronic Exposure to Air Pollution: A Cross-Sectional Analysis of NHANES II. Environ. Res. 50, 309-321.

Timbrell, V. (1982). Deposition and Retention of Fibres in the Human Lung. Ann. Occup. Hyg. 26, 347-369.

Timbrell, V. (1983). Pulmonary Deposition and Retention of South African Amphibole Fibres: Identification of Asbestosis-related Measure of Fibre Concentration. VIth International Pneumoconiosis Conferenece, Bochum. Fed. Rep. Germany.

Timbrell, V., Ashcroft, T., Goldstein, B., Heyworth, F., Meurman, L. O., Rendall, R. E. G., Reynolds, J. A., Shilkin, K. B., and Whitaker, D. (1988). Relationships between Retained Amphibole Fibres and Fibrosis in Human Lung Tissue Specimens. Ann. Occup. Hyg. 32 (Suppl. 1), 323-340.

Timbrell, V., Taikina-Aho, O., Paakko, P., Ashcroft, T., Meurman, L. O., and Shilkin, K. B. (1990). Similarities in the Fibrogenicity of Asbestos Fibers and Other Mineral Particles Retained in Human Lungs. Proceedings of VII Int'l Pneumoconiosis Conference, Pittsburgh, 1988 (in press).

Report of Results: MVA6543

Analysis of Water Putty
Purchased in May, 2006
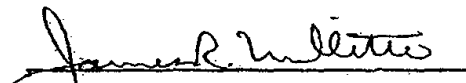
Prepared for:

Early, Ludwick, Sweeney & Strauss
One Century Tower, 11th Floor
265 Church Street
New Haven, CT 06508

Misuse of counting criteria

Example

Respectfully Submitted by:

James R. Millette, Ph.D.
Executive Director

William L. Turner, Jr.
Senior Research Microscopist

MVA Scientific Consultants
3300 Breckinridge Boulevard
Suite 400
Duluth, GA 30096

26 July 2006

MVA SCIENTIFIC CONSULTANTS

Report of Results -- MVA Project No. 6543

Analysis of Water Putty Purchased in May, 2006

INTRODUCTION

This report includes the results of analyses of fourteen containers of Donald Durham Co. Water Putty delivered to MVA Scientific Consultants on 29 May 2006. The information with the samples indicated that the cans had been purchased at a local ACE Hardware store on May 27, 2006. The cans were labeled "Durham's Rock Hard Water Putty" (Figure 1). At the laboratory, the samples were assigned the MVA Numbers R0972 through R0985. Samples R0972 through R0978 are four pound cans; samples R0979 through R0985 are one pound cans. MVA Scientific Consultants was requested to analyze the samples for asbestos content. The analyses were conducted during the period 30 June to 18 July 2006.

METHODS AND EQUIPMENT

The samples were first examined by stereomicroscopy utilizing a Zeiss Stemi 2000 stereomicroscope. They were then analyzed for asbestos by the standard polarized light microscopy (PLM) method using an Olympus BH-2 polarized light microscope. The samples were further analyzed by analytical electron microscopy (AEM) using a Philips 420 transmission electron microscope (TEM) and a Philips 120 TEM equipped with energy dispersive spectroscopy (EDS) x-ray analysis systems.

RESULTS

Sample R0972 is an off-white powder of a fine size that contains approximately 65% hemihydrate gypsum, 20% starch, 8% talc and 7% amphibole fibers. The amphiboles (tremolite by PLM and TEM) occur in a population of particles with an average aspect ratio less than 10:1. While the population of tremolite fibers would generally be considered a cleavage fragment population, many meet the OSHA definition of an asbestos fiber (longer than 5 μm with a 3:1 aspect ratio). PLM and TEM analyses showed the amphibole fibers to be consistent with tremolite (Figures 2 through 4). Some fibers possibly consistent with anthophyllite were also found by TEM.

Sample R0973 is an off-white powder of a fine size that contains approximately 66% hemihydrate gypsum, 25% starch, 5% talc and 5% amphibole fibers. The amphiboles (tremolite by PLM and TEM) occur in a population of particles with an average aspect ratio less than 10:1. While the population of tremolite fibers would generally be considered a cleavage fragment population, many meet the OSHA definition of an asbestos fiber (longer than 5 μm with a 3:1 aspect ratio). PLM and TEM analyses

[handwritten annotation in right margin:] Not true, this is not the OSHA definition. It's a counting criteria for asbestos

showed the amphibole fibers to be consistent with tremolite (Figures 5 through 7). Some fibers possibly consistent with anthophyllite were also found by TEM.

Sample R0974 is an off-white powder of a fine size that contains approximately 63% hemihydrate gypsum, 25% starch, 5% talc and 6% amphibole fibers. The amphiboles (tremolite by PLM and TEM) occur in a population of particles with an average aspect ratio less than 10:1. While the population of tremolite fibers would generally be considered a cleavage fragment population, many meet the OSHA definition of an asbestos fiber (longer than 5 μm with a 3:1 aspect ratio). PLM and TEM analyses showed the amphibole fibers to be consistent with tremolite (Figures 8 through 10). Some fibers possibly consistent with anthophyllite were also found by TEM.

Sample R0975 is an off-white powder of a fine size that contains approximately 70% hemihydrate gypsum, 20% starch, 5% talc and 5% amphibole fibers. The amphiboles (tremolite by PLM and TEM) occur in a population of particles with an average aspect ratio less than 10:1. While the population of tremolite fibers would generally be considered a cleavage fragment population, many meet the OSHA definition of an asbestos fiber (longer than 5 μm with a 3:1 aspect ratio). PLM and TEM analyses showed the amphibole fibers to be consistent with tremolite (Figures 11 through 13). Some fibers possibly consistent with anthophyllite were also found by TEM.

Sample R0976 is an off-white powder of a fine size that contains approximately 65% hemihydrate gypsum, 20% starch, 8% talc and 7% amphibole fibers. The amphiboles (tremolite by PLM and TEM) occur in a population of particles with an average aspect ratio less than 10:1. While the population of tremolite fibers would generally be considered a cleavage fragment population, many meet the OSHA definition of an asbestos fiber (longer than 5 μm with a 3:1 aspect ratio). PLM and TEM analyses showed the amphibole fibers to be consistent with tremolite (Figures 14 through 16). Some fibers possibly consistent with anthophyllite were also found by TEM.

Sample R0977 is an off-white powder of a fine size that contains approximately 65% hemihydrate gypsum, 20% starch, 10% talc and 5% amphibole fibers. The amphiboles (tremolite by PLM and TEM) occur in a population of particles with an average aspect ratio less than 10:1. While the population of tremolite fibers would generally be considered a cleavage fragment population, many meet the OSHA definition of an asbestos fiber (longer than 5 μm with a 3:1 aspect ratio). PLM and TEM analyses showed the amphibole fibers to be consistent with tremolite (Figures 17 through19). Some fibers possibly consistent with anthophyllite were also found by TEM.

Sample R0978 is an off-white powder of a fine size that contains approximately 65% hemihydrate gypsum, 20% starch, 8% talc and 7% amphibole fibers. The amphiboles (tremolite by PLM and TEM) occur in a population of particles with an average aspect ratio less than 10:1. While the population of tremolite fibers would generally be considered a cleavage fragment population, many meet the OSHA definition of an asbestos fiber (longer than 5 μm with a 3:1 aspect ratio). PLM and TEM

analyses showed the amphibole fibers to be consistent with tremolite (Figures 20 through 22). Some fibers possibly consistent with anthophyllite were also found by TEM.

Sample R0979 is an off-white powder of a fine size that contains approximately 65% hemihydrate gypsum, 20% starch, 7% talc and 8% amphibole fibers. The amphiboles (tremolite by PLM and TEM) occur in a population of particles with an average aspect ratio less than 10:1. While the population of tremolite fibers would generally be considered a cleavage fragment population, many meet the OSHA definition of an asbestos fiber (longer than 5 μm with a 3:1 aspect ratio). PLM and TEM analyses showed the amphibole fibers to be consistent with tremolite (Figures 23 through 25). Some fibers possibly consistent with anthophyllite were also found by TEM.

Sample R0980 is an off-white powder of a fine size that contains approximately 65% hemihydrate gypsum, 23% starch, 6% talc and 6% amphibole fibers. The amphiboles (tremolite by PLM and TEM) occur in a population of particles with an average aspect ratio less than 10:1. While the population of tremolite fibers would generally be considered a cleavage fragment population, many meet the OSHA definition of an asbestos fiber (longer than 5 μm with a 3:1 aspect ratio). PLM and TEM analyses showed the amphibole fibers to be consistent with tremolite (Figures 26 through 28). Some fibers possibly consistent with anthophyllite were also found by TEM.

Sample R0981 is an off-white powder of a fine size that contains approximately 65% hemihydrate gypsum, 20% starch, 8% talc and 7% amphibole fibers. The amphiboles (tremolite by PLM and TEM) occur in a population of particles with an average aspect ratio less than 10:1. While the population of tremolite fibers would generally be considered a cleavage fragment population, many meet the OSHA definition of an asbestos fiber (longer than 5 μm with a 3:1 aspect ratio). PLM and TEM analyses showed the amphibole fibers to be consistent with tremolite (Figures 29 through 31). Some fibers possibly consistent with anthophyllite were also found by TEM.

Sample R0982 is an off-white powder of a fine size that contains approximately 62% hemihydrate gypsum, 25% starch, 8% talc and 5% amphibole fibers. The amphiboles (tremolite by PLM and TEM) occur in a population of particles with an average aspect ratio less than 10:1. While the population of tremolite fibers would generally be considered a cleavage fragment population, many meet the OSHA definition of an asbestos fiber (longer than 5 μm with a 3:1 aspect ratio). PLM and TEM analyses showed the amphibole fibers to be consistent with tremolite (Figures 32 through 34). Some fibers possibly consistent with anthophyllite were also found by TEM.

Sample R0983 is an off-white powder of a fine size that contains approximately 65% hemihydrate gypsum, 20% starch, 9% talc and 6% amphibole fibers. The amphiboles (tremolite by PLM and TEM) occur in a population of particles with an average aspect ratio less than 10:1. While the population of tremolite fibers would generally be considered a cleavage fragment population, many meet the OSHA definition of an asbestos fiber (longer than 5 μm with a 3:1 aspect ratio). PLM and TEM

analyses showed the amphibole fibers to be consistent with tremolite (Figures 35 through 37). Some fibers possibly consistent with anthophyllite were also found by TEM.

Sample R0984 is an off-white powder of a fine size that contains approximately 70% hemihydrate gypsum, 20% starch, 5% talc and 5% amphibole fibers. The amphiboles (tremolite by PLM and TEM) occur in a population of particles with an average aspect ratio less than 10:1. While the population of tremolite fibers would generally be considered a cleavage fragment population, many meet the OSHA definition of an asbestos fiber (longer than 5 μm with a 3:1 aspect ratio). PLM and TEM analyses showed the amphibole fibers to be consistent with tremolite (Figures 38 through 40). Some fibers possibly consistent with anthophyllite were also found by TEM.

Sample R0985 is an off-white powder of a fine size that contains approximately 60% hemihydrate gypsum, 20% starch, 9% talc and 6% amphibole fibers. The amphiboles (tremolite by PLM and TEM) occur in a population of particles with an average aspect ratio less than 10:1. While the population of tremolite fibers would generally be considered a cleavage fragment population, many meet the OSHA definition of an asbestos fiber (longer than 5 μm with a 3:1 aspect ratio). PLM and TEM analyses showed the amphibole fibers to be consistent with tremolite (Figures 42 through 45). Some fibers possibly consistent with anthophyllite were also found by TEM.
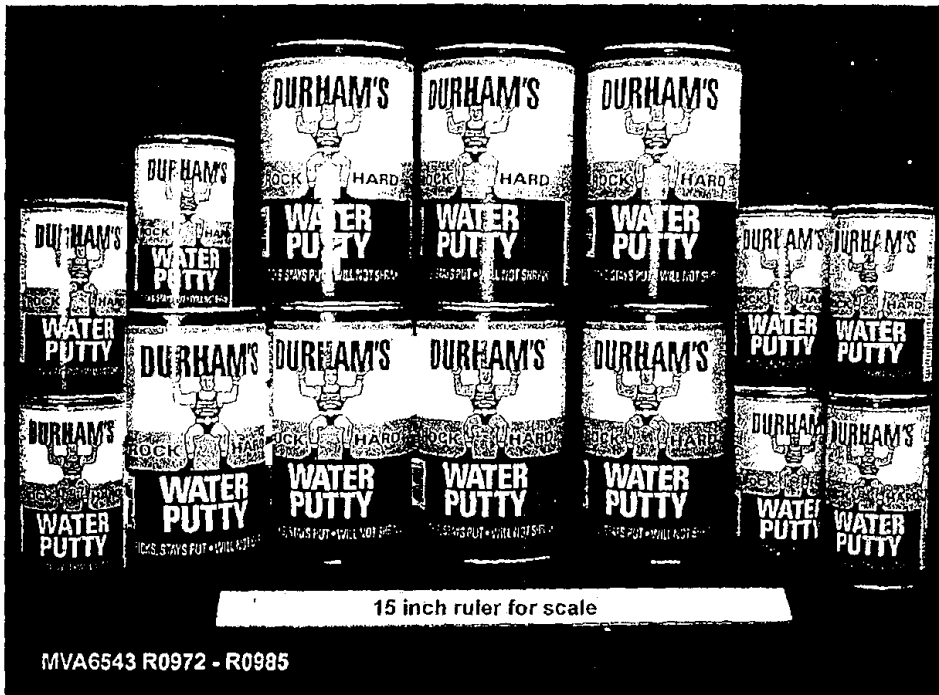
Figure 1. Front of samples of Durham's Water Putty as received.
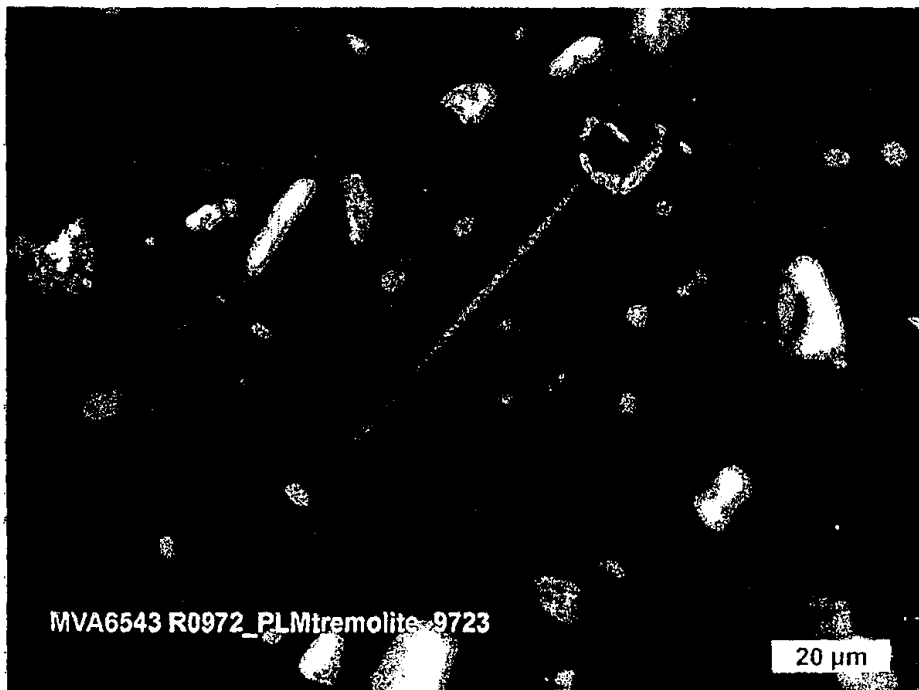
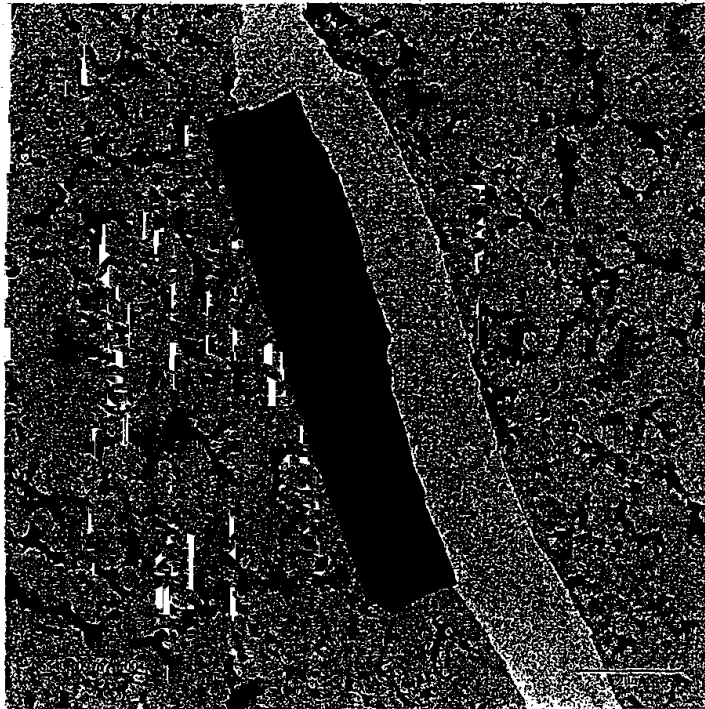**Figure 2.** Polarized light image of a tremolite fiber.
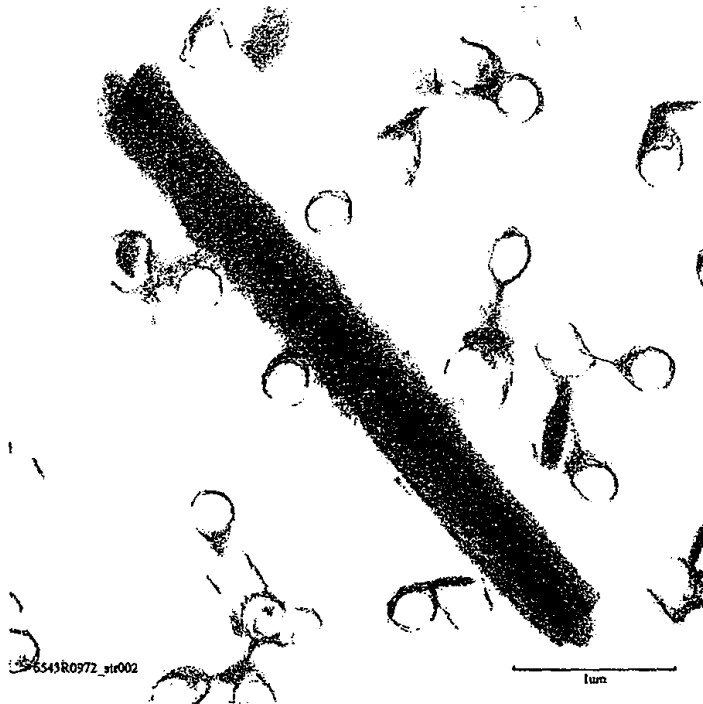
Figure 3. Transmission electron microscope image of tremolite from Sample R0972.
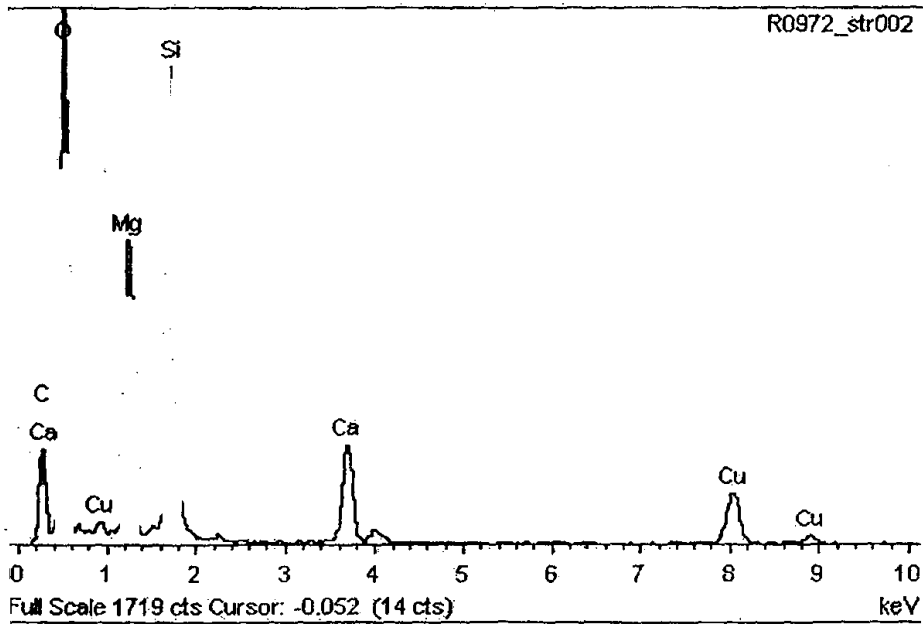
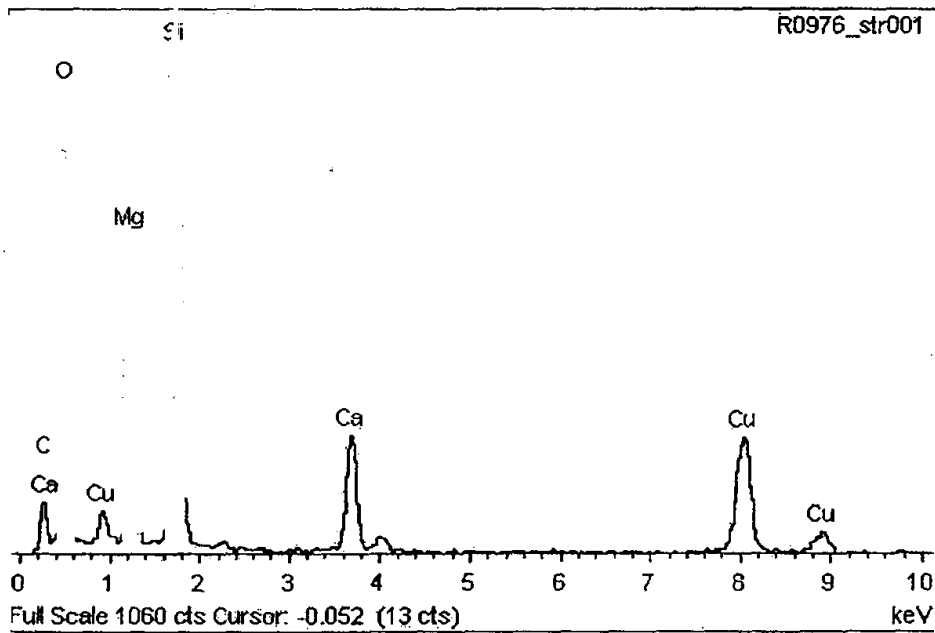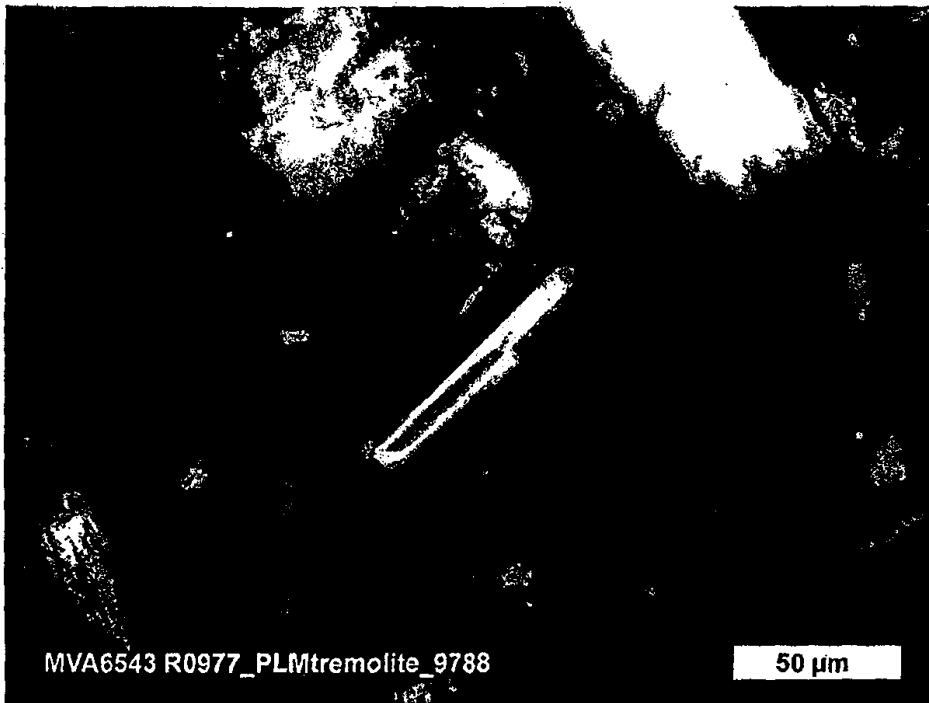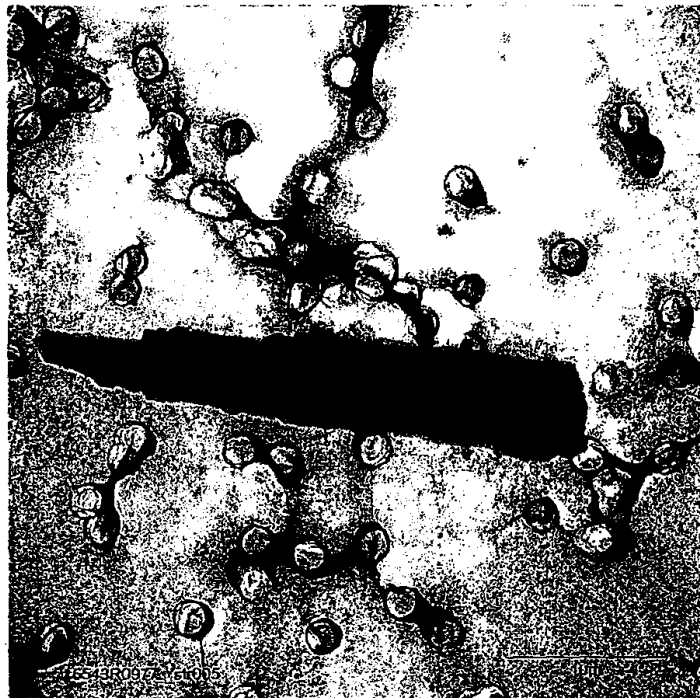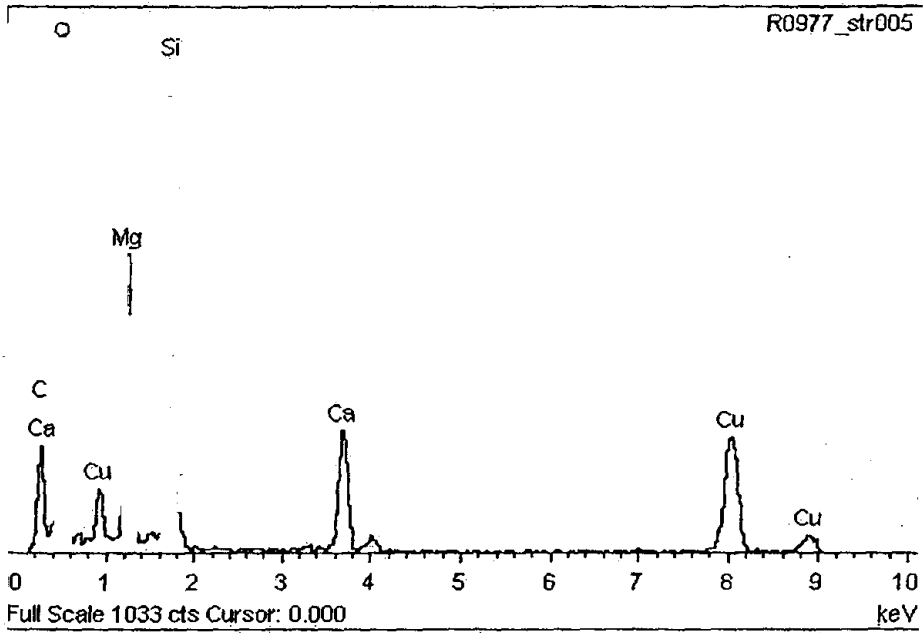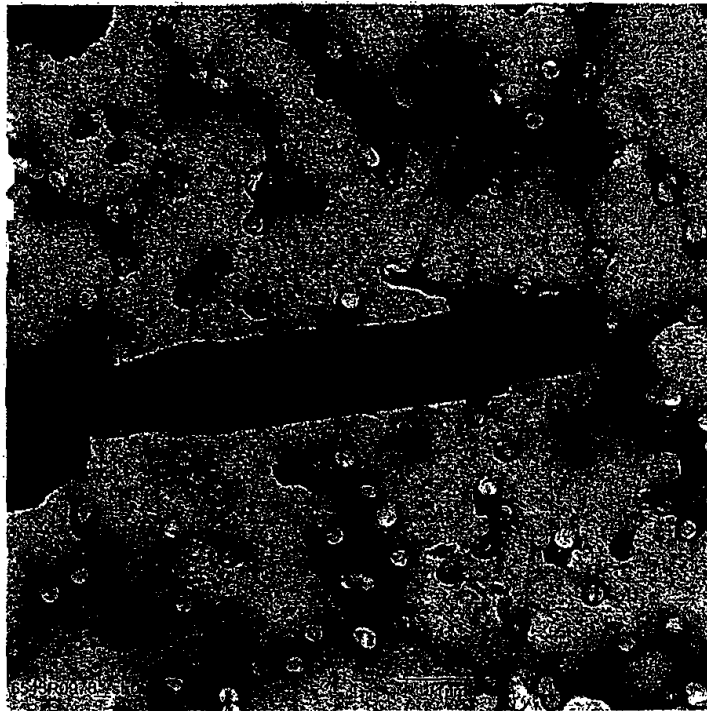**Figure 4.** X-ray spectrum (TEM) of tremolite from Sample R0972.
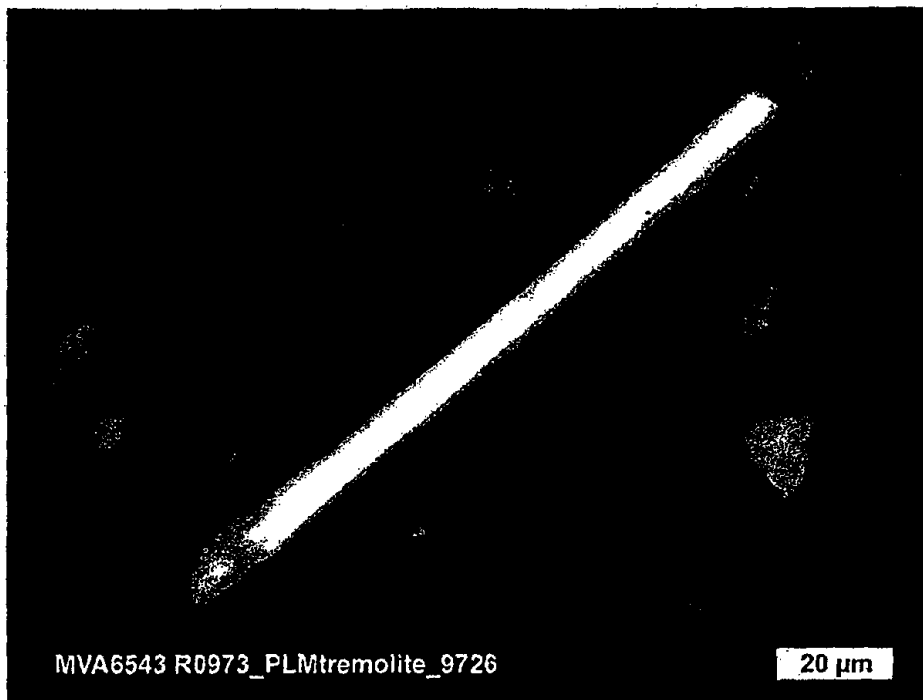
Figure 5. Polarized light image of a tremolite fiber.
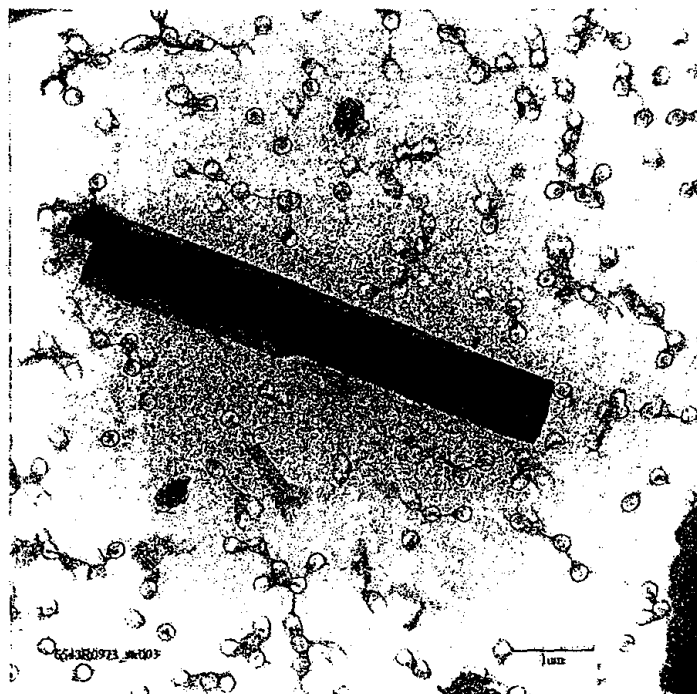
Figure 6. Transmission electron microscope image of tremolite from Sample R0973.
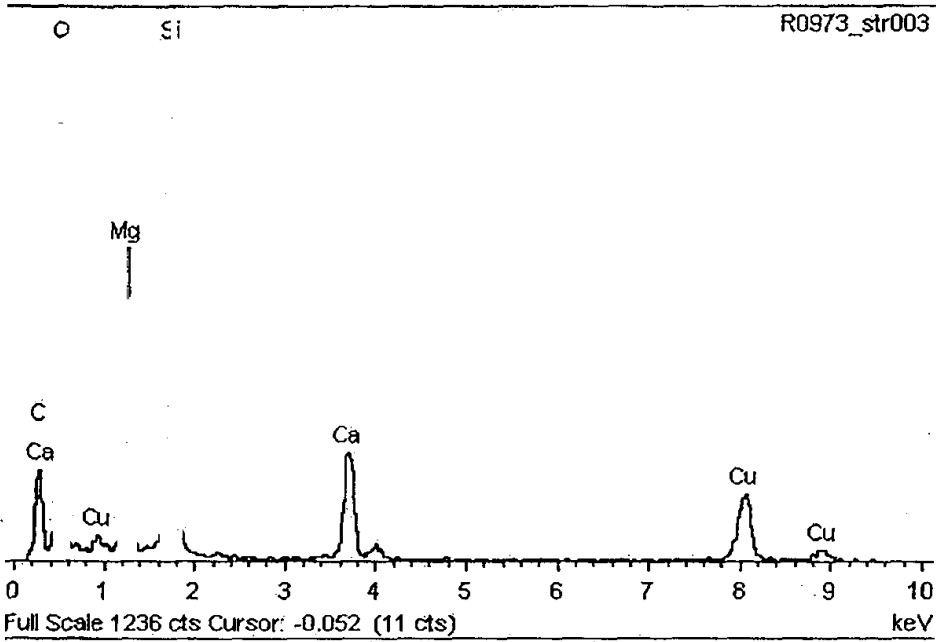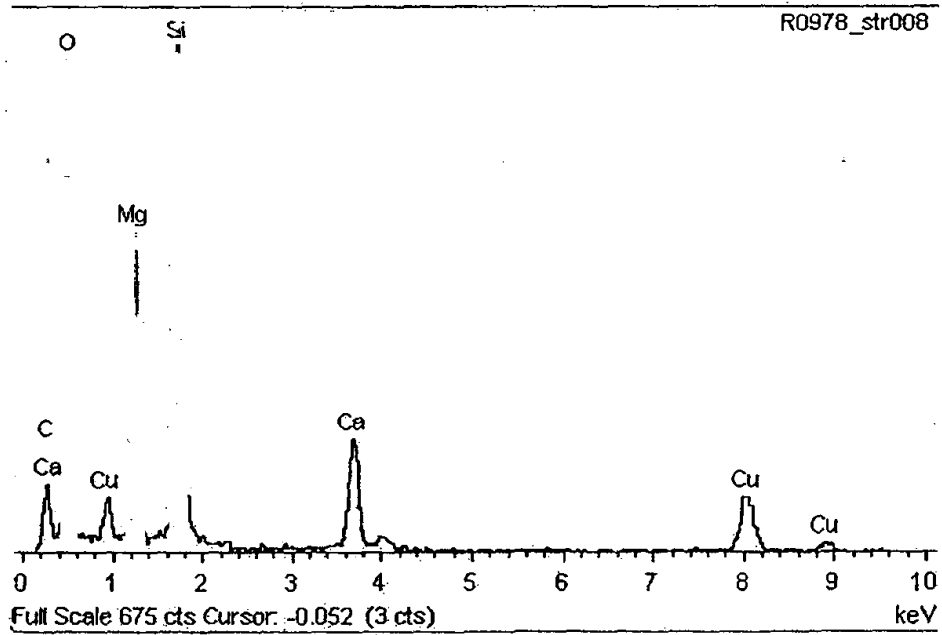
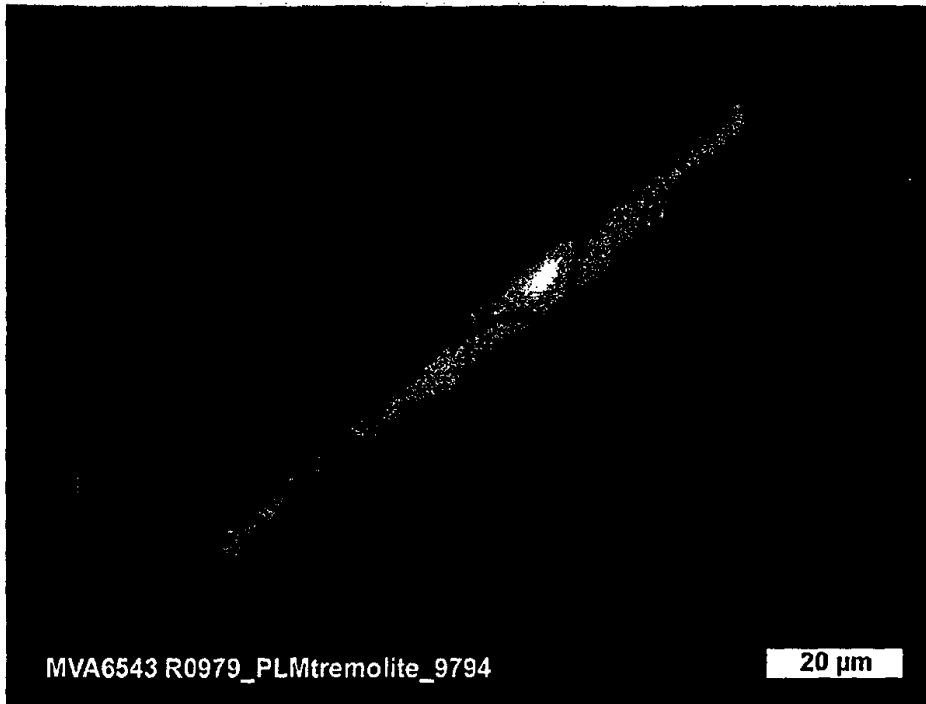**Figure 7.** X-ray spectrum (TEM) of tremolite from Sample R0973.

Figure 8. Polarized light image of a tremolite fiber.
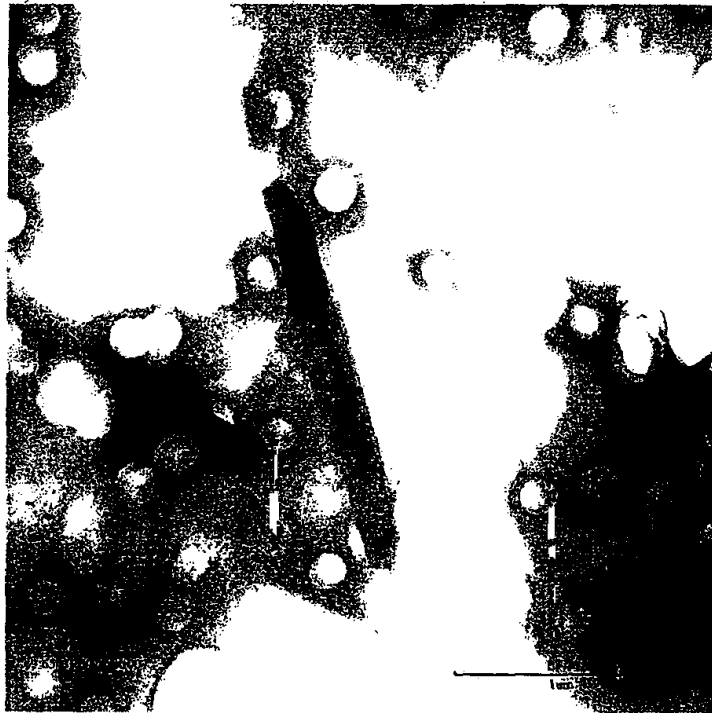
Figure 9. Transmission electron microscope image of tremolite from Sample R0974.
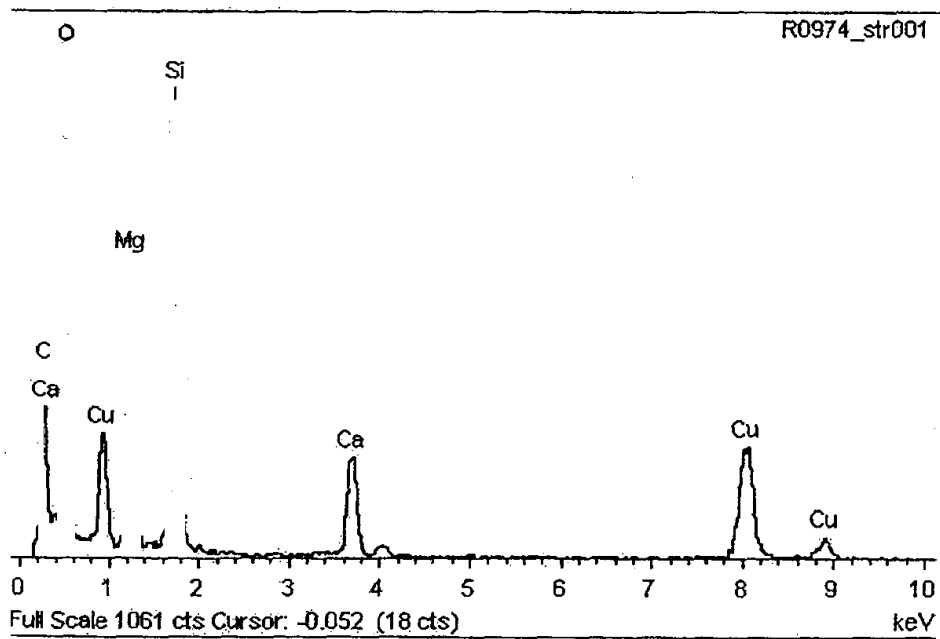
Figure 10. X-ray spectrum (TEM) of tremolite from Sample R0974.

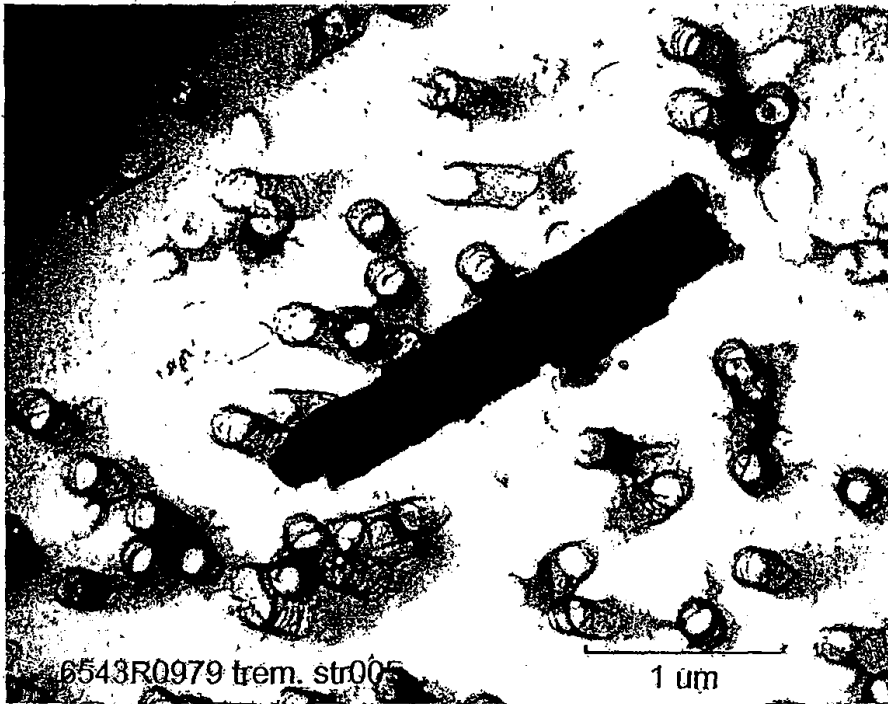**Figure 11.** Polarized light image of a tremolite fiber.
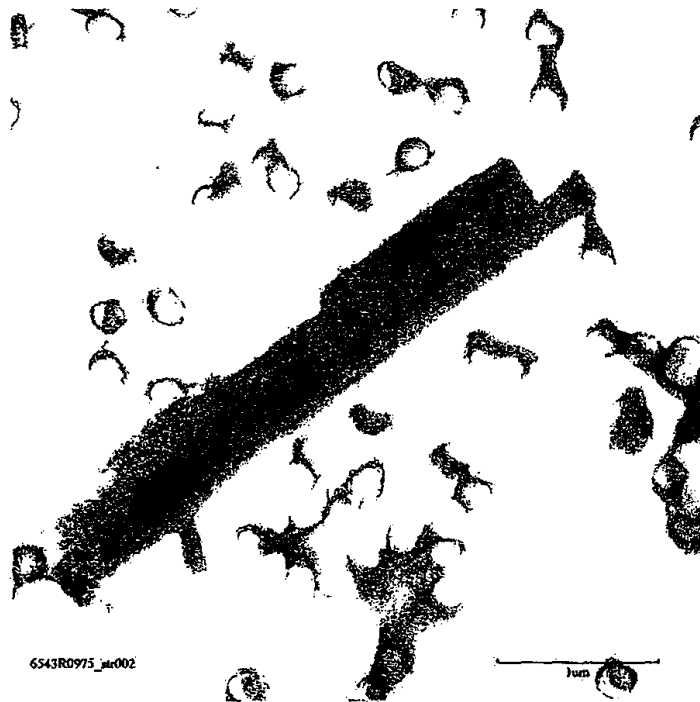
Figure 12. Transmission electron microscope image of tremolite from Sample R0975.
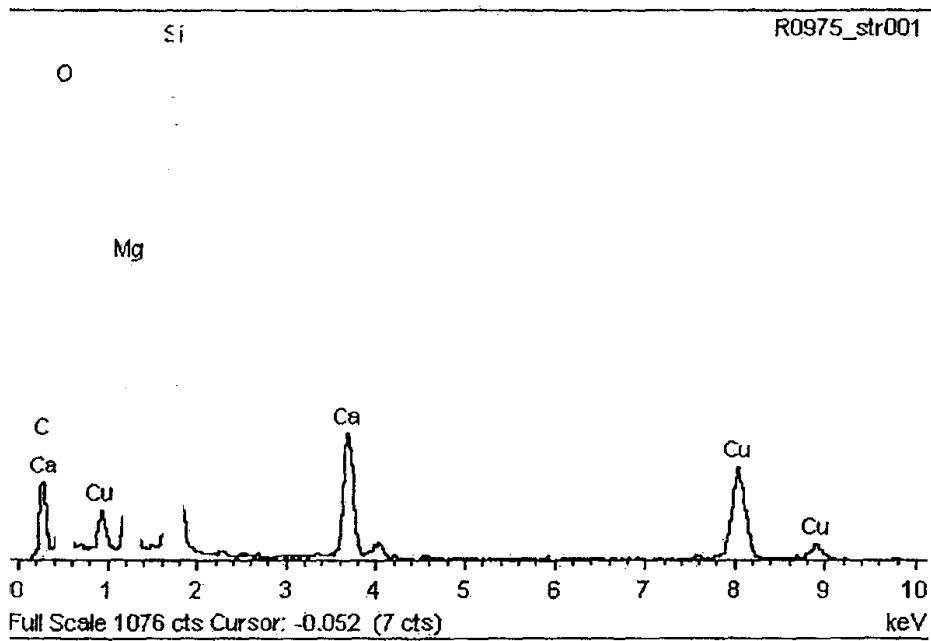
Figure 13. X-ray spectrum (TEM) of tremolite from Sample R0975.

Figure 14. Polarized light image of a tremolite fiber.

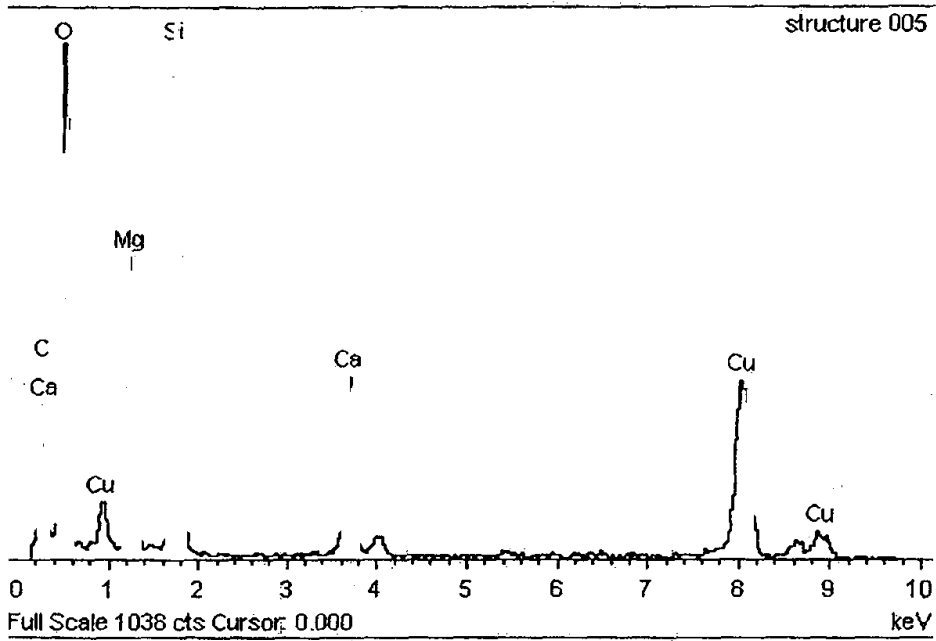**Figure 15.** Transmission electron microscope image of tremolite from Sample R0976.

Figure 16. X-ray spectrum (TEM) of tremolite from Sample R0976.

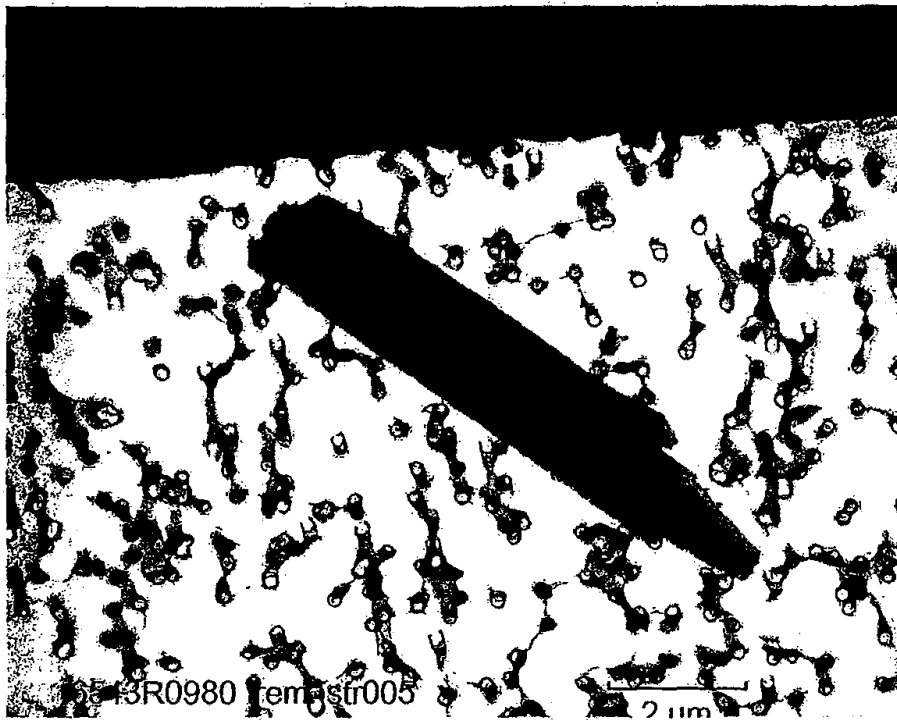**Figure 17.** Polarized light image of a tremolite fiber.

Figure 18. Transmission electron microscope image of tremolite from Sample R0977.

Figure 19. X-ray spectrum (TEM) of tremolite from Sample R0977.

MVA6543 R0978_PLMtremolite_9789   50 μm

Figure 20. Polarized light image of a tremolite fiber.

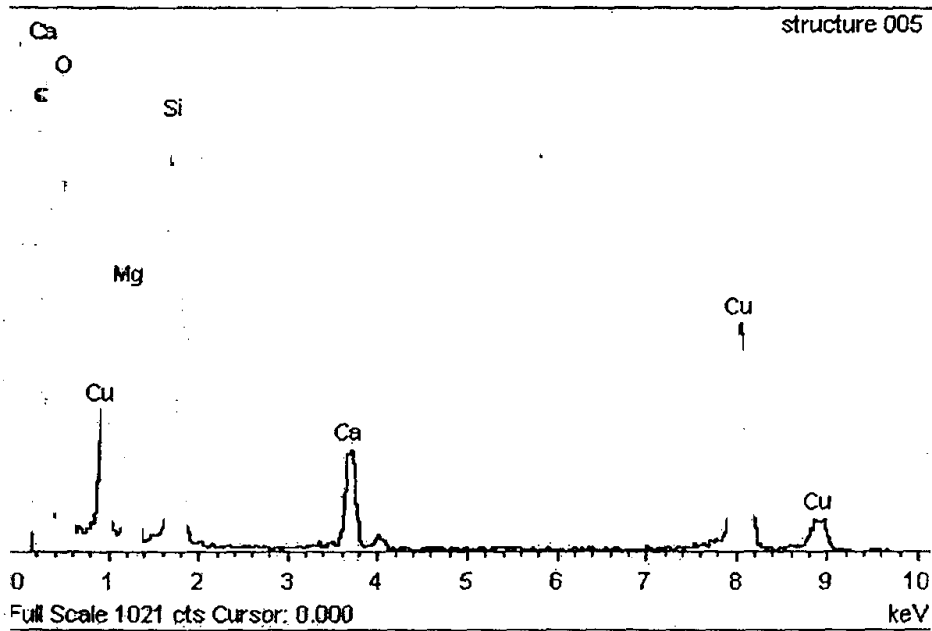**Figure 21.** Transmission electron microscope image of tremolite from Sample R0978.

Figure 22. X-ray spectrum (TEM) of tremolite from Sample R0978.

MVA6543 R0979_PLMtremolite_9794   20 µm

Figure 23. Polarized light image of a tremolite fiber.

6543R0979 trem. str00?   1 um

Figure 24. Transmission electron microscope image of tremolite from Sample R0979.

Figure 25. X-ray spectrum (TEM) of tremolite from Sample R0979.

Figure 26. Polarized light image of a tremolite fiber.

Figure 27. Transmission electron microscope image of tremolite from Sample R0980.

Figure 28. X-ray spectrum (TEM) of tremolite from Sample R0980.

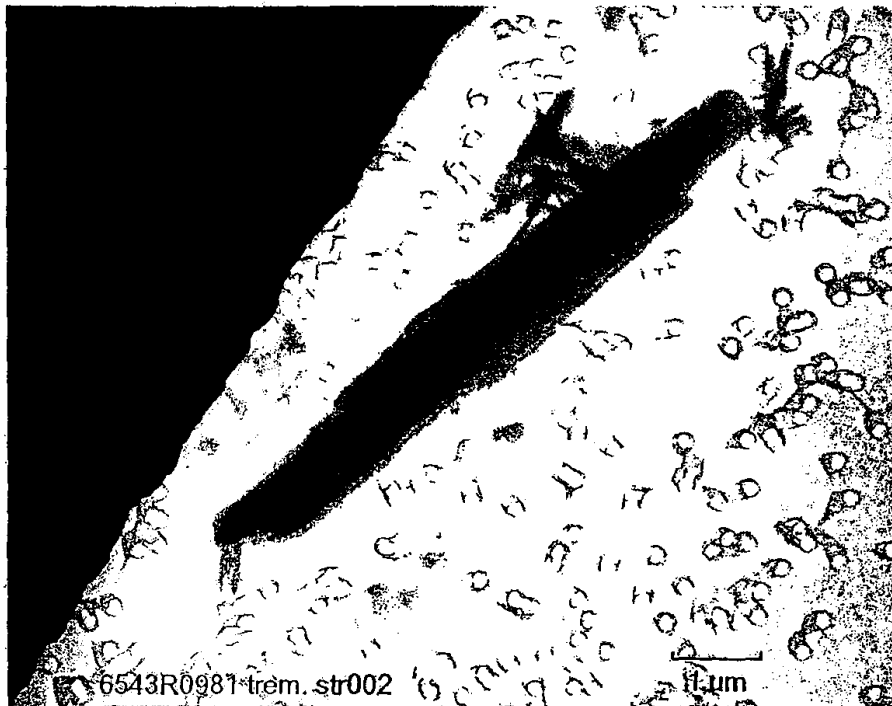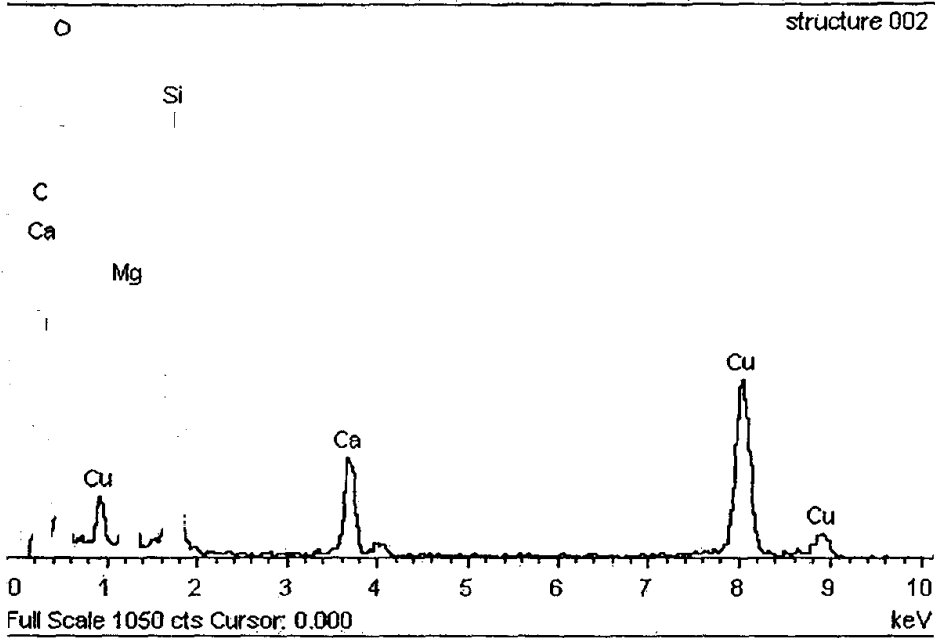**Figure 29.** Polarized light image of a tremolite fiber.

Figure 30. Transmission electron microscope image of tremolite from Sample R0981.

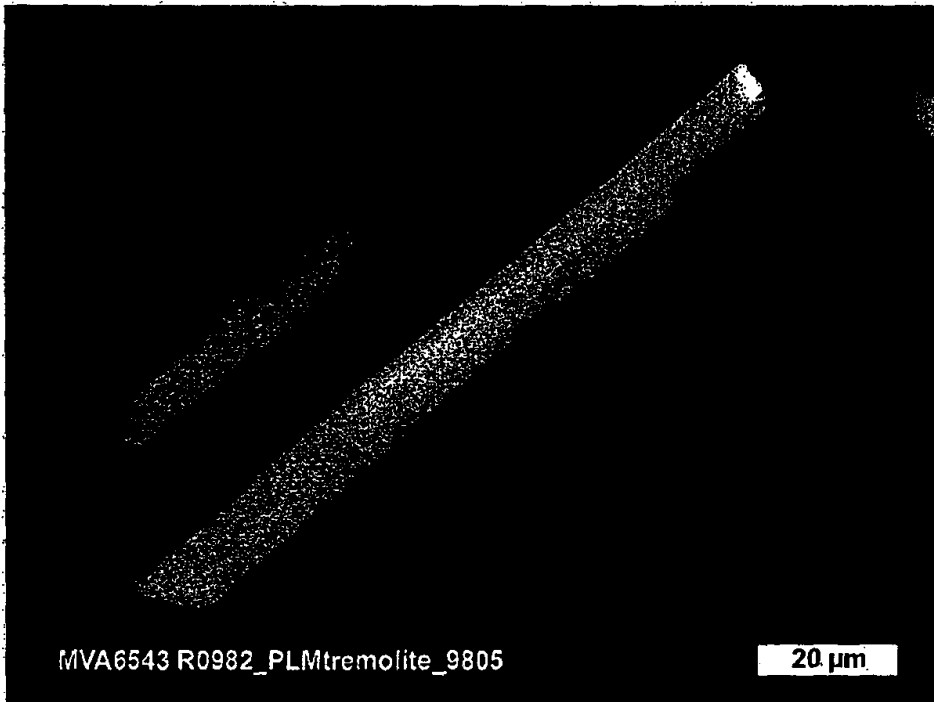**Figure 31.** X-ray spectrum (TEM) of tremolite from Sample R0981.

MVA6543 R0982_PLMtremolite_9805   20 µm

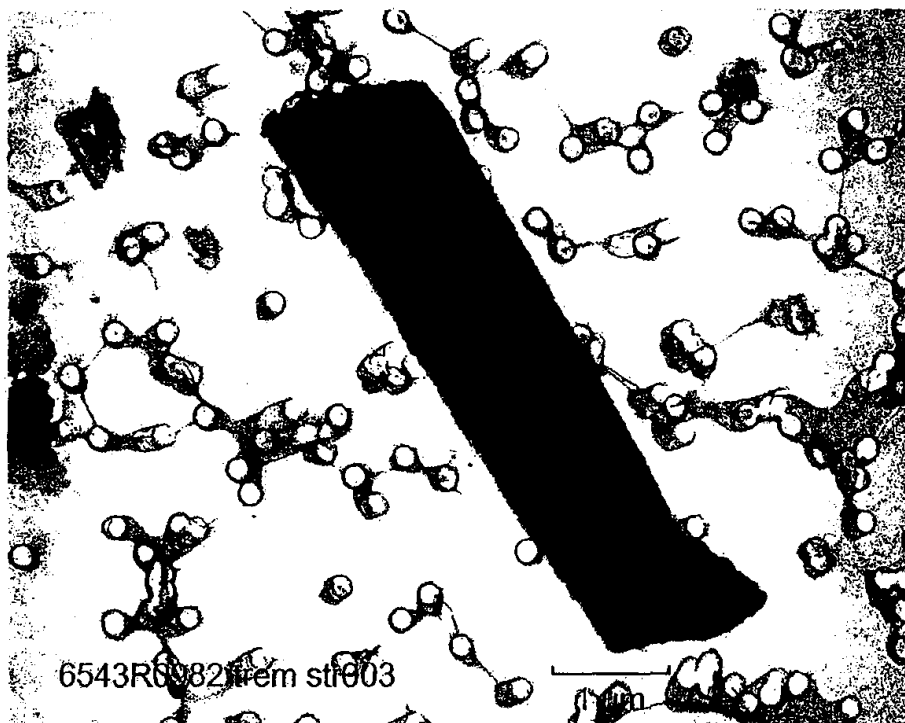**Figure 32.** Polarized light image of a tremolite fiber.

Figure 33. Transmission electron microscope image of tremolite from Sample R0982.
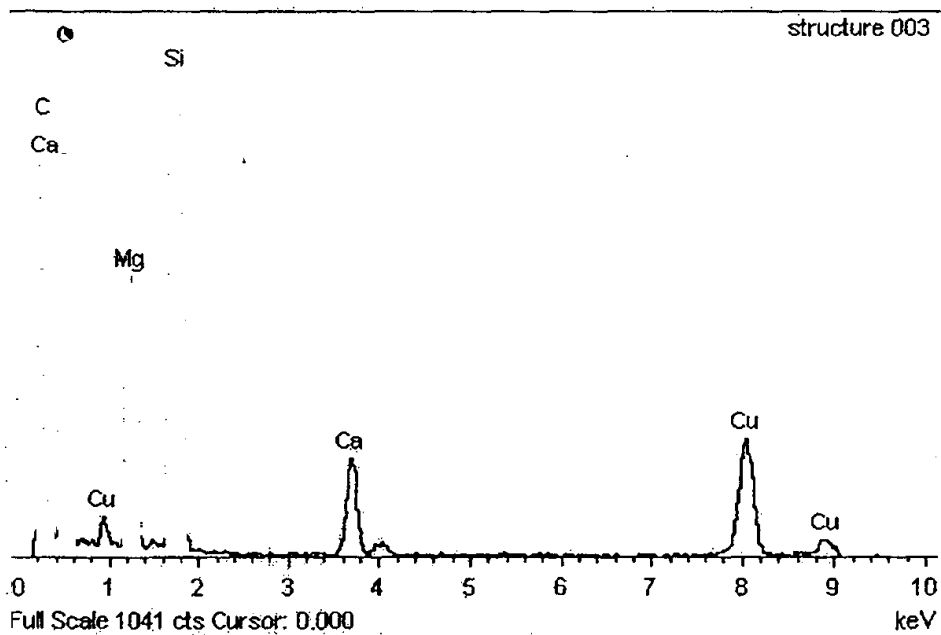

Figure 34. X-ray spectrum (TEM) of tremolite from Sample R0982.

Figure 35. Polarized light image of a tremolite fiber.

Figure 36. Transmission electron microscope image of tremolite from Sample R0983.

Figure 39. Transmission electron microscope image of tremolite from sample R0984.

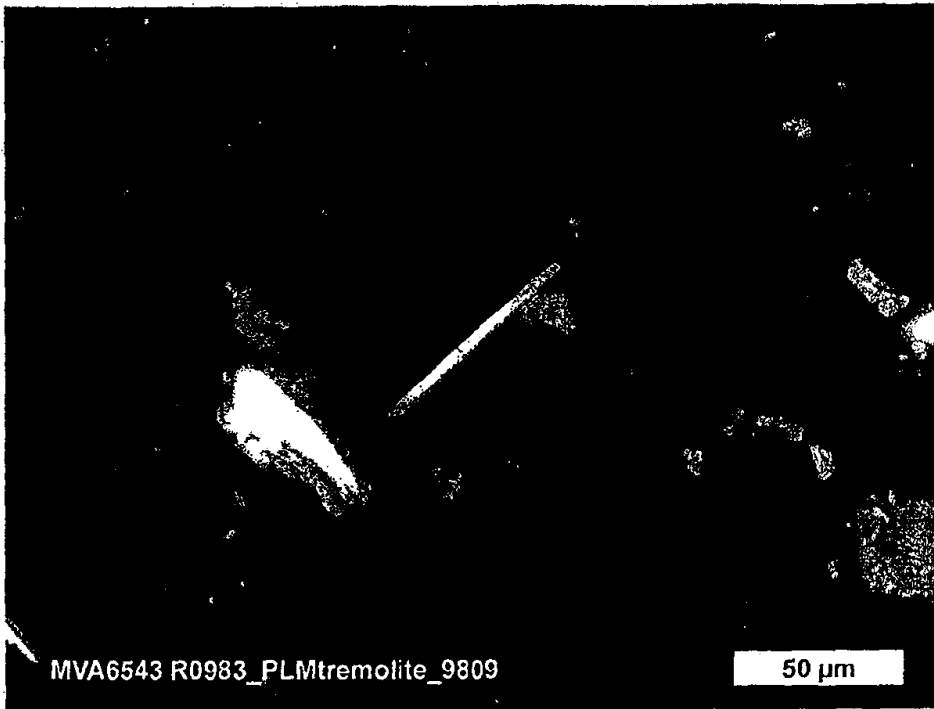**Figure 40.** X-ray spectrum (TEM) of tremolite from Sample R0984.

Figure 37. X-ray spectrum (TEM) of tremolite from Sample R0983.

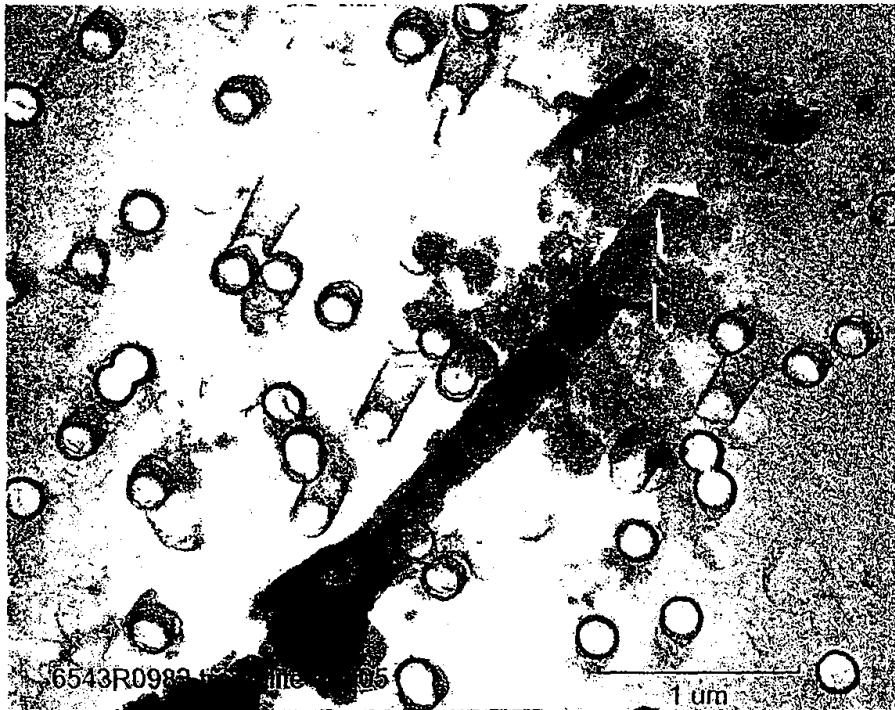Figure 38. Polarized light image of a tremolite fiber.

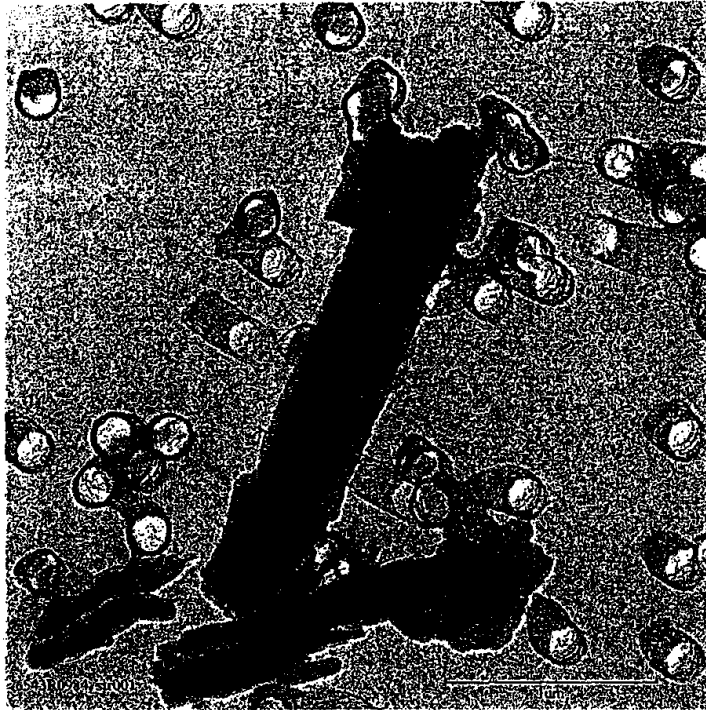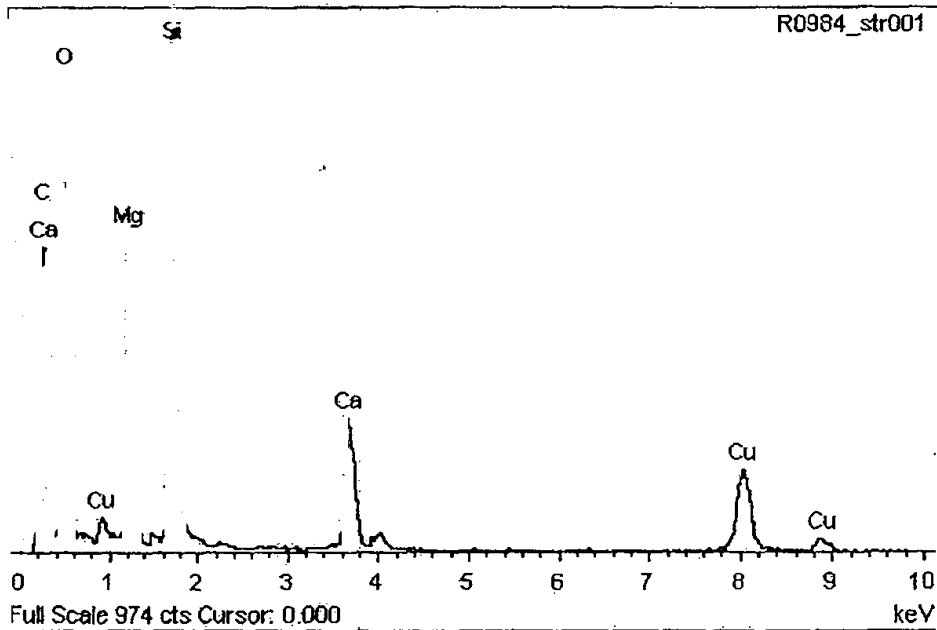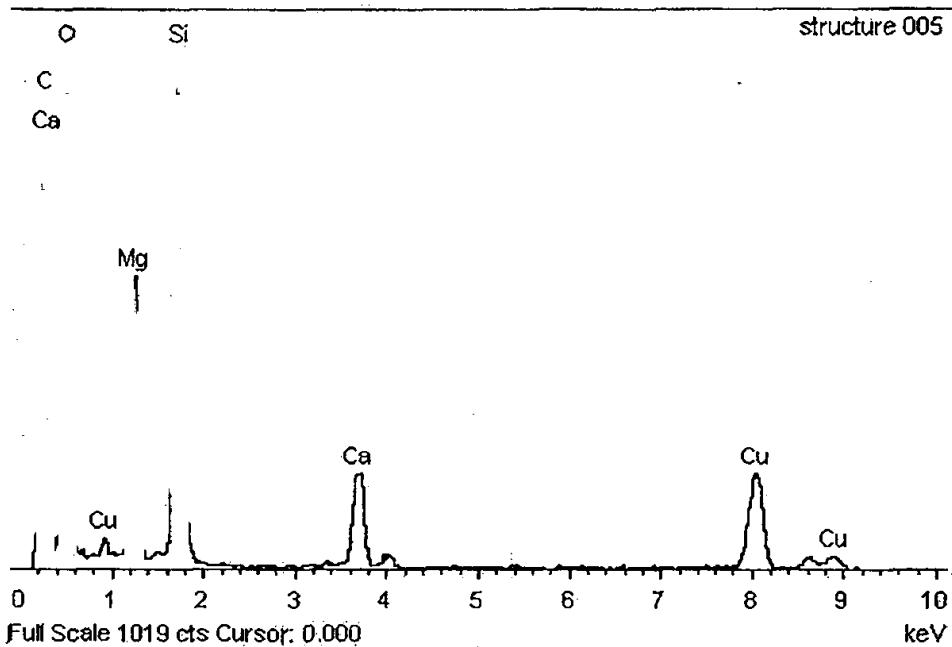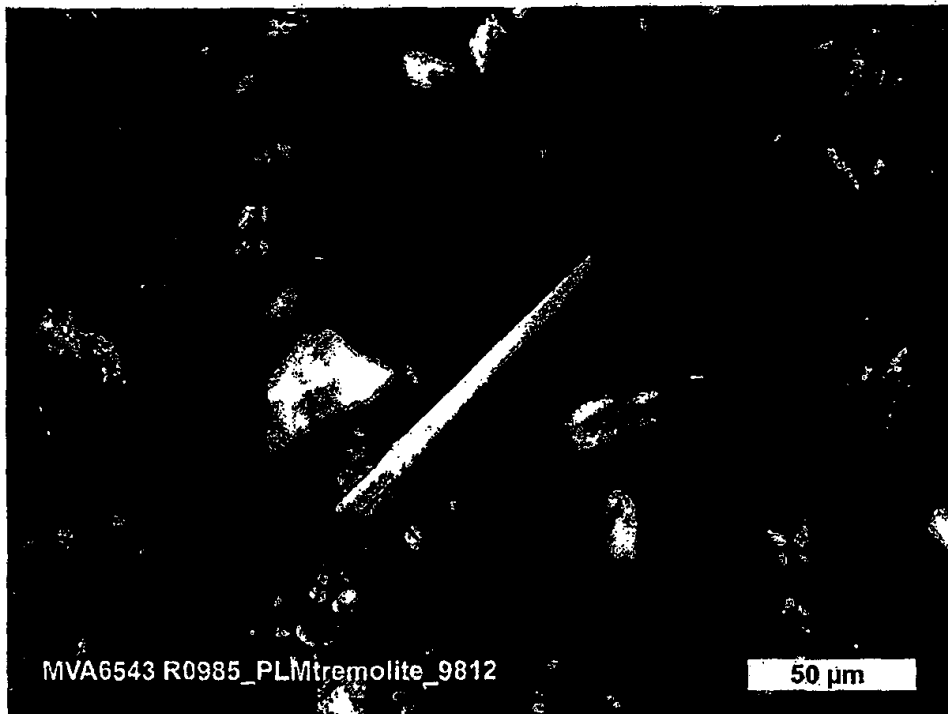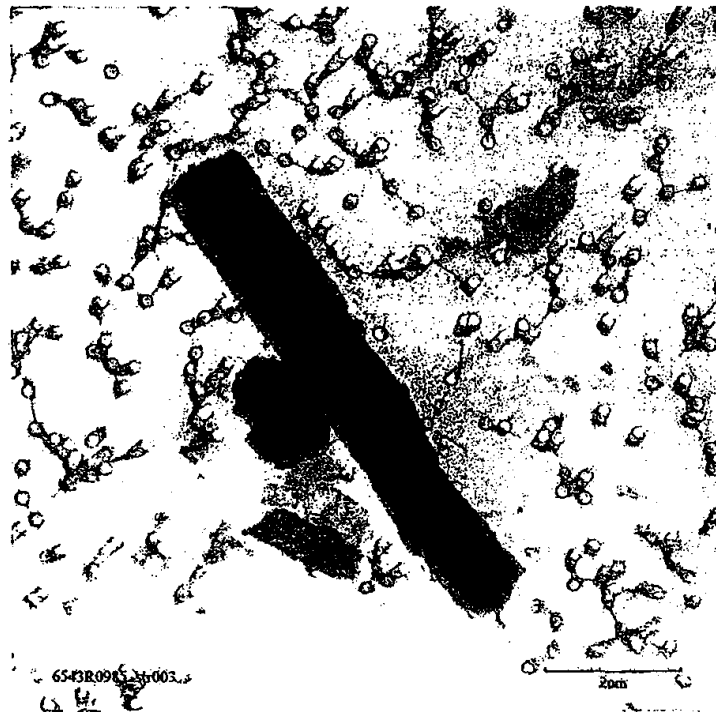**Figure 41.** Polarized light image of a tremolite fiber.

Figure 42. Transmission electron microscope image of tremolite from Sample R0985.
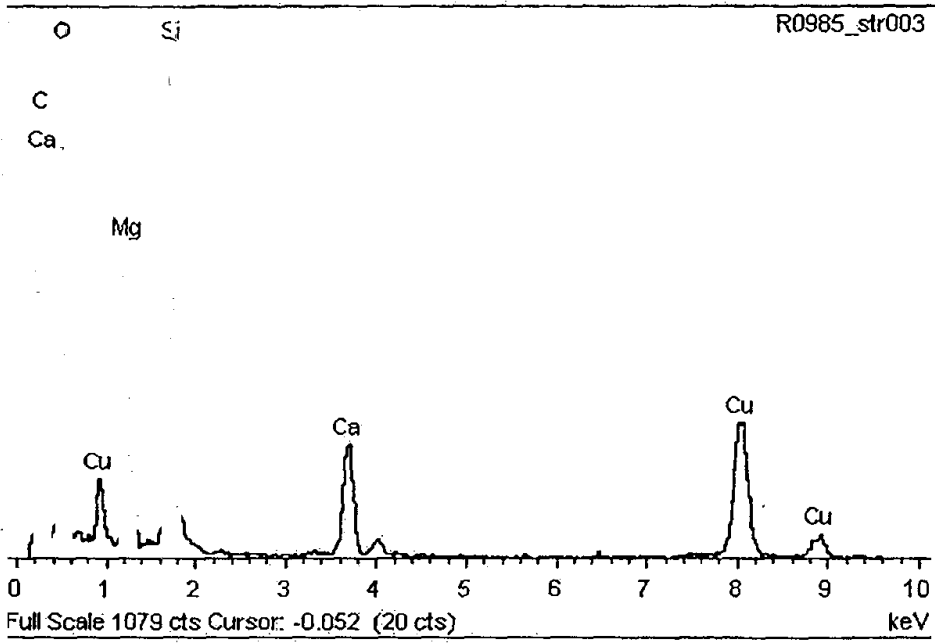
Figure 43. X-ray spectrum (TEM) of tremolite from Sample R0985.

Analytical Performance Criteria

Kevin Ashley, Editor

The Effect of a Proposed Change to Fiber-Counting Rules in ASTM International Standard D7200-06

Martin Harper* and Eun Gyung Lee

Exposure Assessment Branch, Health Effects Laboratory Division, National Institute for Occupational Safety and Health, 1095 Willowdale Road, MS-3030, Morgantown, WV 26505, USA

Bruce Harvey and Michael Beard

Microanalytical Sciences Department, RTI International, 3040 Cornwallis Road, Research Triangle Park, NC 27709, USA

*Corresponding author

Asbestos is a form of certain serpentine or amphibole minerals that has crystallized in a particular habit known as asbestiform.[1] Amphibole minerals are often encountered in metamorphic geological environments, but the majority will not have crystallized in the asbestiform habit.[1] Thus, ore deposits in these environments may include coarsely crystalline amphiboles that can produce cleavage fragments when the rocks are crushed. These fragments may meet morphological criteria that cause them to be designated as fibers, but without them being asbestiform *per se*. In an attempt to distinguish cleavage fragments from asbestiform fibers, the American Society for Testing and Materials (ASTM) International Standard D7200-06[2] includes a procedure for determining whether the particles observable under the phase contrast microscope which meet a morphological definition of a fiber are likely to be asbestiform fibers or cleavage fragments. (The morphological definition of a fiber is that in the National Institute for Occupational Safety and Health (NIOSH) Method 7400[3] "A" counting rules, i.e., > 5

1

μm in length, and with aspect ratio (length:width) ≥ 3:1). Under the ASTM D7200, any particle meeting the definition of a fiber that is curved, or has any morphology that suggests that it is a bundle of fibrils, is automatically assigned to a class of particles ("Class 1") defined as potentially asbestiform, whatever its actual dimensions. In addition, particles meeting the definition of a fiber and > 10 μm in length **or** < than 1 μm in width are also assumed to be potential asbestiform fibers, and are assigned to "Class 2" (see Sections 4.2, 13.13.2, and A4.3 of ASTM D7200). Thus the potentially asbestiform population is considered the sum of Classes 1 and 2. All other particles that meet the definition of a fiber, including possible cleavage fragments, are assigned to Class 3. An alternative definition for Class 2 of length > 10 μm **and** width < 1 μm is being proposed in an upcoming ASTM member ballot. It is important to assess the impact of both the current and proposed criteria.

Taconite is an iron ore that can contain amphiboles in the tremolite-actinolite and cummingtonite-grunerite amphibole series.[1] We have recently analyzed 77 air samples from a taconite mine ore-processing mill. The mine samples have an average of 83.8 fibers (NIOSH 7400 "A" rules) per 85.6 fields, or approximately one fiber per field area. 28% of these fibers met the ASTM International D7200-06 definition of Class 1, and a further 18.6% met the dimensional characteristics of the current criteria for Class 2 (the remainder being Class 3). However, under the microscope, many of these Class 2 fibers have other morphological features (e.g., aspect ratios at the low end of the range, and non-parallel sides) which indicate that they might be mineral cleavage fragments (see Figure 1). Therefore, we hypothesized that the rule used in the current ASTM Standard to classify fibers appears to underestimate proportion of fibers (defined by NIOSH A rules) that are actually cleavage fragments, with many obvious cleavage fragments being placed in Class 2 (potentially asbestiform).

Many experienced microscopists believe they can distinguish cleavage fragments from asbestiform fibers by visual clues, although there is no established reference procedure; the ASTM criteria are the first attempt to establish criteria acceptable by consensus. Given that there is no prior procedure against which the ASTM criteria can be tested, we

decided to test the criteria by examining the results of their application to crushed fragments from samples of massive or coarsely crystalline amphibole minerals that do not have the finely fibrous nature associated with the asbestiform habit. One sample of actinolite was obtained from a mineral dealer who stated it was from near Wrightwood, San Bernardino Co., CA (Figure 2); the mineralogical identification was verified by X-ray diffraction (XRD) analysis. The actinolite was crushed at the RTI International laboratory in a sequential operation using a hydraulic press and a mortar and pestle, in an attempt to maximize the percentage of particles that would meet the definition of a fiber under phase contrast microscopic analysis. In addition, RTI has a stockpile of a previously-crushed tremolite acquired from the National Institute of Environmental Health Sciences (NIEHS), whose provenance is currently unknown. The identity as tremolite was also verified by XRD. A weighed portion of each material was suspended in water, stirred, and aliquots were taken at various time intervals to determine the optimum loading and particle sizing. Approximately 300 particles from each material were examined according to the procedures in ASTM International D7200-06. That is to say, the particles that met the NIOSH 7400 "A" rules definition of a fiber were further classified as to whether they met the definition of D7200-06 Class 2 (potential asbestiform fibers). The results are shown in Table 1. While the presence of a small amount of asbestiform fiber contamination in the mineral specimens used cannot be ruled out, it is unlikely to be more than a few percent at most. As expected, almost none of the particles had the characteristics of Class 1, therefore, it is likely that the large proportions of fibers considered as asbestiform according to the current definition of Class 2 are actually mineral cleavage fragments (along with the remaining fibers which fall into Class 3).

Also shown in Table 1 is the effect of using the alternative definition for Class 2 of length > 10 µm **and** width < 1 µm. This alternative definition removes the majority of fibers from Class 2 and moves them into Class 3 (I.e. non-asbestiform). When applied to the mine samples, a similar result is obtained; while the proportion of Class 1 fibers is unchanged, the proportion of Class 2 fibers using the proposed alternative definition for Class 2 falls to about 0.8%, i.e. nearly all of the Class 2 fibers are re-classified as Class 3.

We have shown that the current definition of Class 2 applied to the non-asbestiform actinolite and tremolite in Table 1 causes many cleavage fragments to be considered as asbestiform fibers. We have further shown that this is likely also to be true for the mixed actinolite-tremolite and cummingtonite-grunerite (non-asbestiform versions of amosite) of the taconite mine samples. We have also shown that this is not the case if the proposed new ASTM International definition of Class 2 is used. However, the question remains as to whether this proposed alternative definition will also cause some actual asbestiform fibers to be classified as non-asbestiform. For example, this may occur when thick bundles of asbestiform fibrils do not show the asbestiform characteristics (curvature or splayed ends) necessary to be included Class 1.

Many of the cleavage fragments with length > 10 µm have quite low aspect ratios and widths > 3 µm. For a fiber of the density of a silicate mineral up to at least 100 µm in length, applying a maximum width of 3 µm should have the same effect as applying the International Organization for Standardisation (ISO) curve for thoracic respirability.[3] It is interesting to examine the effect of using a 3 µm width cut-off as is done in the World Health Organization (WHO) rules.[4] (Note that this is also the case in the NIOSH 7400 "B" rules, but there is a difference in that these rules also include a > 5:1 aspect ratio). For the actinolite sample, the number of particles classified as fibers is reduced from 58% to 48% of the total, while the percentage of those in D7200-06 Class 2 drops even further, from 25% to 14%, or just 7% of the total particles. For the tremolite sample the number of particles classified as fibers is reduced from 63% to 43% of the total, while the percentage of those in Class 2 again drops even further, from 47% to 29%, or just over 12% of the total particles. Thus using the 3 µm upper width limit (or a sampler with a size-selective inlet that performs in an equivalent fashion[3]) may be an alternative to the proposed change in the ASTM International D7200-06 Standard. However, applying this criterion to the taconite mine samples did not produce as much of a reduction in Class 2 particles as with the crushed amphiboles, reducing the average from 18.6% of 83.8 fibers to 15.2% of 80.4 fibers.

In conclusion, the current classification system for fibers in the ASTM International Standard D7200-06 was tested using materials that were expected to contain a large proportion of particles meeting the current NIOSH definition of a fiber, but where those particles would be predominantly cleavage fragments of amphibole minerals rather than asbestiform fibers: crushed samples of coarsely crystalline amphibole minerals, and air samples from a taconite ore-mill. The current classification rules designate many cleavage fragments as Class 2 (i.e. potentially asbestiform), while a proposed change to the definition of Class 2 would place these particles almost exclusively in Class 3 (i.e. non-asbestiform). However, the extent to which asbestiform fibers might also be designated as Class 3 under the proposed change has not been addressed.

Note: Counting rules are often given in terms of less than or greater than a measured value. The precision of measurements under the microscope requires assumptions about rounding errors. The crushed amphibole measurements were made by eye and rounded to the nearest micrometer, except that widths obviously less than 1 μm were assigned a value of 0.5 μm. The analysis provided here assumes all measurements to be greater than the nominal values. For the mine sample data, computer-aided measurements on photomicrographs were made to one-tenth of a micrometer, so that x.0 micrometers was assumed to be not greater than x.

Acknowledgement

We would like to acknowledge the assistance of John Nelson (NIOSH/HELD/EAB) and Owen Crankshaw, Stacy Doorn, Todd Ennis and Lisa Greene (RTI International) with data collection for this column.

Disclaimers

The findings and conclusions in this report are those of the authors and do not necessarily represent the views of the National Institute for Occupational Safety and Health, or RTI International. Mention of ASTM International Standards does not imply endorsement by NIOSH, the Centers for Disease Control and Prevention or RTI International. Data provided in this report are provisional and have not been peer-reviewed.

References

1.   **Virta, R.L.:** "Asbestos: Geology, Mineralogy, Mining and Uses." United States Geological Survey, Open-File Report 02-149, 2002. http://pubs.usgs.gov/of/2002/of02-149 (accessed 11/01/2007)

2.   **American Society for Testing and Materials (ASTM) International:** Standard Practice for Sampling and Counting Airborne Fibers, Including Asbestos Fibers, in Mines and Quarries, by Phase Contrast Microscopy and Transmission Electron Microscopy, D7200-06, ASTM International, West Conshohocken, PA (2006).

3.   **National Institute for Occupational Safety and Health (NIOSH):** NIOSH Manual of Analytical Methods: Asbestos and Other Fibers by PCM. Method 7400 Issue 2, 15 August, 1994. NIOSH, Cincinnati, OH. http://www.cdc.gov/niosh/nmam/pdfs/7400.pdf

4.   **Baron, P.A.:** Application of the thoracic sampling definition to fiber measurement. Am. Ind. Hyg. Assoc. J. 57: 820-824 (1996).

5.   **World Health Organization (WHO):** Determination of airborne fibre concentrations. A recommended method, by phase-contrast optical microscopy (membrane filter method), WHO, Geneva, 1997.

FIGURE LEGENDS

<u>Figure 1</u>

Typical taconite mine ore-mill air sample under phase contrast microscopy (450X) showing a particle very likely to be a mineral cleavage fragment. The area bounded by the darker arcs is 100 μm across.

<u>Figure 2</u>

Coarsely crystalline (non-asbestiform) actinolite (Scale indicated by 25¢ piece).

Figure 1

Figure 2

9

Table 1. Percentage of particles from crushed non-asbestiform amphibole minerals that meet the NIOSH Method 7400 "A" counting rules for a fiber, the percentage of those particles that meet the definition of a potentially asbestiform fiber according to ASTM International Standard D7200-06[1], and the percentage that would meet that definition after a proposed change.

Mineral	% particles meeting 7400 fiber definition	% of 7400 fibers in D7200-06 class 2	% of 7400 fibers in proposed class 2
Actinolite	58.3	25.1	0.6
Tremolite	62.7	46.8	1.6

ASBESTIFORM AND ACICULAR MINERAL FRAGMENTS

Tibor Zoltai

Department of Geology and Geophysics
University of Minnesota
Minneapolis, Minnesota 55455

Although the harmful reaction of the human body to inhaled asbestos particles has been known for over half a century, the full extent of the danger was not recognized in this country until relatively recently. That is, not until the mid sixties when extensive epidemiological surveys and direct electron microscopic observation became available did the full extent of the dreadful picture of asbestos diseases become apparent.

This came at a time when a large segment of our youth was dissatisfied with the "system" and was searching desperately for new values. Some found intellectual incentive and satisfaction in working toward the goal of cleaner environment. The public recognized the value of that drive with the result that agencies were established and laws were passed to improve the long neglected and deteriorating environment. It was a minor revolution and was in general, beneficial for the future of the country. However, it created some undesirable side effects as well. In some instances, emotions overruled realism and some crusaders riding on the crest of the emotional wave lead us to hasty and regrettable decisions. One of the most unfortunate of such decisions was related to asbestos. Instead of accepting available scientific knowledge, the definition of asbestos was modified* to serve the purpose of the crusade, justifying a dramatic and immediate solution to some assumed asbestos pollution problems. The adoption of the distorted definition did not serve the cause of a cleaner and healthier environment. In fact, it delayed enforcement of dust control regulation by drawn out litigation as to whether the acicular particles were truly asbestos. Another effect was that it diverted attention from other equally or perhaps more important pollution problems.

This modified definition limited asbestos to only five minerals; chrysotile, $Mg_6(OH)_8Si_4O_{10}$, actinolite-tremolite, $Ca_2(Mg,Fe)_5(OH)_2Si_8O_{22})$, anthophyllite, $(Mg,Fe)_7(OH)_2Si_8O_{22}$, cummingtonite-grunerite, $(Mg,Fe)_7(OH)_2Si_8O_{22}$, and riebeckite, $Na_2Fe_5(OH)_2Si_8O_{22})$ on the basis of a primarily commercial argument. These are the only five minerals that are known to occur in the rare asbestiform habit in sufficient concentration and quantity to allow their exploitation for profit. These are by no means the only minerals which can crystallize in that habit. Furthermore, this definition specified that all fragments of these minerals which have a minimum axial ratio of 3:1 are to be considered asbestos, or asbestos-like. Since the last four of these

*The definition introduced by the court and accepted by many environmental and public health scientists and regulatory agencies reads:

Asbestos is a generic term for a number of hydrated silicates that, when *crushed* or processed, separate into flexible fibers made up of fibrils."
(U.S. District Court, district of Minnesota, 5th Division. Supplemental Memorandum. No. 5-72. Civil 19, Appendix 5, May 11, 1974, p. 24).

Fibers were:

A mineral which is at least three times as long as it is wide.

For further details see:

ZOLTAI T., 1978. History of asbestos related mineralogical terminology. Natl. Bur. Std. Spec. Publ. No. 506.

ive minerals are amphiboles (chrysotile is a serpentine) and have good prismatic cleavage in all habits other than asbestiform, they all will break into acicular fragments, and most will satisfy the 3:1 aspect ratio. Translated into practical terms, this means that no matter whether these minerals crystallized in the asbestiform habit or not, and whether they possess the peculiar physical and biological properties of asbestos or not, they are considered to be asbestos. On the other hand, minerals other than these five that did in fact crystallize in the asbestiform habit, and may possess the harmful properties of asbestos, are not accepted as asbestos. Unfortunately, this definition is still used today by many environmental and public health researchers. It is adopted in most pollution control laws and is enforced by most regulatory agencies.

The effect is that modification of the asbestos definition, which was designed to improve our environment, poses a major hurdle in the development and execution of appropriate controls of asbestos pollution. We are treating certain minerals as asbestos, when they are not asbestos, and we neglect to consider other minerals as in fact they crystallized in the asbestiform habit and mineralogically are asbestos, although they have no potential commercial value.

ASBESTOS PROPERTIES

This definition cannot be improved by amendment and must be abandoned. A more scientific definition, like the mineralogical one, should be adopted to clear the current confusion concerning the identify of asbestos. for example: "Asbestos is a mineral when crystallized in the asbestiform habit." Of course, all asbestiform crystals will not have exactly the same properties and thus will not be equally harmful. The biological properties of each will have to be determined independently.

Recent biological and epidemiological studies[13] indicate clearly that not only the physical but also the biological properties of amphibole asbestos fibers are different from cleavage fragments, in spite of their similar appearance. Similarly, current epidemiological studies indicate that the cleavage fragments may not be carcinogenic. Although these indications cannot be considered proof at this stage, they are adequate enough for us to change our practices and make the distinction between asbestiform and other crystallization habits of amphiboles and other minerals.

These studies imply strongly that the harmful properties of asbestos fibers must be related more to the peculiar properties of asbestos than the fiber's mineralogic identity.† The unique physical-chemical properties of asbestos fibers, which probably include the crucial carcinogenic factor, can be classified into four divisions:

Shape and Size

Although it is apparent that the shape and size of the asbestos fiber, by itself, is not responsible for the carcinogenic properties of asbestos, this property still constitutes a necessary component of the total properties that render asbestos harmful.

Strength and Toughness

Related or consequential properties, such as hardness, flexibility and durability may also be included in this category. A fiber must be sufficiently strong and tough to

†This argument is supported also by the known carcinogenic properties of some fiber glass which is not even a mineral or a crystalline substance, but may have asbestos properties.

go through industrial processing without destruction and be able to survive in a biological environment to deliver its harmful effect. The asbestiform varieties of silicates, those which are of commercial importance as well as those which are not, are stronger and tougher than other varieties of the same mineral. In the case of amphibole asbestos the increase in tensile strength for example, is 10 to 30-fold.[4]

Relative Chemical Inertness

The fibers also must be chemically inert to survive the different chemical environment of the processing plants and of the human body. Amphibole asbestos for all practical purposes, can be considered to be inert in these two environments. Chrysotile is somewhat less resistant to acids.

Surface Properties

The surface properties of asbestos are probably the most important. Unfortunately, they are also the least understood. The surface properties of asbestiform fibers, single crystals and cleavage fragment must also be different due to the differences in their origins. The surfaces of asbestiform fibers and acicular crystals represent a reasonable equilibrium of the terminated bonds of the structure. The surface of a cleavage fragment is created by external force, and consequently, it is not expected to be as stable as the others, since the stresses must have created a high density of surface defects and also cracks or incomplete fractures. The surface charge of these particles can also be expected to be different and important.[9] The high-charged surface can absorb more foreign ions which may be carcinogenic. Variations in the surface cation exchange properties of the three varieties may also be important. Surface tension may be related to the mobility of fibers and other particles. The study of surface properties should receive high priority in asbestos related research.

ASBESTIFORM HABIT

Under different ranges of physical and chemical conditions most minerals will crystallize in noticeably different habits. Such differences include characteristic crystal forms, crystalline dimensions, ordering or disordering of cations, twinning, and development of various polytypes. Most of these habits are caused by minor and usually negligible changes in the mineral's properties. The asbestiform habit appears to be the only one that displays significantly different properties. The otherwise brittle and relatively weak crystal becomes flexible and extremely strong in that habit. This has puzzled mineralogists for centuries. With the invention of sophisticated instruments, like the high-resolution electron microscope, we can now investigate the causes of these drastic changes. We are far from being able to answer all of the related questions, but we can already explain some of the fiber or fibril-structures and can offer reasonable models for the others. It appears at this stage that there are three categories of fibril structures and either one, or two, or all three may be responsible for the asbestos properties of various types of asbestiform fibers.

Tubular or Scroll Structure

The most important and most abundant asbestos is chrysotile, the asbestiform variety of serpentine. Before the introduction of electron microscope the crystallization

of chrysotile was a very intriguing problem. The basic structure of serpentine is layered. That is, the structure is composed of a layer of tetrahedrally coordinated silicon cations (T-layer) and an octahedrally coordinated layer of magnesium cations (O-layer). These two layers are linked together by sharing common oxygens. These T-O double layers form strong structural units and the bonding between these units is limited to weak residual bonds. Layered silicates, like serpentine, are common rock forming minerals and have numerous variations of layered structures. The tetrahedral layer is approximately the same in all of them (FIGURE 1a), the octahedral layer, on the other hand, has two major types: the trioctahedral and the dioctahedral layers (FIGURE 1b and 1c). Serpentine's octahedral layer is trioctahedral. Some layered silicates contain a unit of one T- and one O-layer (as in serpentine) and some will have the octahedral layer sandwiched between two T-layers (as in talcs). Others will have an additional cation (C-layer) connecting T-O-T units (as in micas) and yet others, the chlorites, will have an extra octahedral layer between the T-O-T layer units. The schematics of the layered silicate structures are illustrated in FIGURE 2. Further variation of the layered silicate structures can be formed by various stacking patterns of the same basic layered units which are referred to as polytypes.

TETRAHEDRAL LAYER   TRIOCTAHEDRAL (or brucite) LAYER   DIOCTAHEDRAL (or gibbsite) LAYER
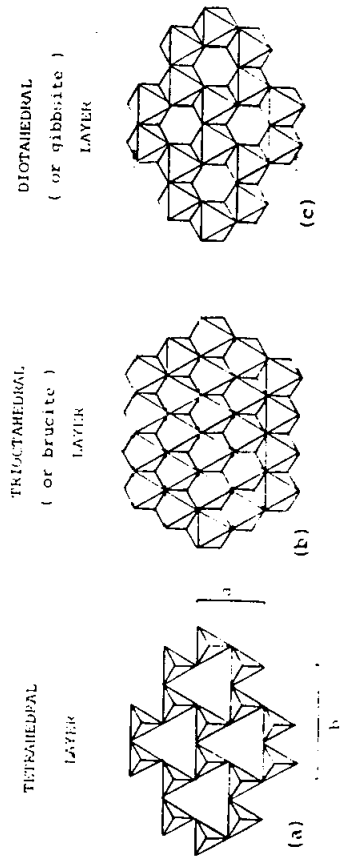
(a)   (b)   (c)

FIGURE 1. Illustration of the idealized models of layers in layered silicates.

All the layered silicates display perfect basal cleavage. Since the bonds between the layer units are weaker than the bonds within the layers, the mineral can easily be cleaved between the layers. This can be well illustrated in micas where sheets can be separated and removed almost like the pages in a book. Although serpentine crystals are never as large as that of micas they will demonstrate the lamellar and platy habit and the perfect basal cleavage. The puzzle about chrysotile was the crystallization of long, one-dimensional fibers of a fundamentally layered and platy mineral. The puzzle remained unsolved until the development of electron microscopy. Bates, Hildebrand and Swineford[10] produced the first electron microscope photograph of the tubular structure of a layered silicate in 1948. The mineral was halloysite, $Al_4(Oh)_8Si_4O_{10} \cdot 4H_2O$, a T-O kaolinite-like clay mineral. One of their photographs and a scheme of interpretation are shown in FIGURE 3. Soon after that, Bates, Sand, Mink,[12] and Whittaker[13] obtained photographs of the cross section of chrysotile fibers and demonstrated their similarity with the structure of halloysite. With subsequent improvement of the instruments, Yada[14] succeeded in obtaining high resolution photographs of the cross sections of chrysotile fibrils and demonstrated the details of both tubular and scroll-like structures (FIGURE 4).

TRIOCTAHEDRAL   DIOCTAHEDRAL

T - O   Serpentine   Kaolinite

T - O - T   Talc   Pyrophyllite

T - O - T + C   Phlogopite   Muscovite
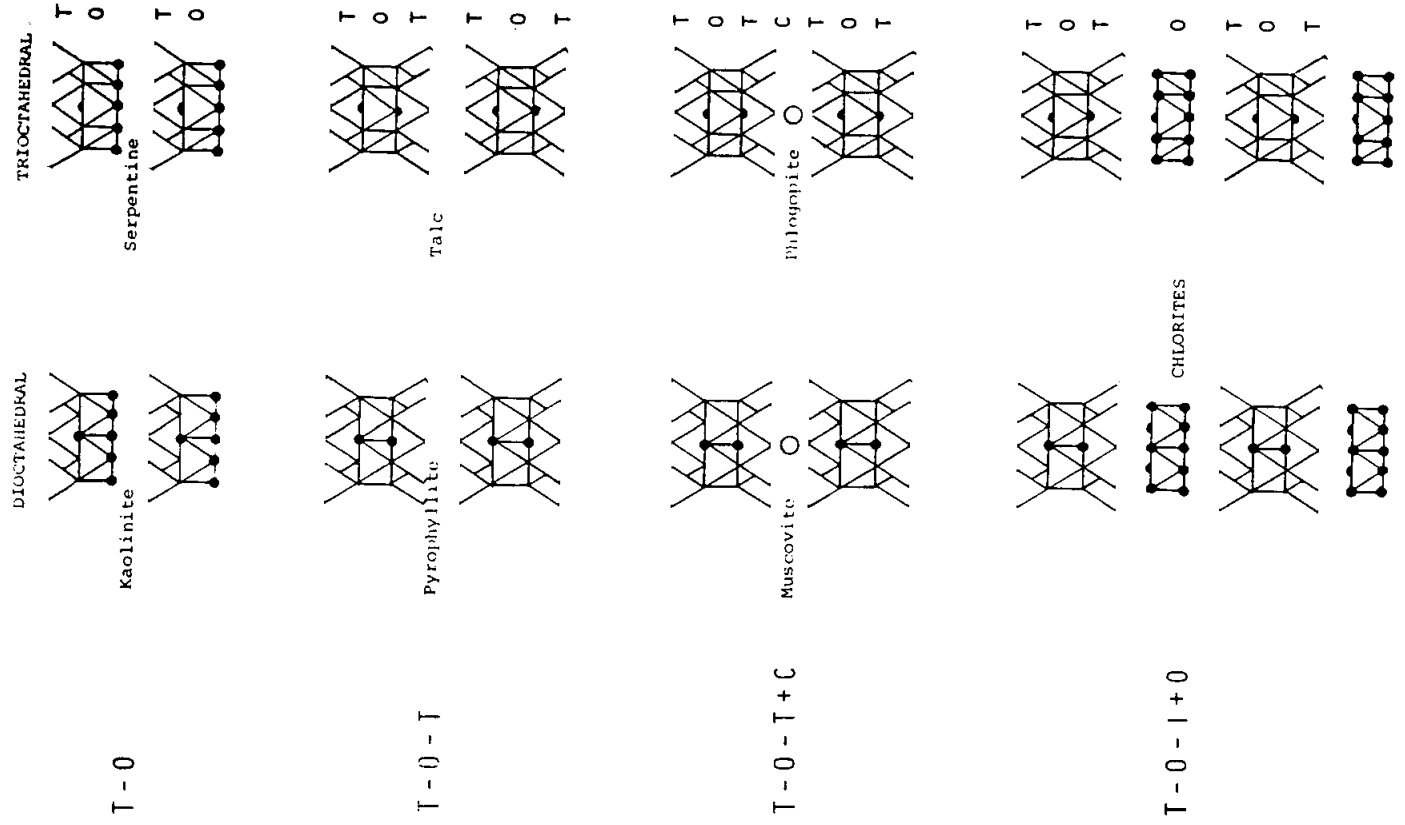
T - O - 1 + 0   CHLORITES

FIGURE 2. Classification of the common layered silicates.

Chrysotile is the only commercially valued asbestiform layered silicate because it is the only one that can be found in sufficiently high quality and quantity to allow profitable exploitation. There are, however, many other layered silicates that are known to occur in the same or similar habit. Some are exceptionally rare, others are more common and in terms of relative quantity they may be comparable to chrysotile. However, they are not of economic interest. Tubular halloysite, as mentioned earlier is a good example. Recently, Kohyama, Fukushima and Fukami[15] have published TEM pictures of tubular halloysite and demonstrated the structural similarities with chrysotile (FIGURE 5). Fibrous or asbestiform varieties of other layered silicates have

In vacuum   10nm

FIGURE 5. Transmission electron microphotograph of tubular halloysite. After Kohyama, Fukushima and Fukami (1978)[15].

also been known. Fibrous talc was long recognized and given the variety names beaconite or agilite by early mineralogists. FIGURE 6 is a might microphotograph of asbestiform talc fibers developed through the alteration of apparently prismatic anthophyllite (pseudomorph?). Fibrous attapulgite (palygorskite) (Mg,Al).(OH)$_2$Si$_4$O$_{10}$·4H$_2$O showing "striking resemblance to asbestos," (see FIGURE 7) and Mg-beidellite and nontronite (CA,Na)$_{0.7}$(Al,Mg)$_4$(Si,Al)$_8$ O$_{20}$·nH2O, was described by Marshall et al.[16] as the common forms of these hydrated layered silicates. A short search in the mineral collection of the University of Minnesota revealed asbestiform varieties of several other layered silicates; pyrophyllite, Al$_2$(OH)$_2$Si$_4$O$_{10}$, the dioctahedral equivalent of the T-O-T structure type of talc (FIGURE 8) and 3 micas, muscovite, KAL$_2$(OH)$_2$Si$_3$Al0$_{10}$ (FIGURE 9a); lepidolite,

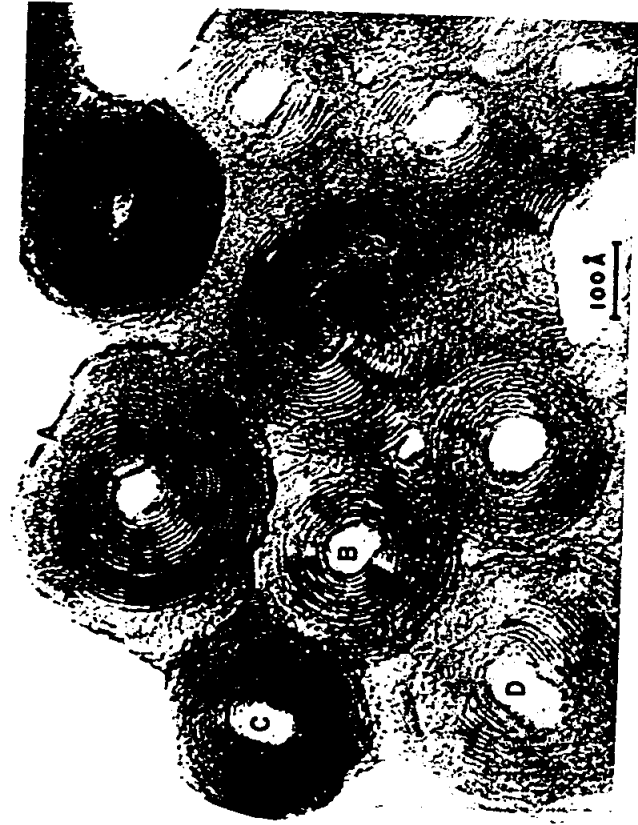FIGURE 3. Scanning electron microphotograph of tubular halloysite. After Bates, Hildebrand and Swinford (1950)[13].

100 Å

FIGURE 4. High resolution electron microphotograph of chrysotile fiber cross sections. After Yada (1967)[14].

KLi2Al(OH)2Si4O10, (FIGURE 10), and glauconite (FIGURE 11). They all displayed good asbestiform fibers.‡ An SEM mount was quickly prepared from the asbestiform muscovite sample and showed that the fibers are composed of smaller fibrils (FIGURE 9b) as in chrysotile. The crystal structure of muscovite is illustrated in FIGURE 12. Other relatively rare layered silicates, like greenalite $Fe_6(OH)_8Si_4O_{10}$, and amesite [not to be mistaken with the trade name of the asbestiform cummingtonite and actinolite mixture, amosite $(Mg,Fe)_8(OH)_8(Si,Al)_4O_{10}$], have T-0 serpentine struc-

tures, and minnesotaite $(Fe,Mg)_3(Si,Al)_4O_{10}$, and stilpnomelane $K(Fe,Mg,Al)_3$ $(OH)_2Si_4O_{10} \cdot nH_2O$, have respectively a talc- and mica-like structure. These were found to crystallize an occasion in relatively poor quality asbestos fibers. Although most of these nonserpentine layered silicate fibers seem to display good asbestos properties, we have no quantitative measurements of these properties. Consequently we can state their similarity with chrysotile asbestos.

‡Some fibers of layered silicates may look asbestiform. Macroscopic examination may, however, be misleading as the fibrous appearance may be a pseudomorphic form in some cases. That is, the layered silicate may be a replacement of an earlier mineral and may assume the shape of the replaced mineral. Fibrous looking talcs are known examples of that.
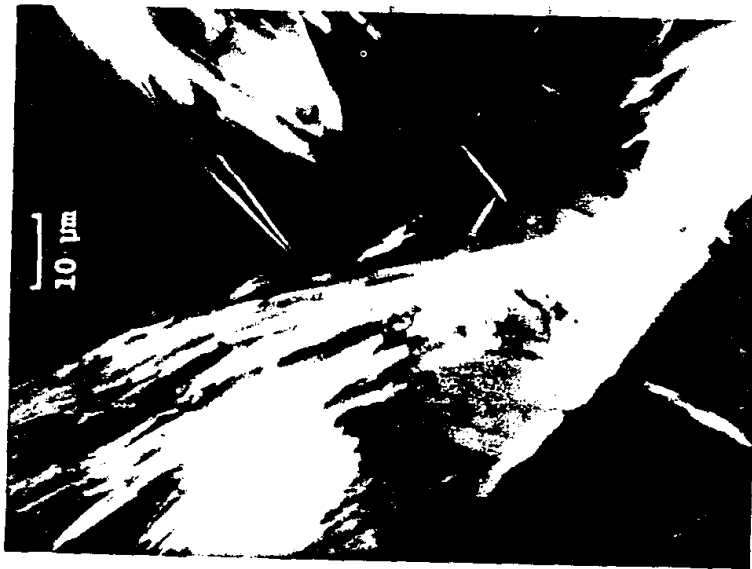

FIGURE 6. Light microphotograph of talc fibers in polarized light. This asbestiform talc is the alteration product of apparently prismatic anthophyllite.

FIGURE 7. Electron microphotograph of attapulgite (palygorskite) showing "striking resemblance to asbestos." After Marshall, Hubert, Shaw and Caldwell (1942)."
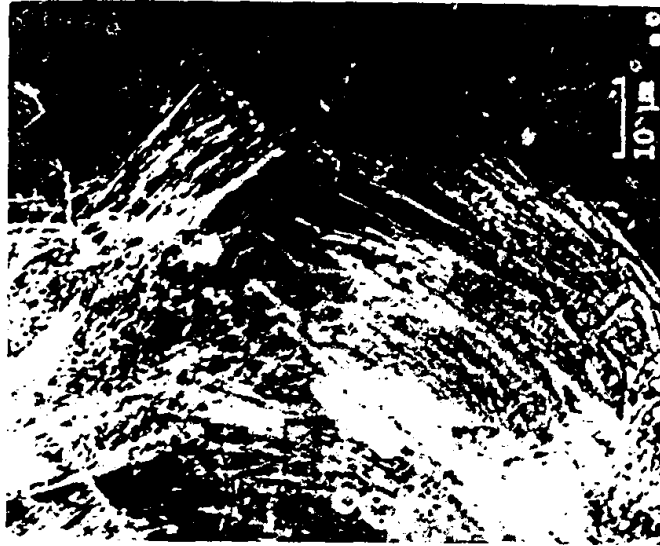

FIGURE 8. Light microphotograph of the partially broken end of a pyrophyllite fiber, in polarized light.
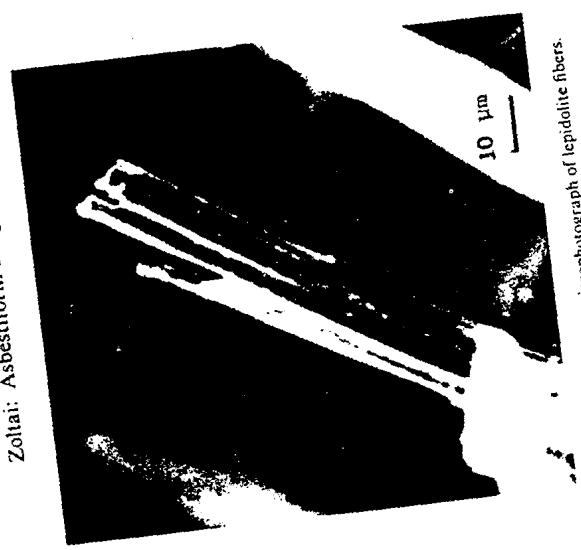
Zoltai: Asbestiform Fragments

FIGURE 10. Light microphotograph of lepidolite fibers.

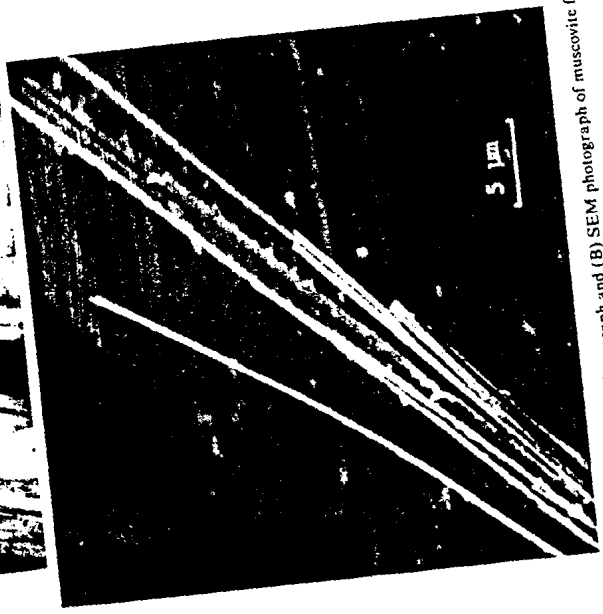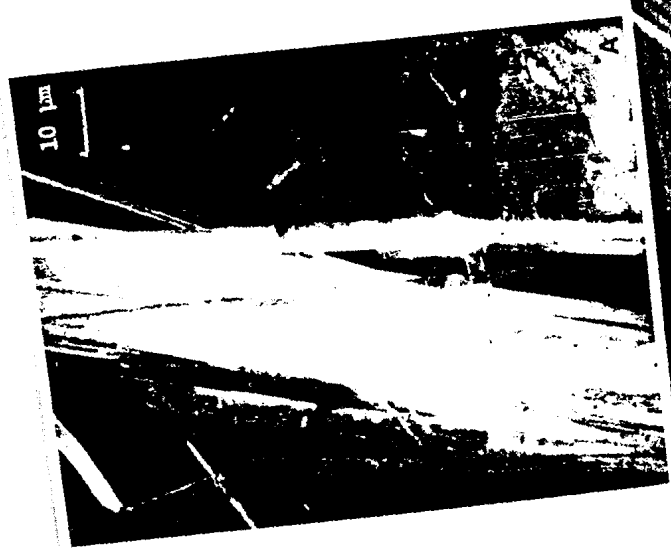FIGURE 11. Light microphotograph of glauconite fibers.

FIGURE 9. (A) Light microphotograph and (B) SEM photograph of muscovite fibers.

Zoltai: Asbestiform Fragments

FIGURE 13. Electron microphotograph of cross section of polygonal chrysotile. After Cressey and Zussman (1976).[20]

picture, however, is not good enough to disclose the rotational equivalence of fibrils in the fiber. This is probably because the 50 μm fiber itself is composed of several smaller fibers and the random orientation of the fibers may shield the more regular orientation of the fibrils in each fiber. The optical properties of monoclinic amphibole asbestos also indicate the random orientation of the fibrils.[19]

Amphiboles are chain silicates; their cystal structures is dominated by the strong chains of silica tetrahedra. The silica chains are connected by weaker bands of usually octahedrally coordinated cations. The difference between the strength of the tetrahedral chains and octahedral bands is due to the high valency and low coordination number of silica in tetrahedra and the lower valency and higher coordination number of the cations in the octahedra. The structure of anthophyllite is illustrated in FIGURE 16. As a consequence of this structural pattern all chain silicates have good prismatic cleavage; their crystals will break along planes between and parallel with the tetrahedral chains. The single chain of the pyroxenes is changed to double chains in

FIGURE 14. Electron microphotograph of cross sections of crocidolite (asbestiform riebeckite) fibers. After Franco et al. (1977).[22]

Polygonal and Faulted Structures

This category of fibril structures is much less understood than the preceeding type. The structure of a lower quality serpentine asbestos, formerly known by names like schweitzerite and Pavlon chrysotile, was recently investigated by Cressey and Zussman[17] and was shown to be different from the usual tubular structure.§ The fibrils are composed of long, parallel units radiating around the central fiber axis as shown in FIGURE 13. A similar but less regular bundle of fibrils was observed by Franco et al.[18] in the electron microscope pictures of crocidolite which is the variety name of 50 μm diameter "amosite" fiber from the classical location of Penge, South Africa (FIGURE 15a). The indices of the diffraction spots (FIGURE 15b) reveal that this picture is not a single reciprocal lattice plane but is composed of many randomly
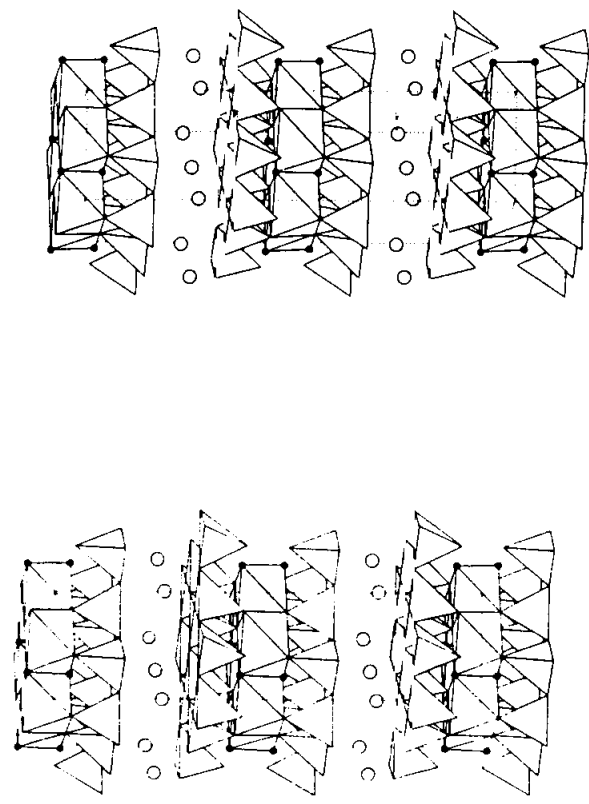

FIGURE 12. Stereoscopic drawing of an idealized muscovite structure.

oriented lattice planes, rotated around the common c-axis there are three diffractions (230), (101) and (102) that violate the C-center of the cummingtonite unit cell indicating the asbestiform crystal may have a primitive cell. The Weissenberg photograph of the same fiber showed lines instead of individual spots which confirms the preceeding observation and proves that the fiber is composed of hundreds of thousands of small fibrils. The diffraction line in the Weissenberg photograph displays variable intensity which indicates that the fibrils have preferred orientation. The

§As the fibril structures of most layered silicate asbestos examples given in the preceeding discussion are not yet known, it is feasible that some have no tubular structures. Some may have polygonal or similar, not yet defined, structures.

Zoltai: Asbestiform Fragments

FIGURE 16. Stereoscopic diagram of the structure of anthophyllite, c-axis horizontal.

the amphiboles. The angle between the two distinct (prismatic) cleavage planes different in these two groups of minerals. The relative orientation of the cleavage planes is different in these two groups of minerals. The relative orientation of cleavage planes is amphiboles is illustrated in FIGURE 17. In this diagram the ch. are perpendicular to the plane o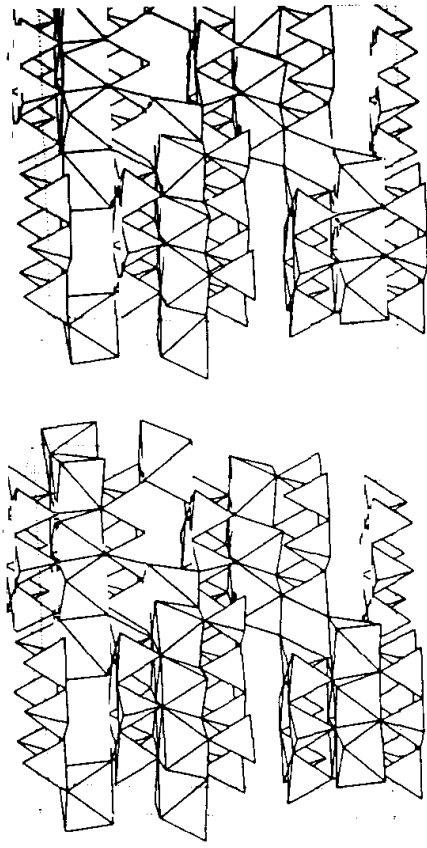f the paper. There are many chain silicates and most important among them are illustrated in FIGURE 18. We know that most of
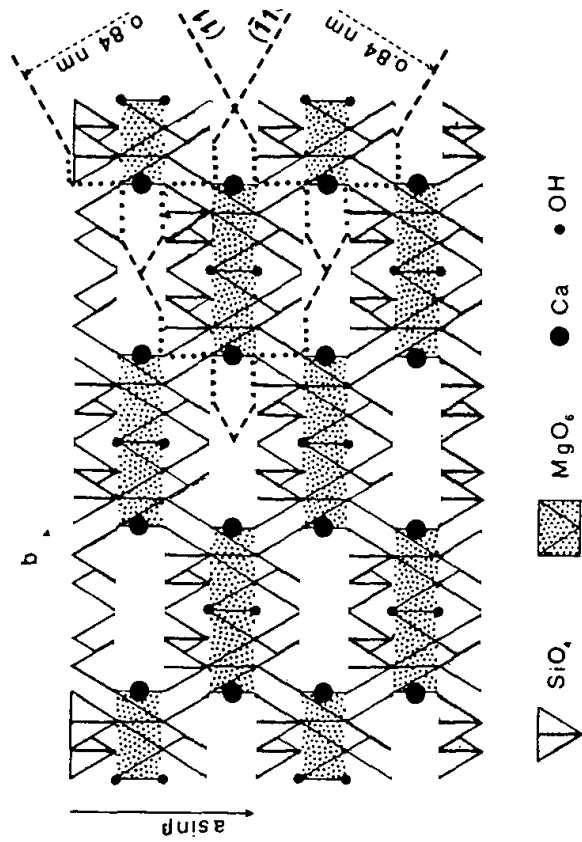
▽ SiO₄   ▨ MgO₆   ● Ca   • OH

FIGURE 17. Illustration of the cleavage pattern in the amphibole structure. Diagram perpendicular to the c- or fiber-axis.
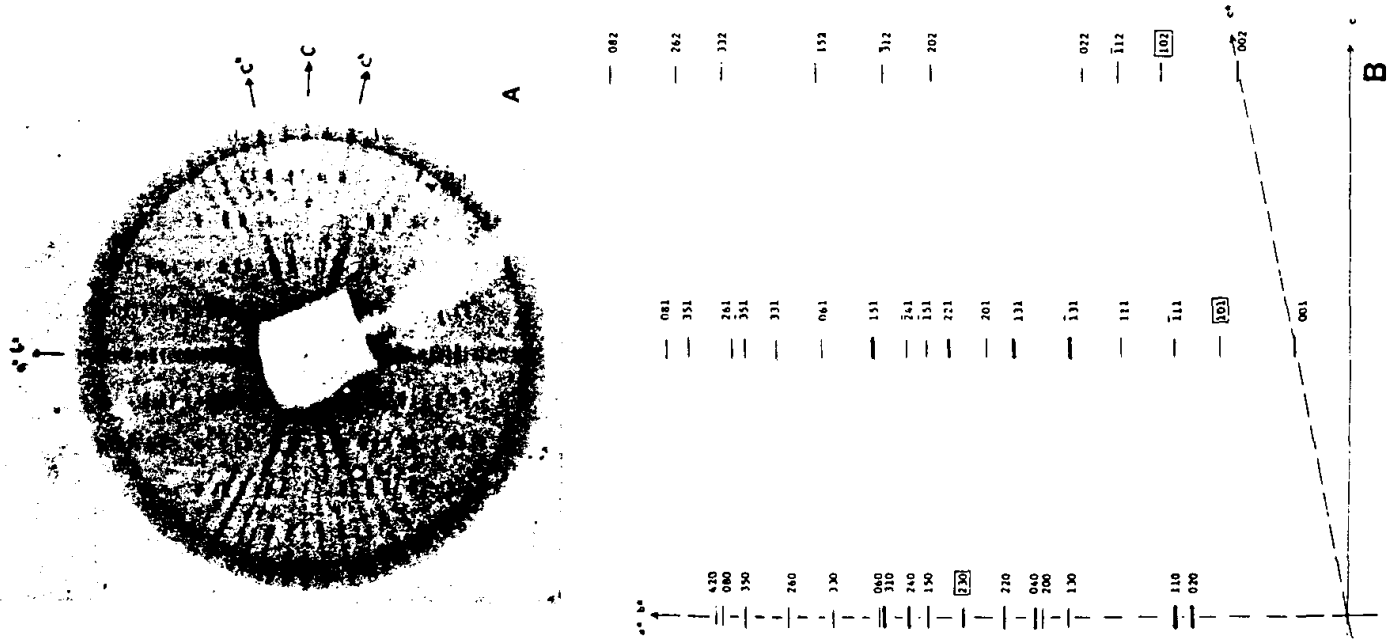
FIGURE 15. (A) Zero level precession photograph of a 50 μm diameter South African "amosite" fiber demonstrating the random orientation of fibers around c-axis (horizontal). MoKα radiation, 20° μ. (B) A portion of the photograph indexed.
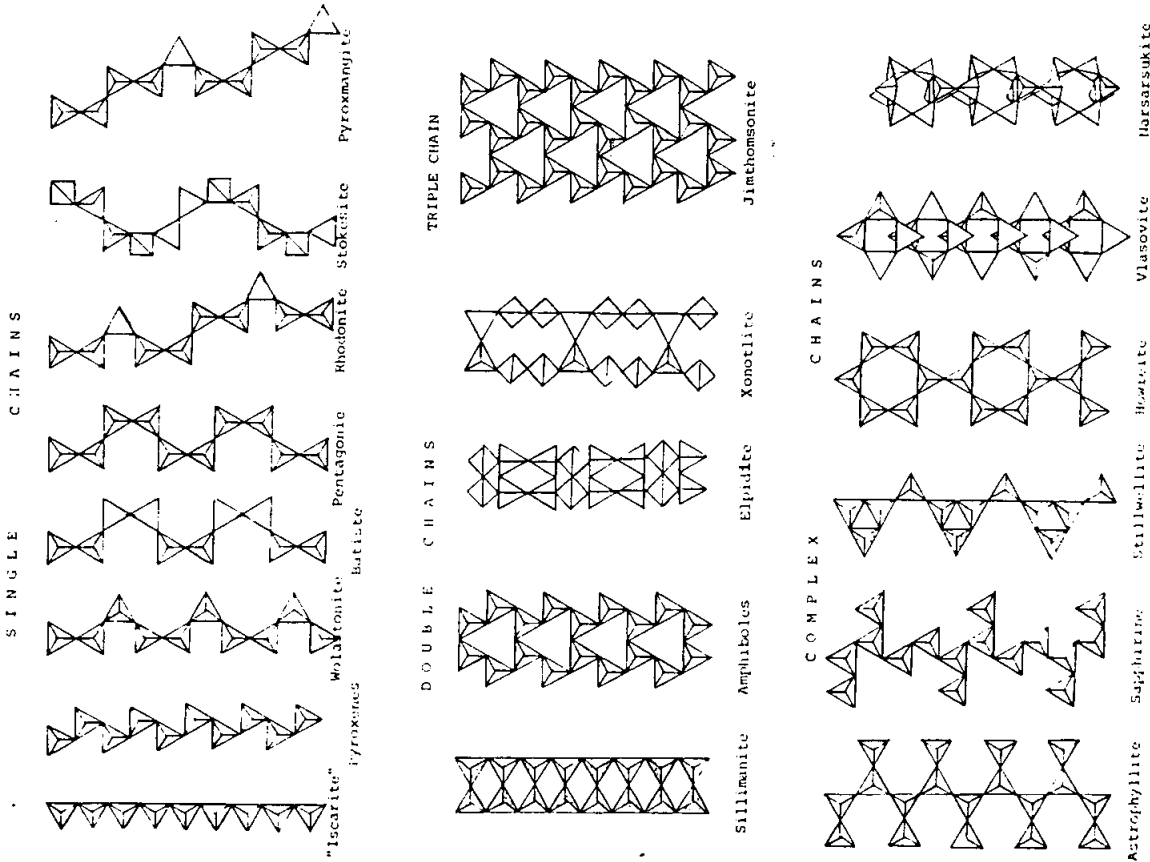
collection which had the appearance of poor quality amphibole asbestos.¶ After separating the fibers, they turned out to be indistinguishable from the best quality amphibole asbestos. The fibers are almost one-inch long, strong and flexible. The asbestos would probably qualify as spin quality in the industry. Some enstatite asbestos fibers are illustrated in FIGURE 19. The mineralogical identity of these fibers has been checked by x-ray diffraction.

The fibril structure of the chain silicate asbestos is less conspicuous than that of the layered silicates, as most chain silicates can grow in fiber-like, acicular crystals. Consequently, the structural reasons for the asbestos properties are not yet fully understood. Several authors have investigated the fibril structures of amphibole asbestos and reported the observation of high density of internal faults and the occasional presence of triple chains, intermixed with the usual double chains.[18-20] More recently Veblen and Burnham[21] described the existence of new chain silicate containing triple chains [jimthompsonite, $(Hg,Fe)_{10}(OH)_4Si_{12}O_{32}$] and others containing even more chains linked into units in a similar manner. The presence of certain faults and of triple chains in the amphibole structure can block the otherwise perfect cleavage planes. The lack of cleavage would strengthen the mineral and could also make it more flexible.‖ In other words, these types of imperfections may be responsible, at least in part, for the development of asbestos properties.

| 10 µm
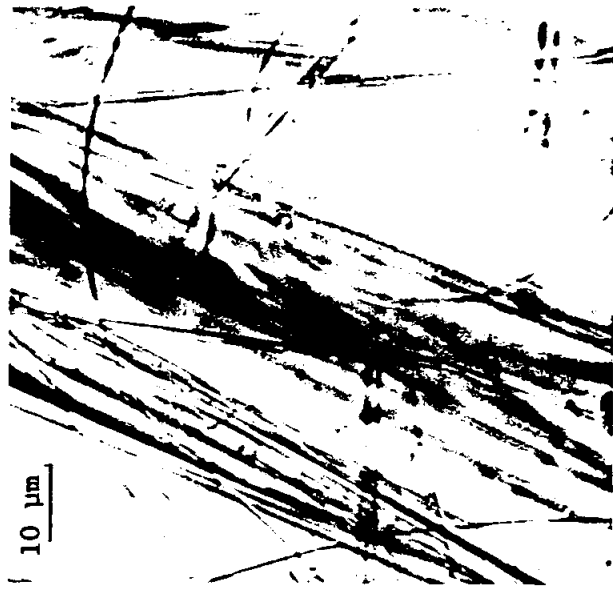
FIGURE 19. Light microphotograph of asbestiform enstatite fibers.

¶This enstatite asbestos displays high industrial qualities. Yet it is not "hydrated." Consequently, the restriction to "hydrated silicates" as given in the modified definition (earlier footnote) is not justified.

‖Due to the absence of cleavage the mineral under relatively high stress will not break but will bend due to slip between planes of atoms.

SINGLE CHAINS

"Iscatite" Pyroxenes

Wollastonite Batisite Pentagonite Rhodonite Stokesite Pyroxmangite

DOUBLE CHAINS

TRIPLE CHAIN

Sillimanite Amphiboles Elpidite Xonotlite Jimthomsonite

COMPLEX CHAINS

Astrophyllite Sapphirine Stillwellite Hoaxite Vlasovite Narsarsukite

FIGURE 18. Illustration of the linkage pattern in the major chain silicates.

amphiboles may crystallize on occasions (less than 1% by volume of all amphiboles) in the asbestiform habit, and some of these make commercially valuable deposits. There is no reason, however, why other chain silicates could not crystallize in the same habit.

We have located an enstatite (a pyroxene), $Mg_2Si_2O_6$, sample in our teaching

Low Density of Surface Defects

The theoretically calculated tensile strength of material is many folds higher than the observed actual strength. Griffith[22] demonstrated in his classical study that the low observed tensile strength of most materials is due to the high density of surface defects and that the density of surface defects is inversely proportional to the tensile strength of the materials. Some of these defects, usually referred to as Griffith cracks, can be observed in light and in electronmicroscopy.

No quantitative studies have been made as yet to determine the relative densities of surface defects in asbestiform fibers and in acicular crystals or cleavage fragments of amphibole. However, the surfaces of asbestos fibers are conspicuously more regular and smoother than that of the other varieties and can be safely assumed to have fewer defects. The apparent absence of Griffith cracks in asbestos fibers, possibly combined with high density of the appropriate structural defects may explain the high tensile strength and flexibility of the amphibole asbestos fibers.

There is no intermediate stage in the development of the tubular or scroll structure of chrysotile. On the other hand, the asbestiform development in the chain silicates is a continuous process. The density of structural faults and surface defects can be variable in different asbestiform fibers crystallized under different physical conditions. Accordingly, the asbestos properties of amphibole and other chain silicates will also be variable, depending on the development of faults and the degree of absence of surface defects. It is reasonable to anticipate that the biological properties will also reflect the same degree of development.

This, of course, complicates the job of public health officials as we do not know at what point of asbestiform development a chain silicate becomes "asbestos." We know that the highly developed asbestiform fibers of commercial asbestos are carcenogenic and we have strong indications that acicular crystals and fragments of the same minerals are probably not. Where should the line be drawn between these two?

We could follow a simplistic approach and call all acicular fragments asbestos, including amphiboles and all or most other chain and layered silicates.** The problem, in this case, becomes unsolvable unless we stop practically all our mining and industrial operations. The other alternative is to initiate systematic studies in the analysis of the development of asbestos properties in minerals and in similar synthetic materials, and coordinate that work with biological and medical research. We can then determine the relative harmfulness of fibrous and acicular particles and can introduce realistic measures for their effective control.

OTHER FIBROUS SILICATES

The minerals discussed in the preceeding section have crystal structures and composition similar to that of serpentines and amphiboles. These minerals are common and constitute about 17% of the earth's crust.[23] Their asbestiform varieties are also comparable to those of chrysotile and amphibole asbestos. In addition, there are a number of other silicates that may also crystallize in the asbestiform habit, and there are also fibrous silicates which have some properties of asbestos. Jade and fibrous zeolites will be discussed as illustrations of these two types.

** In fact we may include elongated particles of most other minerals and synthetic substances, as any one of them may be carcinogenic.

Jade

Actinolite (an amphibole) crystallizes in three distinctly different habits: prismatic or acicular, asbestiform, and microcrystalline-massive. The last one of these is known by the variety name of nephrite and is one of the two accepted jade minerals. Nephrite jade is the toughest‡‡ known natural substance (diamond is the hardest). This property of jade was attributed to the interlocked texture of extremely small, acicular crystals. This explanation, however, does not appear to be adequate since no matter how the acicular crystals are interlocked the strength of the mineral should not exceed

FIGURE 20. Light microphotograph of nephrite jade, in polarized light.

the strength of the composing crystals. Bradt, Newnham and Biggers (1973)[24] have investigated the physical properties of jade and have examined several samples with SEM. They concluded that the tiny actinolite crystals are fibrous and implied that they may be asbestiform. The extreme strength of the asbestiform fibers and their interlocking nature provides a more reasonable explanation for the toughness of nephrite. FIGURE 20 is a microphotograph of a nephrite thin section. The same type of texture can be found in some massive minnesotite (FIGURE 21). Since minnesotite is a layered silicate there seems to be no other explanation feasible

‡‡"Toughness" relates to the amount of work necessary to deform a substance to its rupture point.

and compounds. Some of these may, of course, be carcinogenic. Under these conditions fibrous zeolites may be as harmful as asbestos itself.

SUMMARY

The current definition of asbestos in many environmental studies and in most governmental regulations is arbitrary and is based primarily on a commercial argument: only those minerals are considered to be asbestos which are known to occur in concentrated deposits and can be mined profitably. Four of the five such minerals are accepted as asbestos whether they crystallized in the asbestiform habit and possess the unique physical and biological properties of asbestos or not. Over 90% of the same four amphibole minerals are nonasbestiform and are known to have different physical and biological properties. This definition excludes all other minerals from asbestos even if they actually crystallized in that habit and have the properties of asbestos. Examples of these not-accepted asbestos have been shown. Although these asbestiform varieties make no commercial deposits they are major constituents in certain rocks and can be concentrated in industrial wastes. The current, erroneous and oversimplified definition of asbestos should be abandoned and replaced by a scientifically acceptable one. The toxicity and potential health effects should be determined independently for each of the many types of asbestos as the need arises for their environmental evaluation.

CONCLUSIONS

1. The occasional crystallization in the asbestiform habit is not an exclusive property of chrysotile (serpentine) and amphiboles. This brief survey was limited to silicates which have structures and elemental composition similar to that of the serpentines and amphiboles and demonstrated that many other minerals can occur in the same habit. If the boundaries of the survey would have been extended to include
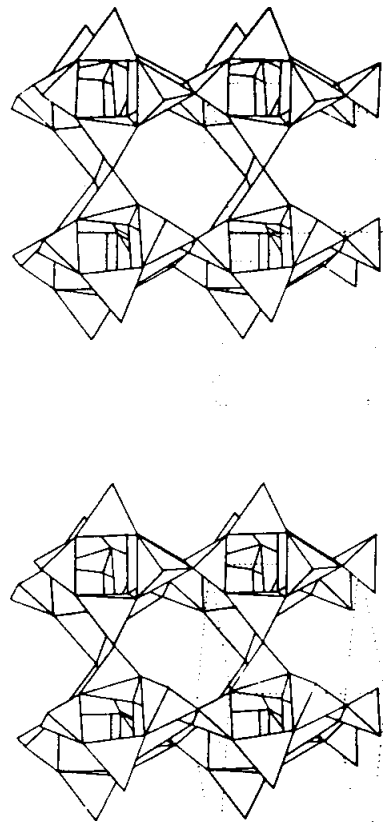
FIGURE 22. Stereoscopic diagram of the tetrahedral frame of the crystal structure of edingtonite, a fibrous zeolite. Tetrahedra are occupied randomly by silicon and aluminum cations.
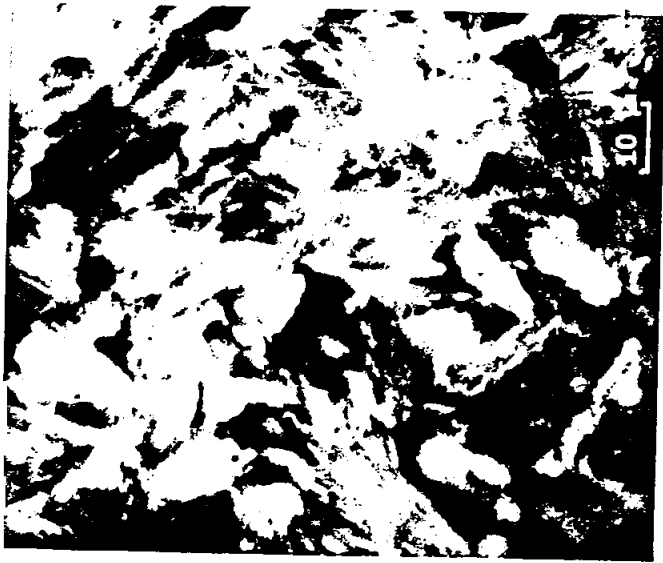

FIGURE 21. Light microphotograph of the minnesotaite "jade" texture, in polarized light.

to account for the fibrous texture than an asbestiform tubular structure. The minnesotaite "jade" displays properties similar to nephrite. It is relatively hard and almost as tough as nephrite.

When jade is crushed sufficiently fine, it will produce fibrous particles. Are these particles asbestos? This question needs investigation.

Fibrous Zeolites

One subgroup of the zeolite minerals (natrolite, edingtonite, thomsonite, and others with general composition of $(Na,Ca,Ba)_{1-2}(Si,Al)_5O_{10} \cdot nH_2O$) usually crystallize in fibrous habit and accordingly they are called fibrous zeolites. These fibers (FIGURE 22) are not believed to be asbestiform. However, the possibility that some may have asbestos properties has not been investigated. It is conceivable that under the appropriate conditions of crystallization they may acquire some asbestos properties.

Whether fibrous zeolites are asbestiform or not, they are reasonably durable and inert in biological environment and have one specific property that makes them comparable with tubular chrysotile. Chrysotile can trap various elements and compounds in the center of the tube. Fibrous zeolites have a strong silica tetrahedral frame which contains large channels and openings. These channels are large enough to let water molecules migrate through the structure and to trap a variety of elements

... ... Academy of Sciences

the more than 4000 other minerals, the list of those having asbestos varieties would undoubtedly be greater.

2. Although only chrysotile and amphibole asbestos is known to occur in sufficient quantity to constitute commercial value, asbestiform varieties of other common minerals are also available in large quantities. They are disseminated in various types of rocks and can be concentrated by industrial processes, and may be major pollutant in some locations.

3. It is apparent that the carcinogenic factor of asbestos is in the realm of the "asbestos properties" of the fibers and the mineralogical identity of the particles is of secondary importance.

4. Asbestiform development is a continuous process in chain silicates and consequently, asbestiform varieties of minerals from different localities may have different degrees of asbestos properties. The gradation in asbestos properties can be expected to be reflected in the biological properties as well.

5. All asbestos cannot be assumed to possess the same carcinogenic properties as chrysotile and amphibole asbestos. The biological properties of each type of asbestos needs to be determined independently.

6. An extensive and systematic research program should be initiated in close cooperation between mineralogists, biologists, medical and public health scientists. Mineralogists should determine and classify the asbestos properties of the asbestiform fibers of the common minerals. Biologist should follow that with the investigation of the biological properties of the different types of asbestos. Medical and public health researchers should then define the various categories of health hazards associated with each type of asbestos.

References

1. PALEKAR, L. C. & D. L. COFFIN, 1977. EPA study of biological effects of asbestos-like mineral fibers. Natl. Bur. Std. Spec. Publ. In press.
2. PALEKAR. L. D., C. M. SPOONER & D. L. COFFIN, 1979. Influence of the fiber character of minerals on *in vitro* cytotoxicity. Ann. N.Y. Acad. Sci. This volume.
3. LANGER, A. M., Epidemiological studies of New York City tunnel workers (personal communication).
4. WALKER, J. S. & T. ZOLTAI. 1979. Comparison of asbestos fibers with synthetic crystals known as "whiskers". Ann. N.Y. Acad. Sci. This volume.
5. LIGHT, W. G. & E. T. WEI, 1977. Surface charge and asbestos toxicity. Nature 265: 537–539.
6. LIGHT, W. G., & E. T. WEI, 1977. Surface charge and hemolityic activity of asbestos. Envir. Res. 13: 135–145.
7. ZOLTAI, T., I VERES, M. J. WAGNER & R. F. HAMMER, 1977. Surface charges of asbestiform amphibole fibers. (in this manuscript).
8. SCHILLER, J. E. 1978. Identification of asbestiform fibers. Qrtr. Rep. Dec. 1977, March, 1978. U.S. Bureau of Mines, Twin Cities Metl. Res. Ctr.
9. BURNEY, J. 1978. Relative surface charge phenomenon as observed in four varieties of the amphibole actinolite. Senior thesis, Univ. of Maryland, College Park, Md.
10. BATES, T. F., F. A. HILDEBRAND & A. SWINEFORD, 1949. Electron microscopy of the kaolin minerals. Am. Mineral. 34: 274.
11. BATES, T. F., F. A. HILDEBRAND & A. SWINEFORD, 1950. Morphology and structure of endellite and halloysite. Am. Mineral. 35: 463-484.
12. BATES, T. F., L. B. SAND & J. F. MINK, 1950. Tubular crystals of chrysotile asbestos. Science Vol. 3: 512-513.
13. WHITTAKIR, E. J. W., 1953. The structure of chrysotile. Acta Crystallogr. 6: 747.
14. YADA, Keiji, 1967. Study of chrysotile asbestos by a high resolution electron microscope. Acta Crystallogr. 23: 704-707.
15. KOHYAMA, N., K. FUKUSHIMA & A. FUKAMI, 1978. Observation of the hydrated form of tubular halloysite by electron microscope equipped with an environmental cell. Clays and Clay Miner. 26: 24-40.
16. MARSHALL, E. C., R. P. HUBERT, B. T. SHAW, & O. G. CALDWELL, 1942. Studies of clay minerals with the electron microscope: II. The fractionation of beidellite, nontronite, magnesium bentonite and attapulgite. Soil Sci. 54: 149-158.
17. CRESSY, B., & J. ZUSSMAN, 1976. Electron microscopic studies of serpentinites. Canad. Miner. 14: 307–313.
18. FRANCO, M. A., J. L. HUTCHINSON, D. A. JEFFERSON & J. R. THOMAS, 1977. Structural imperfections and morphology of crocidolites (blue asbestos). Nature 266: 520–521.
19. WYLIE, A. G., 1978. Optical properties of asbestiform amphiboles and their nonasbestiform analogues. U.S. Bur. Mines. In press.
20. CHISHOLM, J. E. 1973. Planar defects in fibrous amphiboles. J. Mater. Sci. 8: 475–483.
21. VEBLEN, D. R., P. R. BUSECK & C. W. BURNHAM, 1977. Asbestiform chain silicates: New minerals and structural groups. Science 198: 359–365.
22. GRIFFITH, A. A., 1921. VI. Phenomena of rupture and flow in solids. Phil. Trans. Roy. Soc. London, Ser. A. 221: 163–198.
23. AHRENS, I. H., 1965. Distribution of the elements in our planet. Earth and Planet. Ser., McGraw-Hill. New York, N.Y.
24. BRANDT, R. C., R. E. NEWMAN & J. V. BIGGERS. The toughness of jade. Amer. Mineral. 58: 727-732.

8. MINERALOGICAL CHARACTERISTICS OF ASBESTOS

E. Steel and A. Wylie
US Department of Commerce, Washington, DC.

The asbestiform habit is most commonly developed in certain amphiboles and chrysotile, but other minerals also may crystallize with this unusual habit. The habit may be characterized by (1) a fibril structure, single or twinned crystals of very small widths (generally less than 0.5 μm), which have grown with a common fiber axis direction, but are disoriented in the other crystallographic directions; (2) anomalous optical properties, primarily parallel extinction; (3) unusual tensile strength; (4) high aspect ratio; and (5) flexibility. In addition, there is evidence to indicate that some amphibole asbestos may have unusual surface properties.

ASBESTOS AND THE ASBESTIFORM HABIT

Asbestos is defined as a group of highly fibrous silicate minerals that readily separate into long, thin, strong fibers of sufficient flexibility to be woven, are heat resistant and chemically inert, and possess a high electric insulation, and therefore are suitable for uses where incombustible, nonconducting, or chemically resistant material is required (Gary, et al., 1974). The most common minerals that may occur with the asbestiform habit are chrysotile, grunerite (amosite), riebeckite (crocidolite), actinolite, anthophyllite, and tremolite; although the development of this habit among these minerals is rare. Other minerals, most notably other amphiboles, can occur in this habit, but no others have been mined commercially as asbestos.

All asbestos is confined to metamorphic rocks, even though other habits of the amphiboles are common in igneous rocks. Slip fiber veins are the most common deposits (South African amosite, Canadian chrysotile, etc.), but mass fiber deposits also may occur such as California chrysotile or mountain leather. Field relations and experimental data support the hypothesis that metasomatism is the dominant process in the formation of asbestos fibers, amphibole as well as serpentine.

The crystal habit of a mineral is the shape or form a crystal or aggregate of crystals take on during crystallization. The asbestiform habit has a number of characteristics that differentiate it from other habits. Chief among these is the *fibril structure*. A fibril is a single or twinned crystal with a very small width, generally less than 0.5 μm, and an extremely high aspect ratio; bundles of fibrils may have lengths reaching into the cm. Fibrils share a common crystal growth direction along the long axis of the fiber, but appear to be disoriented with respect to one another in the other crystallographic directions. The structure of the individual fibrils, and the organization of fibrils within a fiber may differ among the various types of asbestos.

The fibril structure of asbestos is probably a factor in controlling a number of secondary properties that include high tensile strength, flexibility sufficient for weaving, and anomalous optical properties. The high tensile strength of asbestos is quite remarkable, exceeding that of the ordinary varieties by a thousand fold (Zoltai, 1978). In part, this may be attributed to the lack of defect on the fibril surfaces (Zoltai, 1978), but some contribution also must come from the existance of bundles and the nature of the ordering of and forces among the fibrils. The flexibility is not only enhanced by the fact that the fibrils may slip past one another, but by their small widths and extreme aspect ratios. However, structural defects parallel to the fiber axis also may contribute to this property. Among the common commercial asbestos types, the greatest flexibility is found in chrysotile and the least in grunerite asbestos (amosite), varying inversely with fibril thickness. In addition, at least for chrysotile, composition also may affect the flexibility of the fibers. Finally, most asbestos minerals are monoclinic, but optically display parallel extinction (Heinrich, 1965, and Wylie, 1978). This also must be due, in part, to the ordering or lack of ordering of the fibrils.

The fibril structure is probably a *random*

93

orientation of fibrils about a common fiber axis. This is definitely the case for chrysotile, which has a tubular structure. A single crystal X-ray photograph, Fig. 1, of an amphibole asbestos fiber shows a pattern of lines that indicates multiple orientations of the diffracting lattices in two directions perpendicular to the fiber axis.

The work of Franco, et al., suggests these orientations are random. This would be consistent with the optical properties. However, some amphibole asbestos fibrils appear to have a rectangular cross section, a shape that suggests a more orderly arrangement of growth. Twinning is known to be common (Hutchison, et al., 1975, and Lee 1978), and has shown platelike stacking of grunerite asbestos fibrils. It is possible that some ordering of fibrils, other than random, could produce the same X-ray fiber photograph and parallel extinction. Although unlikely, an orderly arrangement of fibrils spiraling around the fiber axis is one such arrangement and there may be others.

Fibrils vary in size among the asbestos types. Chrysotile fibrils range from 200 to 500Å in diam. Amphibole fibers tend to be more variable in width and are larger in general. They range from close to the size of chrysotile to approximately 0.5 μm. No precise upper limit of thickness is practical because the amphiboles form in a continuum of habits from granular through fibrous to the extremely fibrous and thin asbestiform habit. There is no exact line that can be drawn between the nonasbestiform

Fig. 1. X-ray photograph showing ordering in the c direction and lines indicating disorder in the other crystallographic directions.

acicular habits and the asbestiform habits, but above approximately 0.5 μm in thickness the grains start to lose the properties characteristic of asbestos. There is extensive intradeposit as well as interdeposit variation in size. This is especially true for fiber length that varies from about a microcentimeter to many centimeters among all types of asbestos.

As fiber bundles are broken up during mining, milling, manufacturing, and fabrication, etc., the individual fibrils are liberated. A population of these particles is quite distinct from a similarly sized population of cleavage fragments produced by the mechanical disintegration of nonfibrous materials. These differences easily can be seen from sizing studies done on several types of asbestos and two nonfibrous amphiboles (Siegrist and Wylie, 1979). Fig. 2 shows that the widths of asbestos particles are approximately the same and are independent of length. On the other hand, the widths of the cleavage fragments of the nonfibrous amphiboles, tremolite, and riebeckite are dependent on lengths that increase as the lengths increase.

While much remains to be learned about the true nature of fibrils and fibril structure, there is no doubt that they are fundamental to the development of asbestos and a necessary characteristic of the asbestiform habit. While there may be many fibrous varieties of silicates besides the amphiboles and serpentine minerals, they are not asbestiform unless the fibril structure is present.

THE SERPENTINE GROUP

The serpentine minerals are a group of sheet silicates that have the same general composition of $Mg_6Si_4O_{10}(OH)_8$. Only a few percent weight of iron or nickel substitute into the magnesium site, and a small amount of aluminum can substitute into the silicon site. The serpentine minerals are approximately polymorphic with the possible exception that the aluminum content may control which phase is most stable (Faust and Fehey, 1962).

The serpentine minerals are composed of polymerlike sheets of SiO_4 tetrahedra, the tetrahedral layer is bonded to layers of $Mg(OH)_2$ octahedra, which is the octahedral or brucite layer. There is an apparent mismatch in size between the two layers that puts a stress on the whole structure. The octahedral layer, being somewhat larger than the tetrahedral layer, tends to force the apical oxygens of the tetrahedra further apart than they would be if the two layers matched in size. The ways in which
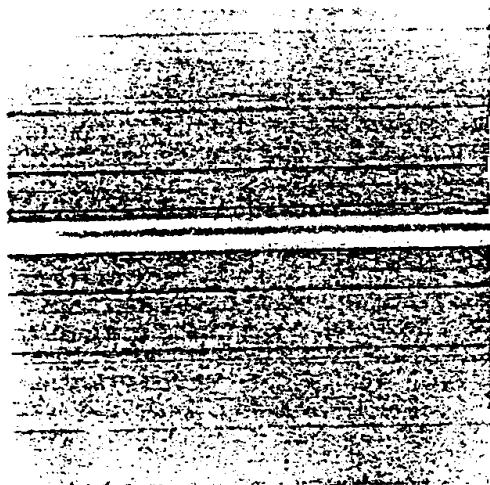
bestiform habits, but
μm in thickness the
·perties characteristic
nsive intradeposit as
ation in size. This is
·ngth that varies from
to many centimeters
·s.
roken up during min·
ring, and fabrication,
; are liberated. A popu·
s quite distinct from a
·ion of cleavage frag·
nechanical disintegra·
·ials. These differences
sizing studies done on
·s and two nonfibrous
·d Wylie, 1979). Fig. 2
·f asbestos particles are
and are independent of
and, the widths of the
f the nonfibrous am·
·l riebeckite are depen·
ncrease as the lengths

to be learned about the
l fibril structure, there is
fundamental to the de·
·nd a necessary charac·
orm habit. While there
·arieties of silicates be·
·nd serpentine minerals,
·n unless the fibril struc·

·NTINE GROUP

·erals are a group of sheet
· same general composi·
·l)s. Only a few percent
·l substitute into the mag·
·all amount of aluminum
· silicon site. The serpen·
·roximately polymorphic
··ption that the aluminum
·hich phase is most stable
2).
·inerals are composed of
·f SiO₄ tetrahedra, the tet·
ded to layers of Mg(OH)₂
the octahedral or brucite
arent mismatch in size be·
· that puts a stress on the
·e octahedral layer, being
·an the tetrahedral layer,
·pical oxygens of the tet·
than they would be if the
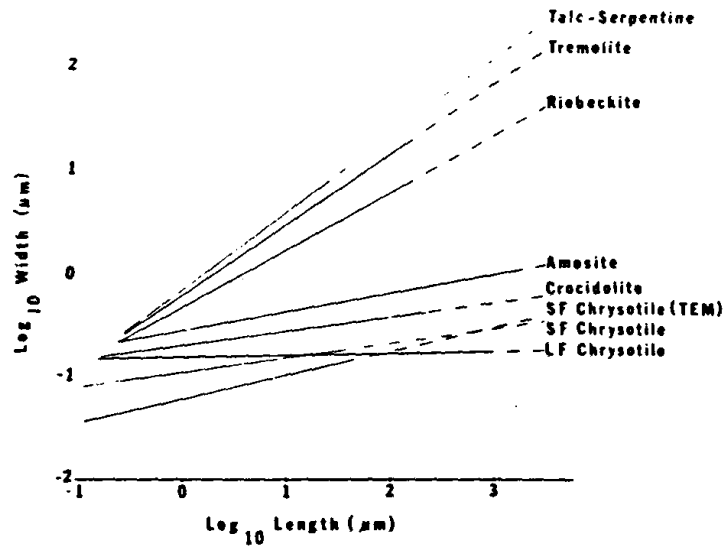·n size. The ways in which

Fig. 2. A graph of the size distributions of a variety of mechanically pulverized mineral samples. The talc serpentine, tremolite, and riebeckite had nonasbestiform habits and, after grinding, the particle width was found to vary as a function of the particle length. For the asbestiform samples amosite, crocidolite, short fiber (SF) chrysotile, and long fiber (LF) chrysotile, the width was found to be very small and approximately constant, showing no or very little relationship to the particle length.

this stress is relieved leads to the three types of serpentine: antigorite, lizardite, and chrysotile (Deer, et al., 1962).

Chrysotile is the only serpentine mineral to exhibit an asbestoform habit. Because of the mismatch of the octahedral and tetrahedral layers, the chrysotile sheet bends so that the smaller tetrahedral layer is on the concave side as shown in Fig. 3.

This bending allows the serpentine sheet to roll up and form concentric cylinders. The coil-
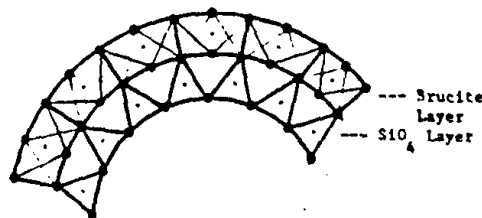
Fig. 3. A schematic of the chrysotile structure showing the way the SiO₄ tetrahedral sheet and the Mg(OH)₂ octahedral layer bend in order to compensate for the mismatch in size between the two layers.

ing effectively relieves the stress between the layers and explains the fibrous nature of chrysotile and its hollow tube appearance on the electron microscope as shown in Fig. 4 (Whittaker, 1956, and Yada, 1967).

The individual fibers or fibrils of chrysotile are approximately 200 to 500Å wide with a hollow tube approximately 50Å wide down the center of the rolled street structure (Zussman, 1978). Chrysotile is found in three forms (1) clinochrysotile, (2) orthochrysotile, and (3) parachrysotile. Clinochrysotile and orthochrysotile differ in their crystal symmetry due to a slight difference in the positioning of the successive brucite and tetrahedral layers, causing clinochrysotile to have monoclinic symmetry, while orthochrysotile has orthorhombic symmetry. Both types have the fiber coiled about the A crystallographic axis, while parachrysotile has the sheet coiled around the B axis.

THE AMPHIBOLE GROUP

The other major asbestos forming group of minerals is called the amphibole group. The amphiboles are a set of minerals based on a

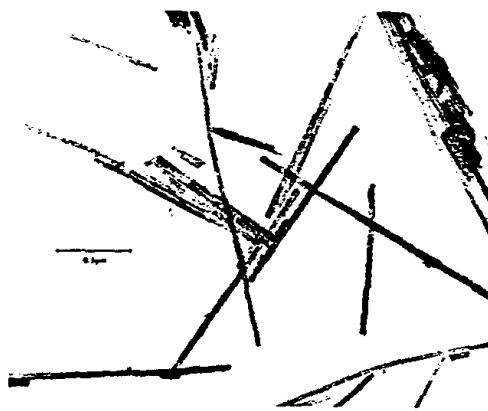Fig. 4. Electron micrograph showing the characteristic hollow canals seen in chrysotile fibrils. The hollow tubes form in the middle of the coiled sheet structure. Note also the very small uniform width of the fibrils.

double chain of silicon-oxygen tetrahedra as shown in Fig. 5. Hauy applied the name amphibole from the Greek word for ambiguous to the group because of its large variation in appearance and composition (Dana and Ford, 1932).
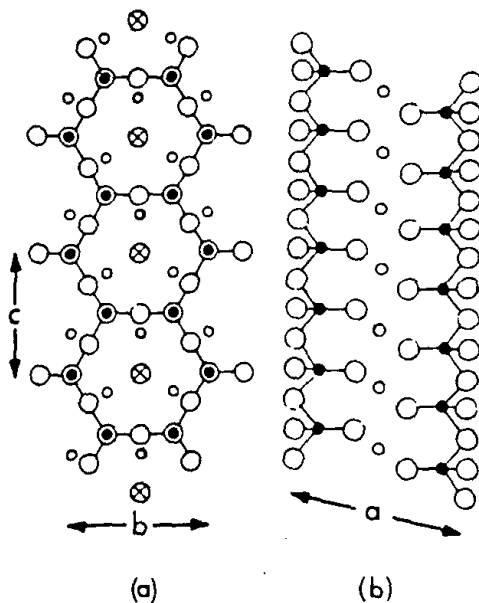

(a)   (b)

Fig. 5. Schematic top view (a) of the double chain structure of the amphiboles and a side view (b) showing the two sets of double chains of SiO_4 bonded together by the octahedrally coordinated cations. The a, b, and c axes are marked on the figure.

The amphiboles are usually first classified by their general crystal symmetry, and are then separated by chemical composition into over 30 different minerals (Leake, 1978).

The amphiboles are divided into two groups (1) those with orthorhombic symmetry (such as anthophyllite and gedrite) that are called orthoamphiboles and (2) those with monoclinic symmetry (such as tremolite, riebeckite, and grunerite) that are called clinoamphiboles. Individuals within each group are further classified by their chemical composition.

In general, the amphibole composition may be defined by the expression: $A_{01} B_2 C_{5VI} T_{8IV} O_{22}$ $(OH_2, F, Cl)_2$. The A position is filled by Na and/or K, the B by Fe^2, Mg^2, Ca^2, Na, Li, and/or Mn, and the C position by Mn^2, Fe^2, Fe^3, Mg^2, and/or Al^3. The T position is filled by Si and/or Al and represents the tetrahedral sites of the double chain structure (Ernst, 1962, and Hurlbut and Klein, 1977).

Table 1 lists some of the more common amphiboles and their compositions.

Not all the amphiboles are known to crystallize in the asbestiform habit. Asbestos seems to be characterized by a low aluminum content. For example, no hornblende asbestos has been reported. The most common amphiboles that have asbestiform varieties are grunerite (asbestiform variety called amosite), riebeckite (crocidolite), tremolite, actinolie, and anthophyllite. Other amphiboles, notably arfedsonite, eckermannite, and winchite also crystallize occasionally in the asbestiform habit.

The structure of the amphiboles is based on double chains of SiO tetrahedra about which other cations are arranged as shown in Fig. 5. Fig. 6 is a view of the structure looking down the double chains of the amphiboles showing the way the double chains are held together by bonding with the cations in the A, B, and C positions. The double chain structure is fundamental to the morphology of the amphiboles and helps to explain the reason cleavage fragments from the amphiboles are generally elongate. Fig. 6 also shows a schematic view of the way the cleavage forms. The cleavage is parallel to (110). It runs parallel to the c-axis and between the long double chains to form elongate fragments. Even though these fragments generally average approximately 7:1 to 9:1 in aspect ratio, they do not possess an asbestiform habit.

In basic structure there doesn't appear to be any difference between the habits of a given amphibole. However, there may be other more subtle differences. For example, the work of Chisolm and Hutchison suggests that amphibole asbestos may be characterized by a high

.ally first classified by
mmetry, and are then
mposition into over 30
. 1978).
vided into two groups
bic symmetry (such as
te) that are called or-
'lose with monoclinic
.olite, riebeckite, and
. clinoamphiboles. In-
i group are further
:al composition.
iole composition may
.on: $A_{01} B_2 C_{5v1} T_{81v} O_{22}$
sition is filled by Na
g², Ca², Na, Li, and/or
y Mn², Fe², Fe³, Mg²,
1 is filled by Si and/or
trahedral sites of the
:! (Ernst, 1962, and

e more common am-
sitions.
are known to crystal-
ut. Asbestos seems to
: aluminum content.
ide asbestos has been
non amphiboles that
- are grunerite (asbes-
mosite), riebeckite
. actinolie, and an-
boles, notably arfed-
winchite also crystal-
)estiform habit.
phiboles is based on
ahedra about which
! as shown in Fig. 5.
acture looking down
imphiboles showing
- are held together by
1 the A, B, and C posi-
ructure is fundamen-
the amphiboles and
1 cleavage fragments
generally elongate.
.utic view of the way
!eavage is parallel to
: c-axis and between
form elongate frag-
fragments generally
to 9:1 in aspect ratio,
-stiform habit.
loesn't appear to be
ie habits of a given
' may be other more
ample, the work of
suggests that am-
iracterized by a high

Table 1. Chemical Composition and Cation Distribution of Several Amphiboles.

Group—Mineral	A	B	C	T	$O_{22}(OH)_2$
Orthorhombic Symmetry					
Fe-Mg group:					
Anthopyllite	—	Mg_2	Mg_2	Si_8	"
Gedrite	—	Mg_2	Mg_3Al_2	Si_6Al_2	"
Monoclinic Symmetry					
Fe-Mg group:					
Cummingtonite	—	Mg_2	Mg_5	Si_8	"
Grunerite	—	Fe_2	Fe_5	Si_8	"
Calcic Group:					
Tremolite	—	Ca_2	Mg_5	Si_8	"
Ferro-actinolite	—	Ca_2	Fe_5	Si_8	"
Hornblende:					
Edenite	Na	Ca_2	Mg_5	Si_7Al	"
Hastingsite	Na	Ca_2	$Fe_4^{2+}+Fe_3^{+}$	Si_6Al_2	"
Na-Ca Group:					
Winchite	—	NaCa	$(Mg,Fe,Al)_5$	Si_8	"
Richerite	Na	NaCa	Fe_5	Si_8	"
Katophorite	Na	NaCa	$(Mg,Fe)_4Al$	Si_7Al	"
Sodic Group:					
Glaucophane	Na	Na_2	Mg_3Al_2	Si_8	"
Riebeckite	Na	Na_2	Fe_3Al_2	Si_8	"

degree of structural defects, primarily involv-ing changes in the positions of the double chains with respect to one another, and defects in chain widths. The two double chains are staggered or slightly shifted in a specific direc-tion, and this stacking sequence is schemati-cally shown in Fig. 7.

The monoclinic amphiboles can be well or-dered with all the shifts being in one direction, or it can be twinned exhibiting a symmetrical
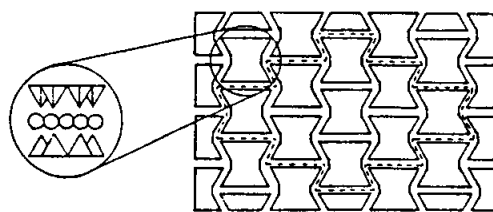
Fig. 6. Schematic view of the way the cleavage forms in the amphiboles. Looking down the c-axis two sets of double tetrahedral chains are strongly bonded to-gether by the octahedral cations as shown in the blowup to form "I beams," named by their simplified shape. The weaker bonds between the I beams, shown by a dashed line, allow for easy breakage and yield the characteristic angles of 56° and 124° of the amphibole cleavage.

change in the stacking direction. There also can be wide-spread disorder on the (100) surface as depicted in Fig. 7c where random changes in the direction of stacking occur.

The other type of defect structure can be seen as variations in the chain widths of the am-phibole structure. These imperfections include single, triple, and larger SiO_4 chains where there are supposed to be double chains. These defects are sometimes referred to as *Wadsley defects* and are parallel to the (010) plane. The fibrous amphiboles have been shown to contain numerous triple chain Wadsley defects ran-domly distributed among the double chains (Hutchison, et al., 1975, and Chisolm, 1975).
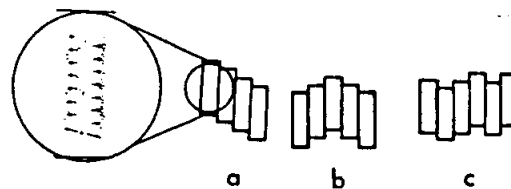
Fig. 7. Schematic of stacking faults in amphiboles. An ordered structure for the monoclinic amphiboles is shown in (a), while (b) shows a single twin plane, and (c) depicts disorder due to the numerous stack-ing faults parallel to the (100).

The stacking faults appear to be much less common in the nonasbestiform amphiboles than in amphibole asbestos (Ross, 1978). There is not enough available data to draw similar conclusions on the chain width defects.

These imperfections may play an important role as fibril makers. The imperfections lie on the (100) and (010) surfaces parallel to the double chain axis. They act as very weak parting planes that contribute to the ease that fibrils break apart laterally.

Experimental evidence suggests that the surface charge on some amphibole asbestos particles may be systematically different than the characteristic of amphibole cleavage fragments of the same composition (Zoltai and Burney, 1978). In part, this may be due to different crystallographic surfaces. Amphibole fibrils are commonly bounded by (100) and (010) surfaces, while cleavage fragments are generally bounded by the (110) faces. The apparent lack of surface defects on fibrils also may contribute to this property. However, much remains to be learned about the surface charges of small particles. It is not yet known if the reports of anomalous surface charge are characteristic of all amphibole asbestos.

RELATED MINERALS

A large number of minerals have fibrous varieties, but few have crystal habits that approach the fibril dimensions and other properties characteristic of asbestos. However, some minerals do have similar habits and therefore may be called asbestiform.

Some of the asbestiform sheet silicates, other than chrysotile, are fibrous talc and the clays palygorskite, sepiolite, and halloysite. The latter is a member of the kaolinite group. Halloysite contains an $Al(OH)_3$ that replaces the brucite layer found in the serpentine structure. The sheet coils to yield a fibril in the same way as chrysotile (Bates, et al., 1950, and Kohyama, et al., 1978). The method of fibril development is not clearly known for the other asbestiform sheet silicates.

Among the chain silicates, only the amphiboles have been described as having asbestiform varieties. Some single chain pyroxenes and pyroxenoids have been described as fibrous, and a few new minerals that are based on triple and alternating double-triple chains have been related to asbestos (Veblen, et al., 1977-78), but have not been shown to have an asbestiform habit.

Other classes of minerals also may occur in fibrous and perhaps even asbestiform habits. For example, individual fibrils of certain zeolites are similar in size to amphibole asbestos. Nemalite or fibrous brucite is another example of a mineral that may be described as asbestiform because of its well developed fibril structure that is probably derived as a pseudomorph after chrysotile.

REFERENCES

Bates, T.F., Hildebrand, F.A., and Swineford, A., 1950, "Morphology and Structure of Endellite and Halloysite," American Mineralogist, Vol. 35, pp. 463-484.

Burney, J., 1978, "Relative Surface Charge in Actinolite Amphiboles," Unpublished Thesis, University of Maryland.

Chisolm, J.E., 1973, "Planar Defects in Fibrous Amphiboles," Journal of Material Science, Vol. 8, pp. 475-483.

Chisolm, J.E., 1975, "Some Implications of the Presence of Planar Defects in Fibrous Amphiboles," Proceedings, 3rd International Conference on the Physics and Chemistry of Asbestos Minerals. Laval, Quebec.

Dana, E.S., and Ford, W.E., 1932, A Textbook of Mineralogy. J. Wiley and Sons, New York, pp. 574.

Deer, W.A., Howie, R.A., and Zussman, J., 1962, Rock Forming Minerals, Vol. 3, J. Wiley and Sons, New York, pp. 170-190.

Ernst, W.G., 1962, Amphiboles. Springer-Verlag, Inc., New York, Chap. 2.

Faust, G.T., and Fahey, J.J., 1962, "The Serpentine Minerals," Professional Paper 384-A, US Geological Survey, Washington, DC.

Franco, MA., et al., 1977, "Structural Imperfection and Morphology of Crocidolite," Nature, Vol. 266, April 7, pp. 520-521.

Gary, M., McAffee, R., and Wolf, C., ed., 1974, Glossary of Geology, American Geological Institute, Washington, DC, p. 41.

Heinrich, E.W., 1965, Microscopic Identification of Minerals, McGraw-Hill, New York, pp. 347.

Hurlbut, C.S., and Klein, C., 1977, Manual of Mineralogy, J. Wiley and Sons, New York, pp. 384-387.

Hutchison, J.L., Irusteta, M.C., and Whittaker, E.J.W., 1975, "High Resolution Electron Microscopy and Diffraction Studies of Fibrous Amphiboles," Acta Crystallographa. A 31, pp. 794-801.

Kohyama, N., Fukushima, K., and Fukami, A., 1978, "Observation of the Hydrated Form of Tubular Halloysite by Electron Microscope Equipped with an Environmental Cell," Clays and Clay Mineralogy, Vol. 26, pp. 24-40.

Leake, B.E., 1978, "Nomenclature of Amphiboles," American Mineralogist, Vol. 63, pp. 1023-1052.

Lee, R.E., 1978. Private communication.

Ross, M., 1978, "The Asbestos Minerals," Workshop on Asbestos, C.C. Gravatt, P.D. LaFleur, and K.FJ. Heinrich, eds., National Bureau of Standards,